UNIVERSITY OF LJUBLJANA
BIOTECHNICAL FACULTY

Boštjan NAGLIČ

NUMERICAL AND EXPERIMENTAL EVALUATION OF WETTED SOIL VOLUME IN SURFACE DRIP IRRIGATION SYSTEMS

DOCTORAL DISSERTATION

Ljubljana, 2014

UNIVERSITY OF LJUBLJANA
BIOTECHNICAL FACULTY

Boštjan NAGLIČ

NUMERICAL AND EXPERIMENTAL EVALUATION OF WETTED SOIL VOLUME IN SURFACE DRIP IRRIGATION SYSTEMS

DOCTORAL DISSERTATION

NUMERIČNO IN EKSPERIMENTALNO VREDNOTENJE VOLUMNA VLAŽNE CONE TAL PRI POVRŠINSKIH KAPLJIČNIH NAMAKALNIH SISTEMIH

DOKTORSKA DISERTACIJA

Ljubljana, 2014

On the basis of the Statute of the University of Ljubljana and by Resolution of the Senate of the Biotechnical Faculty and the Commission for Doctoral study of the University of Ljubljana on 20. 4. 2011, it was confirmed that candidate fulfils conditions to finish a doctorate of science at the Interdisciplinary Doctoral Programme in Biosciences, in the scientific field of agronomy. Prof. dr. Marina Pintar and doc. dr. Cedric Kechavarzi were appointed as a supervisors of this work.

Commission for assessment and defence:

President: prof. dr. Helena Grčman
University of Ljubljana, Biotechnical Faculty

Member: prof. dr. Marina Pintar
University of Ljubljana, Biotechnical Faculty

Member: doc. dr. Cedric Kechavarzi
University of Cambridge, Department of Engineering

Member: doc. dr. Barbara Čenčur Curk
University of Ljubljana, Faculty of Natural Sciences and Engineering

Date of defence: 13th June 2014

The work is the result of my own research work. I agree with publishing of my work in full text on the internet page Digitalna knjižnica Biotehniške fakultete. I declare that the text in the electronic version is identical to the printed one.

Boštjan Naglič

Na podlagi Statuta Univerze v Ljubljani ter po sklepu Senata Biotehniške fakultete in sklepa Komisije za doktorski študij Univerze v Ljubljani z dne 20. 4. 2011 je bilo potrjeno, da kandidat izpolnjuje pogoje za opravljanje doktorata znanosti na Interdisciplinarnem doktorskem študijskem programu Bioznanosti, znanstveno področje agronomije. Za mentorja sta bila imenovana prof. dr. Marina Pintar in doc. dr. Cedric Kechavarzi.

Komisija za oceno in zagovor:

Predsednica: prof. dr. Helena Grčman
Univerza v Ljubljani, Biotehniška fakulteta

Članica: prof.dr. Marina Pintar
Univerza v Ljubljani, Biotehniška fakulteta

Član: doc. dr. Cedric Kechavarzi
University of Cambridge, Department of Engineering

Članica: doc. dr. Barbara Čenčur Curk
Univerza v Ljubljani, Naravoslovnotehniška fakulteta

Datum zagovora: 13. junij 2014

Naloga je rezultat lastnega raziskovalnega dela. Podpisani se strinjam z objavo svojega dela na spletni strani Digitalne knjižnice Biotehniške fakultete. Izjavljam, da je delo, ki sem ga oddal v elektronski obliki, identično tiskani verziji.

Boštjan Naglič

KEY WORDS DOCUMENTATION

DN Dd
DC UDC 631.674.6:626.843:631.432(043.3)
CX Hydrus/ drip irrigation/ numerical modelling/ irrigation systems/ soil/ evapotranspiration/ soil water/ hop/ sweet corn/ irrigation strategies
AU NAGLIČ, Boštjan
AA PINTAR, Marina (supervisor)
PP SI-1000 Ljubljana, Jamnikarjeva 101
PB University of Ljubljana, Biotechnical Faculty, Interdisciplinary Doctoral Programme in Biosciences, Scientific Field: Agronomy
PY 2014
TI NUMERICAL AND EXPERIMENTAL EVALUATION OF WETTED SOIL VOLUME IN SURFACE DRIP IRRIGATION SYSTEMS
DT Doctoral Dissertation
NO XXII, 190 p., 31 tab., 113 fig., 158 ref.
LA en
AL en/sl
AB Information about the horizontal and vertical distances of water distribution in soils under a surface point source is essential for the design of efficient and cost effective surface drip irrigation systems. In this research numerical simulations were carried out with Hydrus-2D/3D to investigate the influence of different emitter discharge rates and initial soil water conditions on the wetting pattern dimensions of a series of soils with varying textures. Based on the simulation results the parameters of Schwartzman and Zur empirical model were refined. Numerical simulations of surface drip irrigation of sweet corn and hop were also conducted on two soil types to evaluate the effect of evapotranspiration and different irrigation management and design strategies on the soil water dynamics. In addition, model accuracy was evaluated against experimental data of hop surface drip irrigation. The simulation results testing influence of different emitter discharge rates showed a small influence of 1.5, 2 and 4 L/h emitter discharge rates on the final size of the wetting pattern. The only major difference was observed for the discharge rate of 0.5 L/h, where the largest wetting pattern in all directions was observed. Higher initial soil water content caused larger wetting pattern sizes in all directions in all contrasting soil textures. However, for a given volume of water applied the wetted radius tended to be larger and wetted depth smaller for fine textured soils. For coarse textured soils the wetted radius of wetting pattern was smaller and wetted depth larger. The numerical data obtained for a wide range of textures provided the opportunity to refine the parameters of the Schwartzman and Zur model, which, when compared to experimental data from the literature, provided good estimates of wetting pattern dimensions. This suggests that this simple model, for which the only soil parameter required is the saturated hydraulic conductivity, could provide a valuable and practical tool for irrigation design in homogeneous soils. Simulation results with sweet corn drip irrigation showed that irrigation strategy strongly affected plants root water uptake. The root water uptake was largest for strategies where high water content was maintained in the zone of maximum root intensity at the time when ETc was highest. It was shown that with the present surface drip system design for sweet corn, the best option is strategy, where irrigation takes place early in the night. When simulations were compared to the experimental field results of surface drip hop irrigation, Hydrus-2D/3D predicted satisfactorily the distribution of water with a root-mean-square-error not exceeding 0.13 cm^3/cm^3. This proposes that the Hydrus-2D/3D can be successfully used for optimizing different irrigation design and management strategies to increase the surface drip irrigation systems efficiency.

KLJUČNA DOKUMENTACIJSKA INFORMACIJA

ŠD Dd
DK UDK 631.674.6:626.843:631.432(043.3)
KG Hydrus/ kapljično namakanje/ numerično modeliranje/ namakalni sistemi/tla/ evapotranspiracija/ voda v tleh/ hmelj/ sladka koruza/ strategije upravljanja namakanja
AV NAGLIČ, Boštjan
SA PINTAR, Marina (mentor)
KZ SI-1000 Ljubljana, Jamnikarjeva 101
ZA Univerza v Ljubljani, Biotehniška fakulteta, Interdisciplinarni doktorski študij Bioznanosti, področje Agronomija
LI 2014
IN NUMERIČNO IN EKSPERIMENTALNO VREDNOTENJE VOLUMNA VLAŽNE CONE TAL PRI POVRŠINSKIH KAPLJIČNIH NAMAKALNIH SISTEMIH
TD Doktorska disertacija
OP XXII, 190 str., 31 pregl., 113 sl., 158 vir.
IJ en
JI en/sl
AI Informacije o horizontalni in vertikalni distribuciji vode v tleh pod površinskim vodnim točkovnim virom so bistvenega pomena za oblikovanje učinkovitih ter stroškovno sprejemljivih nadzemnih kapljičnih namakalnih sistemov. V tej raziskavi smo uporabili numerični model Hydrus-2D/3D z namenom, da raziščemo vpliv različnih pretokov kapljačev ter različnih začetnih vsebnosti vode v tleh na dimenzije omočenih tal v tleh z različnimi teksturnimi razredi. Na osnovi rezultatov numeričnih simulacij smo izboljšali parametre Schwartzman in Zur empiričnega modela. Simulacije nadzemnega kapljičnega namakanje sladke koruze in hmelja so bile prav tako opravljene na dveh tipih tal z namenom vrednotenja vpliva evapotranspiracije, različnih strategij upravljanja namakanja ter različnih oblikovnih parametrov sistema na dinamiko vode v tleh. Natančnost modela Hydrus-2D/3D je bila primerjana z eksperimentalnimi podatki, pridobljenimi iz nadzemnega kapljičnega namakanja hmelja. Rezultati simulacij, kjer smo preizkušali vpliv različnih pretokov kapljačev, so pokazali majhen vpliv – 1,5 in 2 ter 4 L/h pretokov na končno velikost vzorca omočenih tal. Edina večja razlika je bila opažena za pretok kapljača – 0,5 L/h, kjer smo opazili največjo velikost omočenja v vse smeri. Višja začetna vsebnost vode v tleh je povzročila večje velikosti omočenja v vse smeri v preučenih teksturah tal. Ob določeni količini dodane vode sta bila za tla s težjo teksturo opažena večji omočen radij in manjša omočena globina tal. Za tla z lažjo teksturo je bil radij omočenja manjši in globina omočenja večja. Numerično pridobljeni podatki so ponudili priložnost za izboljšanje parametrov Schwartzman in Zur modela, ki je, ko je bil primerjan z eksperimentalnimi podatki, zagotovil dobre ocene dimenzij omočenosti tal. To kaže, da bi lahko ta preprosti model, katerega edini potreben parameter tal je nasičena hidravična prevodnost, predstavljal praktično orodje za oblikovanje površinskih kapljičnih namakalnih sistemov v homogenih tleh. Rezultati simulacij s kapljičnim namakanjem sladke koruze so pokazali, da strategija namakanja močno vpliva na odvzem vode skozi korenine rastlin. Odvzem je bil največji pri strategijah namakanja, kjer se je vzdrževala visoka vsebnost vode v območju največje intenzivnosti korenin v času, ko je bila evapotranspiracija najvišja. Izkazalo se je, da je najboljša strategija namakanja sladke koruze, kjer je namakanje potekalo v nočnih urah. Rezultati primerjave numerične simulacije z eksperimentalnimi rezultati kapljičnega namakanje hmelja so pokazali, da je Hydrus-2D/3D zadovoljivo napovedal vrednosti vsebnosti vode v talnem profilu z vrednostmi efektivne srednje kvadratne napake, manjše od 0,13 cm^3/cm^3. To kaže, da se Hydrus-2D/3D lahko uspešno uporablja za povečanje učinkovitosti nadzemnega kapljičnega namakanja.

TABLE OF CONTENTS

LIST OF TABLES

LIST OF FIGURES

ABBREVIATIONS

Roman alphabet

Symbol	Description
A	Surface area
A_1	Constant for the cylindrical flow model
A_2	Constant for the cylindrical flow model
D^*	Dimensionless diameter
h	Soil water pressure head
ha	Hectares
h_i	Initial pressure head
h_a^i	Average water tension
Ka	Apparent dielectric constant
h_1	Value of the pressure head below which roots start to extract water from the soil
h_2	Value of the pressure head below which roots extract water at the maximum possible rate
$h_{3\,high}$	Value of the limiting pressure head below which roots can no longer extract water at the maximum rate (assuming a potential transpiration rate of *TH*)
$h_{3\,low}$	As above, but for a potential transpiration rate of *TL*
h_4	Value of the pressure head below which root water uptake ceases (usually taken at the wilting point)
$h50\ (P50)$	The coefficient in the root water uptake response function associated with water stress
$K_{ij(iz)}^{A}$	Components of the dimensionless anisotropy tensor K*A*
$K(h)$	Unsaturated hydraulic conductivity function
K^A	Dimensionless anisotropy tensor for the unsaturated hydraulic conductivity K
Ks	Saturated hydraulic conductivity of the soil
L	Litre
l	Shape parameter (pore connectivity parameter)
m	Parameter in the soil water retention function
Mha	Mega hectares (million)
$\bar{M}$	Mean of observed data
Mi	Observed (measured) values
n	Shape parameter (exponent of soil water retention function)
n	Number of observations

n_1	Constant for the cylindrical flow model
n_2	Constant for the cylindrical flow model
P3 ***(p3)***	The exponent in the root water uptake response function associated with water stress
PW	Pressure head at wilting point below which transpiration stops
R^2	Correlation coefficient
Q	Discharge rate (emitter, dripper)
Qa	Actual flow rate
q_i	Volumetric flux density
Qr	Irrigation requirement
q_{fc}	Drainage flux from the soil at field capacity
r	Radius
$TH\ (T_p)$	Potential transpiration rate (set at 0.5 cm/day)
$TL(T_p)$	Potential transpiration rate (set at 0.1 cm/day)
S	Sink term
S_e	Effective soil water saturation
$S(h)$	Root water uptake
Si	Simulated values
S_p	Potential water uptake rate
t	Irrigation duration
T_p	Potential transpiration rate
V	Applied volume of water
V	Total amount of water in the soil
V^*	Dimensionless amount of water applied
X^*	Dimensionless parameter wetted radius
x_i	Spatial coordinate
Y^*	Dimensionless wetted depth

Greek symbols

α	Shape parameters (coefficient in the soil water retention function)
$\alpha(h)$	Dimensionless stress response function of the pressure head
$\Delta\theta$	Average change in volumetric water content
θ	Volumetric water content
θ_i	Initial value of water content
$\theta_a^{\ i}$	Average water content
θ_f	Free pore space
θ^i	Initial water content
θ_r	Residual water content

θ_s	Saturated water content
θ_f	Free pore space
θ_{fc}	Soil field capacity
ρ_b	Bulk density

2D	Two-dimensional
3D	Three-dimensional
ASCE	American Society of Civil Engineering
ASAE	American Society Of Agricultural Engineers
AW	Available water
Aw	Area wetted by one emitter
BC	Boundary condition
BD	Below dripper (emitter)
C	Coarse
COZ	Centre of the overlap zone
CP	Critical point
D	Diameter
EF	Modelling efficiency
ET	Evapotranspiration
ETc	Crop water requirements (crop evapotranspiration)
ETo	Reference crop evapotranspiration
EU	European Union
EWRI	Environmental and Water Resources Institute
F	Fine
FAO	Food and agricultural organisation
FC	Field capacity
GUI	Hydrus graphical user interface
ICID	International Commission on Irrigation and Drainage
IHPS	Institute of Hop Research and Brewing
Kc	Crop coefficient
NSRI	National Soil Resource Institute
Pw	Average percentage of the wetted area
PWP	Permanent wilting point
RAW	Readily available water
RMSE	Root mean square error
SCL	Societe de Cultures legumieres
SD	Surface drip
SDI	Subsurface drip

Se	Short dimension and is representing 80 % of maximum expected diameter
SEISMIC	Spatial Environmental Information System for Modelling the Impact of Chemicals
T	Transpiration
TAW	Total available water
TDR	Time Domain Reflectometry
UK	United Kingdom
USA	United States of America
v.	Version
VG	van Genuchten
X	Wetted radius (horizontal direction)
Y	Wetted depth (vertical direction)
w	The long dimension; the expected maximum horizontal diameter of the wetted soil volume
WRC	Water release curve

1 INTRODUCTION

1.1 BACKGROUND AND RATIONALE

As the population grows and urban water use increases, irrigated agriculture is being called on to produce more food using less water. Fischer et al. (2007) analyzed that mitigation of greenhouse gas emissions should play an important role in reducing the impacts of climate change on agricultural water resources, regionally and globally. Around 18 % of total cultivated land today presents irrigated crops which produce about 40 % of total agricultural output. According to Fischer et al. (2007) the area of worldwide irrigated land has since 1960 increased at a rate of around 2 % per year, from 140 million hectares (ha) in 1961/1963 to 270 million ha in 1997/1999. In a study by de Fraiture and Wichelns (2010), study it was estimated that irrigated area grew at about 0.6 % per year during the last 20 years. If this trend is extended to 2050 this will result in a 35 % increase of irrigated area.

Today about 70 % of total water withdrawals worldwide is due to irrigation causes which represent more than 90 % of consumptive water use. In a study by Bruinsma (2003), a 14 % increase in irrigation water withdrawal for countries in development is expected by 2030 without taking into account impacts of climate change. The projections show that under climate change the changes in water availability and demand in the 21st century will affect security of food and agricultural activities. Modified precipitation patterns and water storage cycles will change availability of water for aquatic and terrestrial agro-eco systems. Therefore the future water availability for food production and for competing human and environmental needs will need to be assured. Climate change will increase irrigation water demand because of a combination of increased evapotranspiration caused by higher temperatures and decreased rainfall in the majority of world regions (Bates et al., 2008).

As discussed by Bruinsma (2003) and Bates et al. (2008) the future improvements in irrigation, as modified irrigation technology or techniques, will play a very important role. These improvements can in the future increase the productivity of water used by irrigation and may provide significant adaptation potential under a changing climate. However, as mentioned by de Fraiture and Wichelns (2010), it is not easy to improve irrigation performance (i.e., increase of water productivity). In order to increase water productivity, capacity buildings, technical assistance and the right incentives and policies are required to motivate farmers. The great potential of drip irrigation lies in improving water management by improving crop yield and quality using less water, and by localising chemical and fertiliser applications to enhance their efficient use and to reduce the risk of pollution (Fischer et al., 2007). Drip irrigation systems consist of point or line source emitters. Point source emitters sometimes interact. For instance, for the irrigation of row crops, emitters along the laterals have to be closely spaced to maintain the necessary

wetted strip of soil along the row. During water infiltration into the soil the water content changes spatially and temporally. Soil water distribution is strongly dependent on the drip irrigation system design parameters, like emitter discharge rate, spacing between the emitters, system pressure, drip emitter type, soil physical properties, climatic conditions, vegetation properties and root distribution. To design drip irrigation systems effectively, the soil water dynamics needs to be predicted using all above mentioned variables. Information about temporal evolution of the wetted soil volume can be helpful in establishing the optimal emitters spacing and the duration of irrigation for the volume of soil where the main crop roots are located (Provenzano, 2007).

There are some guidelines published (for instance Keller and Karmeli, 1974; Vermairen and Jobling, 1984; Keller and Bliesner, 1990; Benami and Ofen, 1995; FAO, 2002a) to help end users operate surface drip irrigation systems. Unfortunately, there are few, if any, clear guidelines on how to design surface drip irrigation systems by taking into account differences in soil hydraulic properties. Some irrigation manuals and guidelines, such as Vermairen and Jobling (1984), propose excavation of the soil beneath the emitters to visually observe the wetting pattern geometry. In engineering terms, systems are often designed to an economic optimum, which may result in insufficient or excessive irrigation. On the other hand, models that simulate the dynamics of water in the soil beneath surface drip irrigation can help in predicting soil water content distribution. One such model is the numerical model Hydrus (Šimůnek et al., 2006). The model has been used extensively to simulate water distribution under surface and subsurface drip irrigation systems (e.g. Aussaline, 2001; Cote et al., 2003; Skaggs et al., 2004, 2010; Gardenas et al., 2005; Lazarovitch et al., 2005; Provenzano, 2007; Bufon et al., 2011; Kandelous et al., 2011; Phogat et al., 2011; Dabach et al., 2013). The use of such models can, in comparison to field experiments, save financial resources and time-demanding laborious work, which would have to be undertaken to examine the dimensions of wetting patterns under different drip irrigation strategies and field/soil conditions. Once all the necessary soil parameters are determined, Hydrus can simulate distribution of water under drip irrigation systems for a wide range of conditions which include different drip irrigation scheduling options, emitter discharge rates, amount of water applied, pulsing irrigation and different soil water initial conditions.

1.2 AIMS AND RESEARCH HYPOTHESES

1.2.1 Aim and objectives

The main purpose of this project is to investigate numerically and experimentally the influence of soil texture, relevant hydraulic properties, evapotranspiration, vegetation root distribution and rate of water applied on the size of the wetted area and therefore emitter

spacing under surface drip irrigation systems that are appropriate for Slovenian climate conditions. This research addresses the interrelation between all the above mentioned parameters, which are important for efficient drip irrigation.

The aim is to maintain/produce water distribution between the emitters uniformly and to achieve sufficient water content at the depth of the root zone which is important for growing row crops, without losses of water to the groundwater.

These considerations lead to the following specific objectives:

- To simulate water infiltration and calculate depths and widths of wetted area using the numerical model Hydrus-2D/3D for a series of soils with contrasting textures.
- To correlate wetted width and depth with soil texture and hydraulic parameters in order to develop a predictive equation for the wetted area dimensions.
- To study the influence of emitter flow rates and initial soil water conditions on the wetted area.
- To study the influence of bulb interaction between adjacent emitters on wetting pattern geometry and water content distribution using 3D numerical simulations.
- To study numerically the influence of evapotranspiration for two specific crops using real meteorological and crop data as model boundary conditions.
- To verify the model results under realistic Slovenian conditions through a field experiments under drip irrigated hop production.

In this dissertation the specific objectives mentioned above were investigated through five dependent parts of research. In the first part of research numerical simulations were done for soils from arable land use which were covering all texture classes according to the UK soil textural triangle and were selected from the Spatial Environmental Information System for Modelling the Impact of Chemicals database. Hydrus-2D/3D was used to simulate the wetting pattern extent under point source drip irrigation for 11 soil textural classes, four different emitter discharge rates and three different initial soil moisture conditions (depletions). This set of data contained results of wetting patterns extent in the X and Y directions for every litre of water applied and up to 20 L of continuously added water. All together the data set included 880 measurements. Numerically generated data from the first part of research was used for the second part of research where the parameters of the empirical model of Schwartzman and Zur (1986) were refined. In the third part of this research numerical simulations were carried out with Hydrus-2D/3D to investigate the influence of five different irrigation management strategies of sweet corn on the spreading of water from the surface emitter when at the same time considering realistic plants and

meteorological data. This part of the research is a case study and does not relate in any way to previous parts of research, but presents a good basis for subsequent more complex numerical modelling parts with real weather and plants conditions. In the fourth part of research the accuracy of Hydrus-2D/3D simulations of 3D water infiltration and redistribution from a surface point source for a layered silty clay loam soil when considering plants root water uptake, was evaluated in a hop field. Volumetric soil water content distribution, measured with 20 TDR probes inserted in the soil profile, was compared with the Hydrus-2D/3D simulated values at the same locations. Because simulated soil volumetric water contents were found to be in good agreement with TDR measured experimental data the last, fifth part of the research was carried out. With other words, the evaluated model allowed evaluation of the effects of various surface drip irrigation design and management parameters for surface drip hop irrigation, such as different soil water initial conditions at the onset of irrigation, different emitter (dripper) spacings and volumes of water applied.

1.2.2 Research hypotheses

The dissertation examines numerically and experimentally the influence of different drip irrigation system design and management factors on the wetted soil geometry. The hypotheses to evaluate this are:

- Wetting volumes will strongly correlate with soil texture (% sand, % silt, % clay), they will be wider and shallower for finer textured soils.
- Higher flow rate for equal irrigated volumes will create wider shallower wetting patters for all drip systems.
- Different initial soil water conditions at given evapotranspiration will affect size of the wetting pattern.

2 LITERATURE REVIEW

2.1 DRIP IRRIGATION

2.1.1 Introduction

The plastic revolution started after World War II and the equipment for installing subsurface drip irrigation systems had been developed by the 1970s. Surface drip irrigation systems, including fertilizer injection were developed at about the same time in Israel (Dasberg and Or, 1999). When plastic drip emitters and tubing became more reliable, surface drip irrigation systems grew at a greater rate than subsurface ones. This happened because of problems with emitter clogging and root intrusions of the subsurface systems (Camp, 1998). The International Commission on Irrigation and Drainage (ICID) estimated that in 2010 – 2011 the total irrigated area in the world was 299 Mha. According to Bucks (1995) (cited in Dasberg and Or, 1999), the area under drip irrigation in year 2000 was estimated to be around 3 Mha, which represented only 2 % of the total world irrigated area. However, according to Reinders (2007), the irrigated area by microirrigation in the world increased from 0.43 Mha in 1981 to more than 6 Mha in 2006 (Table 2.1) and was, after ICID estimations, 10.3 Mha in 2013 (ICID, 16.7.2013).

Table 2.1: The worldwide area of microirrigation (ha) (Reinders, 2007)
Preglednica 2.1: Svetovne površine pod mikro namakanjem (ha) (Reinders, 2007)

Year	1981	1986	1991	2000	2006
Area (ha)	436 590	1 030 578	1 826 287	3 201 300	6 089 534
Increase (%)		136.1	77.2	75.3	90.2

2.1.2 Definitions

Microirrigation is a general defined term meaning slow application of water on or below the soil surface. It can be also called localised irrigation, to emphasize that only part of the soil volume is wetted (Lamm et al., 2007). In ASAE (2007) microirrigation is defined as the ″frequent application of small quantities of water as drops, tiny streams, or miniature spray through emitters or applicators placed along a water delivery line. The microirrigation method encompasses a number of systems or concepts, such as bubbler, drip, trickle, line source, mist, or spray″. Drip irrigation is, according to ASAE (2007), defined as a ″method of microirrigation wherein water is applied to the soil surface as drops or small streams through emitters. Emitter (dripper) discharge rates (Q) are generally less than 8 L/h for single-outlet emitters and 12 L/h per meter for line-source emitters″. In the literature, trickle irrigation is used interchangeably with drip irrigation. Term drip irrigation will be used throughout this work.

2.1.3 Surface drip irrigation (SD)

Surface drip irrigation systems have been at the beginning used for irrigation of widely spaced perennial crops. Today this type of irrigation can be used for irrigating annual or row crops too. Surface drip irrigation system typical components are presented on Figure 2.1 and include irrigation controllers, pump, primary and backup filters, system valves, injection systems, underground pipelines and other components (Lamm et al., 2007).

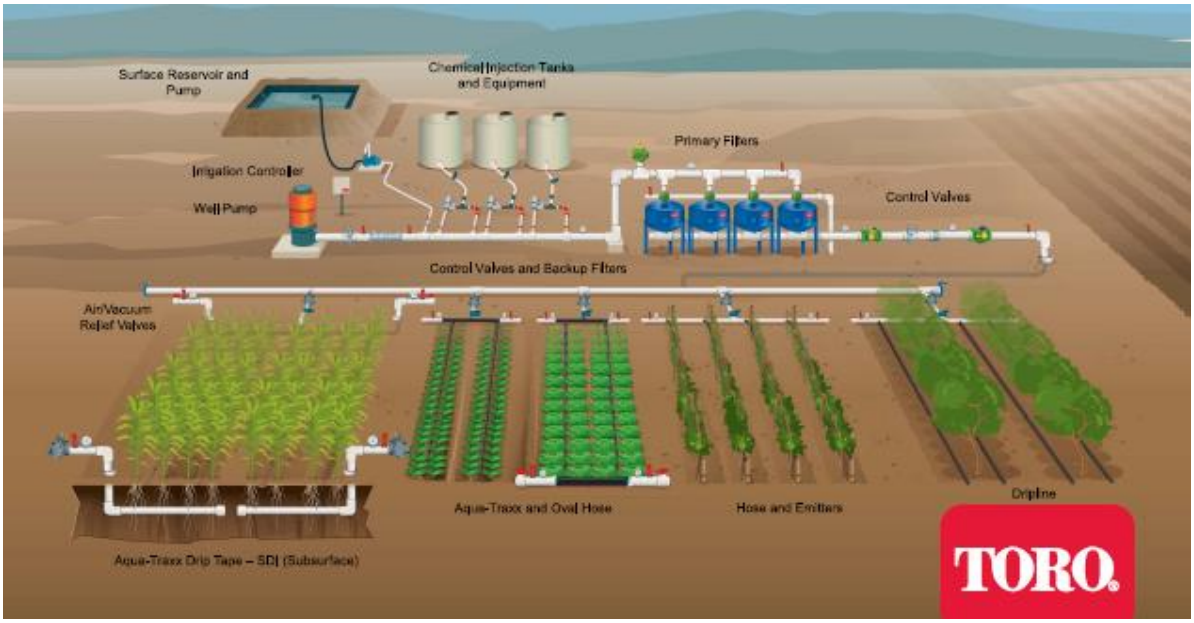

Figure 2.1: Drip irrigation layout and its parts (DripTips, 2013)
Slika 2.1: Postavitev kapljičnega namakalnega sistema in njegovi deli (DripTips, 2013)

2.1.3.1 Surface drip irrigation for row crops

Management and design of surface drip irrigation systems for annual row crops and for perennial crops (trees and vines) is different. For some vegetable crops or other density-planted crops, wetting of the entire growing area is needed by overlapping the wetted soil volume formed beneath each emitter. For perennial crops, like trees, a dry zone along the row and between the rows may separate the trees. When drip irrigating the row crops the aim is to wet the plat row uniformly and leave the soil between the rows dry. For irrigation of row crops drip tape emitting hose or point source emitters, usually used to irrigate trees in orchards, can be utilised. To maintain the necessary wetted strip of soil (at the desired depth) along the row, the emitters along the lateral need to have appropriate spacing.

2.1.3.2 Surface drip system design and crop water needs

Drip irrigation systems design and installation must be site-specific and are governed by soil type, climate, topography, water quantity and quality, proposed crops and cropping systems. These factors will, in the design process, guide the selection of the emitters, emitter spacing and tubing. Water is transported from a source, to a crop, through a network of emission water devices and pipes. The general goal of drip irrigation system design is to choose appropriate layout and components to achieve adequate water distribution throughout the field to meet the crop evapotranspiration (ET) needs and deliver water efficiently and uniformly to a crop. At the same time, the ability of a system to maintain the desired water content at a root zone depth is of great importance (Lamm et al., 2007; FAO, 2002a; Evans et al., 2007). It is important to design drip irrigation systems as simple as possible or to meet the user level of expertise. The system also has to be reliable, easy to maintain, sustainable, able to manage salts and allow tillage and harvest operations.

Drip irrigation systems distribute water directly to the crops root zone and therefore selection of the drip emitters must consider the characteristics of crop rooting system, the expected wetted volume of soil, the total amount of water that will need to be applied and the total estimated time of irrigation per day. The emitters selection (discharge rate and spacing) will be based on the estimated time of irrigation, maximum application amounts, water supply and soil hydraulic properties.

Perennial crops (such as trees or vines) may require up to five drip laterals per plant row, to provide enough water to meet the plants ET needs. This mainly depends on soil type, climate characteristics and size of the plants. Closely spaced perennial crops, such as grapes or hops will need only one drip lateral per plant row. Drip irrigation systems can apply water as a point source or a line source. Line sources apply water in a continuous or near-continuous pattern along the length of the lateral and are most suitable for irrigation of row crops or shallow rooted and closely spaced crops. They are designed based on discharge rate per length unit. Soaker hoses or porous pipes (line-source emitters) in which the entire pipe wall is a seepage surface, as well as drip tapes with closely spaced (e.g., 15-30 cm) emission points whose water application patterns overlap belong to this category. Tubings with discrete or point-source emitters usually used for irrigation of wide spaced crops are designed using discharge rate per one outlet (emitter). Point source emitters are grouped based on their flow properties. Thin walled driplines with periodically spaced emitters infiltrate upon pressurization and have usual emitter spacings ranging from about 50 mm to 1 m. Usually water discharge from emission points which are spaced more than 1 m apart are called point source application (emitters) (Dasberg and Or, 1999; Evans et al., 2007; Lamm et al., 2007).

In cropped field water can be lost from the bare soil surface or wet vegetation through the evaporation (E) process which is affected by climatological factors such as air temperature, solar radiation, wind speed and air humidity. The second process of water loss is transpiration (T), where water vaporizes from the plant tissues into the atmosphere through stomata, located on the plant leaves. Both transpiration and evaporation depend on the vapour pressure gradient, wind and energy supply. When assessing transpiration, air temperature, air humidity, wind speed and solar radiation should be considered. Transpiration is also dependent on many other factors, such as crop characteristics and cultivation practices, environmental aspects, soil salinity, waterlogging and the soil water content. The two processes mentioned above are usually combined into a process known as evapotranspiration.

Distinguishing between evaporation and transpiration is not simple because they occur simultaneously. At the beginning of the crop growth, while the crop is small and most of the soil surface is exposed, the prevailing process is evaporation. Later in the crop development process or when the crop completely covers the ground the transpiration process becomes dominant. At the time of the crop sowing, 100 % of the total ET comes from evaporation process. Once the crop develops its full cover, evaporation accounts for roughly 10 % of ET and transpiration accounts for the remaining 90 % (FAO, 2002b). Coelho and Or (1996) compared soil surface evaporation from drip irrigated corn. The results showed that when the crop is fully grown, the evaporation represents only 7 to 10 % of the total water losses. When calculating crop irrigation water requirements the ET_c (crop evapotranspiration) has to be calculated by multiplying ET_o (reference crop evapotranspiration) with crop coefficient (K_c). For calculation of ETo from meteorological data several empirical and semi-empirical methods have been developed over the last fifty years. Some of the methods that have been developed are the Pan Evaporation, Modified Penman, Radiation and Blaney-Criddle methods. More details of these methods are given in Dorenbos and Pruitt (1977).

Advances in research and science resulted in the development of more accurate methods for assessing crop water use. This revealed that the methods did not behave the same way in different locations around the world which presented their major weakness. This revealed the need for derivation of a standard and more consistent method for ETo calculations. For that reason in 1990 Food and Agricultural Organisation (FAO) organized a conference with scientists, experts and researchers. An outcome of this meeting was the new FAO Penman-Monteith method which is now recommended as the standard method for calculation of the ETo. This method has a good probability of correctly predicting ETo for a wide range of climates and even in the case of missing meteorological data (Allen et al., 1998; FAO, 2002b). In the Penman-Monteith method ETo is defined as a hypothetical

reference crop which is not short of water, with an assumed crop height of 0.12 m, a fixed surface resistance of 70 sec/m and an albedo of 0.23. It has to be noted that if the crop receives some of its water from other sources (rainfall, water stored in the ground, upward seepage), then the irrigation requirement can be considerably less than the crop water requirement (Dorenbos and Pruitt, 1977; FAO, 2002b).

Irrigation scheduling can be prepared when the crop water irrigation requirements are determined. In order to compile a good irrigation scheduling, all the elements of the system's hydraulic design and maintenance with various aspects of the soil and the crop characteristics with the atmospheric evaporative demand have to be integrated. Drip irrigation scheduling is controlled by determining soil and plant water status and by estimating or measuring crop water needs (Lamm et al., 2007).

2.1.3.3 Surface drip system management

In ASAE, 2007 irrigation water management is defined as ″managing plant, soil, and water resources (precipitation, applied irrigation water, humidity) to optimize water use by the crop″. Irrigation scheduling for drip irrigated plant production requires constant attention. Clark (1992) discussed drip irrigation management as dynamic process which requires knowledge of the soil hydraulic properties, plant growth characteristics, crop water requirements, evapotranspiration demand, irrigation scheduling method and drip system characteristics. Also, as mentioned in Evans et. al. (2007), the microirrigation management is associated with questions when to irrigate and how much water to apply, how to accurately calculate the plant water status and its needs and how to integrate other cultural practices with irrigation needs.

Microirrigation management in arid and humid areas differs greatly. In the latter, the crop root system volume is not limited to irrigated zone since water supplies are not a problem and because of frequent precipitation events. Therefore the root water uptake also occurs outside of the irrigated zone. In this situation it is generally recommended that microirrigation system should wet at least 50 % of the root zone volume (Evans et al., 2007).

2.1.4 Drip irrigation efficiency

When considering all above mentioned surface drip design and management practices or more specifically, when appropriate components and layout to achieve suitable water distribution over the field and, at the same time, meet crop need with consideration of

economical, operational, water quality and quantity are determined and well designed, the drip irrigation systems should provide equal soil water availability to all plants in the irrigated field at high irrigation efficiency. In ASAE, 2007 irrigation efficiency is defined ″as the ratio of the average depth of irrigation water that is beneficially used to the average depth of irrigation water applied, expressed as a percentage″.

2.1.5 Advantages and disadvantages of surface drip irrigation systems

Surface drip irrigation has, when compared to other irrigation systems, many advantages and disadvantages. In Keller and Bliesner (1990), Dasberg and Or (1999) and Lamm et al. (2007) they are discussed in more detail, here only the most important ones are presented.

The most important surface drip irrigation advantages are: increased water use efficiency, improved water management (because a smaller soil surface area is wetted the evaporative losses are lower than for surface, sprinkler or micro-sprinkler irrigation), improved crop yield and quality (because only a proportion of soil is wetted, the irrigation is possible right up to time of harvest), improved crop establishment, improved weed control, improved crop yields and quality (water content in the soil is constant because water is applied slowly and frequently), reduced nonbeneficial use (because of irrigation of smaller soil volume, reduced or eliminated runoff, reduced deep percolation and decreased surface evaporation, the water requirements are smaller when compared to other irrigation methods), reduced deep percolation (drip irrigation offers a great potential to reduce the losses to a minimum), improved fertilizer and other chemical application (to improve crop production the fertilizers, herbicides, insecticides, fungicides, rodenticides, nematocides, growth regulators and carbon dioxide can be applied efficiently), lower costs, reduced insects problems (because of smaller discharge openings the surface drip systems are less likely to be plugged by insects when compared to micro-sprinklers), decreased energy requirements (because of lower operating pressures).

The most important surface drip irrigation disadvantages are: limited wetting of crop root zone, high system costs (extensive lateral networks and supportive equipment can make drip irrigation systems expensive at the initial stage. Costs of operation are comparable to other pressurized irrigation methods), limitations with the cover crop (surface drip irrigation can exclude the use of cover crops in arid climates), persistent maintenance requirements (drip emitters are because of smaller flow passageways than micro-sprinkler irrigation systems, more easily clogged), extensive maintenance requirements (clogging, whether complete or partial represents a serious problem whereas damages to pipelines and other components can occur), potential for excess deep percolation (because water is applied to a small soil volume, deep percolation losses can occur), restricted root

development (because water is applied to a specific part of a soil volume, root development may be limited to the wetted soil volume near each emitter or along each lateral line), cleaning difficulties (for example, clogged emitters are almost impossible to clean).

2.2 HOP (HUMULUS LUPULUS L.) IRRIGATION

2.2.1 Hop plant

Hop (*Humulus lupulus* L.) is a perennial herbaceous climbing plant from the *Cannabaceae* family. It is native to Europe, western Asia and North America. Only female plants are grown in hop fields, while male ones are not desired, to prevent the pollination of the female plants. The life expectancy of hop plant is from 10 to 20 years and depends mainly on the growth conditions, variety and agricultural practices. The hop plant consists of above-ground and below-ground vegetative parts. The above-ground parts of the plant die back to ground level every winter, but below-ground parts (or rootstock) are perennial. The commercial value of hops lies in the lupuline glands that contain resins (α-acid, β-acid) which give beer its bitterness and essential oils which contribute to hop flavour (Neve, 1991; Rode et al., 2002).

Wirework is attached to the permanent structure of wooden or concrete poles and is the main support for a hop plants. A string or thick wire is attached to the wire which provides support for the hop plants. Plant spacing depends mostly on hop variety and growing area conditions. In Slovenia they vary between 2.4 to 3.0 m between the rows and about 1.1 to 1.4 m between the plants in the row. Usually two strings are used per each plant. The height of the wires on which hop plants climb varies from 6 to 7 meters. Pruning and shedding are two of very important cultural operations in hop production. With pruning the one-year-old wood and the redundant developed eyes above the rootstock are removed. With this process the growth and development of the plants is controlled. With shedding the soil is added to the plant and ridges along the hop rows are created. This fastens the bines, so that wind does not break them, cover and suffocate the weeds and enable growth for adventitious roots. Hop plants are shed twice or three times per season (Pavlovic, 2012).

The hop production industry is one of the highest work-intensive and capital demanding types of agricultural production. In study of Pavlovic (2012) it was estimated that in the European Union (EU), in 2008, hop was produced by fourteen member states but that 80 % of the total EU hop, by volume, was produced by Germany and the Czech Republic. In 2008 the total hop production was around 57 000 t which represents more than 50 % of

total world hop production. The largest hop producers in EU were Germany (39 676 t), Czech Republic (6 735 t), Poland (3 446 t), Slovenia (2 359 t), France (1 469 t), the UK (1 410 t).

2.2.2 Root system

The hop roots below-ground parts are composed from roots tissue and stem tissue. Together they form a rootstock (Figure 2.2). The upper part of the rootstock is actually a stem tissue. The root system can, if plant is mature, extend downwards for 1.5 m or more and laterally for 2 – 3 m, but this mainly depends on soil characteristics. Hop has two types of roots. The first type is horizontal roots that are tough, wiry and branching and produce fibrous or adventitious roots within upper 20 cm of the soil. They also form on the lower part of the upper rootstock. These roots constantly renew themselves and have the main function of water and nutrients absorption. These roots are maintained with shedding. The second type is vertical roots which arise from the crown and are fleshy, irregularly swollen and fragile and have a function of food and nutrient storage. The plant regenerates each spring from buds on the branched stem tissue, which lies below ground level and forms the upper part of the rootstock (Neve, 1991; Rode et al., 2002).

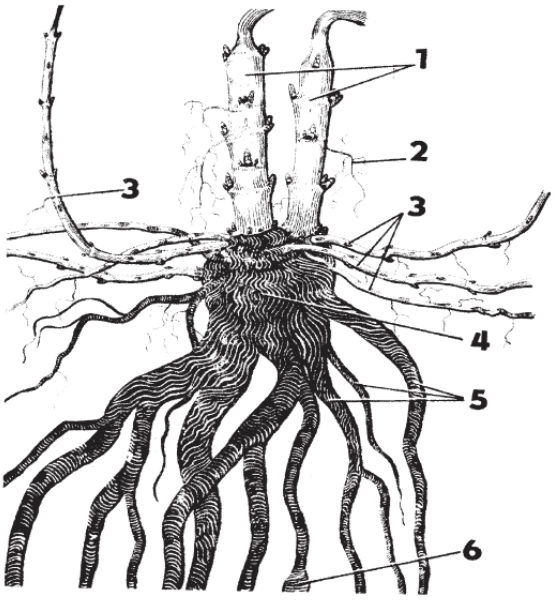

Figure 2.2: Below ground hop plant parts or rootstock. 1 - stem tissue with sleeping buds, 2- adventitious roots, 3 – new shoots, 4 – old stem, 5 – vertical roots (Rode et al., 2002)
Slika 2.2: Podzemni deli rastline hmelja (korenike ali štora). 1 – stebelno tkivo s spečimi očesi, 2 – adventivne korenine, 3 – stranski poganjki, 4 – koreninsko tkivo, 5 – glavne korenine, 6 – odebeljena glavna korenina (Rode in sod., 2002)

2.2.3 Technology of hop irrigation

To produce the highest yields, the hop plants require a good supply of water. Irrigation as an agri-technical measure was quickly established in hop production especially in the drier regions of the world (Neve, 1991). Today two basic technologies of hop irrigation are widely used. First technology is a sprinkler type of irrigation or, more specifically, hose pull irrigators and second one is different varieties of drip irrigation.

The hose-pull irrigator consists of a rain gun mounted on a sledge (Figure 2.3). The sledge is connected to its own hose which is pulled to a large drum (hose reel) which is located on the other end of the field. The drum is rotating and therefore pulling the hose. The drum is mounted on a chassis, which is parked at the headland and has water supply from the hydrant or main water supply. The drum is fitted on the chassis with a drive mechanism, which is driven by water power or diesel engine (FAO, 2001). After Knapič (2002) with hose-pull irrigator in one run from 20 to 30 mm of water is added in Slovenian conditions, depending on the soil type.

Figure 2.3: Hose-pull irrigator on the field (left) and its rain gun (right)
Slika 2.3: Bobnasti namakalnik na polju (levo) in njegove sani z razpršilci (desno)

Technology of drip irrigation is becoming more and more popular in hop production industry. There are three different versions of drip irrigation used in hop. First one is subsurface drip irrigation where a dripline is placed beneath the plants (10-15 cm beneath the plants), usually before the hop garden is established. Once the hop garden is established, the dripline is placed around 30 cm from the hop row at the soil depth of around 40 cm. Second one is surface drip system placed on the top of the ridge along the hop row. With this system the dripline has to be placed and picked up and stored each growing season. The third version is dripline placed at the top of the wirework structure. In

this case additional wire, on which the dripline is fixed, needs to be installed at the top of the wirework along the hop row (Knapič, 2002).

2.3 SOIL WATER DISTRIBUTION UNDER SURFACE DRIP IRRIGATION

2.3.1 Introduction

As mentioned in the surface drip systems design chapter (section 2.1.3.2), factors such as soil hydraulics, water quantity, crop properties have a strong influence on the selection of the emitters, their spacing and tubing size. Based on this it is clear that information about the dimensions of the wetted zone in the soil which forms beneath the emitter(s) is an important prerequisite at the beginning of the drip irrigation design process.

2.3.2 Importance of wetted volume

The distances between the emitters along the laterals have to be adapted to crop water requirements. Distances should be based on soil hydraulic properties and emitter discharge rate (Q). The knowledge about wetted soil volume shape in relation to peak crop water requirements, crop root zone extend and irrigation frequency can be considered as a unifying design objective for various emitter layouts, discharges and spacings. The plant root water uptake during water infiltration into the soil is, at the design stage, usually neglected (Dasberg and Or, 1999). The selection of optimum emitter spacing is not an easy matter, considering all the variables (which usually have nonlinear relationship) involved. In recent years a number of physically-based, analogue and mathematical models have been developed to help estimate wetting patterns dimensions from a point source. They are discussed in upcoming chapters.

At the stage of surface drip irrigation system installation, the placement of the emitters above the soil surface causes water infiltration within a very small area compared to the total soil surface area. According to Vermeiren and Jobling, (1984), Cote et al. (2003), Gardenas et al. (2005), Skaggs et al. (2010), the shape of the wetted soil volume under single drip emitter is influenced by soil hydraulic properties, soil texture, soil structure, impermeable layers in the soil profile and anisotropy such as horizontal and vertical permeability. The soil wetting and drying are continuous processes under cropped conditions. In this case the soil water content patterns depend also on water management (volume of water applied per irrigation, the rate of application, irrigation frequency), emitter distance (number of drippers), dripper placement (above or below soil surface), initial soil water content and lateral positioning with respect to the plant row. According to Benami and Ofen (1995) the wetted zone beneath the surface point source emitter consists

of three phases (Figure 2.4). Around and under point source emitter a transition zone forms in which the soil water content is near saturation and soil is poorly aerated. Around the transition zone a wetting zone forms. In this zone the water spreading is governed by capillarity and gravitational forces and the water content decreases with the distance from the point source. The third zone is the wetting front, where the soil water content equals the initial water content.

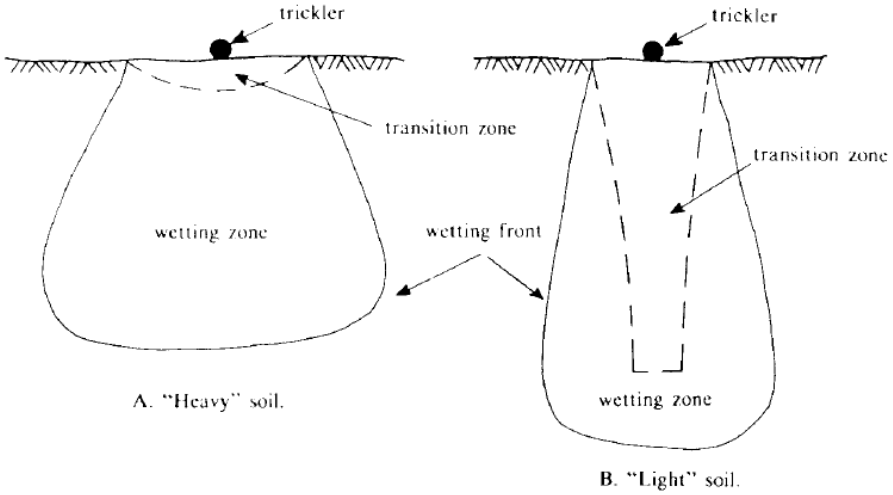

Figure 2.4: Phases of water distribution in the soil profile for two soil types from a point source emitter at a low discharge rate (Benami and Ofen, 1995)
Slika 2.4: Faze distribucije vode v talnem profilu iz točkovnega vira z nizkim pretokom za dva tipa tal (Benami in Ofen, 1995)

As mentioned by Lamm et al. (2007) the monitoring, management and modelling of water distribution in the soil under cropped conditions requires also information on patterns of plants root water uptake. Root water uptake patterns influence water distribution in the soil profile and are essential for obtaining reliable information of water and matric potential distributions within the volume of wetted soil. Root water uptake information is important for drip irrigation design purposes. Irrigation system emitter spacing, application uniformity and discharge rate have to match with the extent of plant root system.

The knowledge acquired on other irrigation systems cannot be directly applied to drip irrigation. Usually, because of the lack of necessary financial resources or time, it is difficult to carry out experiments with all possible drip irrigation design factors and scheduling strategies under specific field conditions to determine the optimal soil wetting. Hence, scientists developed various models to describe water dynamics in the soil which can be used to evaluate a series of possible drip irrigation scheduling strategies. The most promising modelling strategies could be selected and tested under field conditions.

Lubana and Narda (2001) and more recently Subbaiah (2011) presented an extensive review of models of soil water dynamics during drip irrigation. They pointed out that

knowledge gaps still exist in the field of water dynamics in the soil under drip irrigation. Possible improvements on this topic include more fieldwork experiments to supplement modelling progress.

2.3.3 Influence of drip system design and management on soil water distribution

Wang et al. (2006) carried out a research on the effect of drip irrigation frequency on potato growth and wetting patterns dimensions. He used six different drip irrigation scheduling strategies (irrigation once every day (N1), once every two days (N2), once every three days (N3), once every four days (N4), once every six days (N6) and once every eight days (N8)). Equal amount of water was applied for all frequencies studied. The results showed that water distribution, wetted soil depth and distance from the emitter were affected by different irrigation frequencies. Distribution of water varied with the potato growth stage. In the middle of the potato growing season, at the depth greater than 30 cm, decreased irrigation frequency increased water content variations. During the late growth stages the treatment N8 showed larger variation at the depth of 50 – 90 cm in comparison to other treatments. This happened because of longer water application duration, which extended soil wetting pattern in the horizontal direction. Also, more water was depleted at that depth because of denser root system. Higher irrigation frequency caused higher root length density at the soil depth of 0 – 60 cm and the lower root system density at 0 – 10 cm. Results also showed that irrigation frequency reduction (from N1 to N8) resulted in significant yield reduction.

Li et al. (2003) studied the effect of a surface point source emitter Q and volume of applied water on the shape of the wetted area in a loam soil. The emitter discharge rates varied from 0.6 to 7.8 L/h. Results showed that the wetting front moved fast at the beginning and slowed down with increasing time. The saturated wetted radius at the soil surface increased with increase of discharge rate. The wetted radius and depth at the soil surface were proportional to the volume of applied water. Radius of saturated water entry zone become larger as time increased, and after around 3.5 h approached to a constant size. The constant surface saturated wetted radius was reached faster with the higher emitter Q. Higher discharge rate resulted in faster wetting front movement in all directions. Emitter discharge rate increase, after adding the same volume of water, resulted in a wetting pattern increase in the horizontal direction and decrease in the vertical direction. The same results were reported from other studies too (e.g. Khan et al., 1996). Also, the increase in volume of applied water increased the wetting pattern depth and had little effect on wetting pattern horizontal directions. Li et al. (2004) studied the wetting pattern movement in sand and loam soil and concluded that the increase in emitter discharge rate allowed more water to

redistribute in the horizontal direction when the same volume of water is applied. Emitter *Q* decrease caused more water to redistribute in the vertical direction.

Ah Koon et al. (1990) studied the effect of three emitter discharge rates (1, 2 and 3 L/h) on the water distribution and drainage beneath a sugarcane crop compared to fallow plot on clay and silty clay soil. Similar to results of Li et al. (2003, 2004) increase of emitter *Q* increased lateral water spreading.

Also the distribution of water was studied by Bar-Yosef and Sheikholslami (1976). In their research a sand soil was irrigated with a surface drip source. Their results showed that when adding the same amounts of water and increasing the emitter *Q* at the same time, the wetting pattern size in vertical direction increased and decreased in horizontal one.

Mostaghimi et al. (1981) also studied water movement in silty clay loam soil under single emitter source. He carried out a laboratory experiments and showed that emitter discharge rate increase results in a wetting pattern increase in the vertical direction and a decrease in the horizontal direction.

Bresler et al. (1971) examined the surface drip emitter discharge rate effect on the distribution of water content in sandy and loamy soil. He carried out field and laboratory experiments which showed that emitter discharge rate increase caused in larger wetted area in horizontal direction and decreased soil wetted depth. Research done by Levin et al. (1979) for sand soil, confirmed the findings of Bresler et al. (1971).

Acar et al. (2009) investigated the effect of emitter discharge rate and volume of applied water under drip irrigation for loam and clay loam soil. The emitter discharge rates examined were 2 and 4 L/h. Results showed that different discharges did not have significant effect on the size of the wetting pattern. However, different amounts of applied water significantly affected vertical wetted front size, but had no significant effects on later soil water movement within the soil profile and on the soil surface. The results also showed that the wetted volume increased with higher emitter discharge rates affecting both vertical and lateral soil water movement.

Thabet and Zayani (1998) carried out a study with a loamy sand soil to determine the effect of different surface drip emitter discharge rates (1.5 and 4 L/h) on the size of the wetting pattern. They concluded that at the given amount of water applied low water application rates extend the wetting pattern in horizontal direction and high application rates in vertical direction.

Badr and Taalab (2007) concluded that when applying the same amount of water, the higher *Q* causes more water to spread in horizontal direction and while decreasing the discharge rate causes more water to spread in vertical direction. The study was carried out under active root water uptake of tomato plants growing on sandy soil.

2.3.4 Guides for estimating percentage of wetted area

The percentage of wetted area is the average horizontal area wetted within the upper 30 cm of the crop root zone in relation to the total area which is cropped. Many times the question of how many emitters per plant are required arises and this number will depend on the desirable percentage wetted area and the area wetted by one emitter.

Keller and Karmeli (1974) presented a guide for estimating an average percentage of wetted area (Pw). Table 2.2 estimates Pw for coarse (C), medium (M) and fine (F) textured soils for various emitter discharge rates and spacings. The emitter spacings, suggested in the table, should provide a continuous wetted strip of soil with uniform width approximately 30 cm beneath the soil surface. The values presented in the table are valid for predictions of Pw for a single straight lateral, with uniformly spaced emitters, when applying approximately 40 mm of water per irrigation cycle. As already mentioned, the optimum value for Pw is unclear; but, considering the current state of knowledge, Pw for widely spaced crops should be held below 67 %. But for closely spaced crops (crops spaced less than 1.8 m apart) Pw can approach to 100 %.

Keller and Bliesner (1990) presented a Table 2.3 for estimating the wetted area (Aw). The estimation is based on a standard 4 L/h emitter for different soil types and depths. They stated that the Aw, wetted by one emitter at the soil surface, is usually less than half as large as Aw measured at a depth of 15 to 30 cm. They provided the values for different soil texture classes, soil depths and degrees of soil stratification. The values are based on daily or every-other-day irrigations, which apply sufficient volumes of water to slightly exceed the water crops need. Wetted area is approximated by a rectangle; the long dimension, w, is the expected maximum horizontal diameter of the wetted soil volume caused by one emitter. Se is the short dimension and is representing 80 % of maximum expected diameter. Se represents the emitter spacing, which should give a continuous wetted strip of soil. If those two values are multiplied, the result is approximately the same as the circular wetted area. As clearly stated by the authors, these values should be used as guidelines only.

Table 2.2: Percentage of soil wetted by various emitter discharge rates and spacing for emission points in a straight line applying 40 mm of water per cycle (Keller and Karmeli, 1974)
Preglednica 2.2: Odstotek omočenih tal z različnimi pretoki kapljačev in njihovimi medsebojnimi razdaljami za ravno namakalno linijo ob aplikaciji 40 mm vode na cikel (Keller in Karmeli, 1974)

Effective spacing between laterals, m [1] (1.0 m = 3.3. ft	Effective emission point discharge rate [2]														
	Under 1.5 L/h			2 L/h			4 L/h			8 L/h			Over 12 L/h		
	Soil texture and recommended emission point spacing on the lateral [3] – m														
	C	M	F	C	M	F	C	M	F	C	M	F	C	M	F
	0.2	0.5	0.9	0.3	0.7	1.0	0.6	1.0	1.3	1.0	1.3	1.7	1.3	1.6	2.0
	Percentage of soil wetted [4]														
0.8	38	88	100	50	100	100	100	100	100	100	100	100	100	100	100
1.0	33	70	100	40	80	100	80	100	100	100	100	100	100	100	100
1.2	25	58	92	33	67	100	67	100	100	100	100	100	100	100	100
1.5	20	47	73	26	53	80	53	80	100	80	100	100	100	100	100
2.0	15	35	55	20	40	60	40	60	80	60	80	100	80	100	100
2.5	12	28	44	16	32	48	32	48	64	48	64	80	64	80	100
3.0	10	23	37	13	26	40	26	40	53	40	53	67	53	67	80
3.5	9	20	31	11	23	34	23	34	46	34	46	57	46	57	68
4.0	8	18	28	10	20	30	20	30	40	30	40	50	40	50	60
4.5	7	16	24	9	18	26	18	26	36	26	36	44	36	44	53
5.0	6	14	22	8	16	24	16	24	32	24	32	40	32	40	48
6.0	5	12	18	7	14	20	14	20	27	20	27	34	27	34	40

[1] Where double laterals (or laterals with multiple outlet emitters) are used in orchards, enter the table with both the spacing between outlets to either side of the tree row and across the space between the rows and proportion the percentages
[2] Where relatively short pulses of irrigation area applied, the effective emission point discharge rate should be reduced to approximately half of the instantaneous rate for safety t
[3] The texture of the soil is designated by C. course; M, medium; and F, fine. The emission point spacing is equal to approximately 80 percent of the largest diameter of the wetted area of the soil underlying the point. (Closer spacings on the lateral will not affect the percentage area wetted)
[4] The percentage of soil wetted is based on the area of the horizontal section approximately 0.30 m (1.0 ft) beneath the soil surface. Caution should be exercised where less than 1/3 of the soil volume will be wetted.

Table 2.3: Estimated wetted area by 4 L/h drip emitter operating under various field conditions (Keller and Bliesner, 1990)
Preglednica 2.3: Ocenjena omočena površina s kapljačem s pretokom 4 L/h v različnih terenskih pogojih (Keller in Blesner, 1990)

Soil or root depth and soil structure	Degree of soil stratification and equivalent wetted soil area (m×m)		
	Homogeneous (Se×w)	Stratified (Se×w)	Layered (Se×w)
Depth 0,75 m			
Coarse[1]	0.4 × 0.5	0.6 × 0.8	0.9 × 1.1
Medium	0.7 × 0.9	1.0 × 1.2	1.2 × 1.5
Fine	0.9 × 1.1	1.2 × 1.5	1.5 × 1.8
Depth 1,5 m			
Coarse	0.6 × 0.8	1.1 × 1.4	1.4 × 1.8
Medium	1.0 × 1.2	1.7 × 2.1	2.2 × 2.7
Fine	1.2 × 1.5	1.6 × 2.0	2.0 × 2.4

[1] Coarse includes coarse to medium sands; medium includes loamy sands to loams; fine includes sandy clay to loam to clays.

2.4 MODELLING OF WATER INFILTRATION FROM POINT SOURCE

For prediction of water flow in the soil or for prediction of wetting patterns dimensions from a water point source, a number of models exist. Modelling approaches vary from relatively simple to more complex codes. We can group them in empirical, analytical or numerical models.

2.4.1 Richards' equation based models

Richards' equation is the governing equation for water movement in unsaturated soils. This equation is described in more detail in the Materials and methods section. The methods that solve Richards' equation (Richards, 1931) can be analytical, semi-analytical and numerical methods (Subbiah, 2011).

2.4.2 Analytical models

Analytical models for prediction of water flow usually solve the governing water flow equation under specific conditions. Because Richards's equation is highly nonlinear it can be analytically solved only in a limited number of cases. Therefore analytical models rely on assumptions, such as soil homogeneity and simple geometries of transport domain, simplified initial soil water conditions and homogeneous and simplified soil hydraulic properties (Ravi and Williams, 1998, Šimůnek and van Genuchten, 2006; Subbiah, 2011). For this purposes, Richards' equation has to be linearized, which involves use of mathematical transformations (i.e. Kirchhoff integral transformation is commonly used in water flow modelling) (Šimůnek, 2005). However, despite some simplifying assumptions, analytical models have some advantages as direct relationship between input and output parameters, simplicity of use and predictive capabilities (Dashberg and Or, 1999). Analytical solutions can be further separated in steady-state solutions, quasi-linear approximation solutions and transient infiltration solutions (Ravi and Williams, 1998). Analytical solutions for complex problems (e.g. transient water flow) cannot be derived and are therefore not available and in that case the numerical models have to be used. The extensive review and more detailed discussion of various analytical models is given by Subbiah (2011) and Ravi and Williams (1998). Only selected models are discussed below.
Analytical solutions have been derived for steady infiltration from a buried point source and from cavities (Philip, 1968, 1984), from a surface point (Warrick, 1974) and from shallow circular ponds (Wooding, 1968). More recently Cook et al. (2003) presented a user friendly Microsoft Windows based programme WetUp. The programme provides visualisation of the wetting patterns (Figure 2.5) and estimates their dimensions. Different soil hydraulic characteristics and soil textures can be used for surface or subsurface point

sources. WetUp contains a database of predefined soil types, emitter flow rates (from 0.503 to 2.7 L/h), different water application times (1 – 24 h), different soil water initial conditions (3, 6 and 10 m of suction) and drip emitter positions.

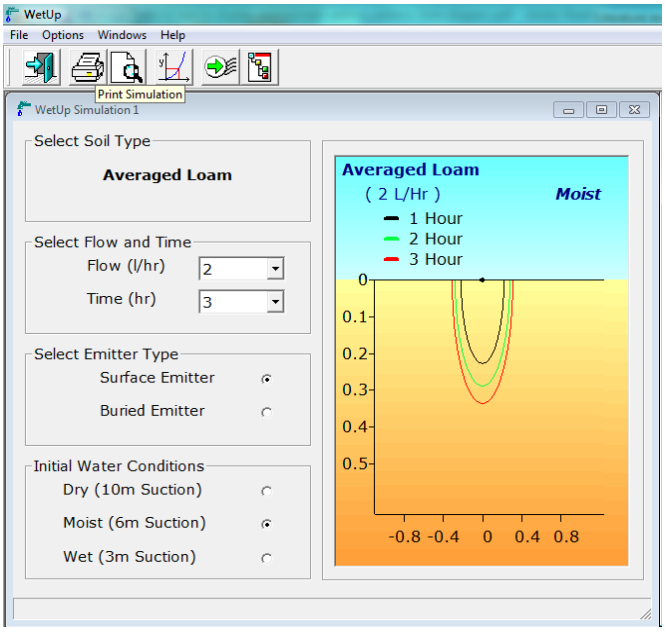

Figure 2.5: WetUp window programme showing wetting pattern under surface drip irrigation for averaged loamy soil, at emitter discharge rate of 2 L/h, 3 h of water application and initial soil water content of 6 m suction

Slika 2.5: Okno programa WetUp, ki prikazuje vzorec omočenosti pod površinskim kapljičnim namakalnim sistemom za povprečna ilovnata tla, s pretokom kapljača 2 L/h, 3 h namakanja ter začetno vsebnostjo vode v tleh pri 6 m sukcije.

WetUp uses Philip's (1984) analytical solution for water flow from surface and subsurface source. The solution is based on a quasi-linear analysis and determines the travel time of water.

2.4.3 Semi-analytical models

Semi-analytical models can solve the mathematical problem using analytical and partly numerical approach. Semi-analytical methods are, when compared to pure analytical ones, applicable to a wider range of problems which still have to be simple (Subbiah, 2011). Mmolawa and Or (2000) presented a semi-analytical model for calculating water flow and solute transport with and without plant uptake for surface or subsurface drip irrigation.

2.4.4 Numerical models

With the increasing power of computers and advances in development of more accurate and stable numerical solutions, numerical models have become widely used in recent years. Numerical methods are able to solve practical problems (as water flow under drip irrigation) and allowing users to control various parameters in time and space, design complicated geometries which are close to natural hydrologic conditions and to determine and regulate more realistic boundary and initial conditions. A number of numerical algorithms have been proposed in recent years to solve Richards' equation. Those numerical algorithms can solve variably saturated flow problems. They usually subdivide the spatial and time coordinates into small discrete elements, such as finite elements, finite difference or finite volumes and reformulate the continuous form of partial governing differential equations. Finite difference methods are today mainly used in one-dimensional models. Finite elements and finite volume methods are usually used in three and two-dimensional models. A brief review of the history of development of various numerical models used in vadose zone models are presented by Šimůnek (2005) and Subbaiah (2011).

Brandt et al. (1971) developed a finite difference model to analyse multidimensional transient infiltration from a drip source. Their model was widely used for simulations of various field and laboratory experiments (Subbaiah, 2011). Bresler et al. (1971) compared their model, with experimental data for two soils and found a good agreement. They concluded that, despite some discrepancies, between the experimental and theoretical results which occurred at high emitter Q, the agreement is good enough for the practical implementation of the model. Levin et al. (1979) used the same model to compare it to experimental data.

Bresler (1975) presented a numerical model for multidimensional simultaneous transfer of a non-interacting water and solute transport. He found quite good agreement between measured and predicted soil water content. The model was applicable to the infiltration from a drip source. Mostaghimi et al. (1981) studied water movement under single emitter source in silty clay loam soil. They also used the model of Bresler (1975) and compared it to experimental results. The results showed that increasing the emitter discharge rate Q results in an increase in the wetted zone in the vertical direction and a decrease in the horizontal direction. Those results are in contradication with the results of Bar-Yosef and Sheikholslami (1976), Khan et al. (1996) and Li et al. (2003).

Lafolie et al. (1989) presented the numerical solution for water content distribution predictions under drip irrigation for Cartesian and axicylindrical flow geometries. The

model can be used for solving saturated and unsaturated water flow problems in stratified soils.

Elmaloglou and Diamantopoulos (2010) used a cylindrical flow model which incorporates evaporation and root water uptake (Figure 2.6). Alternating direction implicit finite difference method was used to solve mathematical model which describes the axisymmetric infiltration from surface point source.

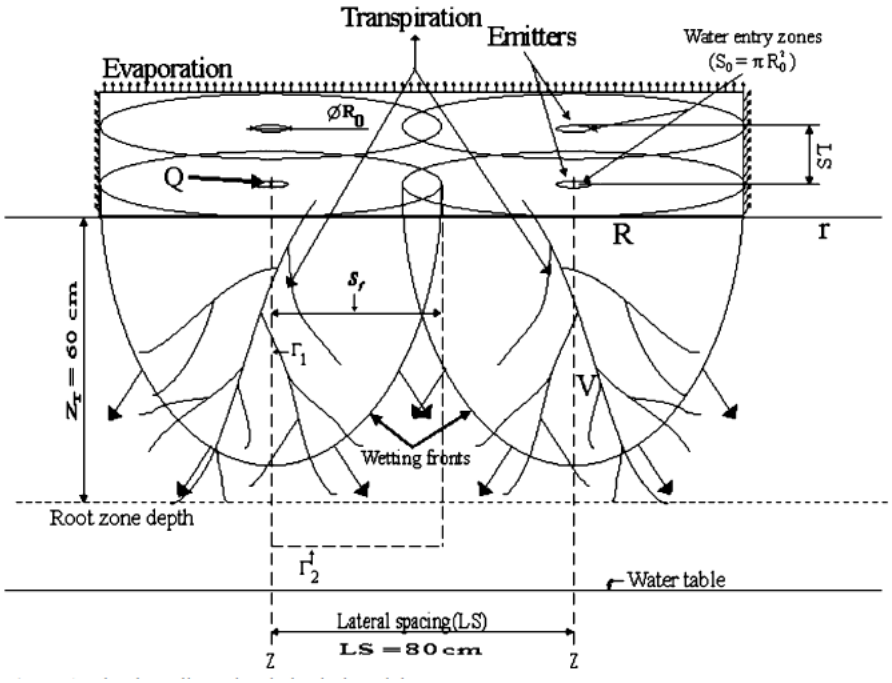

Figure 2.6: Cylindrical flow model as presented by Elamaloglou and Malamos (2007)
Slika 2.6: Model cilindričnega pretoka po Elamaloglouu in Malamosu (2007)

They studied the effects of emitter *Q*, irrigation duration and inter-emitter distances on the size of the wetting front and deep percolation were also investigated. The mathematical model was applied to loamy sand and silt soil types. Two emitter *Q*, two irrigation depths and two spaces between the emitters were investigated. The results of numerical experiments show that when the same irrigation depth, the same dripper spacing and the same soil type are used, a smaller emitter discharge rate (when compared to a higher one) results in a larger wetted zone in the vertical direction. Wetted zones overlapped faster in the fine-grained soils and deep percolation was lower in the fine-grained soil compared to the coarse-grained soils. The results also showed that deep percolation increased with increasing irrigation depth.

Šimůnek et al. (1996) developed a software package, Hydrus-2D, which was in 2006 updated to provide three dimensions, now called Hydrus-2D/3D (Šimůnek et al., 2006). Hydrus-2D is an update of SWMS-2D (Šimůnek et al., 1994) and Chain-2D (Šimůnek and van Genucten, 1994). Hydrus software enables implementation of three-dimensional water flow, heat, multiple solute transport and root–water and nutrient uptake based on numerical solutions of finite-elements for the transport and flow equations. For the variably saturated flow module the program numerically solves Richards' equation (Richards, 1931). The flow equation incorporates a sink term to simulate plant water root uptake. The main unit of the programme is the graphical user interface (GUI) which defines the overall computational environment of the Hydrus (Figure 2.7). In 2011 a Hydrus-2D/3D version 2.0 was released which included many new features compared to version 1.0. New features, which can be used for different drip irrigation design and management simulations include new special boundary conditions options (i.e. surface – with dynamic wetting pattern and subsurface drip irrigation - with a drip characteristic function reducing irrigation flux based on the back pressure) and triggered irrigation (irrigation can be triggered by Hydrus when the pressure head drops below a specific value) (Šejna et al. 2011).

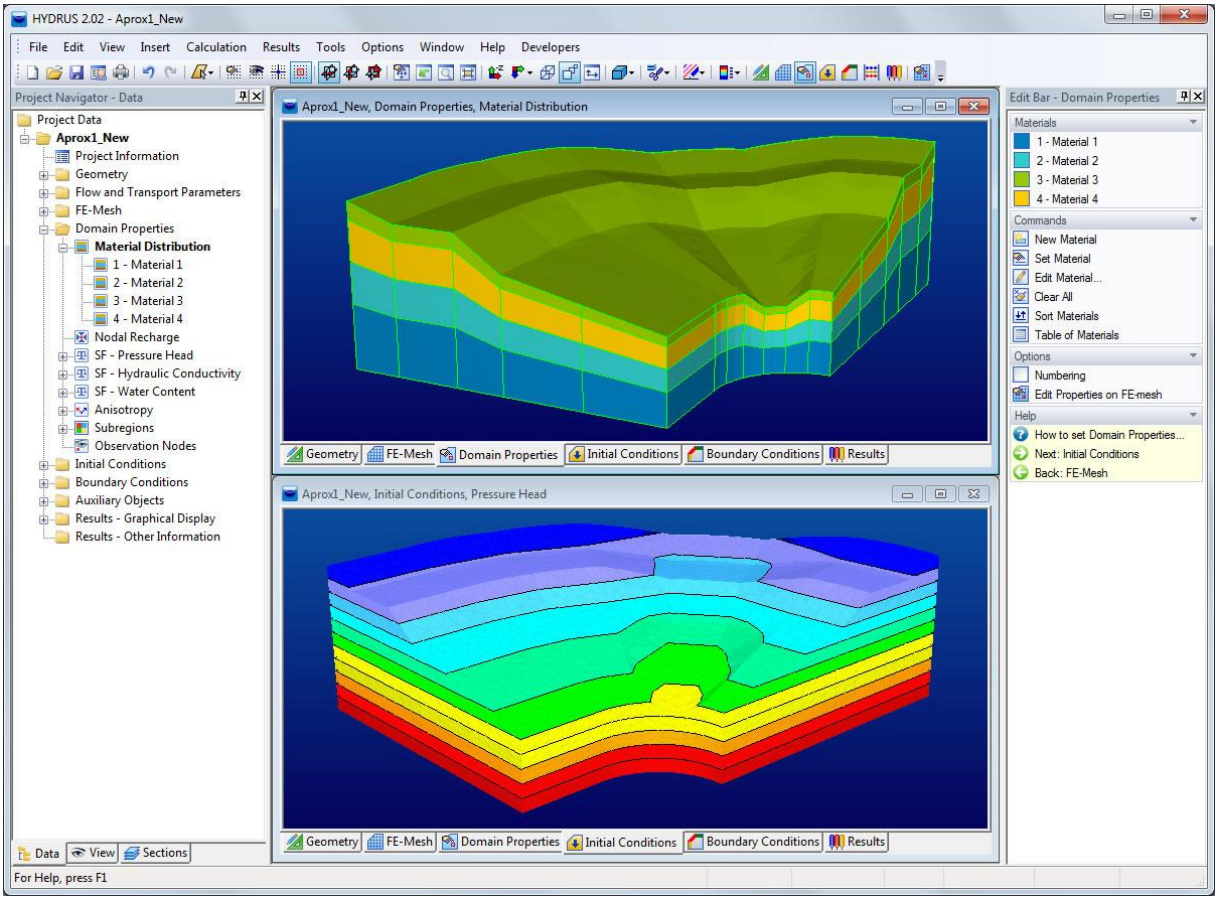

Figure 2.7: Hydrus graphical user interface, including its main components
Slika 2.7: Grafični vmesnik programa Hydrus ter njegove glavne komponente

The performance of Hydrus-2D/3D to simulate water movement from microirrigation systems has been in recent years assessed by many researchers. For example Assouline, 2002; Schmitz et al., 2002; Cote et al., 2003; Skaggs et al., 2004; Lazarovitch et al., 2005, 2007; Fernandez-Galvez and Simmonds, 2006; Dahiya et al., 2007; Provenzano, 2007; Patel and Rajput, 2008; Elmaloglou and Diamantopolus, 2009; Kandelous and Šimůnek, 2010a, 2010b; Rodriguez-Sinobas et al., 2010; Skaggs et al., 2010; Bufon et al., 2011; Kandelous et al., 2011; Phogat et al., 2011. In the majority of these studies a subsurface drip irrigation (SDI) process as a line source (a lateral) was analysed (Ben-Gal et al., 2004; Skaggs et al., 2004; Patel, 2008; Bufon et al., 2011; Kandelous et al., 2011; Wang et al., 2013). In some other studies SDI was simulated by means of a point source (Lazarovitch et al., 2005; Provenzano, 2007; Kandelous and Šimůnek, 2010a, 2010b). Some authors assessed the ability of Hydrus to simulate water dynamics under surface drip systems (Assouline, 2002; Gardenas et al. 2005; Dabach et al., 2011; Phogat et al., 2011, 2013; Shan and Wang, 2012; Kanzari, 2013). But because of the lack of appropriate surface boundary conditions in Hydrus the number of such studies has been limited. This problem was resolved in 2011 by the introduction of Hydrus version 2.0.

Assouline (2002) numerically and experimentally investigated the effect of different emitter discharge rates on water distribution under surface drip irrigated corn. Three emitter discharge rates (0.25, 2.0 and 8 L/h) were compared (Figure 2.8). Field experiments showed that emitter discharge rate of 0.25 L/h produced highest relative water content in the upper 30 cm and the lowest in the 60 to 90 cm layer of the soil profile. Numerical simulations, using Hydrus-2D, showed that under discharge of 0.25 L/h wetted volume of soil was smallest in all directions. The water content gradients for 0.25 L/h treatment were also less extreme in both directions, compared to 2.0 and 8.0 L/h discharges. The saturated zone beneath the emitter was obtained only with 8.0 L/h dripline. The wetting front depth was shallowest under 0.25 L/h irrigation treatment.

Kandelous and Šimůnek (2010a) compared numerical, empirical and analytical models to estimate wetting patterns extend for surface and subsurface drip irrigation. The accuracy of several popular approaches used to estimate wetting zone size was evaluated by comparing their predictions with laboratory and field data. These approaches included the numerical Hydrus-2D model, selected empirical models (Schwarzman and Zur, 1986; Amin and Ekhmaj, 2006; Kandelous et al., 2008) and the analytical WetUp (Cook et al. 2003). The mean absolute error was used to compare the model predicted and observed values of wetting zone dimensions. Results showed that mean absolute error varied from 0.9 to 10.4 cm for Hydrus, from 1.3 to 12.2 cm for empirical models and from 1 to 58.1 cm for WetUp software.

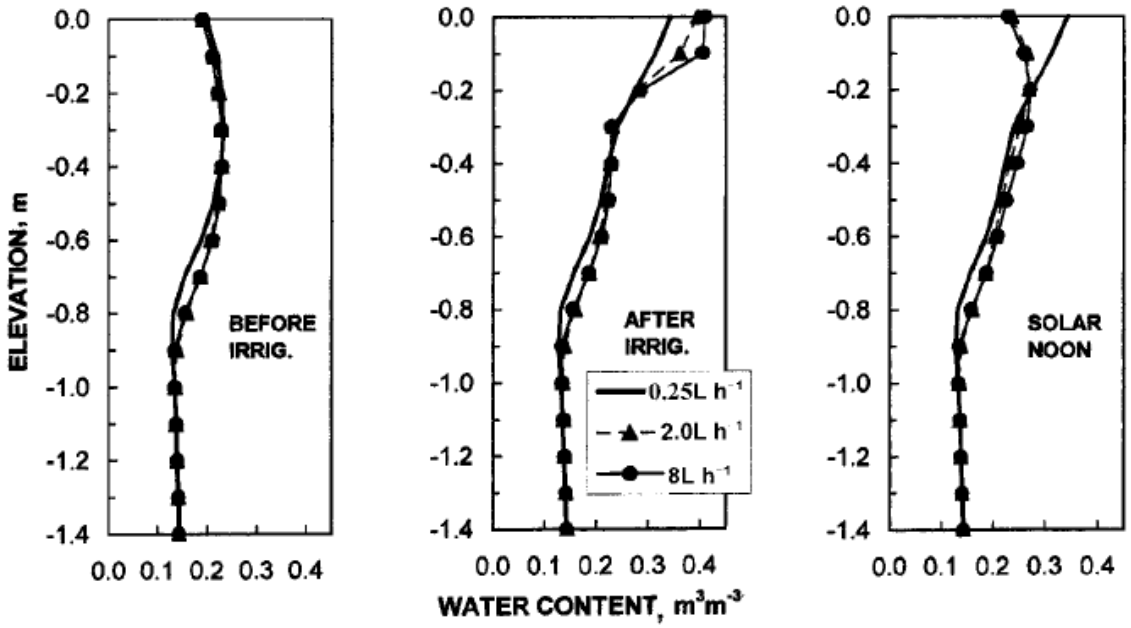

Figure 2.8: Simulations of water content distribution for three emitter discharge rates, 0.10 m from the emitter, before and after irrigation and at solar noon (Assouline, 2002)
Slika 2.8: Simulacije distribucije vode v tleh za tri petoke kapljačev v oddaljenosti 0,10 m od kapljača, pred in po namakanju, ob poldnevu (Assouline, 2002)

Dabach et al. (2011) investigated the accuracy of Hydrus-2D/3D simulations of water movement and root water uptake under surface drip irrigation on two soils (loamy sand and sandy loam). The effect of different transpiration rates and management strategies of triggered irrigation were investigated. The new system-dependent boundary condition, which is now included in Hydrus-2D/3D version 2.0) which triggers irrigation when the matric potential head at selected point drop below a certain threshold, was used in his study. The results showed that Hydrus simulated matric heads at selected positions were in good agreement with experimental results (Figure 2.9) which suggests that Hydrus can be used for investigating different irrigation management strategies. Results also showed that Hydrus can be used for irrigation threshold optimisation and optimisation of amount of water applied in irrigation cycle which helps to increase water use efficiency.

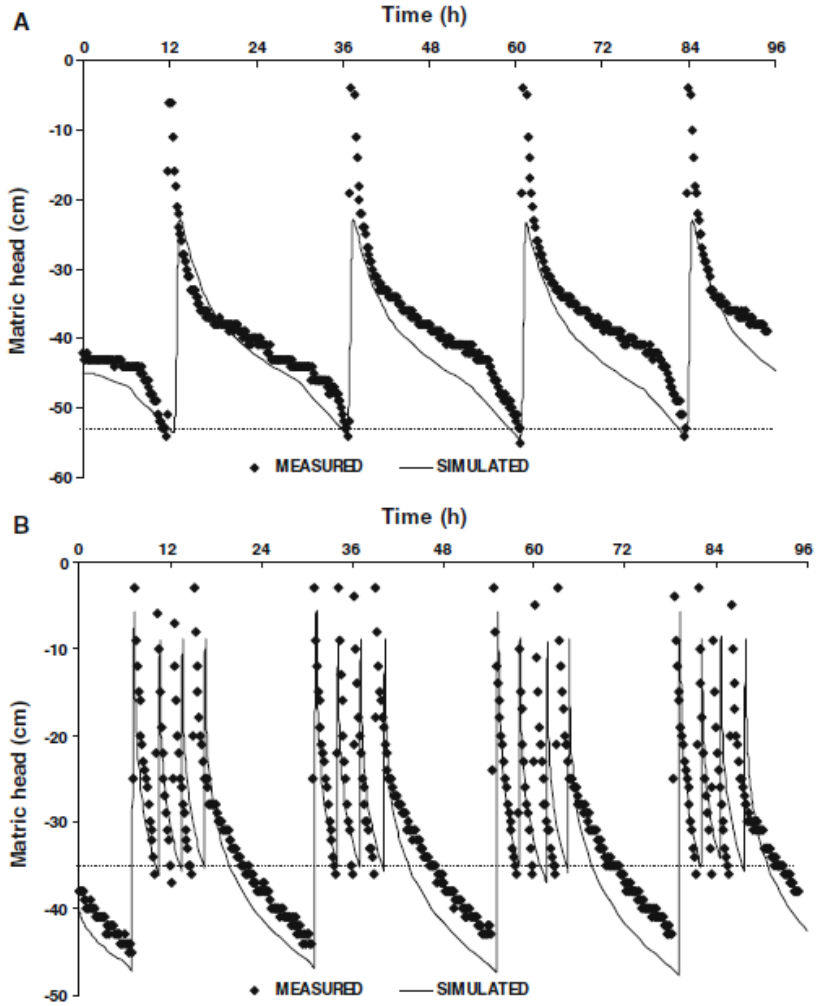

Figure 2.9: Simulated and measured matric heads during 96 hours of experiments. The potential transpiration rate was set to 3.5 mm/day with irrigation amounts varying from 4 mm (A) to 1 mm (B). Dotted line represents irrigation threshold (Dabach et al. 2011)
Slika 2.9: Simulirani in izmerjeni matrični potencial med 96-urnim eksperimentom. Potencialna transpiracija je bila določena pri 3,5 mm/dan z namakalnimi obroki, ki so variirali od 4 mm (A) do 1 mm (B). Pikčasta črta predstavlja prag namakanja (Dabach in sod., 2011).

Gardenas et al. (2004) used a three-dimensional axisymmetrical modelling approach incorporating root water uptake to examine the influence of soil type and fertigation strategy on nitrate leaching potential for four different microirrigation systems. In his study the Hydrus code was modified to include a new special boundary condition which allowed simulation of surface drip irrigation (Figure 2.10) with dynamic wetting (this boundary has been later included in Hydrus-2D/3D version 2.0 in 2011).

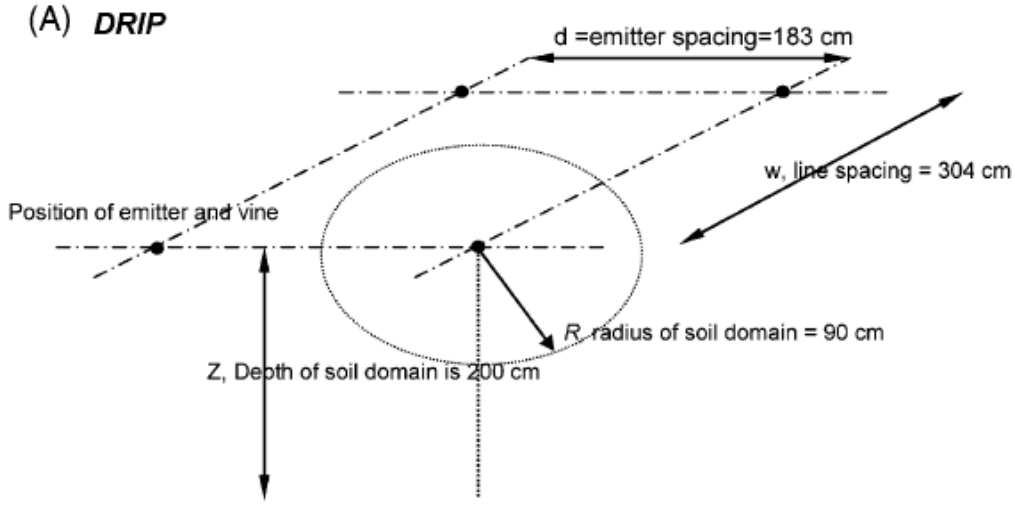

Figure 2.10: Layout for surface drip irrigation for grapes (Gardenas et al., 2004)
Slika 2.10: Postavitev površinskega kapljičnega namakanja za grozdje (Gardenas in sod., 2004)

Phogat et al. (2011) experimentally verified HYDRUS-2D model for water and salinity distribution during the stage of soil profile establishment of almond trees under pulsed and continuous surface drip irrigation. The simulated water content values obtained at different lateral distances from a dripper, different soil depths and different times, were compared with values obtained with neutron probe. The model closely predicted water content distribution at all distances, times and soil depths with Root mean square error (RMSE) values ranged between 0.017 and 0.049. Therefore it was concluded that HYDRUS-2D can successfully simulate the dynamics in soil water content change and soil water salinity. Results showed that he influence of water pulsing on water content in the soil, drainage flux and salinity distribution vanished completely when irrigation was applied daily on the basis of crop evapotranspiration (ETc) with a suitable leaching fraction. Research also showed that initial soil water content and irrigation duration or scheduling of water application represent a significant role in the design of surface drip irrigation systems for light textured soils.

Phogat et al. (2013) used HYDRUS-2D to simulate field data recorded for a surface drip irrigated almond trees. Hydrus was used to evaluate the daily changes in water content under full pulsed, sustained deficit pulsed and full continuous drip irrigation. Influence of pulsing water on the dynamics of the water distribution was also assessed. In the sustained deficit pulsed treatment, 65 % of calculated crop ETc needs were replaced, compared to replacement of 100 % ETc in other two treatments. Results showed that irrigation water productivity under sustained deficit irrigation compared to full irrigation, increased for 37 % and around 35 % of irrigation water was saved. On the other hand almond yield was reduced by 8 %.They concluded that in regions with severe water scarcity, sustained deficit

pulsed irrigation method for almond cultivation appears to be a promising strategy of deficit irrigation. Almonds irrigated above the sustained deficit pulsed level may enhance unproductive water usage.

Cote et al. (2003) used Hydrus-2D model to investigate the effect of pulsed water applications on the wetting pattern size for the for subsurface drip irrigation for three soil types (sand, silty and silty clay loam). Research showed that irrigation frequency caused slight increase of wetting pattern dimensions in coarse textured soils. They found that the geometry of wetting pattern is strongly influenced by soil hydraulic properties. Also, similarly to Skaggs et al. (2010) results, high emitter *Q* tend to increase wetting pattern more in vertical than in horizontal direction. The research highlighted that the drip irrigation system discharge rate has to be matched with particular soil type or its hydraulic properties.

Hydrus-2D/3D was used to analyse field data in study of Kandelous et al. (2011). Different modelling approaches were assumed in which SDI emitters were represented as a point source (in axisymmetrical two-dimensional domain), a line source (in planar two-dimensional domain) or a point source (in a fully three-dimensional domain). Results showed, that SDI systems can be entirely described using only a fully three-dimensional model. Use of an axisymmetrical two-dimensional domain can accurately describe the SDI only before wetting patterns start to overlap, and a planar two-dimensional domain, only after full merging of the wetting fronts from neighbouring emitters occurs.

Skaggs et al. (2010) used field trials and Hydrus-2D numerical simulations to investigate the effect of application rate, pulsed water application and antecedent water content on the water spreading from drip irrigation emitters located 5 cm below the soil surface. Results showed that water spreading from drip irrigation systems is higher with increase of antecedent water content. The increase is bigger in a vertical than a horizontal direction. Only minor increases in horizontal spreading of water were produced with lower water application rates and pulsed water application. Overall, they found out that pulsing and emitter *Q* have very little effect on the soil water distribution. On the other hand, soil hydraulic properties and antecedent water content largely determine the soil water distribution at a given water application rate.

Provenzano (2007) studied wetted soil volume formed under subsurface drip irrigation in sandy loam soil. Hydrus-2D was verified on the basis of experimental results. The subsurface single dripper was presented with 2D axisymmetrical domain. He presented the dimensions of wetted soil volume as a function of irrigation duration, soil water initial conditions and emitter *Q* (Figure 2.11). The comparison between measured and predicted

soil matric potentials showed a reasonably good agreement, indicating that the model can used as a tool to design and managing SDI systems. Research also showed that for fixed initial water content, wetting pattern dimensions increase with increasing irrigation duration and for a fixed irrigation duration, greater is the initial water content higher the correspondent wetting pattern dimensions.

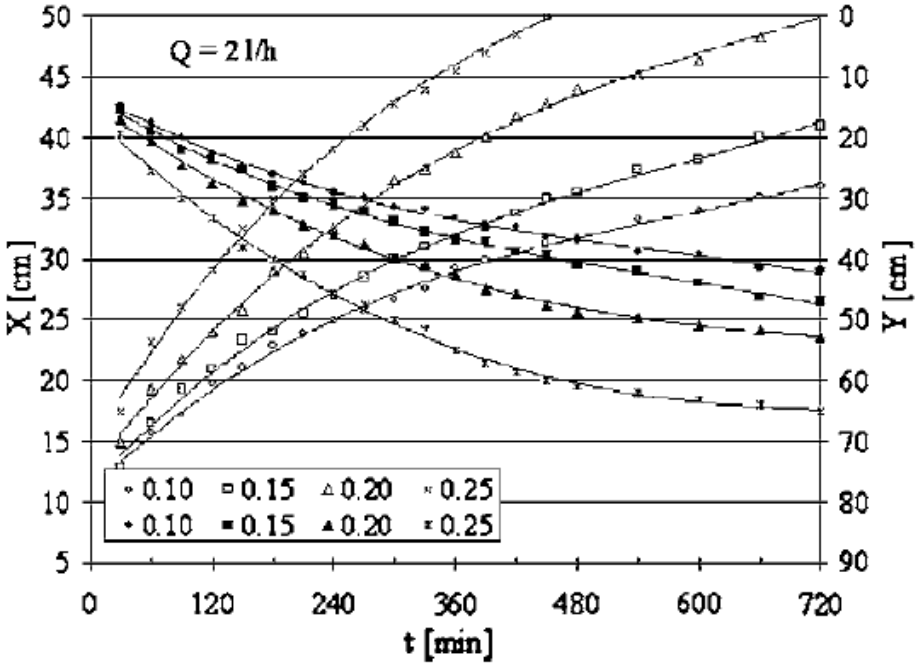

Figure 2.11: Dimensions of the wetted soil volume for horizontal (X) and vertical (Y) direction, as a function of flow rate (*Q*) of 2 L/h, initial soil water conditions varying from 0.10 cm^3/ cm^3 to 0.25 cm^3/ cm^3 and irrigation duration (min) (Provenzano, 2007)
Slika 2.11: Dimenzije omočenega volumna tal v horizontalno (X) in vertikalno (Y) smer, kot funkcija pretoka kapljača (*Q*) pri 2 L/h, začetne vsebnosti vode v tleh (od 0,10 cm^3/ cm^3 do 0,25 cm^3/ cm^3) in trajanjem namakanja (min.) (Provenzano, 2007)

Shan and Wang (2012) assessed the accuracy of Hydrus-3D to simulate the salinity distribution in the overlap zone caused by double point source surface drip emitters in sandy soil. Hydrus predictions were also in good agreement with observed data.

Mmolawa and Or (2003) used the numerical model (Hydrus-2D) and analytical model that uses a local volume balance approach (Warrick, 1974) to compare soil water dynamics under the point source with and without plant root water uptake. When the plants root water uptake was not considered, dynamics of water content by the analytical model was in good agreement with Hydrus-2D model simulations. When considering plant root water uptake the analytical model, when compared to Hydrus-2D simulations, overestimated root water uptake at some locations.

Above only a small part of Hydrus modelling applications like drip irrigation, is presented. There are many more Hydrus applications published, showing that such numerical models play an important role in vadose zone research. In addition, HYDRUS (PC Progress) website lists over one thousand references, in which HYDRUS has been used. Also, the frequency of downloading the programme from the HYDRUS website is reflecting the need for codes such as Hydrus. For example, in 2012, HYDRUS-1D was downloaded more than 10,000 times by users from around 50 different countries. The HYDRUS web site daily receives on average around 700 individual visitors. (Šimůnek, 2013).

2.4.5 Empirical models

Empirical models for determining the geometry of wetting patterns have been developed based on field observations, regression analysis, dimensional analysis or Artificial Neural Networks. They usually require only simple intake parameters, such as infiltration rate, saturated hydraulic conductivity, volume of applied water, soil porosity, saturated water content and other simple soil properties. Empirical models can be according to Dasberg and Or (1999) used when information about soil hydraulic properties, which are required for numerical or analytical predictions, are not available, or when simplicity of mathematical model is of primary importance.

An extensive review on older empirical models is given by Lubana and Narda (2001) and Subbaiah (2011). Below only more recent or the most popular simple empirical models are presented.

Schwartzman and Zur (1986) developed a well-known semi-empirical model (Equations 1 and 2) for determining the width, X, and the depth, Y, of the wetted soil volume under a surface point source.

$$X = 1.82\, V^{0.22} \left(\frac{Ks}{Q}\right)^{-0.17} \quad \text{... (1)}$$

$$Y = 2.54\, V^{0.63} \left(\frac{Ks}{Q}\right)^{0.45} \quad \text{... (2)}$$

Wetted soil volume was assumed to depend on the hydraulic conductivity of the soil (*Ks*), on emitter discharge rate (*Q*) and on the total amount of water in the soil (*V*). Using dimensional analysis, analytical expressions for wetted depth and width were obtained as functions of the above parameters. The equations coefficients were then obtained empirically based on experiments carried out on two types of soils (Gilat loam and Sinai sand). This model is one of the most practical for determination of soil wetted geometry

from point sources. However, using the model for a wide range of conditions is questionable because it was calibrated only on two sets of experimental data, with only two soil types and two emitter discharge rates. The model of Schwartzman and Zur (1986) is presented in more details in materials and methods chapter (Section 3.5.1).

Healy and Warrick (1988) presented a method for estimating the time-variant extent of the wetting front that develops in the soil in response to water infiltrating from a surface point source. The method was based on numerical finite-difference solution of a dimensionless form of Richards' equation. The generalised solutions were obtained from empirical equations. The coefficients for these equations were tabulated for a variety of soil types and volumetric inflow rates by the same authors. Despite some assumptions (homogeneous soil, uniform initial soil water conditions, no evapotranspiration) the generalised empirical model presented, provided good results when compared with experimental data.

Amin and Ekhmaj (2006) presented an empirical model (Equations 3 and 4) for estimating surface wetted radius, X, and vertical distance (depth), Y, of the wetting pattern front from the surface drip emitter:

$$X = \Delta\theta^{-0.5626} V^{0.2686} Q^{-0.0028} Ks^{-0.0344} \quad \text{... (3)}$$

$$Y = \Delta\theta^{-0.383} V^{0.365} Q^{-0.101} Ks^{0.195} \quad \text{... (4)}$$

Their model assumes that the wetting pattern dimensions are a function of average change of volumetric water content within the wetted zone, $\Delta\theta$, total volume of water applied, *V*, application rate, *Q*, and saturated hydraulic conductivity, *Ks*. Their approach is empirical as they modified the Schwartzman and Zur (1986) model by adding the average change in volumetric water content as one of the parameters in their equation and used published experimental data from Taghavi et al. (1984), Anglelakis et al. (1993), Hammami et al. (2002), and Li et al. (2003) to determine the equation coefficients using nonlinear regression. They concluded, based on these experiments which included sand, loamy sand, loam, silty clay and sandy loam soils, that the soil type, volume of applied water and emitter *Q* were the most important factors that affected the wetted zone width and depth.

More recently Malek and Peters (2011) presented a new empirical formula (Equations 5 and 6), of the same type as that of Amin and Ekhmaj (2006), for prediction of soil wetted dimensions around the surface drip emitter. The coefficients were obtained by using regression analysis on the results of field experiments done in Iran. Based on those results, the models of Schwartzman and Zur (1986), Amin and Ekhmaj (2006) and analytical model WetUp (presented above) were also evaluated. The best results were obtained with

the newly proposed model. They demonstrated that the suggested equations can be used for a wide range of soils and emitter discharge rates.

$$X = Q^{0.543}\, Ks^{0.772}\, t^{0.419}\, \Delta\theta^{-0.687}\, \rho_b^{0.305} \quad \ldots (5)$$

$$Y = Q^{0.398}\, Ks^{0.208}\, t^{0.476}\, \Delta\theta^{-1.253}\, \rho_b^{0.445} \quad \ldots (6)$$

Wetted widths (X) and depths (Y) depend on discharge rate (Q), hydraulic conductivity (Ks), average volumetric water content during irrigation ($\Delta\theta$), soil bulk density (ρ_b) and irrigation duration (t).

Ainechee et al. (1999) used Schwartzman and Zur (1986) model and obtained good agreement between observed and simulated values for sand, loam and silty clay loam soils. Kandelous and Šimůnek (2010a) compared the two empirical models of Schwartzman and Zur (1986) and Amin and Ekhmaj (2006) against field data, to evaluate their accuracy in predicting wetted zone dimensions. Results showed better prediction capability of the Amin and Ekhmaj (2006) model in comparison with the Schwartzman and Zur (1986) model. In some cases the Amin and Ekhmaj (2006) model predicted wetting pattern geometry even better than numerical models results. The better predictive capability of the Amin and Ekhmaj (2006) model can be explained by its use of $\Delta\theta$. Kandelous and Šimůnek (2010a) concluded that soil water content plays an important role when predicting wetted geometry for surface drip irrigation systems.

Importance of the roots function in soil water transport is becoming increasingly acknowledged as pressure is imposed on agricultural resources because of the environmental and water limitation concerns. According to Dasberg and Or (1999) modelling and monitoring of soil water distribution for management of drip irrigation systems, under cropped conditions requires information on plants root water uptake patterns. Root water uptake patterns influence water distribution and are thus essential for obtaining reliable information of water distribution within the wetted soil volume. Information about root water uptake is important for drip irrigation design purposes and as mentioned before, to match water application uniformity, emitter spacing and discharge rate with the plant root system extent.

According to Subbaiah (2011) and Vrugt et al. (2001) the root water uptake depends mainly on the soil physical properties, such as hydraulic conductivity and water retention, root density distribution (root system architecture) and the absorption capability of roots.
Today there are two major approaches used for the simulation of root water uptake. They differ in the way they predict the sink term of Richards' equation. The first approach is

microscopic or mesoscopic or bottom-up approach which considers a single root to be equivalent to infinitely long cylinder of uniform radius with water absorbing properties (Gardner, 1960). The steady state water flow in the soil is solved analytically assuming radial flow and imposed root water uptake rates. Distributions of soil water matric heads around the idealized roots are then calculated. This concept was presented by Gardner (1960) and later extended in Gardner (1964, 1965). The microscopic approach proved to be very insightful, but impractical also, since it requires detailed data about root geometry and soil heterogeneity that is generally not available, is difficult to measure or very computational and time demanding (Vrugt et al., 2001; Šimůnek and Hopmans, 2008).

The second approach, generally used by most vadose zone models, is a so called macroscopic approach. This approach predicts root water uptake based on distribution of potential transpiration over the root zone proportionally to root density and is locally reduced based on soil water content and salinity status. In the macroscopic approach, a sink term, representing water extraction by plant roots is included in the dynamic water flow equation, allowing spatially and temporally variable uptake as controlled by soil water and plant demand.

This approach combines the root water uptake processes which can then be represented as a single term (sink term) that can be added to the governing mass balance equations (Šimůnek and Hopmans, 2008; Feddes and Raats, 2004). In Hydrus-2D/3D the sink term represents the volume of water removed per unit time from a unit volume of soil. It uses a complex function suggested by Feddes et al. (1978) or an S-shaped function suggested by van Genuchten (1987) (Šimůnek et al., 2011). Various other terms have also been suggested, like Molz (1981), Jarvis (1989) and Vrugt et al. (2001).

Feddes et al. (1978) modelled root water uptake as a function of soil water pressure head (h) (Equation 7):

$$S(h) = \alpha(h) S_p \quad \text{... (7)}$$

where $S(h)$ is the root water uptake or volume of water removed from a unit volume of soil per unit time (T^{-1}), S_p is the potential water uptake rate (T^{-1}) and $\alpha(h)$ is a dimensionless stress response function of the pressure head ($0 \leq \alpha \leq 1$). The stress response function is shown on the Figure 2.12.

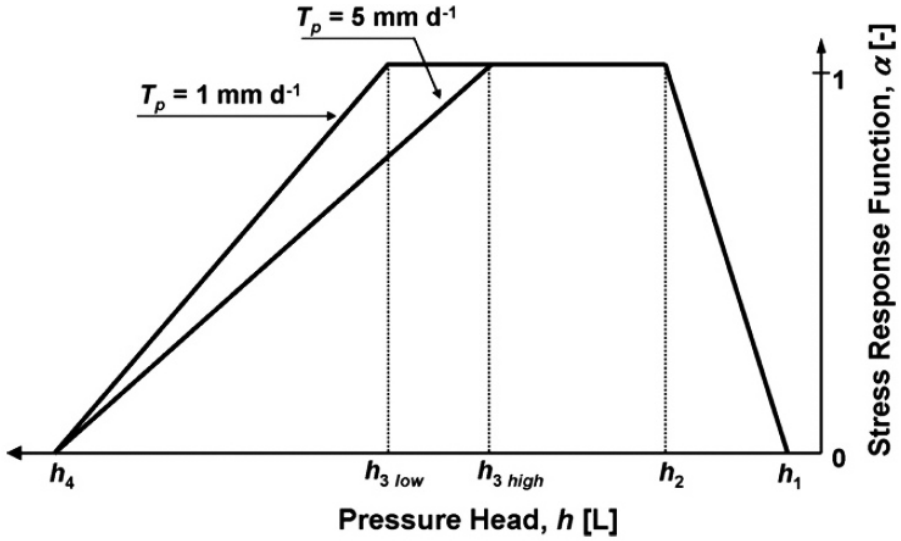

Figure 2.12: Plant water stress response function α(h) as used by Feddes et al. (1978)
Slika 2.12: Funkcija stresnega odziva rastlin za vodo α(h) kot jo je predstavil Feddes in sod., 1978.

Root water uptake is assumed to be zero close to soil water saturation point due to lack of the oxygen in the root zone - h_1. h_4 is the value of the pressure head below which root water uptake ceases (usually taken at the wilting point), h_2 represents the value of the pressure head below which roots extract water at the maximum possible rate, $h_{3\ high}$ presents a value of the limiting pressure head below which roots can no longer extract water at the maximum rate (assuming a potential transpiration rate of *TH*). T_p is the potential transpiration rate (in Hydrus set at default at 0.5 cm/day (*TH*) and 0.1 cm/day (*TL*)). $h_{3\ low}$ is the same as $h_{3\ high}$ but for a potential transpiration rate of *TL*, In Hydrus. Root water uptake is optimal between pressure heads of h_2 *and* h_3.

As long as the soil is wet and the pressure head is larger than h_3, the actual uptake will be the same as potential uptake. Only when the soil dries out to less that h_3, the potential uptake will be reduced to the actual uptake. The point in time when this reduction starts then depends on the values of *TL* and *TH*. Some believe that this initial reduction (*TL*) should depend on the potential transpiration rate (i.e., if the potential transpiration is larger the reduction starts earlier). The initial reduction becomes independent of potential transpiration if one specifies that *TL* = *TH* and $h_{3\ low} = h_{3\ high}$.

S-shaped root water stress response function was suggested by van Genucten (1987) (Figure 2.13).

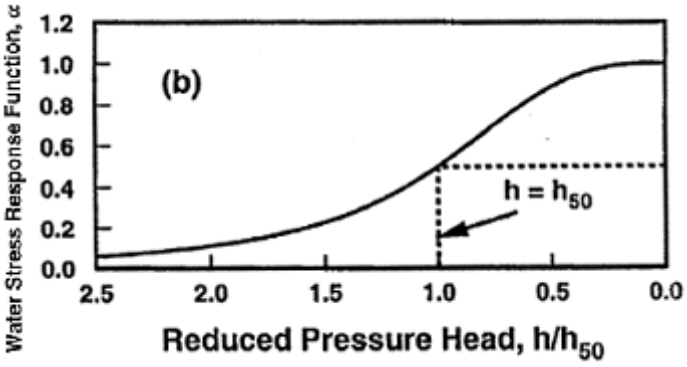

Figure 2.13: Plant water stress response function *α(h)* as used by van Genucten (1987)
Slika 2.13: Funkcija stresnega odziva rastlin za vodo *α*(h) kot jo je predstavil van Genuchten (1987)

The parameter *h50* represents the coefficient, (In Hydrus S-shape parameter P50) in the root water uptake response function associated with water stress. Root water uptake at this pressure head is reduced by 50 %. The parameter *p3* is the exponent (S-shape parameter P3) in the root water uptake response function associated with water stress; its recommended value is 3. In Hydrus model the parameter PW is additionally included and represents the pressure head at wilting point (WP), below which transpiration stops. In contrast to the response function of Feddes et al. (1978) this function does not consider the root water uptake near soil water saturation due to the lack of oxygen.

In the Hydrus-2D/3D model the root water uptake is distributed over the root zone according to the 2D or 3D spatial root distribution following Vrugt et al., 2001a, 2001b.

Hydrus can simulate root water uptake with compensation when the Critical Stress Index is set to smaller than one (Šimůnek et al. 2006). This compensatory is an important aspect of irrigation and drainage practices, where a non-uniform water stress is imposed to the plants root zone. In this situation plants can respond with increasing water uptake from root zone sections with more favourable conditions. According to Skaggs et al. (2006) these practices include deficit irrigation, partial root zone drying and deficit irrigation in combination with shallow groundwater management.

The root water uptake functions in combination with drip irrigation simulations using the Hydrus software have been used by several researchers, like Assouline (2002), Gardenas et al. (2005), Bufon et al. (2011), Phogat et al. (2011, 2013), Sansoulet et al. (2008), Dabach et al. (2011), Šimůnek and Hopmans (2009), Hanson et al. (2008).

Recently Couvreur et al. (2012) introduced a promising simple three-dimensional macroscopic root water uptake model which is based on the root system hydraulic

architecture. The model has three macroscopic parameters defined at the soil element scale, or the plant scale, rather than for each segment of root system architecture.

Because it is not the aim of this work to give in depth review of the root water uptake modelling, for further details about microscopic and macroscopic root water uptake approaches the reader is referred to Hopmans and Bristow (2002), Subbaiah (2011), Lubana and Narda (2001), Šimůnek and Hopmans (2009) and Skaggs et al. (2006).

3 MATERIALS AND METHODS

3.1 RESEARCH FRAMEWORK

The main purpose of this project is to investigate numerically and experimentally the influence of soil texture, relevant hydraulic properties, evapotranspiration, vegetation root distribution and amount of water applied on the size of the wetted area and therefore emitter spacing under surface drip irrigation systems, which are valid for different climate conditions. For the first part of this work, numerical simulations were done for soils, from arable land use, covering all texture classes according to the UK soil textural triangle which were selected from the Spatial Environmental Information System for Modelling the Impact of Chemicals (SEISMIC) database. In the second part selected empirical model parameters were improved based on simulations data from the first part. In the third part numerical model was used to investigate surface drip irrigation management of sweet corn when considering root water uptake. In the fourth part, numerical model results were compared with experimental data from hop surface drip irrigation. Finally, in the fifth part, numerical simulations were carried out to investigate the influence of different hop surface drip irrigation design parameters on soil water dynamics between two adjacent emitters. The Hydrus-2D/3D numerical model was chosen for modelling because, as presented in the previous chapter, it has been validated and used extensively for modelling drip irrigation systems under varied boundary conditions.

3.2 HYDRUS-2D/3D MODEL

In this research the modelling of water flux under surface drip irrigation was performed using the numerical model Hydrus-2D/3D Version 1.0 (v.1.0) and v.2.0. Recently, in 2011, Hydrus-2D/3D v.1.0 was upgraded and replaced by Hydrus-2D/3D v.2.0. (Šejna et al., 2011; Šimůnek et al., 2011). A notable feature in v.2.0 is new boundary condition, which allows the dynamic evaluation of the wetted area for surface drip irrigation. Although, initial simulations with the SEISMIC soils in this study were carried out with version 1.0. prior to the release of version 2.0, the simulations of soil water movement in all other studies were carried out with this new boundary condition (BC). The Hydrus developers, PC-Progress, are continuously introducing new versions of the programme. For simulations of hop irrigation, the Hydrus-2D/3D (v.2.02.0700) was used, which, in comparison to v. 2.0, includes new option for determining water flow initial conditions which are equal to field capacity of the soil, following Twarakavi et al. (2009) approach.

3.2.1 Soil hydraulic model and water flow parameters

The theory behind Hydrus-2D/3D model is given by Šimůnek et al. (2006), and more recently by Radcliffe and Šimůnek (2010). This section focuses only on details, relevant to this research. Transient or variably saturated water flow in soils occurs when water enters the soil surface whether in the form of precipitation or irrigation (Figure 3.1).

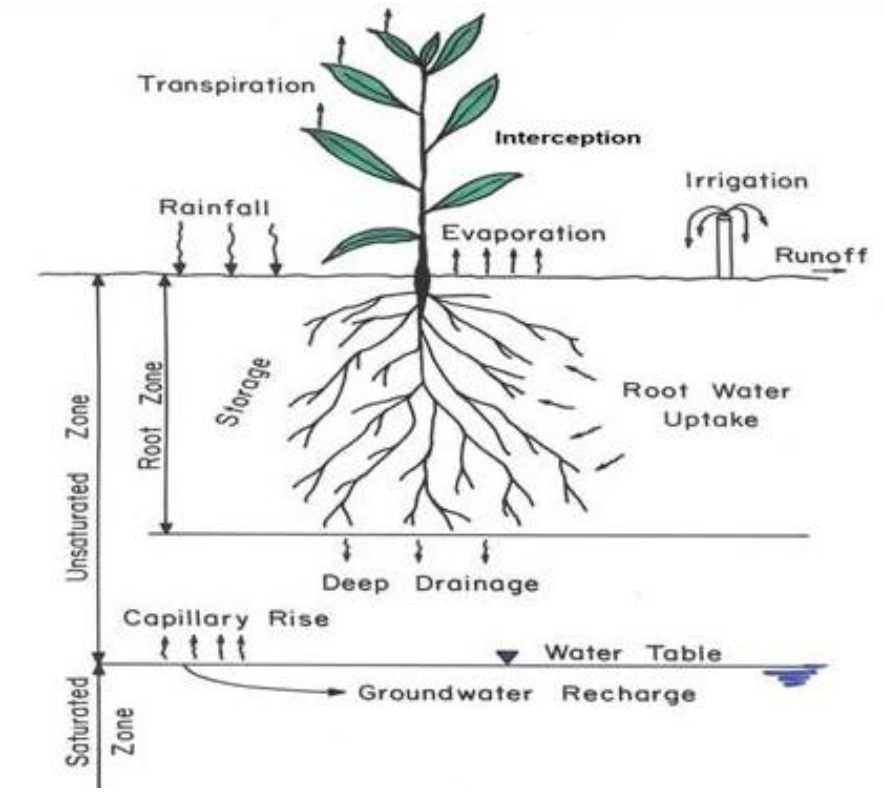

Figure 3.1: Transient water flow process in soils (Šimůnek et al. 2006)
Slika 3.1: Prehodni proces toka vode v tleh (Šimůnek in sod., 2006)

The equation that governs transient water flow in soils is Richards's equation (Richards, 1931). This equation combines the mass balance or continuity equation (Equation 8) with a Darcy-Buckingham equation (Equation 9) which is describing uniform flow in soils.

$$\frac{\partial \theta}{\partial t} = \frac{\partial q_i}{\partial x_i} - S \quad \text{... (8)}$$

$$q_i = K(h)\left(K_{ij}^A \frac{\partial h}{\partial x_j} + K_{iz}^A\right) \quad \text{... (9)}$$

where, *K(h)* is the unsaturated hydraulic conductivity function , h is the soil water pressure head, x_i (*i=1,2* for two-dimensional model and *i=1,2,3* for three-dimensional model) are spatial coordinates, K_{ij}^A and K_{iz}^A are components of a dimensionless anisotropy tensor K^A

(which reduces to the unit matrix when the medium is isotropic), θ is the volumetric water content, t is time, q_i is the volumetric flux density and S is a sink term, usually representing the root water uptake which is in more detail described in literature review section.

Combining equations 8 and 9 leads to the general form of Richards's equation (Equation 10):

$$\frac{\partial \theta(h)}{\partial t} = \frac{\partial}{\partial x_i}\left[K(h)\left(K_{ij}^{A}\frac{\partial h}{\partial x_j} + K_{iz}^{A}\right)\right] - S(h) \quad \ldots (10)$$

Equation 10 is partial differential equation and is governing variably saturated water flow in the saturated zone that can be easily expandable to two and three dimensions. The right side term accounts for the effect of capillarity on soil water movement and the second term on the right side accounts for the effect of gravity on movement of water. The coefficient *K(h)* that multiplies the gradient term is a function of the dependent variable θ or *h.* The Richards equation is, in any form, nonlinear. Because of its nonlinearity only a few simple analytical solutions can be derived, meaning that analytical solution usually exists only for steady conditions. The most practical applications of the equation 10 requires numerical solutions. As already mentioned in the literature review, there are two most common numerical methods used to solve the Richards equation: finite elements and finite differences (Radcliffe and Šimůnek, 2010).

Hydrus-2D/3D uses a numerical finite element approach in space (where the flow region is divided into a network of triangular (2D) or tetrahedral (3D) elements. The corners of these elements are taken to be the nodal points and finite difference approach in time (with discretizing the time domain into a sequence of finite intervals and replacing the time derivatives by finite differences).

The Galerkin linear finite element method is used to obtain a solution of Richards's equation and can be used to solve two and three dimensional problems (Šimůnek et al., 2006, 2011). Also, the two-dimensional form of Richards's equation can be used to solve three-dimensional problems. In this case the vertical axis (z coordinate) must coincide with the vertical axis of symmetry. These problems are then called quasi-three-dimensional or axisymmetrical problems and are good for simulations of water flow from a point source.

Richards's equation can be solved numerically or analytically only when the initial and boundary conditions are specified. In Hydrus-2D/3D the initial conditions, which characterize the initial state of the system, can be specified in terms of water content (Equation 11) or pressure head (Equation 12).

$$\theta\ (z,t) = \ \theta_i(z,0) \quad \text{... (11)}$$

$$h\ (z,t) = \ h_i(z,0) \quad \text{... (12)}$$

where θ_i (cm^3/cm^3) is the initial value of water content and h_i (cm) is the initial pressure head.

In Hydrus two types of BC can be specified on the transport domain boundaries. The first one is the system-independent BC, for which the specified boundary values (water content, pressure head, water flux, gradient) do not depend on the status of the soil system. The second one are system dependent BC for which the actual BC (water content, pressure head, water flux, gradient) depends on the system status and is calculated by the model itself.

System independent BC may be applied when the pressure head at the boundary is known. In this case one can use the Dirichlet or type-1 BC. This BC must be used for simulations with ponded infiltration, to specify a water level in a well or define a position of the water table. Water flux across Dirichlet BC must be calculated from the mathematical solution of the governing flow problem, because it is not known a priori. When the water flux across the BC is known, the Neumann or type-2 BC can be used. This BC must be used along boundaries where the flux is known. This BC therefore cannot be used with irrigation or precipitation modelling, because they can exceed the infiltration capacity of the soil and cause water ponding and consequently decrease the actual boundary flux.

System dependent BC may be applied when a flux, pressure head or gradient across boundary are not known a priori and follow from interactions between the surrounding and the soil. Hydrus considers several different types of system-dependent boundary conditions, for example atmospheric BC, seepage face, special time-variable flux/head BC, subsurface drip characteristic function, irrigation scheduling (triggered irrigation), surface drip irrigation – dynamic evaluation of the wetted area and irrigation scheduling – triggered irrigation (Šimůnek and van Genuchten, 2006; Radcliffe and Šimůnek, 2010; Šimůnek et al. 2012).

The $\theta(h)$ and K(h) in Richards' equation are in general highly nonlinear functions of the pressure head. They can be determined in Hydrus using six different analytical models for the hydraulic properties: the van Genuchten-Mualem model (van Genuchten, 1980), the van Genuchten-Mualem model with an air-entry value of -2 cm, modified van Genuchten type equations (Vogel and Cislerova, 1988), the equations of Brooks and Corey (1964), the

lognormal distribution model of Kosugi (1996), and a dual-porosity model (Durner, 1994; Šimůnek et al. 2012).

In this chapter only the the van Genucten-Mualem hydraulic function (van Genuchten, 1980; Mualem, 1976) is presented because it was used for modelling in this study and because it is, according to Radcliffe and Šimůnek, 2010, the most widely implemented function in vadose zone hydrology.

Similarly as for water retention curve, analytical models were also developed to describe soil hydraulic conductivity function. Mostly these functions were derived using the pore size distribution models, as that of Burdine (1953) or Mualem (1976) combined with one of the water retention functions. For instance, Brooks and Corey (1964) model is commonly used with Burdine's pore size distribution model and van Genuchten (1980) retention function is commonly coupled with the statistical pore size distribution model of Mualem (1976) to obtain unsaturated hydraulic conductivity function.

Van Genuchten (1980) model is given with Equation 13:

$$\theta(h) = \begin{cases} \theta_r + \dfrac{\theta_s - \theta_r}{[1 + |\alpha h|^n]^m} & h < 0 \\ \theta_s & h \geq 0 \end{cases} \quad \text{... (13)}$$

Mualem's (1976) unsaturated hydraulic conductivity function is presented with Equation 14:

$$K(h) = K_s S_e^l \left[1 - (1 - S_e^{1/m})^m\right]^2 \quad \text{... (14)}$$

Where

$$m = 1 - \frac{1}{n}, \qquad n > 1$$

$$S_e = \frac{\theta - \theta_r}{\theta_s - \theta_r}$$

In the above equations θ_s and θ_r are saturated and residual water content (cm^3/cm^3), α (1/cm), n, m and l are shape parameters, and S_e is the effective soil water saturation. The pore connectivity parameter l in Equation 14 was estimated by Mualem (1976) to be equal to 0.5 for most soils (Mualem, 1976; Šimůnek et al., 2011).

3.2.2 Dynamic boundary conditions for surface drip irrigation simulations and field capacity prediction model

The new special BC for surface drip irrigation with dynamic evaluation of the wetted area (Figure 3.2), which is implemented in Hydrus-2D/3D v. 2.0, was first used by Gärdenas et al. (2004) who at that time had access to the Hydrus source code. With this BC, a Neumann BC (discharge rate) is applied to the node which represents the dripper. As the pressure head needed to maintain this constant flux at the node exceeds 0, the BC is switched from a Neumann (flux) to a 0 pressure head Dirichlet (head) BC and the actual flow rate (*Qa*), corresponding to this head, is computed (Šimůnek et al., 2011). The excess irrigation flux (*Q* – *Qa*), again, using a specified Neumann BC, is applied to the neighbouring node. This procedure is repeated iteratively until the entire specified *Q* is applied over a radius corresponding to the wetted area. This option can be used in 2D and 2D axisymmetrical geometry definitions only.

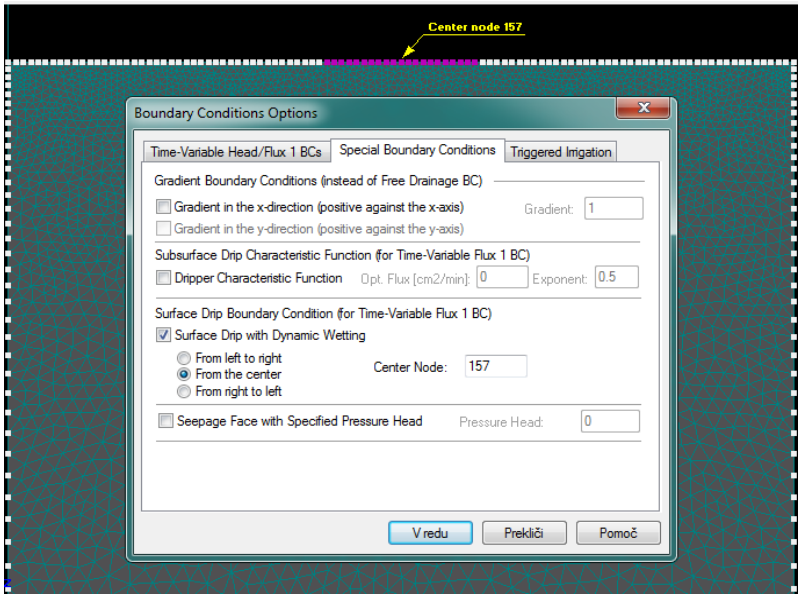

Figure 3.2: The new surface drip boundary condition window options in Hydrus-2D/3D
Slika 3.2: Nova možnost izbire robnih pogojev za površinsko kapljični namakanje v Hydrusu-2D/3D

A new option in Hydrus-2D/3D (v.2.02.0700), where initial conditions for water flow can be set equal to field capacity of the soil, follow approach of Twarakavi et al. (2009). He found out that field capacity shows a relationship with van Genuchten-Mulaem model parameters θ_s, θ_r, n and Ks. Based on that he developed an accurate empirical relationship to estimate the soil field capacity. Assuming negligible drainage flux (as suggested by Dirksen and Matula, 1994), from the soil at field capacity (q_{fc}) is 0.01 cm/day which is according to Twarakavi et al. (2009) a reasonable approximation at which one may assume that θ_{fc} is attained, the final simplified equation was obtained (Equation 15):

$$S_{fc} = \frac{\theta_{fc} - \theta_r}{\theta_s - \theta_r} = n^{-0.60(2+log_{10}(Ks))} \quad \text{... (15)}$$

where *Ks* is saturated hydraulic conductivity of the soil in cm/day, *n* is shape parameter of van Genuchen-Mualem equation and θ_{fc} is field capacity of the soil (cm^3/cm^3).

3.2.3 Surface boundary condition used with SEISMIC soils compared to new dynamic boundary condition

As already mentioned, simulations with SEISMIC soils have been done with Hydrus-2D/3D (v. 1.0), assuming that the flow rate per unit area was equal to the soil *Ks*. This approach was used because Hydrus-2D/3D v.1.0. cannot simulate surface flow, which occurs at the onset of drip irrigation, as the discharge rate exceeds the infiltration capacity of the soil. A constant flux boundary was applied to a fixed surface area representing the infiltration area that is achieved at steady state, after water has spread across the soil surface. This area represents the area that would be obtained with the new BC in v. 2.0 after all the fluxes have been redistributed, assuming a maximum pressure head of zero (i.e. no ponding) at the soil surface (see section 3.2.2). The radius of this surface area (Equation 11) is calculated by considering that, at zero pressure head, the flow rate per unit area is equal to the soil saturated hydraulic conductivity (Equation 16, 17, 18, 19):

$$q = \frac{Q}{A} \quad \text{... (16)}$$

$$A = \pi r^2 \quad \text{... (17)}$$

$$q = Ks \quad \text{... (18)}$$

$$r = \sqrt{\frac{Q}{\pi \times Ks}} \quad \text{...(19)}$$

where Q is the flow rate (cm^3/h), A is surface area (cm^2), K_s is saturated hydraulic conductivity (cm/day), q is the water flux per unit area (cm/day) and r is the radius (cm) of the infiltrating surface.

All other simulations were carried out with the new surface drip BC with dynamic wetting which was included in Hydrus-2D/3D (v.2.0). To test, if any discrepancies in the wetting pattern size between using the new and the old BC exist, some randomly selected simulations (with different soil types and emitter discharge rates), where the old BC was

used, were rerun using the new BC. Results showed that in general the differences of wetting pattern size when using the original and new BC was remarkably small (Figures 3.3. and 3.4.). The results are presented in more detail in Naglič, 2011.

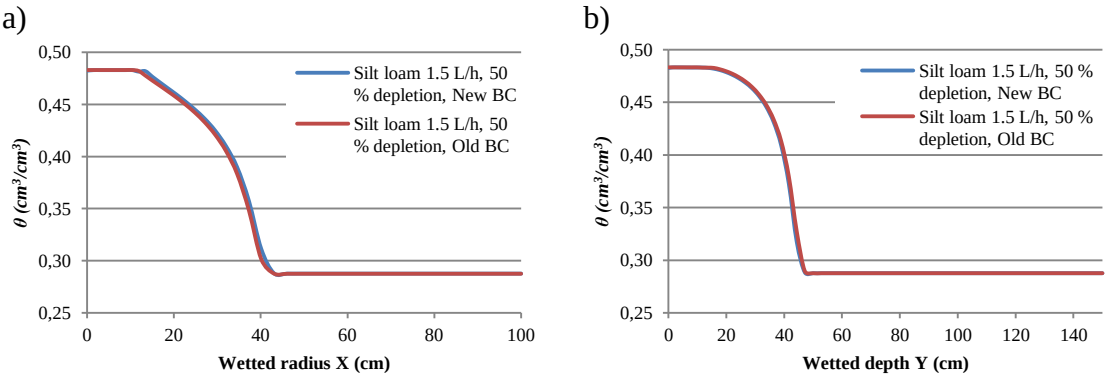

Figure 3.3: Comparison of simulated wetted radius (a) and wetted depth (b) using old and new boundary conditions for emitter discharge rate of 1.5 L/h and 50 % depletion for silt loam soil at the end of irrigation (20 L of water applied)
Slika 3.3: Primerjava simuliranega omočenega radija (a) in omočene globine (b) z uporabo starih in novih robnih pogojev za pretok kapljača pri 1,5 L/h in pri 50 % stanja razpoložljive vode v meljasto ilovnatih tleh, pri koncu namakanja (pri 20 L dodane vode)

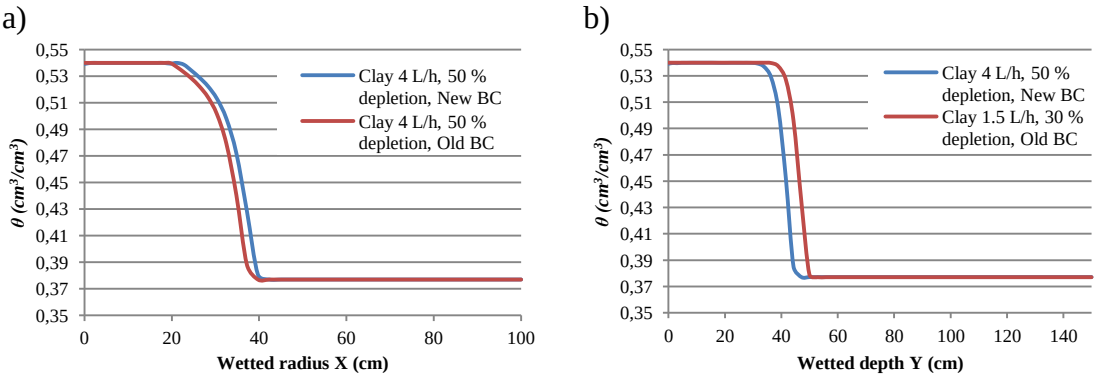

Figure 3.4: Comparison of simulated wetted radius (a) and wetted depth (b) using old and new BC for emitter discharge rate of 4 L/h and 50 % depletion for clay soil at the end of irrigation (20 L of water applied)
Slika 3.4: Primerjava simuliranega omočenega radija (a) in omočene globine (b) z uporabo starih in novih robnih pogojev za pretok kapljača pri 4 L/h in pri 50 % stanja razpoložljive vode v glinastih tleh, pri koncu namakanja (pri 20 L dodane vode)

3.3 NUMERICAL AND EXPERIMENTAL STUDY OF WETTING PATTERNS

3.3.1 Numerical simulations for soils from SEISMIC database

In this section the numerical model Hydrus-2D/3D (v.1.0) was used with a purpose to simulate the wetting pattern size dynamics under surface drip irrigation for 11 soil textural classes, different emitter discharge rates and different initial soil water conditions. This part is an expansion of work which has been already started in Naglič (2011) by introducing additional emitter discharge rate of 0.5 L/h. Therefore the dataset was extended for additional 180 measurements, which will be used for the Schwartzman and Zur (1986) empirical model parameters improvement.

3.3.1.1 Soil textural classes and hydraulic parameters

Soils, from arable land use, covering all soil texture classes according to the UK soil textural triangle (Figure 3.5), were selected from the Spatial Environmental Information System for Modelling the Impact of Chemicals (SEISMIC) database. The SEISMIC database was developed by the National Soil Resource Institute (NSRI) at Cranfield University. It provides soil data for 412 soil series of England and Wales and uses pedotransfer functions derived from multiple regression analysis from measured data to predict soil hydraulic properties. At a given volumetric water content, these pedotransfer functions return an overall root mean square error (RMSE) of 4.6 % and a model efficiency of 0.77.

The database provides all the van Genuchten-Mualem model parameters needed as input for Hydrus-2D/3D modelling. These are saturated water content (θ_s), residual water content (θ_r), saturated hydraulic conductivity (Ks) and shape parameters α, and n which are presented in Table 3.1. The pore connectivity parameter (l) was taken as 0.5, as suggested by Mualem (1976) for all soils.

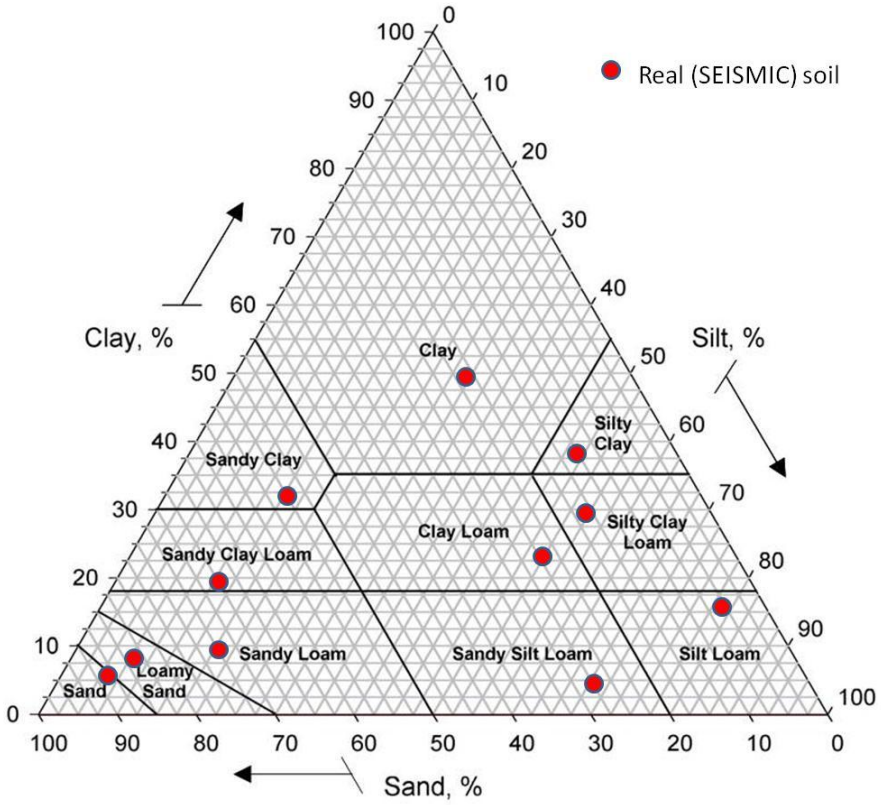

Figure 3.5: Selected soil textural classes selected from SEISMIC database according to the UK textural triangle (James, 2010)
Slika 3.5: Talni teksturni razredi izbrani iz zbirke podatkov SEISMIC, kot prikazuje UK teksturni trikotnik (James, 2010)

Table 3.1: Soil classification, texture, bulk density (ρ_b) and van Genuchten (VG) parameters used for Hydrus-2D/3D modelling (SEISMIC, 2011)
Preglednica 3.1: Klasifikacija tal, tekstura tal, gostota tal (ρ_b) in van Genuchtnovi (VG) parametri, uporabljeni za Hydrus-2D/3D modeliranje (SEISMIC, 2011)

Soil series	Texture	Layer	Particle size fraction (%)			ρ_b (g/cm^3)	VG		*Ks* (cm/day)
			Clay	Silt	Sand		α (1/cm)	n	
Blackwood	Sandy Loam	A	11	19	70	1.3	0.08	1.32	242.6
Bridgnorth	Loamy Sand	A	8	8	84	1.48	0.11	1.41	117
Isleham	Sandy Clay Loam	A	20	13	67	1.03	0.08	1.29	333
Bridgnorth	Sand	BW1	7	6	87	1.42	0.12	1.48	289.8
Wittering	Silty Clay	A	38	49	13	0.88	0.03	1.21	141
Carswell	Sandy Clay	Bc	31	16	53	1.37	0.06	1.24	161.2
Fladbury	Clay	A	50	30	20	1.05	0.04	1.2	78.9
Chatteris	Silty Clay Loam	A	30	54	16	0.83	0.03	1.22	185.6
Coprolite washing	Clay Loam	A	25	52	23	1.38	0.04	1.23	47.9
Rowton	Silt Loam	A	16	79	5	1.25	0.03	1.25	80.8
Poundgate	Sandy Silt Loam	A	4	68	28	1.1	0.06	1.35	226.9

The influence of initial water content was investigated by varying the % depletion of the available water (AW). AW corresponds to the amount of water between field capacity of the soil (FC) and soil permanent wilting point (PWP) and therefore % depletion represents the % of AW that is no longer available to the plant. A FC was selected corresponding to water content at 10 kPa (-100 cm) (Li et al., 2004) pressure head for all soils. θ_r was used for the PWP. The three depletion rates of 30, 50 and 70 % were used for all soils. This approach allows the investigation of the relative influence of dry and wet initial conditions rather than that of a set initial water content value which might correspond to dry conditions for one soil but wet conditions for another one. Soil water initial conditions for three most contrasting soil textural classes, with which the simulations were done, are presented in Table 3.2.

Table 3.2: Water content (θ (cm^3/cm^3)) at different depletion rates for 11 soil textural classes
Preglednica 3.2: Vsebnost vode (θ (cm^3/cm^3)) pri različnih stanjih razpoložljive vode v tleh za 11 teksturnih razredov

	Depletion (initial conditions)		
Texture	30 %	50 %	70 %
Sandy Loam	0.24	0.21	0.18
Loamy Sand	0.20	0.17	0.15
Sandy Clay Loam	0.30	0.26	0.22
Sand	0.15	0.13	0.11
Silty Clay	0.42	0.37	0.33
Sandy Clay	0.27	0.25	0.23
Clay	0.41	0.38	0.34
Silty Clay Loam	0.41	0.36	0.31
Clay Loam	0.32	0.28	0.25
Silt Loam	0.33	0.29	0.24
Sandy Silt Loam	0.30	0.25	0.21

3.3.1.2 Hydrus-2D/3D setup

Three different sets of numerical simulations were carried out. A total of 20 L of water was applied in all cases. The first set of simulations, which aimed at studying the influence of texture alone, was performed for the eleven soils at a given discharge rate of 2 L/h and a fixed initial soil water depletion of 50 %. (Table 3.3).

Table 3.3: Emitter discharge rate (*Q*), soil initial condition and soil textures used for first set of simulations
Preglednica 3.3: Pretok kapljača (*Q*), začetna vsebnost vode v tleh in talni teksturni razredi, uporabljeni za prvi set simulacij

Q (L/h)	Initial conditions (% depletion)	Soil texture
2	50	Sandy Loam Loamy Sand Sandy Clay Loam Sand Silty Clay Sandy Clay Clay Silty Clay Loam Clay Loam Silt Loam Sandy Silt Loam

With the second set of simulations the influence of initial water content on wetting patterns was evaluated and was carried out on three soils with contrasting textures (sand, silt loam and clay) at one given emitter discharge rate of 2 L/h, for the three initial water depletion rates of 30, 50 and 70 %. (Table 3.4).

Table 3.4: Emitter discharge rates (*Q*), soil initial conditions and soil textures used for second simulation set
Preglednica 3.4: Pretok kapljača (*Q*), začetna vsebnost vode v tleh in talni teksturni razredi, uporabljeni za drugi set simulacij

Q (L/h)	Initial conditions (% depletion)	Soil texture
2	30	Sand Silt loam Clay
2	50	Sand Silt loam Clay
2	70	Sand Silt loam Clay

Finally, for the same three soils, a third set of simulations was carried out with a purpose to study the influence of four different emitter discharge rates (0.5, 1.5, 2 and 4 L/h) for initial soil water conditions set to 50 % depletion (Table 3.5).

Table 3.5: Emitter discharge rates (*Q*), soil initial conditions and soil textures used for third set of simulations
Preglednica 3.5: Pretok kapljača (*Q*), začetna vsebnost vode v tleh in talni teksturni razredi, uporabljeni za tretji set simulacij

Q (L/h)	Initial conditions (% depletion)	Soil texture
0.5	50	Sand Silt loam Clay
1.5	50	Sand Silt loam Clay
2	50	Sand Silt loam Clay
4	50	Sand Silt loam Clay

All together 44 simulations were carried out, which included:

- three distinct soil types at three different emitter discharge rates and at three different soil water initial conditions and
- 11 soil textural classes at discharge rate of 2 L/h and 50 % depletion. With a purpose to study the influence of soil texture, emitter discharge rate and soil water initial conditions on the size of the wetting pattern only the simulations presented in tables 3.3, 3.4 and 3.5 were used (32 simulations). All 44 sets of simulations were used only for selected empirical model parameters improvement in section 3.5.

The wetting patterns radii size, X (horizontal direction) and depth, Y (vertical direction), were measured using the boundary line chart function in Hydrus-2D/3D for every litre of water applied. Hence, for simulations with 0.5 L/h measurements were carried out every 0.08 days (120 min), for1.5 L/h measurements were carried out every 0.03 days (40 min), for 2 L/h every 0.02 days (30 min) and for 4 L/h after every 0.01days (15 min). The total irrigation time was 1.7 days (40 h) for the 0.5 L/h emitter discharge rate, 0.56 days (13.3 h) for the 1.5 L/h emitter discharge rate, 0.42 days (10 h) for the 2 L/h emitter discharge and 0.21 days (5 h) for the 4 L/h emitter discharge (Figure 3.6).

The boundary between the wetted area and the initial soil conditions was defined as the point in the wetted front where water content just exceeds the initial water content, as suggested by Bresler et al. (1971).

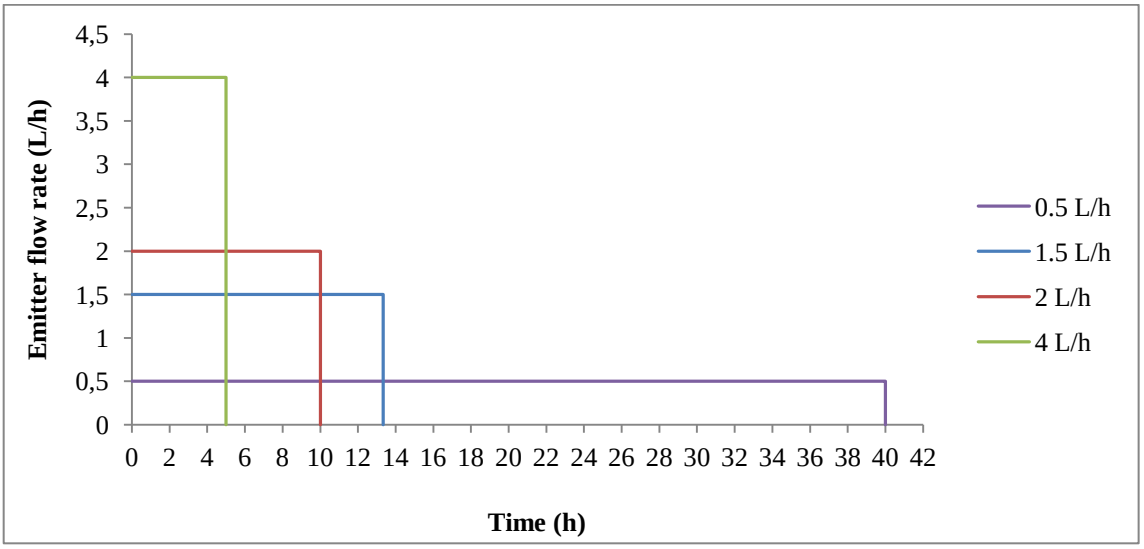

Figure 3.6: Time of water application for four investigated emitter discharge rates
Slika 3.6: Čas aplikacije vode za štiri preučevane pretoke kapljačev

Similarly to other studies, axisymmetrical two-dimensional geometry, where the emitter is represented as a point source, was used (Gardenas et al., 2005; Provenzano, 2007; Cote et al., 2003; Kandelous and Šimůnek, 2010a; Kandelous et al., 2011). Simulations were done using a 150 cm deep and 100 cm wide rectangular flow domain (Figure 3.7).

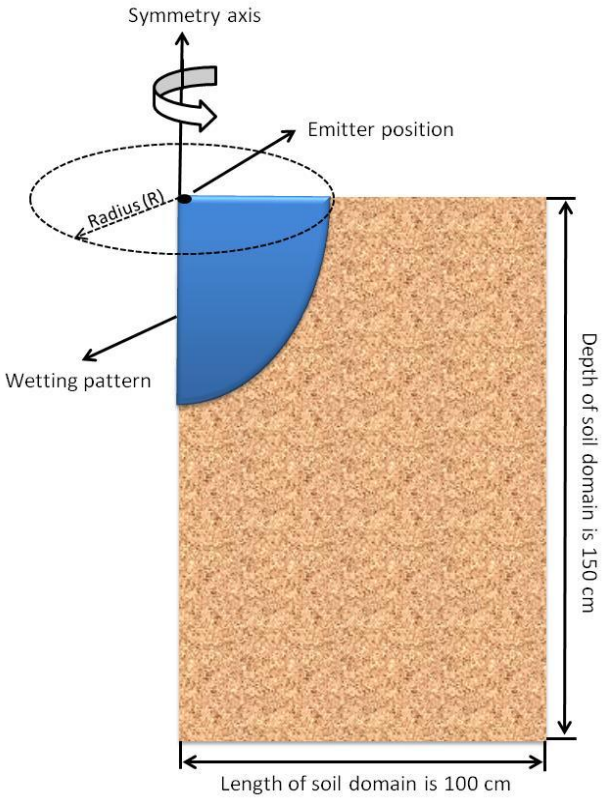

Figure 3.7: Flow domain used in SEISMIC soils simulations
Slika 3.7: Pretočna domena, uporabljena za simulacije SEISMIC tal

Along the upper boundary absence of flux was considered except a small part on the left, close to the axis of symmetry, where a surface drip boundary condition (BC), representing the dripper, was used. A free drainage BC was used along the bottom boundary, and a zero-flux BC for all remaining boundaries of the domain (Figure 3.8).

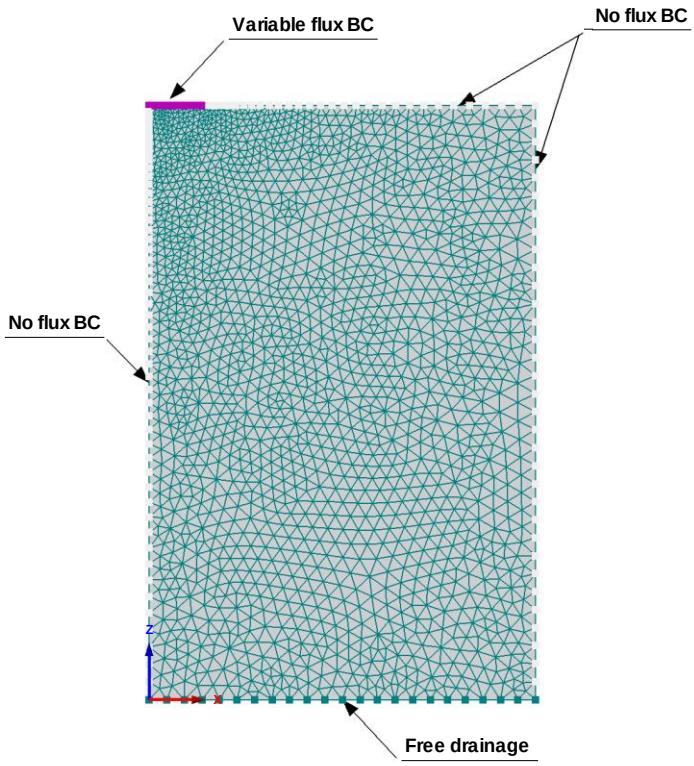

Figure 3.8: Spatial discretization of the 2D axisymmetrical flow domain and its boundary conditions (BC)
Slika 3.8: Prostorska diskretizacija 2D aksisimetrične pretočne domene in njeni robni pogoji (BC)

An unstructured mesh was automatically generated to discretise the flow domain into between 1789 and 1917 nodes, depending on the radius of BC representing dripper at the surface of the soil. Smaller finite elements were selected around the emitter, where the hydraulic gradient is higher.

3.3.2 Soil tank experiments

The soil tank experiments were conducted in the Soil Laboratory at Cranfield University with a purpose to evaluate the ability of Hydrus 2D/3D (v.2.0) to determine to which extend observed and simulated results agree when the measured soil hydraulic properties are used rather than optimised through inverse modelling and when the new special boundary condition for surface drip with dynamic wetting is used.

3.3.2.1 Experimental setup

The soil tank experiments were conducted in the Soil Laboratory at Cranfield University. Experiments were carried out on a 40.3 cm long, 30 cm high and 2.5 cm deep 2D soil tank (Figure 3.9). The front wall of the soil tank was transparent and made of tempered glass. The back panels were made from stainless steel alloy. A thin 4 mm diameter polyethylene pipe, representing a surface emitter, and fitted with a water flow regulator was installed at the upper boundary of the soil tank, approximately 2 mm above the soil surface (Naglič, 2011).

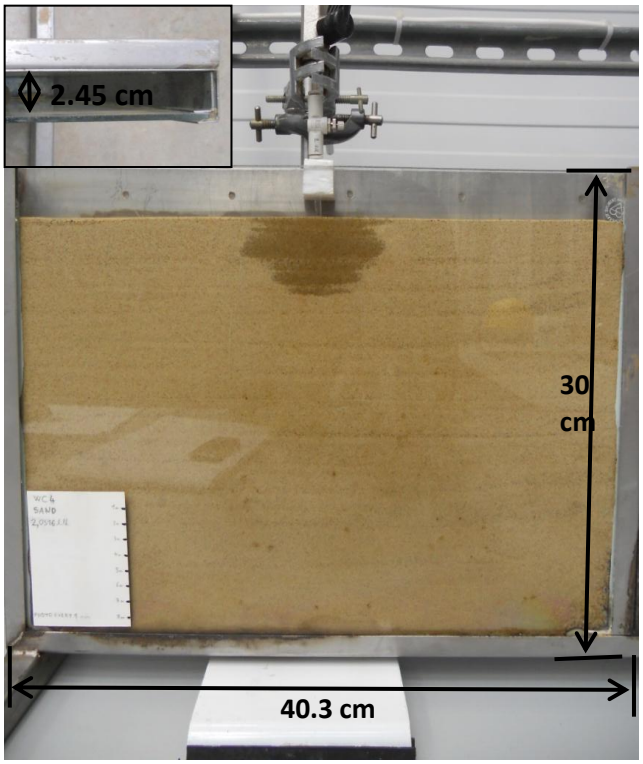

Figure 3.9: Soil tank used in laboratory experiment and its dimensions
Slika 3.9: Tank za zemljo, uporabljen v laboratorijskem poskusu, in njegove dimenzije

The sand and silty clay loam soils used for the experiment were first sieved through a 2 mm sieve and packed in the soil tank in 2 cm layers. The soil bulk density was determined after packing, using a steel cylinder with fixed volume. Soil physical properties are presented in Table 3.6.

Table 3.6: Soil texture and bulk density (ρ_b) for selected soils used in soil tank experiment
Preglednica 3.6: Tekstura in gostota tal (ρ_b) za izbrana tla, uporabljena v poskusu s tanki, napolnjenimi s tlemi

Soil texture	Sand (%)	Silt (%)	Clay (%)	ρ_b (g/cm^3)
Sand	99.52	0.32	0.16	1.58
Silty clay loam	18.27	46.77	34.96	1.29

The emitter discharge rates used with the sandy soil are presented in Table 3.7. In total 0.15, 0.41, 0.47, 0.48 and 0.44 L of water was applied for emitter discharge rates of 0.11, 0.49, 0.99, 1.51 and 2.05 L/h, respectively. Because of surface ponding and water spreading to the sides of the soil tank at higher flow rates, the experiments in the silty clay loam soil could only be done with one *Q* where 0.23 L of water was applied. All together six soil tank experiments have been done.

When the experiment started, the shapes of the wetting patterns in both directions were recorded, taking pictures at different predetermined times. The interval between two pictures depended on the *Q* and soil type and ranged from 5 to 1 min which resulted in 15 to 30 taken images for one experiment. A scale was drawn on the soil tank which enabled determination of the wetting pattern dimensions from the pictures using the computer programme ImageJ 1.43u (National Institutes of Health, USA) (Naglič, 2011).

Table 3.7: Desired and averaged emitter discharge rates (*Q* (L/h)) used for soil tank laboratory experiment
Preglednica 3.7: Željeni in povprečni pretoki kapljačev (*Q* (L/h)), uporabljeni v laboratoriskem poskusu s tanki

Soil	*Q* (L/h)	
	Desired	Average
Sand	0.1	0.11
	0.5	0.49
	1	0.99
	1.5	1.51
	2	2.05
Silty clay loam	0.1	0.12

3.3.2.2 Soil hydraulic properties

Water retention data for the sand soil were determined using a sand table and a pressure-plate apparatus. For the silty clay loam soil the laboratory evaporation method (Peters and Durner, 2008) HYPROP® was used. In both cases the the Mualem - van Genuchten model was fitted to the data and the model parameters used as inputs in Hydrus. For sandy soil the RETC software (van Genuchten et al. 1991) was used to fit the unknown van Genuchten - Mualem equation parameters (θ_s, θ_r, α and n) from observed water retention data. The For silty clay loam soil the HYPROP software was used to fit van Genuchten-Mualem model to water retention data. The parameters of van Genucten-Mualem soil hydraulic properties model selected for both soils, are presented in Table 3.8. The soil water *Ks* was determined in the laboratory using a falling head method. All soils used in soil tank experiment were air-dried and initial soil water content was close to θ_r. Initial soil water content for both soils was close to θ_r, resulting in 0.02 and 0.14 cm^3/cm^3 for sand and and silty clay loam soil (Naglič, 2011).

Table 3.8: Parameters of van Genuchten-Mualem model for soils used in laboratory experiment
Preglednica 3.8: Parametri van Genuchtnovega modela za tla, uporabljena v laboratorijskem poskusu

Soil texture	θ_s (cm^3/cm^3)	θ_r (cm^3/cm^3)	α (1/cm)	n	K_s(cm/min)	l
Sand	0.459	0.018	0.029	3.437	0.481	0.5
Silty clay loam	0.52	0.13	0.0215	1.281	0.007	0.5

The hydraulic parameters obtained were used as inputs for the numerical model Hydrus-2D/3D which was used simulate the experiments (Naglič, 2011).

3.3.2.3 Hydrus-2D/3D setup

The experimental data were compared to Hydrus-2D/3D (version 2.0) simulation results. The dripper lateral on the soil surface was assumed to represent a 2.5 cm section of an infinite line source. Simulations were done considering a 30 cm deep and 40.3 cm wide 2D rectangular transport domain, where a single emitter was placed at the centre (Figure 3.10). An unstructured mesh was automatically generated to discretise the flow domain into 3733 nodes in all cases. Finite elements were smaller at the upper boundary of the transport domain, where the hydraulic gradient is higher, and larger with increasing depth. Absence of flux was considered for all boundaries, except at the centre of the domain where a time-constant flux BC, representing the dripper, was used (Naglič, 2011).

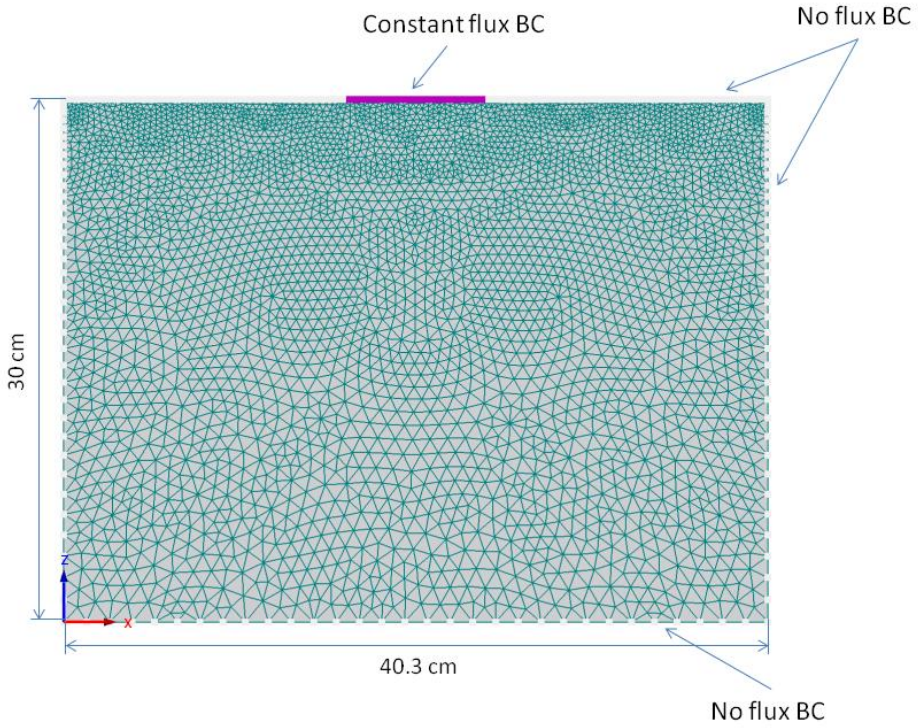

Figure 3.10: Spatial discretization of the 2D flow domain and its boundary conditions (BC)
Slika 3.10: Prostorska diskretizacija 2D pretočne domene in njeni robni pogoji (BC)

A new special BC for surface drip with dynamic wetting, incorporated into recent second version of Hydrus-2D/3D, was used. This BC was previously used by Gardenas et al. (2004). The emitter discharge rates and total volumes of applied water for numerical simulations are presented in Table 3.9 and are equal to those used in soil tank experiments. Selected initial conditions were identical to those determined in the experiment. Because of the short duration of the experiments and small surface area, the evaporation from the soil surface was neglected (Naglič, 2011).

Table 3.9: Irrigation duration (min) and volume of applied water (L) for all soil tank laboratory experiments
Preglednica 3.9: Trajanje namakanja (min) in volumen dodane vode (L) za laboratorijske poskuse s tanki, napolnjeneimi s tlemi

Soil	*Q* (L/h)	Irrigation time (min)	Applied volume (L)
Sand	0,11	84	0.15
	0,49	50	0.41
	0,99	28	0.47
	1,51	19	0.48
	2,05	13	0.44
Silty clay loam	0,12	120	0.23

The constant water flux per unit area (q) is equal to the emitter discharge rate (Q) at the modelled drip surface length (2.45 cm wide) (Equation 20), which varied from 0.1 to 2 L/h, and was calculated as below:

$$q = \frac{QL/h * 1000}{60 * 2.45\ cm}\ in\ cm^3/min \quad \text{... (20)}$$

3.4 CORRELATIONS BETWEEN SOIL TEXTURE, HYDRAULIC PROPERTIES AND HORIZONTAL AND VERTICAL WETTING PATTERN DIMENSIONS

The multiple linear regression analyses were carried out to investigate the effects of the soil texture, volume of applied water, emitter discharge rate (Q) and other soil hydraulic properties as *Ks*, free pore space (θ_f) and van Genuchten α and n, on the wetting pattern radius and depth dimensions. θ_f was calculated subtracting initial soil water content from θ_s. The purpose of the analysis was to identify if any of the above parameters can explain the variation of soil wetting pattern radius and depth. Analysis was performed for 35 simulation results with SEISMIC soils using different emitter discharge rates and initial soil water conditions (% depletion), as presented in section 3.3.1, but with difference, that three contrasting soil types (sand, silt loam and clay) with Q of 0.5 L/h at 30, 50 and 70 % depletion rates were excluded from analysis (all together 9 simulations). The software package STATISTICA Version 10 (StatSoft, Inc., USA) was used for this purpose.

3.5 SELECTED EMPIRICAL MODELS FOR WATER INFILTRATION FROM A POINT SOURCE

Simple empirical models of Li et al. (2003), Amin and Ekhmaj (2006) and Schwartzman and Zur (1986) were compared in Naglič (2011) with a purpose to assess their predictive capabilities. They were compared to simulations data of wetting pattern radius and depth using SEISMIC soils. Good performance Schwartzman and Zur (1986) model was observed. Therefore model can be very attractive for drip irrigation design by the end users because the number of variables required is limited and easily available but also because it proposes a universal set of parameters. Therefore its parameters were in this research further improved, extending it with additional 0.5 L/h emitter discharge rate at different soil water initial conditions.

3.5.1 Model improvement

Schwartzman and Zur (1986) empirical model parameters were fitted to the data set obtained with the Hydrus-2D/3D simulations results. This data set contained results of wetting patterns extend in the X and Y directions for every litre of applied water and up to 20 L of continuously added water. This dataset included 11 different soil textures irrigated with Q of 2 L h^{-1} and depletion rate of 50 % and three contrasting soil textures irrigated at three different antecedent soil water conditions and four different Q. All together 880 measurements, in each direction (X and Y), were fitted with the model of Schwartzman and Zur (1986).

Several empirical models proposed that wetting pattern X and Y are mostly influenced by volume of applied water, as suggested by Li et al. (2003), Ks, Q, changes in volumetric water content ($\Delta\theta$) (Amin and Ekhmaj, 2006) and soil bulk density (Malek and Peters, 2011). In all above mentioned models, X and Y of the wetting patterns are power functions of the above parameters and can be determined using a nonlinear regression approach.

However, as already noted, these parameters were obtained for a very limited number of soil types, Q rates and initial soil water conditions. Therefore their universality is unclear (Ainechee et al. 2009). In Schwartzman and Zur (1986) these parameters were obtained through regression analysis based on Bresler (1978) experimental results for a point source surface dripper for only two soil types and two Q rates. Bresler (1978) used two soils from Israel. First is Gilat loam soil with 48 % sand and 20 % clay, which is according to UK textural triangle, a clay loam, and second one Sinai sand with 97 % sand and 1 % clay. Ks was 2.4×10^{-6} m/s for Gilat loam and 7.6×10^{-6} m/s for Sinai sand soil. The used Q rates were 1.1×10^{-6} m^3/s (4 L/h) and 5.6×10^{-6} m^3/s (20 L/h).

According to Schwartzman and Zur (1986), the wetted soil volume under a surface point source is mainly dependent on the hydraulic conductivity of the soil (*Ks*), the emitter discharge rate (*Q*) and the total volume of water applied (*V*). Authors used dimensional analysis to develop an semi-empirical model to predict horizontal and vertical wetting pattern positions under surface drip irrigation. The following functions were considered for wetted soil dimensions under point source (Equations 21 and 22):

$$D = f_1(V, Q, Ks) \quad \text{... (21)}$$

$$Y = f_2(V, Q, Ks) \quad \text{... (22)}$$

where *D* (cm) is diameter of the wetted soil volume at its widest point and Y (cm) is depth of the wetting.
In order to reduce the number of variables, the dimensionless forms of the above parameters were presented as below (Equations 23, 24 and 25).

$$V^* = V \left(\frac{Ks}{Q}\right)^{\frac{3}{2}} \quad \text{... (23)}$$

$$D^* = D \left(\frac{Ks}{Q}\right)^{\frac{1}{2}} \quad \text{... (24)}$$

$$Y^* = Y \left(\frac{Ks}{Q}\right)^{\frac{1}{2}} \quad \text{... (25)}$$

The dimensionless parameters, *V**, *D** and *Y** were extracted from experimental or simulated results. It was assumed, that the relationship between the dimensionless parameters was (Equations 26 and 27):

$$D^* = A_1 V^{*n_1} \quad \text{... (26)}$$

$$Y^* = A_2 V^{*n_2} \quad \text{... (27)}$$

where, A_1, A_2 n_1 and n_2 are constants for the cylindrical flow model.

To convert dimensionless equations to dimensional ones, the relationship in equations 23, 24 and 25 are used, which results in following equations (Equations 28 and 29).

$$D = A_1 V^{n_1} \left(\frac{Ks}{Q}\right)^{\frac{3n_1}{2} - 1/2} \quad \text{... (28)}$$

$$Y=A_2\ V^{n_2}\ \left(\frac{Ks}{Q}\right)^{\frac{3n_2}{2}\ 1/2} \quad \text{... (29)}$$

In this work Equations 28 and 29 will be used to fit to the data of simulation results as opposed to the original model parameters presented below which is the Schwartzman and Zur (1986) model (Equations 30 and 31).

$$D=1.82\ V^{0.22}\ \left(\frac{Ks}{Q}\right)^{-0.17} \quad \text{... (30)}$$

$$Y=2.54\ V^{0.63}\ \left(\frac{Ks}{Q}\right)^{0.45} \quad \text{... (31)}$$

3.6 NUMERICAL INVESTIGATION OF SURFACE DRIP IRRIGATION MANAGEMENT OF SWEET CORN (*ZEA MAYS* L. VAR. SACCHARATA) FROM SENEGAL

3.6.1 Site description

Sweet corn was grown at Société de Cultures légumières (SCL) which is located in Diama, close to the Saint-Louis in the north of Senegal. Availability of water and favourable climate allow that 2 to 3 corn crops can be grown on the same field each year. SCL is cultivating around 500 ha which are divided into five farms: Diama, Djama, Agrinord, Agroval and Bango. The main crops at SCL are: sweetcorn, butternut squash, peanut, asparagus and sweet potatoes (Hess, 2011).

3.6.2 Climate and plants characteristics

Long term climate data are available from the Saint Louis airport (16.050°N, 16.458°E, altitude: 4 m) weather station, which is in 17 km range from Diama. The climate in Senegal is tropical and divided into two seasons. Rainy season lasts from June to October and dry season lasts from November to May when there is virtually no rain. Based on analysis no evidence was found suggesting that ETo at the SCL farm was significantly different from Saint Louis airport (Hess, 2011; Kaiser, 2012). The SCL farm provided hourly ETo data for period of three days, which were multiplied by Kc of 1.15 (mid-season) and resulted in ETc values, as shown on Figure 3.11.

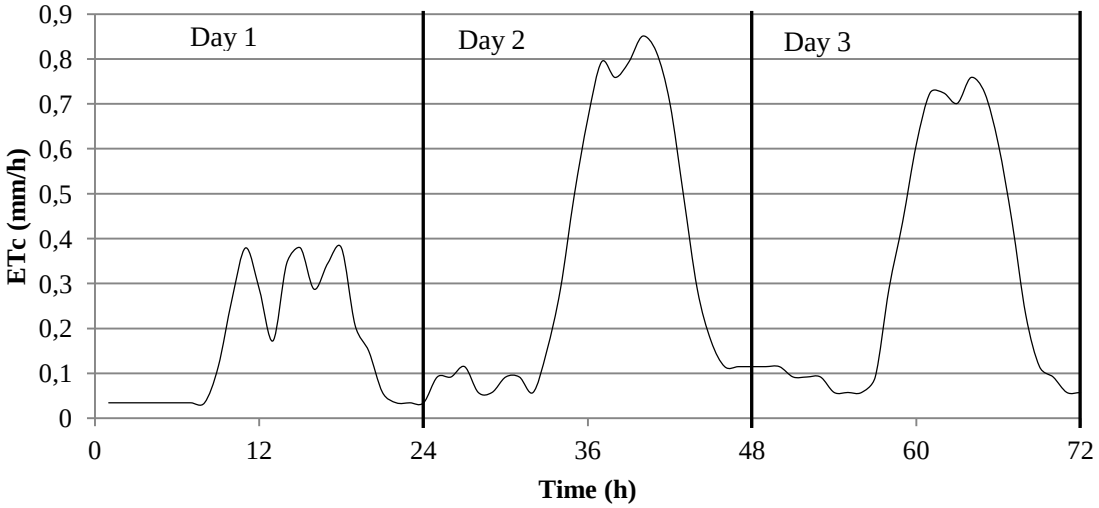

Figure 3.11: Potential evapotranspiration (ETc) characteristics at SCL farm for a period of three days (7.6.2011 (Day 1), 11.6.2011 (Day 2) and 12.6.2011 (Day 3))
Slika 3.11: Karakteristike potencialne evapotranspiracije (ETc) za SCL kmetijo za obdobje treh dni (7. 6. 2011 (Dan 1), 11. 6. 2011 (Dan 2) in 12. 6. 2011 (Dan 3))

The sum of hourly ETc was 3.75 mm/day, 8.27 mm/day and 7.34 mm/day for day 1, day 2 and day 3, respectively

3.6.3 Corn irrigation characteristics

For corn irrigation at SCL T-tape drip tape with emitter spacing of 0.33 m and *Q* of 1 L/h is used. The drip line (lateral) spacing is 0.75 m (one drip line per row), resulting in 4.04 mm/h application. The crop is irrigated on the daily basis. Water is at SCL usually applied in 30 min intervals or 2.02 mm applications. The corn plants have the spacing of 0.75 m between rows and 0.18 m within a row which gives a density of 7.41 plants/m^2 (Figure 3.12).

There is a concern that large amounts of water and nutrients are lost because of inadequate sweet corn irrigation management in the very permeable sandy soil. No design and scheduling programme tools or excavations, to observe water distribution on the site, have been used to better manage the irrigation system. In addition, irrigation is not adjusted to crop water demand for different crop growth stages; the application rate is set close to the maximum plant water demand of 7 mm/day during the whole crop growth period. It was estimated by Hess (2011) that irrigation water application exceeds sweet corn crop water requirements by 50–100 % which is indicating substantial over irrigation and consequently waste of water and nutrients.

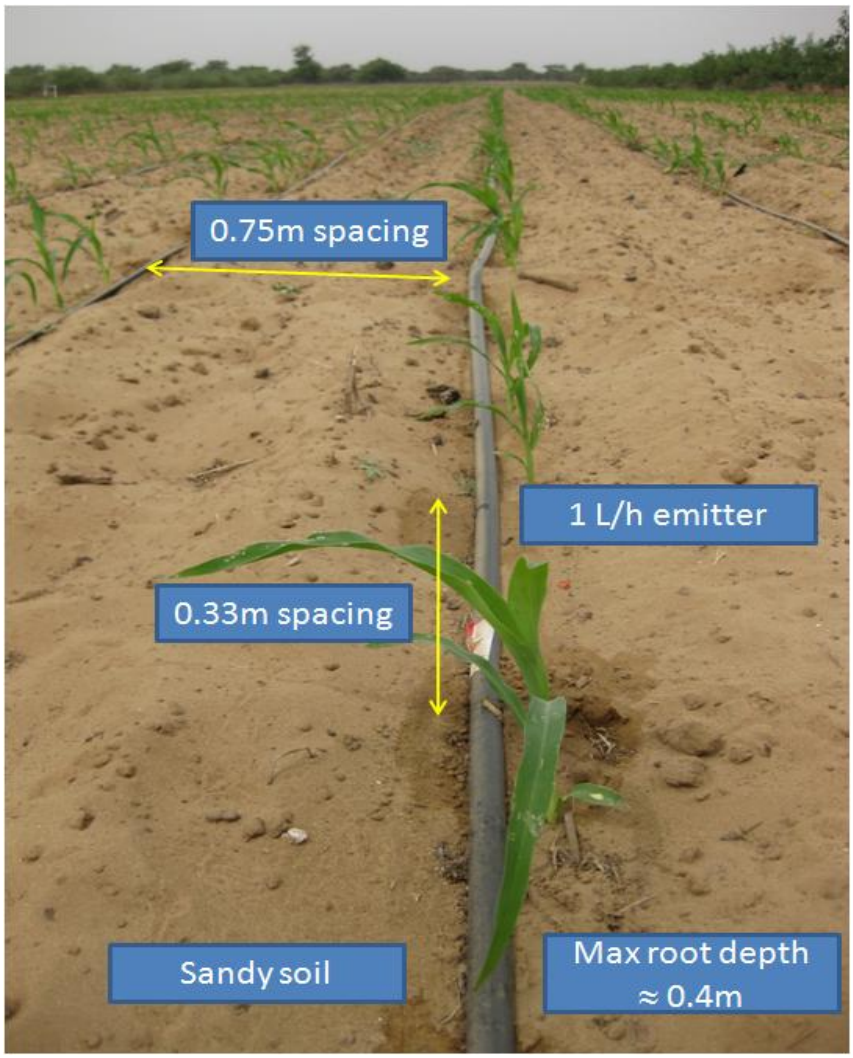

Figure 3.12: Layout of corn irrigation at SCL farm in Senegal
Slika 3.12: Postavitev namakanja koruze na SCL kmetiji v Senegalu

3.6.4 Soil hydraulic properties

The soil analyses showed that the soil at the corn irrigation site is deep uniform sand, with the mean soil particle distribution of 87.5 % sand, 9 % silt, 3.5 % clay, bulk density of 1.6 g/cm^3 and saturated hydraulic conductivity of 0.49 m/day (2.04 cm/h). Particle size distribution was determined on a peroxidised, oven-dry basis. Bulk density and water holding characteristics were determined on an oven-dry basis.

3.6.5 Hydrus-2D/3D setup

Water movement under corn crop was simulated for period of 15 or 16 days (depending on irrigation strategy) using the Hydrus-2D/3D (v2.0). Simulations were done with three

dimensional axisymmetrical domain geometry. The modelled domain was 40 cm wide and 50 cm deep. It was assumed to have uniform soil physical properties. A new special BC for surface drip with dynamic wetting was used for the upper BC, no flux BC for vertical boundaries and free drainage BC for lower boundary (Figure 3.13).

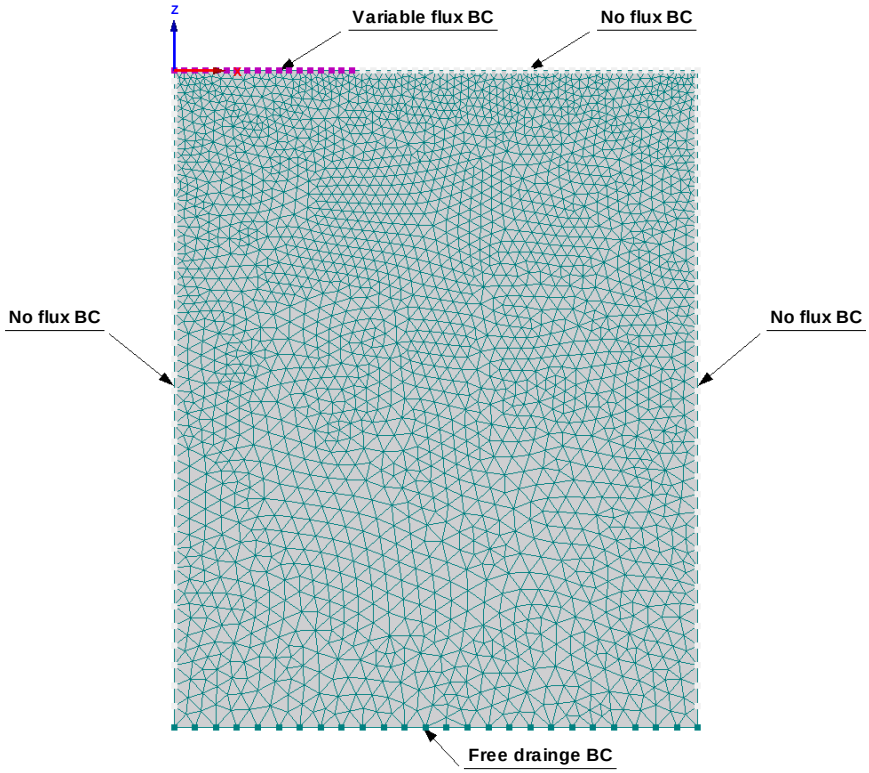

Figure 3.13: Spatial discretization of the 2D axisymmetrical flow domain and its BC used for simulations of corn irrigation
Slika 3.13: Prostorska diskretizacija 2D aksisimetrične pretočne domene in njeni robni pogoji, uporabljeni za simulacije namakanja koruze

Soil properties needed as input for model are presented in Table 3.10. Water retention data for the sand soil were determined using a pressure-plate apparatus. *Ks* was determined usinga a constant head method. The Code for Quantifying the Hydraulic Functions of Unsaturated Soils (RETC) software (van Genuchten et al. 1991) was used to fit the unknown van Genuchten - Mualem equation parameters (α and n) from observed water retention data. θ_s and θ_r were selected according to volumetric water content at soil saturation and PWP.

Table 3.10: Parameters of van Genuchten-Mualem model used for Hydrus simulations
Preglednica 3.10: Parametri van Genuchtnovega-Mualem modela, uporabljeni za Hydrus simulacije

Soil texture	θ_s (cm^3/cm^3)	θ_r (cm^3/cm^3)	α (1/cm)	n	Ks (cm/h)	l
Sand	0.502	0.0335	0.0492	1.89	2.04	0.5

Root depth was assumed to be 40 cm (Hess, 2011) with the maximum radius of 16.5 cm (Figure 3.14). Corn root distribution assessed by Laboski et al. (1998) for sandy soil showed that on average 94 % of total root length within the upper 0.60 m of soil with 85 % in the upper 0.30 m of soil. Depth of maximum root intensity was set at 15 cm with radius of maximum intensity was 16.5 cm. The root radial extend and depth of maximum intensity was set according to research done by Coelho an Or, 1999 and Gao et al. (2010). Simulation period corresponded to the mid growth period, during which plants were fully developed and root system was constant. To reduce the potential root water uptake to actual root water uptake the water stress response function as suggested by Feddes et al. (1978) was used. The parameter TH (potential transpiration rate) was set to 8.2 mm to meet the simulated local conditions.

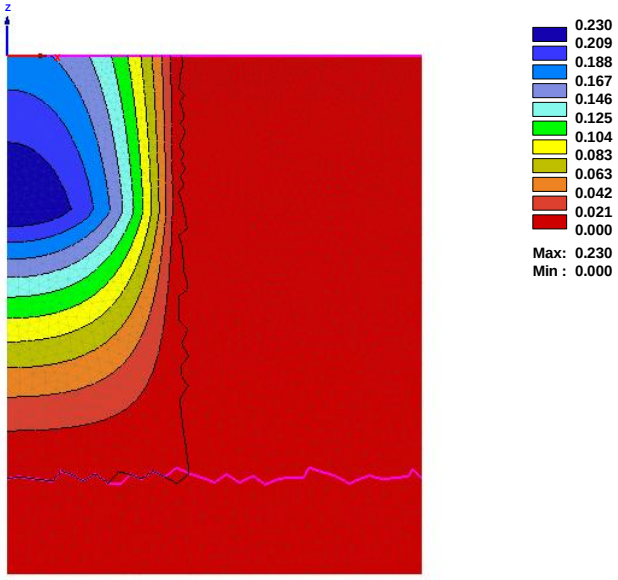

Figure 3.14: Root distribution used for Hydrus-2D/3D simulations. The legend shows the root distribution, where red means there are no roots and dark blue means there is maximum root density
Slika 3.14: Distribucija korenin, uporabljena za Hydrus-2D/3D simulacije. Legenda prikazuje distribucijo korenin, pri čemer rdeča barva pomeni, da korenin niso prisotne, in temno modra barva pomeni, da je gostota korenin največja.

The required Fedde's parameters are presented in Table 3.11 and were selected as suggested in Hydrus-2D/3D database. The parameters $h_{3\ high}$ and $h_{3\ low}$ were chosen as to represent the 50 % of soil water depletion for specified soil. 50 % was selected as depletion fraction of available water according to the Allen et al. (1998) recommendations.

Table 3.11: Fedde's parameters for sweet corn root water uptake used as input for Hydrus simulations
Preglednica 3.11: Feddesovi parametri za odvzem vode skozi korenine sladke koruze, uporabljeni za Hydrus simulacije

Fedde's parameters	h_1 (cm)	h_2 (cm)	$h_{3\ high}$ (cm)	$h_{3\ low}$ (cm)	h_4 (cm)	TH (cm/h)	TL (cm/h)
	-10	-50	-116	-116	-15000	0.034	0.004

Irrigation requirement *Qr* (L/day) was calculated from the crop ETc (cm/day) and the area of irrigated soil allocated to one emitter. Hourly values of ETo, provided from SCL farm, for 11th of June 2011 were normalised to obtained a function representative of hourly ETo variations. This function was used to derive hourly ETo over the 15-16 days simulation period by using daily ETo data. Hourly amounts of water applied and transpiration rates were used as a time-variable boundary conditions in Hydrus. Daily irrigation amount of 8.3 mm/day was provided by 4.04 emitters per m^2 (given by the line and emitter spacing), the daily application rate per 1 emitter was calculated as 2.05 L. The surface area associated with transpiration was set as 2475 cm^2 (given by irrigation system design characteristics). The amount of applied water through irrigation and amount of water lost through transpiration were about the same. It was assumed no rain occurred during irrigation period. Evaporation from the soil surface was neglected as it was fully covered by the plants canopy during simulation period. Initial water content of 0.21 cm^3/cm^3 was chosen close to soil field capacity (FC) of the soil. FC was selected at -5 kPa or -50 cm resulting in 0.228 cm^3/cm^3.

Five irrigation strategies were selected to represent possible drip irrigation management of sweet corn (Figures 3.15 and 3.16). Water applied with irrigation was covering 100 % of the corn daily ETc in all cases.

The strategies were as follows:

- Strategy 1 – Continuous irrigation starts every day at 7.00 h in the morning and lasts until 9.03 h.
- Strategy 2 – Continuous irrigation starts every day at 21.30 h in the night and lasts until 23.33 h.
- Strategy 3 – Irrigation is divided into 4 daily pulses. Each pulse lasts for half an hour and 0.5 L of water is added, except in the last pulse, where 0,546 L is applied. First pulse starts at 8 h, second at 10 h, third at 12.30 h and fourth at 14.30 h.
- Strategy 4 – Water is continuously applied every two days. Irrigation starts at 7.00 h in the morning and lasts until 11.06 h.
- Strategy 5 – Water is applied every two days. Irrigation is divided into 8 pulses and, the same as for strategy 3, 0.5 L of water is applied with each pulse. Irrigation pulses start a t 8 h and follow at 10 h. 12 h, 14 h, 16 h, 18 h, 20 h and 22 h.

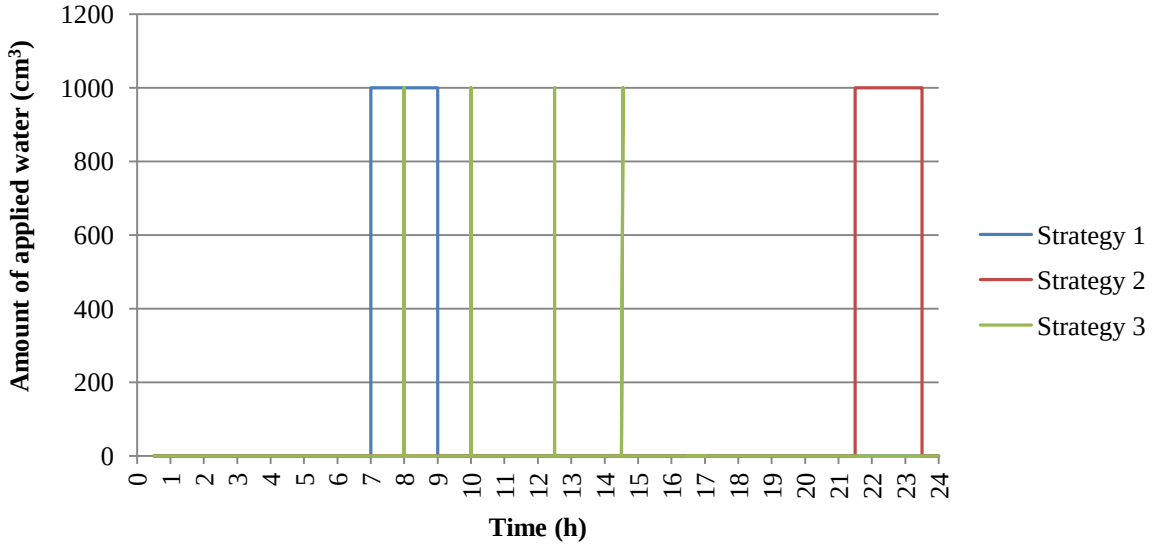

Figure 3.15: Different irrigation strategies where water was applied daily. In strategies 1 and 2 water was applied continuously and in strategy 3 with 0.5 L pulses
Slika 3.15: Različne strategije namakanja sladke koruze, kjer je bila voda aplicirana vsak dan. Pri strategijah 1 in 2 je bila voda dovajana neprekinjeno, pri strategiji 3 pa v kratkih 0.5 L pulzih.

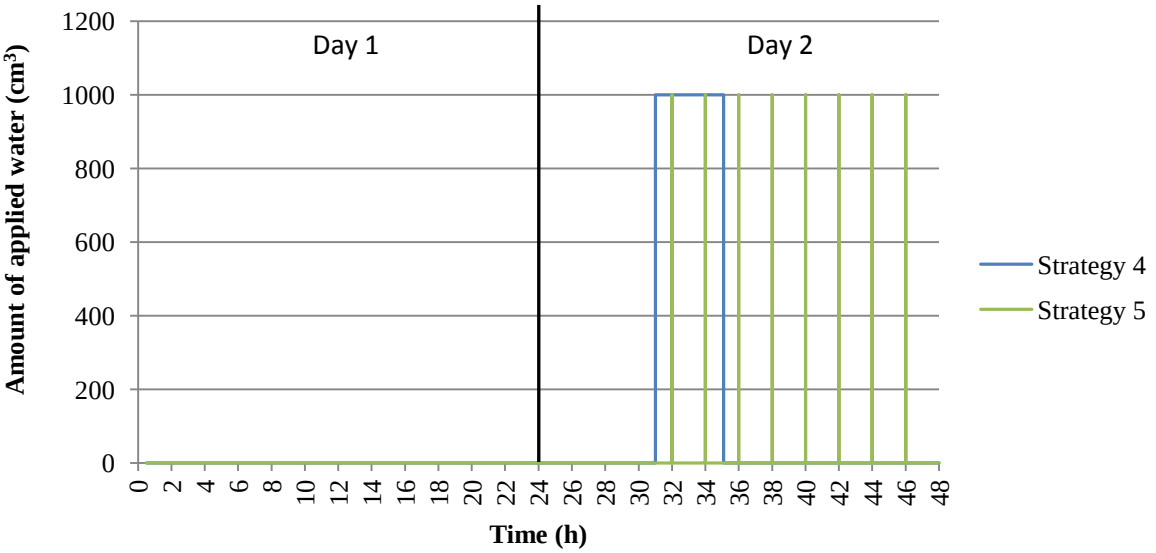

Figure 3.16: Sweet corn irrigation strategies 4 and 5 where water was applied every 2 days. In strategy 4 water was applied continuously and in strategy 5 with 8 pulses
Slika 3.16: Strategije (4 in 5) namakanja sladke koruze, kjer je bila voda aplicirana vsak drugi dan. Pri strategiji 4 je bila voda dovajana neprekinjeno, pri strategiji 5 pa v 8 pulzih.

Strategies 1, 2 and 3 were simulated for 15 days and in all cases 2.05 L of water was applied (equal to plants ETc). Strategies 4 and 5 were simulated for 16 days and 4.1 L of water was applied every two days to meet plant water needs.

The water content distribution was measured for the last irrigation cycle (15th day) or, for pulsed treatments, for the last irrigation pulse (16th day).

With the purpose of water content monitoring during irrigation simulations three observation nodes were placed beneath the emitter at three different soil depths. Node 1 was placed at 10 cm, node 2 at 20 cm and node 3 at 40 cm.

3.7 NUMERICAL AND EXPERIMENTAL STUDY OF HOP SURFACE DRIP IRRIGATION

3.7.1 Experimental site description

The experimental site was located at the field of Institute of Hop Research and Brewing (IHPS) in Žalec, Slovenia, with coordinates 46°24'N, 15°16'W, and elevation of 255 m above sea level (Figure 3.17).

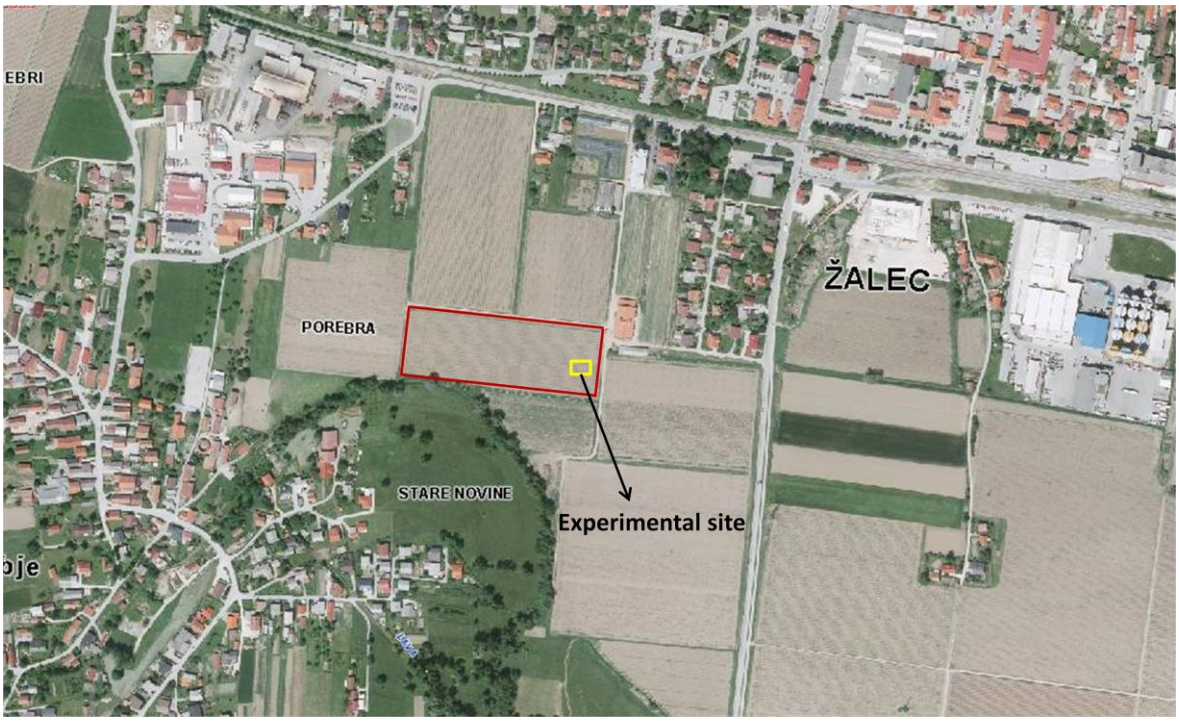

Figure 3.17: Experimental site (yellow rectangle) at the field of IHPS in Žalec and surrounding area (MKO, 30.8.2013)
Slika 3.17: Eksperimentalno območje (rumen kvadrat) na polju IHPS v Žalcu in okolica (MKO, 30.8.2013)

3.7.2 Climate and plants characteristics

The site is characterised by interaction of alpine and continental climate with mild to hot summers and cold winters. Air distance between Žalec and nearest meteorological station, located in Celje (Medlog), is 4.43 km. The monthly average rainfall and temperatures for period 1991 – 2000 for Celje station are presented in Table 3.12 (ARSO, 30.8.2013). Slovenia gets enough annual precipitation, but the rainfall is unevenly distributed over the plants growth season. As a consequence severe summer droughts are common phenomenon (Knapič and Pintar, 1998).

Table 3.12: Average monthly temperatures (°C) and rainfall (mm) for period 1971 to 2000 and for 2012 for agrometeorological station Celje-Medlog
Preglednica 3.12: Povprečne mesečne temperature (°C) in padavine (mm) za obdobje od 1971 do 2000 in za 2012 za agrometeorološko postajo Celje-Medlog

	Jan	Feb	Mar	Apr	May	Jun	Jul	Aug	Sep	Oct	Nov	Dec	Year
Average temp. (°C)	-0,7	1.0	5.1	9.4	14.6	17.9	19.6	18.9	14.8	9.6	4.1	0.3	9.6
Average precipitation (mm)	49	52	70	77	90	134	132	123	109	117	102	76	1129
Average temp. for 2012(°C)	0.7	-3.1	7.8	10.8	15.2	20.3	21.4	20.8	16	10.6	8.1	0.2	10.7
Average precipitation for 2012(mm)	16.1	31.5	7.4	97.6	143.3	79.8	95.7	47.4	200.2	205.3	109.0	72.6	1105.9

Average monthly reference evapotranspiration values for 30 years period compared to average monthly values for 2012, for station Celje, are given on Figure 3.18.

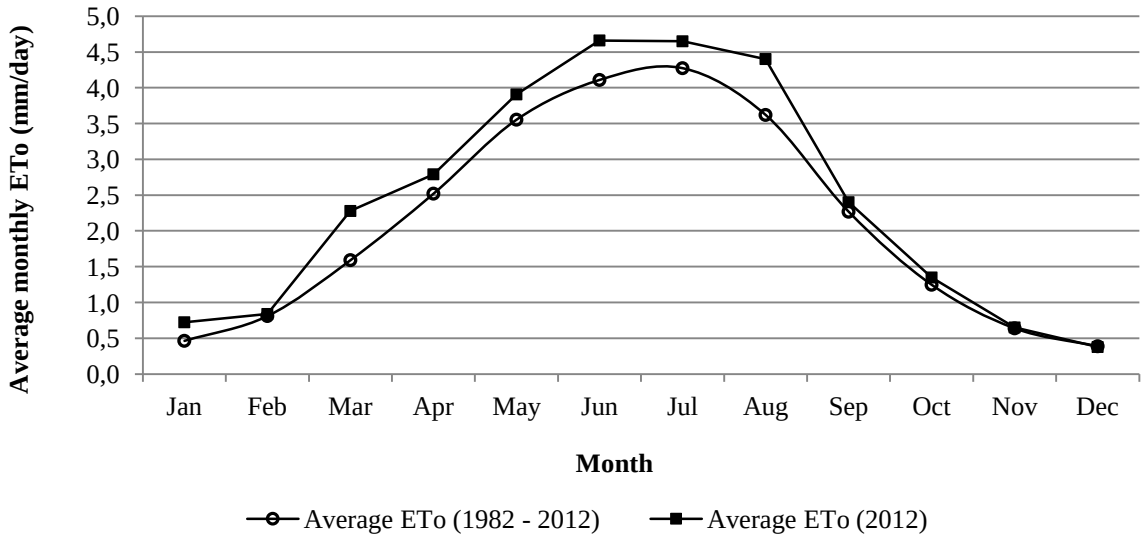

Figure 3.18: Average monthly reference evapotranspiration (ETo) for 30-years period (1982-2012) and 2012 for agrometeorological station Celje-Medlog
Slika 3.18: Povprečna mesečna referenčna evapotranspiracija (ETo) za 30-letno obdobje (1982-2012) in za leto 2012, za agrometeorološko postajo Celje-Medlog

On Figure 3.19 the ETo and ETc from the meteorological station Celje are shown for the time of experiment duration. The Kc values used were gained from Knapič (2002) and are presented in Table 3.13. A Kc of 1.15 was selected as representative for ETc calculations.

Table 3.13: Crop coefficients (Kc) with regard to hop plants development and growth stage (Knapič, 2002)
Preglednica 3.13: Faktorji rastlin (Kc) glede na rastno obdobje in razvoj hmelja (Knapič, 2002)

Month	Kc
April	0,3
May	0,6
June	0,9
July	1,15
August	1,15 (until technological maturity)

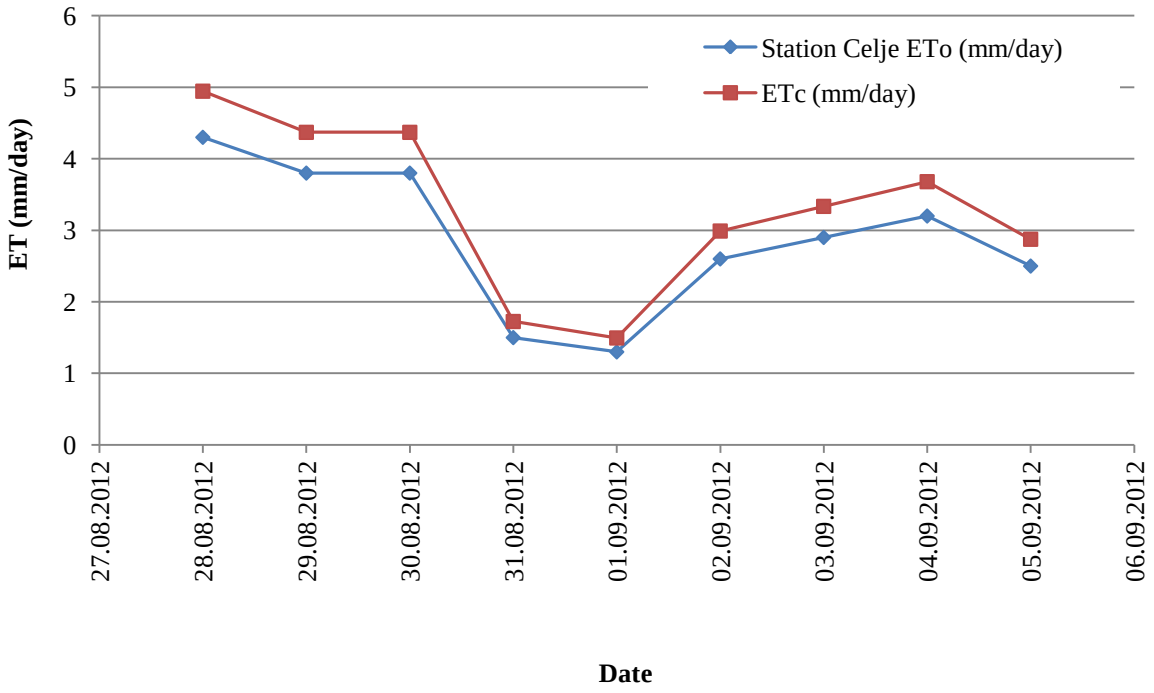

Figure 3.19: Crop reference (ETo (mm)) and potential (ETc (mm)) evapotranspiration for the duration of the experiment (from 28.8.2012 to 5.9.2012)
Slika 3.19: Referenčna (ETo (mm)) in potencialna (ETc (mm)) evapotranspiracija hmelja za obdobje trajanja poskusa (od 28. 8. 2012 to 5. 9. 2012)

For the purpose of Hydrus simulations the ETo (mm/day) daily values were converted to hourly ETo (mm/h). The Penman - Monteith hourly reference evapotranspiration was calculated from daily values as recommended by the Environmental and Water Resources Institute (EWRI) and American Society of Civil Engineers (ASCE) in the ASCE-EWRI Task Committee Report (ASCE-EWRI, 2005) titled The ASCE standardized reference evapotranspiration equation. The calculation software to calculate hourly ETo values from daily ones, following the approach described in the ASCE-EWRI report, was developed by

Snyder and Eching (2006). The programme requires input data of longitude, latitude and elevation of the site and hourly data about solar radiation, mean air temperature, mean wind speed and mean dew point temperature. Hourly ETo values were multiplied by Kc of 1.15 and are given in Figure 3.20.

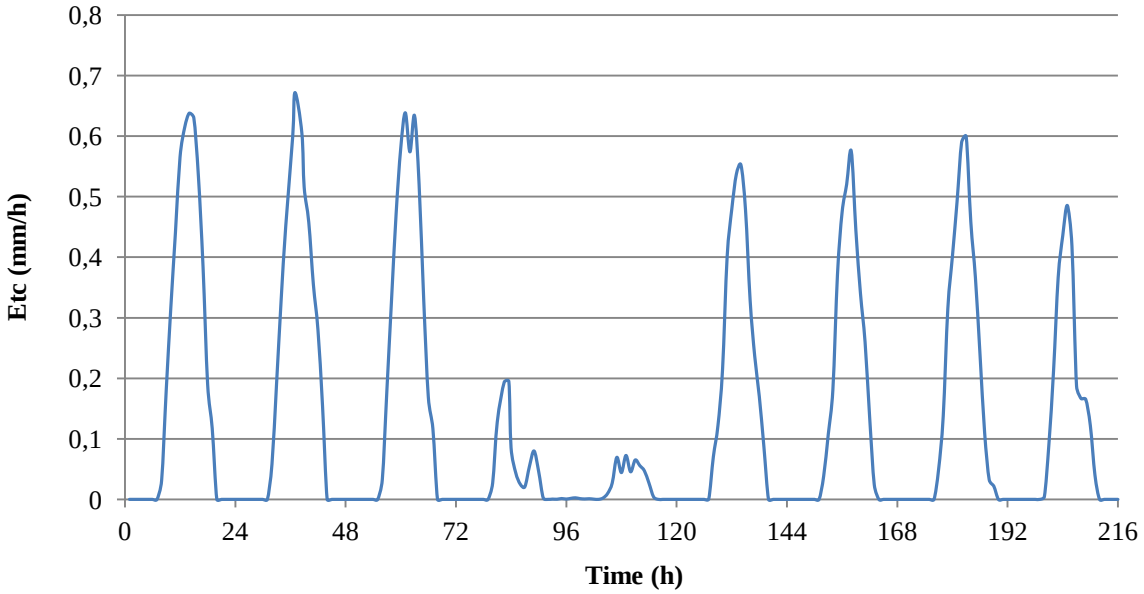

Figure 3.20: Hourly values of ETc (mm/h) obtained from agrometorological station Celje-Medlog for period from 28. 8. 2012 to 5. 9. 2012

Slika 3.20: Urne vrednosti potencialne evapotranspiracije ETc (mm/h), pridobljene iz agrometeorološke postaje Celje-Medlog, za obdobje od 28. 8. 2012 do 5. 9. 2012

Calculated ETo hourly values were summarized for each day of the experiment and compared to daily ETo values from meteorological station Celje. The results are presented in Figure 3.21. It has to be noted that the sum of hourly ETo values, using standardized ETo equation for plants with short canopies, fitted better with measured ETo values from station Celje, when compared to the sum of ETo for tall canopies. Therefore ETo calculation for short canopies was used as a reference throughout this research.

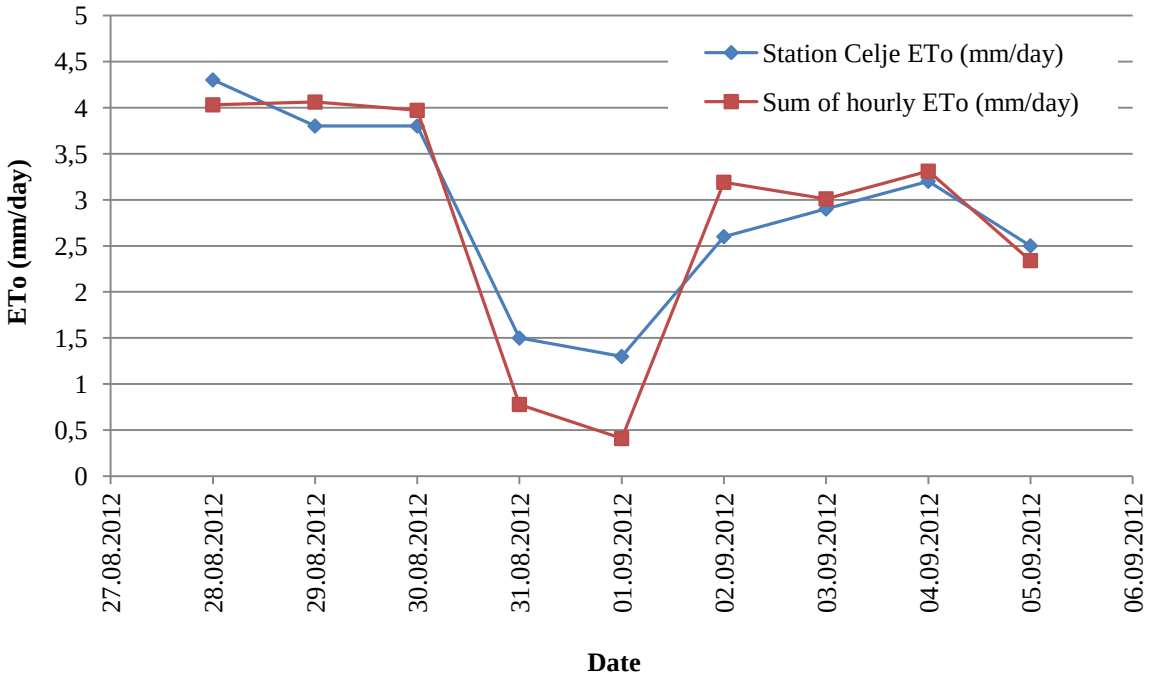

Figure 3.21: Comparison of reference evapotranspiration (ETo (mm/day)) values and daily sum of hourly ETo (mm/day) values for short canopy obtained at agrometeorological station Celje-Medlog for period from 28. 8. 2012 to 5. 9. 2012
Slika 3.21: Primerjava referenčnih evapotranspiracijskih (ETo (mm/dan)) vrednosti in vsot urnih ETo (mm/dan) vrednosti za kratko krošnjo, pridobljenih na agrometeorološki postaji Celje-Medlog za obdobje od 28. 8. 2012 do 5. 9. 2012

The hop field at the experimental site was planted in 2006 with hop variety Dana. The spacing between the rows was 2.8 m and 1.1 m within a row. Rows were oriented in east-west direction. Hop field was pruned on the 13th of April and shed three times: on the 17th of May, 20th of June and on 19th of July 2012. The field was fertilised and sprayed according to standard agricultural practices of hop production in the surrounding area.

3.7.3 Experiment setup

The experiment was conducted in the summer 2012, from 23rd of August until 6th of September. Because of technical problems with TDR probes the experiment started on the 28th of August. The experiment was terminated on the 6th of September, when TDR probes were removed and calibrated.

The pedological characteristics of soil profile were determined on the experimental site, which was a part of the 2.04 ha big hop field (240 m×85 m). The hop field was not irrigated, but for the purpose of the experiment, the 5 m long drip line (Netafim®, 17 mm) was placed along a single hop row, on the top of the soil ridge. One emitter representing

the water point source was isolated, to prevent wetting patterns overlapping from the neighbouring emitters (Figure 3.22).

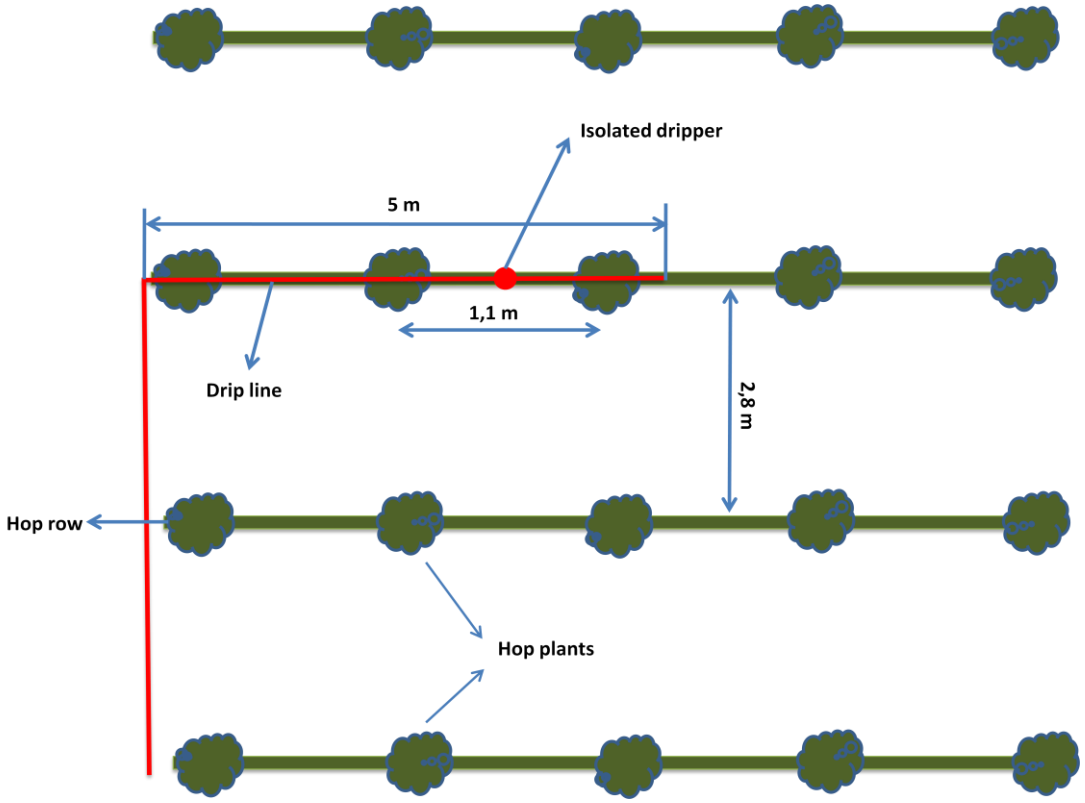

Figure 3.22: Schematic presentation of the experimental setup at the IHPS hop field in Žalec
Slika 3.22: Shematski prikaz eksperimentalne postavitve v nasadu hmelja na IHPS v Žalcu

Emitter nominal discharge rate was 1.6 L/h and it was placed 30 cm from the vertical wall of excavated soil profile. The average measured discharge rate per one dripper was 1.47 L/h. Water for irrigation system was provided by a nearby groundwater pumping station. Plants water demand was not important for this experiment, since the purpose was only to assess the accuracy of Hydrus simulations when compared to realistic field conditions. During duration of field experiment irrigation was carried out as shown in Table 3.14.

Table 3.14: Days with irrigation events and duration (h) at the experimental site in 2012
Preglednica 3.14: Dnevi z izvajanjem namakanja in trajanje namakanja (ure) na lokaciji poskusa v letu 2012

Date	Irrigation interval (h)		Irrigation duration (h)
	From	To	
29.8. 2012	12:30:00	14:30:00	2
31.8.2012	10:31:00	11:31:00	1
4.9.2012	11:00:00	13:00:00	2
5.9.2012	11:00:00	14:00:00	3

3.7.4 Soil physical and hydraulic properties

The soil profile was dug out perpendicularly to the hop row. The soil type was classified as Riverside, Groundwater Deep Gley. The soil on the site was composed out of 5 distinctive soil layers to the depth of 80 cm. The soil layers were determined as follows: P horizon (from 20 – 0 cm, which is an artificially made hop ridge), A_1 horizon (from 0 – 20 cm), A_2 horizon (from 20 – 35 cm), AG_o horizon (from 35 – 50 cm) and G_oA horizon (from 50 – 80+ cm) (Figure 3.23). On each side of the hop ridge a compacted soil zone was located which extended to a soil depth of around 50 cm ± 2 cm (Figure 3.24). Soil compaction was assessed on the basis of soil structure aggregates expression, which were, in the compacted zone, destroyed and highly compressed. Below this zone the structure of soil layers was well expressed. The occurrence of this zone was due to regular heavy machinery traffic. To prevent soil compaction in hop production industry a subsoiler is used in the autumn. With this operation the soil is loosened between the rows to a depth of approximately 30 to 40 cm. It has to be noted, that subsoilers destroy the roots which, during the hop growing season, penetrate in the compacted zone. Also, during the hop growing season, the cultivators are used to loosen the topsoil and destroy the weeds between the rows. Their working depth varies from 5 to 20 cm and depends on the type of cultivator (Friškovec, 2002). Because subsoilers are used only in autumn, during the hop growing season compaction zone forms again and is influencing soil water movement, water infiltration, soil aeration and roots development in this zone (Hillel, 2004). Also, as mentioned by Chesworth (2008) the soil compaction results in slightly higher bulk density, lower macroporosity and lower *Ks*.

Figure 3.23: Soil profile excavated between two hop plants along the ridge showing four soil layers
Slika 3.23: Izkopan talni profil s štirimi sloji tal med dvema rastlinama hmelja, gledano vzdolž grebena.

The soil horizon G_oA which occurs at the depth of 50 – 80+ cm was not included in further analysis because, as mentioned by Knapič (2002), the decision when to start with irrigation, is based on 50 % depletion (Allen et al., 1998) of plant total available water in the upper 40 cm of the soil.

Figure 3.24: Compacted soil zone on one side of the hop ridge at the IHPS experimental field. The compacted zone extends to a soil depth of around 50 cm
Slika 3.24: Zbita cona tal na eni strani grebena na eksperimentalnem polju IHPS. Zbita cona tal sega do globine približno 50 cm.

The analysis revealed that the soil was on average (combining soil layers) silty clay loam, with 18.27 % sand, 46.77 % silt and 34.96 % clay. Three undisturbed soil samples were taken in each soil layer (Figure 3.25). The laboratory evaporation method HYPROP® was used to determine water retention data and to fit van Genuchten-Mualem function to the measured data.

Hyprop is a registered trademark of the UMS Company (Germany). Evaporation method is a fast and simple technique to determine the soil water retention curves. The method was first proposed by Wind, 1968. Hyprop uses the simplified evaporation method, developed by Schindler (1980), where pressure head measurements are carried out at two different depths using two small tensiometers. The soil in between the two tensiometers represents the volume of soil which is analysed. The soil sample in a 250 ml soil sampling ring is first saturated, placed on the scale and closed on the bottom. The upper side of the sample stays open, so the evaporation process at the soil surface can occur. The mean water content is derived from the mean pressure head and column weight, and is assessed at every time step, to get the water flow rate and data for the water retention function. From the total loss of water the initial water content (θ^i) can be determined. Average water content $\theta_a{}^i$ can be

derived from the θ^i and weight loss and the average water tension $h_a{}^i$ gives a retention function value $\theta_a{}^i(h_a{}^i)$ at every time step. The measurements lasts until the tensiometers run dry (at -85 kPa; with proper filling they may sometimes work beyond -250 kPa) or the change in mass becomes negligible. The procedure is based on the assumption that water content and water tension distribute through the column linearly. Another assumption is that the changes between the water tension and weight of the sample are linear between two tensiometer heights (Peters and Durner, 2008). Peters and Durner (2008) investigated the errors that result from the linearization assumptions, and show how systematic and stochastic measurement errors affect the calculation of water retention and hydraulic conductivity data and the resulting fits of soil hydraulic functions. They found that linearization errors with respect to time are negligible if cubic Hermite splines are used for data interpolation.

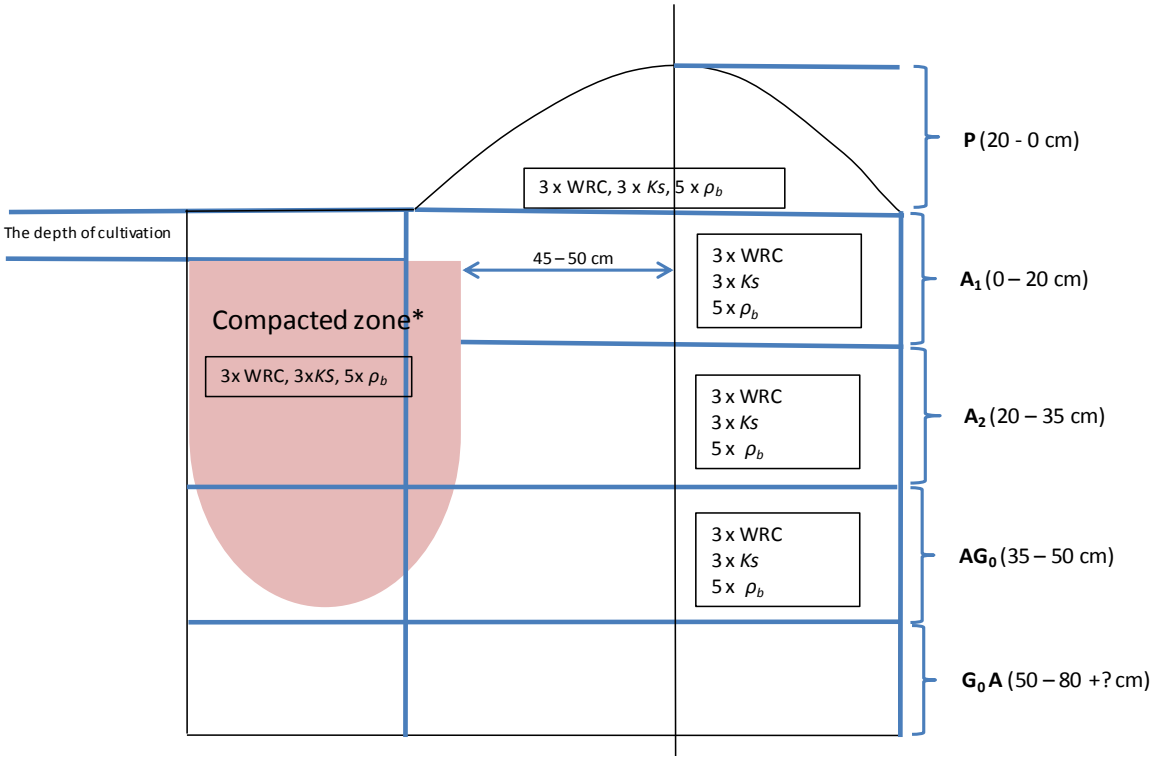

Figure 3.25: Schematic presentation of the soil profile characteristics at the IHPS experimental field with number of samples taken from each soil layer (WRC – water release curve, ρ_b – bulk density, *Ks* – saturated hydraulic conductivity)
Slika 3.25: Shematski prikaz značilnosti talnega profila na eksperimentalnem polju IHPS s prikazanim številom odvzetih talnih vzorcev iz vsakega sloja tal (WRC – vodnoretenzijska krivulja, ρ_b – gostota tal, *Ks* – nasičena hidravlična prevodnost)

Schindler et al. (2010) presented a new approach where the tensiometer-cup air-entry pressure is used as additional tension measurement. This extends the tension measurement range towards the dry soil conditions range considerably and accordingly stretches the water range where soil hydraulic functions can be better quantified. Because the above

mentioned method does not define the fitting towards dryness so well, the soil water content at PWP was also determined on disturbed soil samples for all soil layers, using a pressure plate apparatus (Richards, 1942). This additional measured point improves the VG fit towards the dry end of the retention curve. The VG curve was then fitted to the replicate measurements and the best fit and the most realistic (visually observed) retention curve was selected (Table 3.15, Figure 3.26).

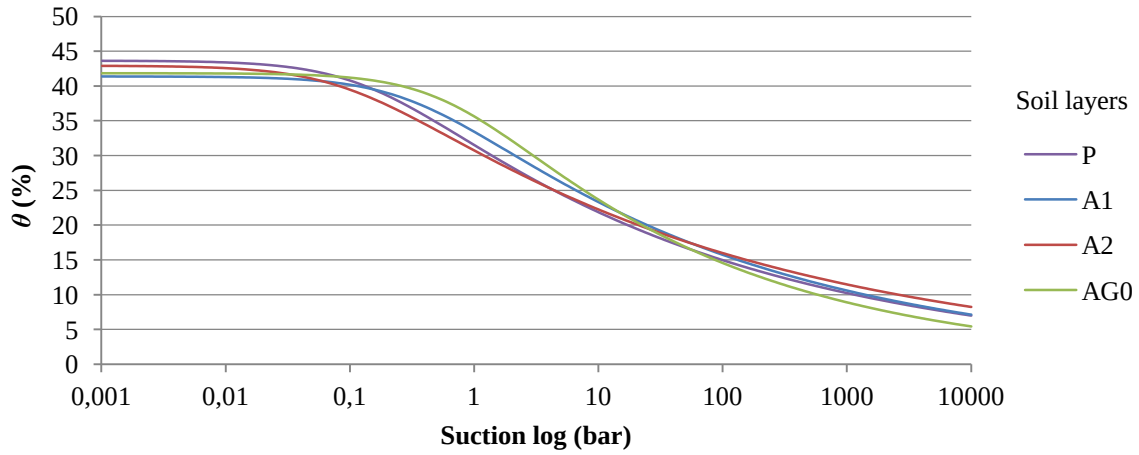

Figure 3.26: Selected water retention curves as resulted in Hyprop for all soil layers occurring in the soil profile at the experimental site
Slika 3.26: Izbrane vodnoretenzijske krivulje za vse sloje tal v talnem profile na eksperimentalnem polju, ki so rezultat Hyprop metode.

For all soil samples *Ks* was determined in the laboratory with constant head method using Darcy apparatus (Table 3.15). Undisturbed soil samples were taken with the Kopecky rings (5.1 cm height, 5 cm diameter and 100 cm^3 volume). As shown on Figure 3.21, three soil samples were taken from each soil layer. It is well known, that determined *Ks* values of a given soil profile can vary by orders of magnitude between the layers. The variability can occur even within a specific soil layer (Deb and Shukla, 2012). As suggested by Oosterbaan and Nijland (1994) a representative value of *Ks* can be obtained from the geometric mean. The same approach was followed in this research. It has to be noted that the samples taken in the compacted zone were considered impermeable (*Ks* was equal to 0 cm/h), because water did not penetrate through the soil sample in 12 days of samples saturation in Darcy apparatus.

Soil ρ_b was determined as suggested in Grossman and Reinsch (2002) following the core method approach. Five undisturbed soil samples were taken from each soil layer using the Kopecky rings. Soil dry mass divided by the ring volume yielded in soil dry ρ_b which was for the final result averaged for each soil layer (Table 3.15). All together 25 soil samples were analysed for soil ρ_b determination.

Table 3.15: Parameters of van Genuchten-Mualem model for soil layers at the IHPS experimental site in Žalec
Preglednica 3.15: Parametri van Genuchtnovega-Mualem modela za sloje tal na eksperimentalnem polju IHPS v Žalcu

Soil layer	Soil depth (cm)	Soil bulk density (g/cm^3)	θ_s (cm^3/cm^3)	θ_r (cm^3/cm^3)	α (1/cm)	n	Ks (cm/h)	l
P	20-0	1.30	0.437	0	0.0066	1.165	11.24	0.5
A_1	0-20	1.42	0.414	0	0.0028	1.172	1.74	0.5
A_2	20-35	1.49	0.440	0	0.0036	1.183	1.28	0.5
AG_o	35-50	1.49	0.418	0	0.0014	1.214	2.37	0.5
Compacted zone		1.63	0.410	0	0.0031	1.164	0	0.5

Soil FC was determined for each soil layer as suggested by Cassel and Nielsen (1986). FC measurements were necessary for determination of Feddes' parameters for the root water uptake modelling in Hydrus-2D/3D. Four different approaches for determining soil FC were used for the purpose of this study. Firstly, for determination of FC, the soil profile was saturated and soil water content in each soil layer was measured 2 and 3 days after saturation, as suggested by Chesworth (2008). For this purpose a rectangular box was placed on bare soil which was subsequently flooded with water. Two tensiometers were installed at different depths, 20 and 40 cm, to ensure the soil was fully saturated (Figure 3.27). To prevent the evaporation from the soil surface, the soil was covered with a plastic sheet. Three disturbed soil samples from each soil layer were taken with steel auger after 48 (2 days), 72 (three days) and 120 h (5 days). Volumetric water content was calculated multiplying gravimetric water content with soil ρ_b. Second approach followed Cassel and Nielsen (1986) study, which reported that soil FC can be obtained in the laboratory where a wide range of matric potentials (from -2.5 kPa to -50 kPa) can used for this purpose, although suctions of 5 kPa, 6 kPa, 10 kPa, and 33 kPa are the most common. In Slovenia a FC is commonly approximated at -33 kPa (-0.33 bar) in heavier soils (Pintar, 2006). The water content at -33 kPa (-0.33) bar was determined from the water release curves presented in Figure 3.26. However, as mentioned by Hillel (2004), there is no satisfactory universal criterion of this sort suggesting the suction values for the determination of soil FC. The third approach was to use a new version of Hydrus-2D/3D which includes new option, where soil water conditions can be set equal to its field capacity, following approach of Twarakavi et al. (2009). At last, as a fourth approach, the situation under consideration was simulated with Hydrus-2D/3D without considering root water uptake. The simulation was started with saturated soil and a free drainage BC was selected for bottom boundary of the domain.

Figure 3.27: Soil field capacity (FC) determination (rectangular box with two tensiometers installed at two different soil depths of 20 and 40 cm)
Slika 3.27: Določanje poljske kapacitete tal za vodo (FC) in pravokotna škatla z dvema vstavljenima tenziometroma na globinah 20 in 40 cm

The observation nodes were inserted in the middle of each soil layer and water content was determined after 48 and 72 hours of drainage for each node. It has to be noted that FC was not measured in the compacted zone. All above mentioned different approaches for soil FC determination are presented in Table 3.16.

Table 3.16: Different approaches for determination of soil field capacity (FC) at the IHPS experimental field
Preglednica 3.16: Različni pristopi za določanje poljske kapacitete tal za vodo (FC) na eksperimentalnem polju IHPS

FC determination approach	Soil layer			
	P	A_1	A_2	AG_o
FC measured after 72 h	0.32	0.33	0.34	0.36
FC simulated with Hydrus after 72 h	0.32	0.34	0.30	0.35
FC 0.33 bar	0.37	0.37	0.35	0.39
Twarakavi et al. (2009) Hydrus	0.33	0.34	0.33	0.30
Selected values	0.32	0.34	0.32	0.36

Based on the results from Table 3.16, the FC of the soil was selected after 72 h of water redistribution. The FC measured at the field and the FC simulated with Hydrus model, were in very good agreement, except for the soil layer A_2. Twarakavi et al. (2009) model

performed well, when compared to measured and simulated FC after 72 h. The only mayor difference was observed for AG_o layer. The decision was made, that average of measured and simulated water content at FC after 72 h gives representative FC estimate. The selected soil FC values are shown in the bottom row of Table 3.16.

Not much data can be found in the literature about hop root extent in the soil profile. Some data about the root depth can be found in Allen et al. (1998), where the range of maximum effective rooting depth is given at 1.0 to 1.2 m (the value of 1.2 m represents the root depth for soils with no significant layering or other characteristics that can restrict rooting depth; this value can be used for rainfed conditions also). As mentioned by the authors, the smaller value of 1.0 m may be used for irrigation scheduling purposes. According to Rode et al. (2002) and Neve (1991) the hop roots can, in a mature plant, extend downwards for 1.5 m or more and laterally for 2 – 3 m, but this mainly depends on soil characteristics. According to Allen et al. (1998) and Pintar (2006) 40 % of the root water uptake occurs in the first quarter of the total rooting depth, 30 % in the second quarter, 20 % in the third and only 10 % in the fourth quarter. To provide better water use efficiency under surface drip irrigation, only the upper half of total rooting depth is usually taken into account (Pintar, 2006). This agrees well with Knapič (2002) who noted that only the total available water in the soil (root) depth of 40 cm is important for irrigation scheduling for the hop.

However, as mentioned before, because of hop cultivating practices and consecutive soil compaction, the root lateral extent may be limited. To simulate water uptake by roots, Hydrus simulations require data on the plant roots spatial distribution (both, in vertical and horizontal direction) and root density. Because no convenient data about hop roots spatial distribution under given conditions was available, the hop root system was examined on the site. Methods of uncovering the root system are time and energy demanding and because of a lack of financial resources, the hop root system was examined directly, partly following the approach of Weaver (1926).

Site for root examination included two typical hop plants and was free of weeds. The trench was excavated 70 cm from the plants row and was 110 cm long and 50 – 55 cm deep. The roots were isolated from the trench wall using hand tools. The vertical trench wall was removed gradually moving towards the centre of the plants row. When the root system was completely excavated, the photographs were taken. It was observed that roots extend around 30 cm in horizontal direction (Figures 3.28) and more than 50 cm in vertical one (Figure 3.29). However, the highest root density was observed around the root stock and to a soil depth of around 40 cm, excluding the soil ridge.

Figure 3.28: Root horizontal distance (cm) from centre of hop row. The ridge was 70 cm wide and therefore extended 35 cm on each side of the centre of plants row
Slika 3.28: Horizontalna razdalja (cm) korenin od sredine grebena. Celotna širina grebena je 70 cm oziroma 35 cm na vsako stran od sredine grebena.

Figure 3.29: Root depth (cm) from the centre of the hop row. The ridge was 20 cm high and represented soil layer P (20-0 cm). Most of the ridge containing upper part of the root stock is removed each year with the pruning process
Slika 3.29: Globina korenin (cm) pod sredino grebena. Greben je bil širok 20 cm in je predstavljal talni sloj P (20-0 cm). Večina grebena, kjer je lociran zgornji del štora, je vsako leto odrezana.

During the experiment θ in the soil profile was measured using a TDR system (TDR System Trace 6050 with 6005L Buriable Waveguides, Soilmoisture Equipment corp., California, USA). A theory behind TDR method is in detail presented in Ferre and Topp (2002). TDR probes used for this study were 20 cm long. 22 TDR probes (Figure 3.30) were inserted in excavated soil profile and were directed parallel to the soil surface. The TDR probes were set to measure the soil θ in 30 min intervals for the entire duration of the experiment.

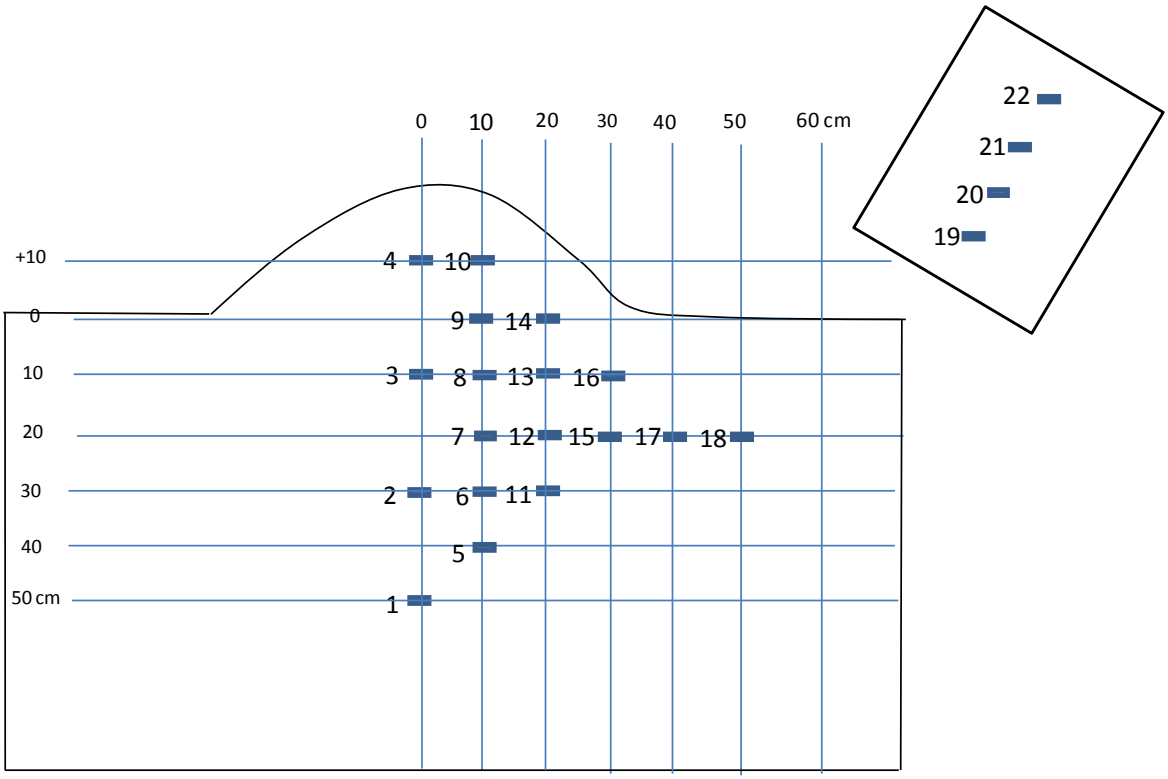

Figure 3.30: Schematic layout of the experimental location with 22 inserted TDR probes. Probes from 19 to 22 were inserted vertically along the ridge
Slika 3.30: Shematski prikaz eksperimentalne lokacije z vstavljenini 22 TDR sondami. Sonde od 19 do 20 so bile vstavljene vertikalno vzdolž grebena.

It was assumed the soil wetting pattern, which forms beneath the surface water point source (dripper) located at the top of the soil ridge, will be symmetrical. Therefore, the TDR probes were inserted only in the right side from the centre of the plant row. As shown on Figure 3.30, probes 1, 2, 3 and 4 were positioned 20 cm apart to a depth of 50 cm, and lay directly beneath the centre of the plant (in a middle of the plant row and ridge). Probes from 10 to 18 were inserted 10 cm apart (vertically and horizontally). Probes from 19 to 22 were inserted vertically, starting at the soil depth of 10 cm. Once they were installed, the etop of the soil ridge was reformed to its original shape (Figure 3.31). The first vertical probe (probe 19) was inserted 30 cm from the excavated trench vertical wall and was located directly beneath the dripper.

a) b)

Figure 3.31: Layout of the location of TDR probes inserted horizontally (a) and vertically (b) to monitor soil volumetric water content in the soil at the IHPS experimental site
Slika 3.31: Postavitev TDR sond, ki so vstavljene horizontalno (a) in vertikalno (b), namenjene za spremljanje volumskega deleža vode v tleh na eksperimentalnem polju IHPS.

Excavated soil trench was not refilled with the soil after TDR probes were installed but remained opened during the experiment. In some studies (e.g. Bufon et al., 2011) the excavated trench with inserted probes was refilled 4 months before beginning of measurements. Because of complexity of the soil properties on the site (e.g. soil layering, artificially made ridge, compacted zones on the side of the ridge) this was not possible in this study.

TDR calibration was conducted at the end of experiment to obtain site specific information on θ values. For this purpose, the gravimetric soil water content was measured for each TDR probe at three locations along each probe. Gravimetric soil water contents were converted to volumetric ones (θ) using measured ρ_b of the soil. θ values for three samples taken for each probe were averaged and compared to actual TDR θ measurements at exactly the same time as the samples were collected. Measured average θ was divided by TDR measured θ to obtain multiplication factor for each probe (Table 3.17). It has to be noted that measured θ values are above soil FC at almost all TDR probes locations. This happened because of last irrigation event which took place three hours before soil samples for TDR calibration were taken.

Table 3.17: Volumetric water content θ (cm^3/cm^3) for last TDR reading, when measured using gravimetric method and multiplication factor for each of 22 TDR probes at the IHPS experimental site
Preglednica 3.17: Volumski delež vode v tleh θ (cm^3/cm^3) za zadnje TDR meritve, izmerjene ob uporabi gravimetrične metode in pomnožene z ustreznim faktorjem, za vseh 22 TDR sond, na eksperimentalni lokaciji IHPS

TDR probe number	Last TDR reading (θ)	Measured average (θ)	Multiplication factor
1	35.8	38.38	1.07
2	36.2	40.8	1.13
3	36.4	39.48	1.08
4	28.6	37.46	1.31
5	34.2	37.09	1.08
6	30.2	38.74	1.28
7	37.5	36.91	0.98
8	38.8	39.27	1.01
9	36.1	37.37	1.04
10	25.5	38.04	1.49
11	29.1	36.67	1.26
12	29.3	36.99	1.26
13	29.8	37.51	1.26
14	26.8	38.05	1.42
15	29	32.96	1.14
16	26.2	32.76	1.25
17	25.7	31.55	1.23
18	28.7	33.33	1.16
19	36.1	36.28	1.00
20	33	36.19	1.10
21	27.7	35.07	1.27
22	18.2	23.93	1.31

The calibration parameters given in Table 3.17 were used for TDR probes calibration for data gained during nine days of field experiments.

Figure 3.32 shows θ values for last TDR reading, measured average θ values and, for comparison purposes, Topp et al. (1980) empirical equation (Equation 32), which is widely used for TDR calibration when site specific calibration is unavailable.

$$\theta = -5.3*10^{-2} + 2.92*10^{-2}*Ka - 5.5*10^{-4} * Ka^2 + 4.3*10^{-6} * Ka^3 \quad \text{... (32)}$$

This empirical approach relates TDR measured apparent dielectric constant (Ka) to the soil θ.

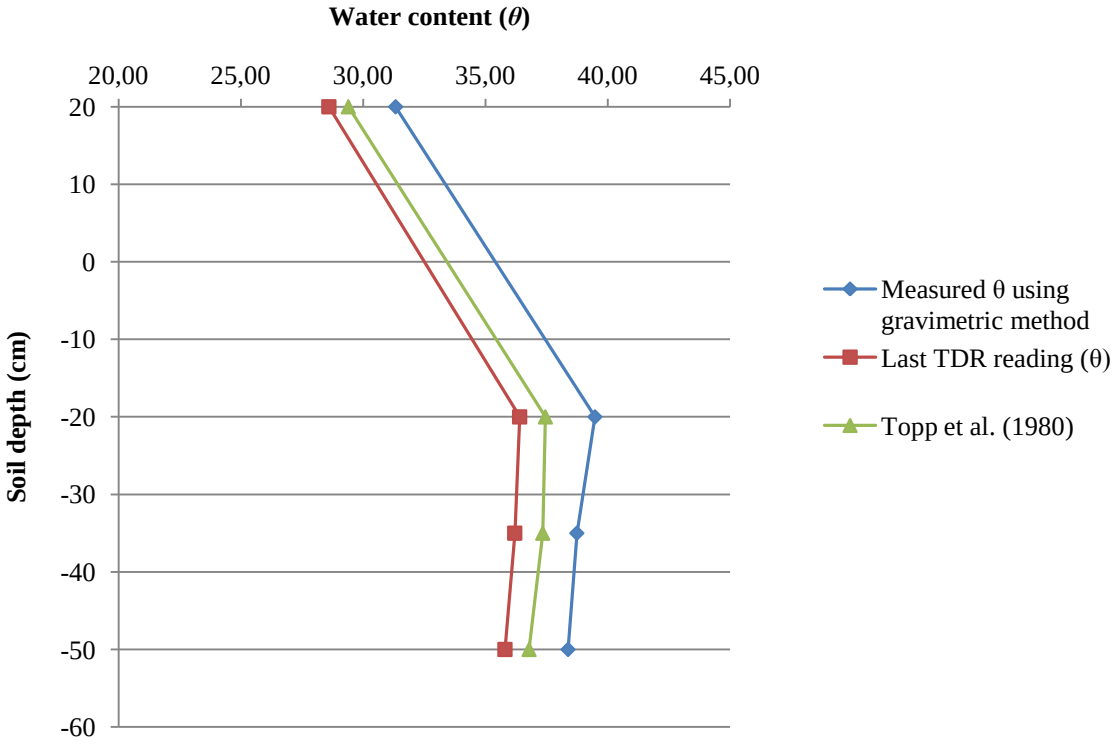

Figure 3.32: Average volumetric water content (θ (cm^3/cm^3)) distribution in the soil profile for last TDR reading compared to averaged measured (θ (cm^3/cm^3)) with gravimetric method and Topp et al. (1980) equation

Slika 3.32: Distribucija povprečnega volumskega deleža vode (θ (cm^3/cm^3)) v profilu tal, za zadnje TDR meritve, primerjane s povprečnimi izmerjenimi volumskimi deleži vode (θ (cm^3/cm^3)) z gravimetrično metodo in Topp in sod. (1980) enačbo.

3.7.5 Hydrus-2D/3D setup

Water movement under hop field was simulated for period of 9 days (from 28th of August to 5th of September 2012) using Hydrus-2D/3D (v2.0). Simulations were done using three dimensional layered soil domain. The emitter *Q* (L/h) was the same as used for field experiment and were calculated by dividing emitter *Q* by the area associated with variable flux BC.

Days with irrigation and irrigation duration were the same as those of field experiment (Table 3.14). The modelled domain was 120 cm wide, 100 cm deep and 80 cm high. The ridge was 70 cm wide and 20 cm high (Figure 3.33).Variably finite element mesh was automatically generated. However, around expected higher soil water potentials (surface boundaries and dripper), nodes were made smaller, to provide better stability and accuracy of the model (Figure 3.34).

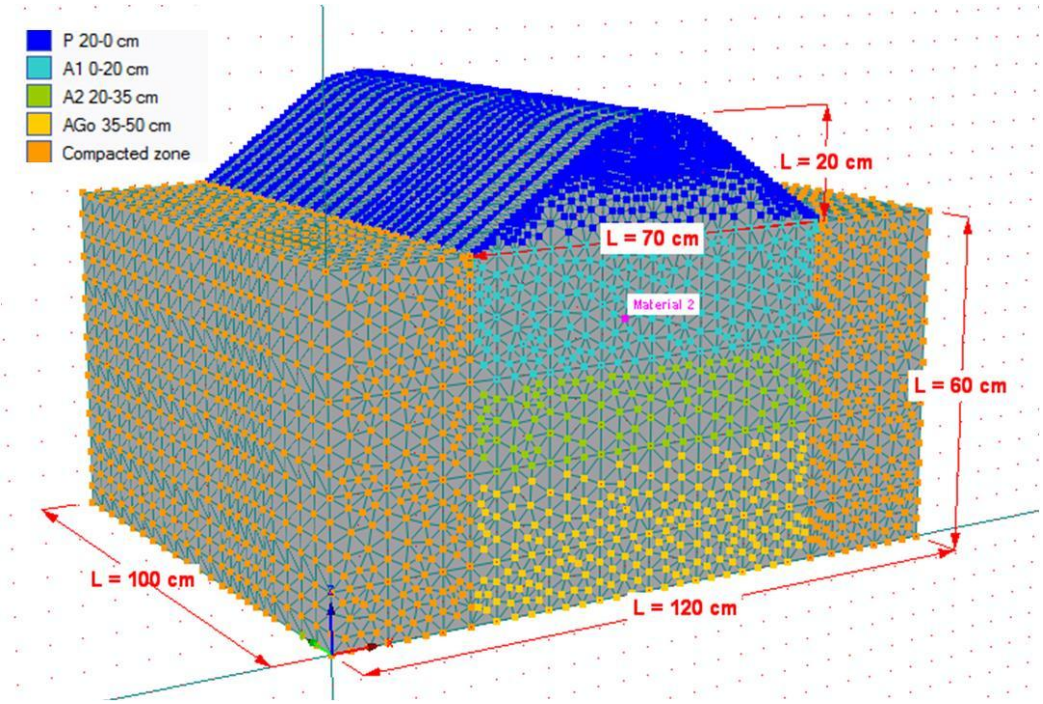

Figure 3.33: Spatial discretization of the 3D flow domain and material distribution used for Hydrus-2D/3D simulations of hop irrigation
Slika 3.33: Prostorska diskretizacija 3D pretočne domene in distribucija materiala za Hydrus-2D/3D simulacije namakanja hmelja

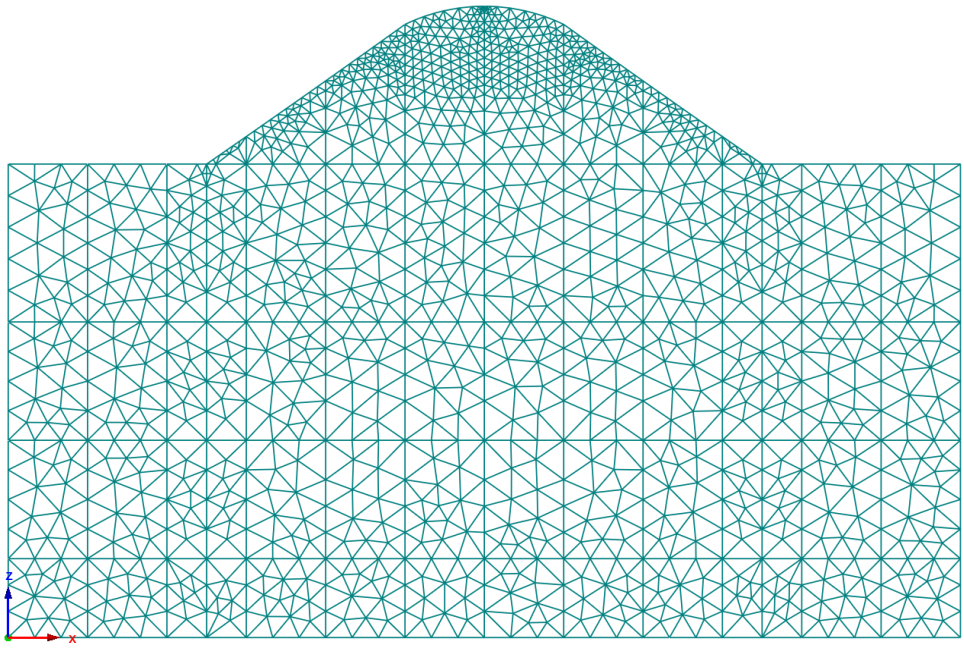

Figure 3.34: Generated finite element mesh used for Hydrus-2D/3D simulations. The mesh elements were made smaller around expected higher soil water potentials
Slika 3.34: Generirani končni elementi mesh, uporabljeni za Hydrus-2D/3D simulacije. Mesh elementi so bili manjši okoli pričakovanih višjih vodnih potencialov.

Soil material distribution and soil layers depth was set according to data presented in Table 3.15.

Variable flux BC representing a surface dripper with its centre located 30 cm from the front vertical wall was used on the top of the ridge. Free drainage BC was used for lower boundary and seepage face BC for entire front vertical domain boundary. All other boundaries were no flux BC (Figure 3.35).

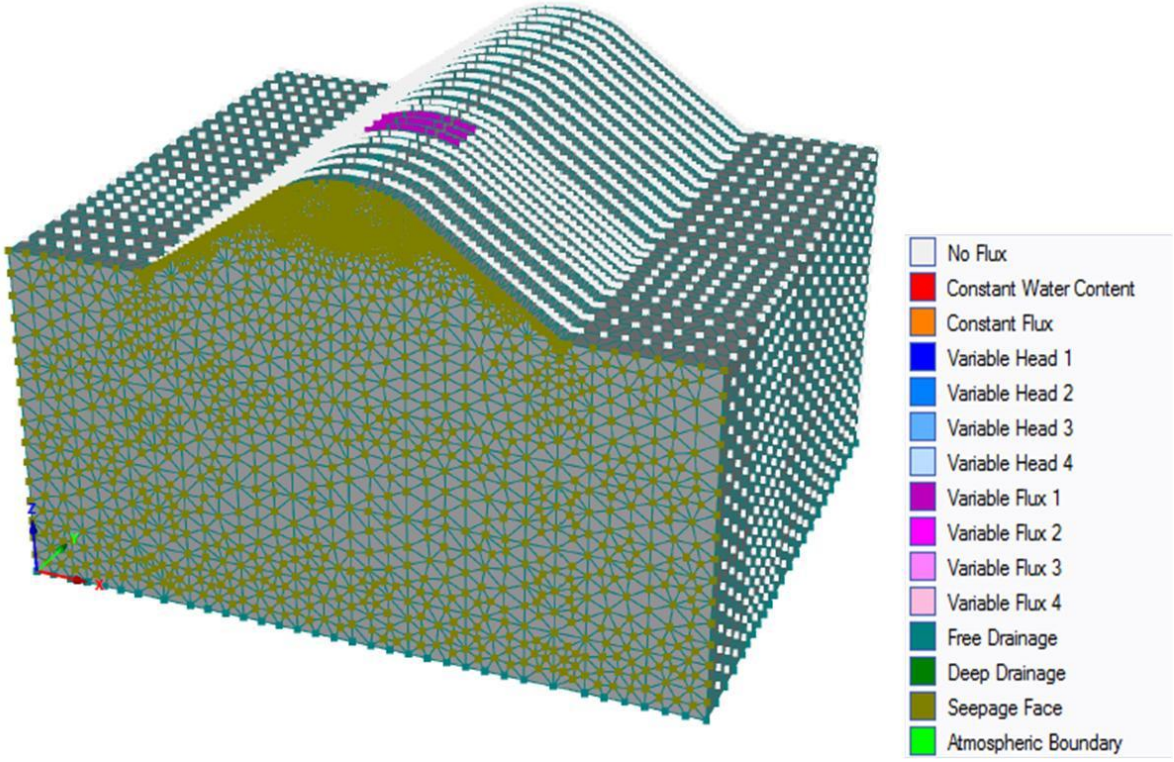

Figure 3.35: Boundary conditions (BC) used for Hydrus-2D/3D simulations of hop irrigation
Slika 3.35: Robni pogoji (BC) uporabljeni za Hydrus-2D/3D simulacije namakanja hmelja

Soil properties needed as input for model are presented in Table 3.15. All necessary soil van Genuchten - Mualem parameters were determined with HYPROP® software, as presented in section 3.7.4.

Soil water initial conditions were selected according to θ values measured with TDR. For this purpose in each soil layer representative TDR nodes were selected. For soil layer P probes 4 and 10 were selected, following with soil layer A_1 with probes 3, 8 and 13, layer A_2 with probes 2, 6 and 11, layer AG_o with probe 5 and for compacted zone probe 17. Measured water content data with TDR probes was averaged for each soil layer and used for simulations. Initial θ (%) for layer P was selected at 31.47 %, for layer A_1 at 36.09 %, for layer A_2 at 37.47 %, for layer AG_o at 35.50 % and for compacted zone at 31.86 %.

Root depth was assumed to be 40 cm, excluding the soil ridge. Roots distribution was, according to observations, selected as shown on Figure 3.36.

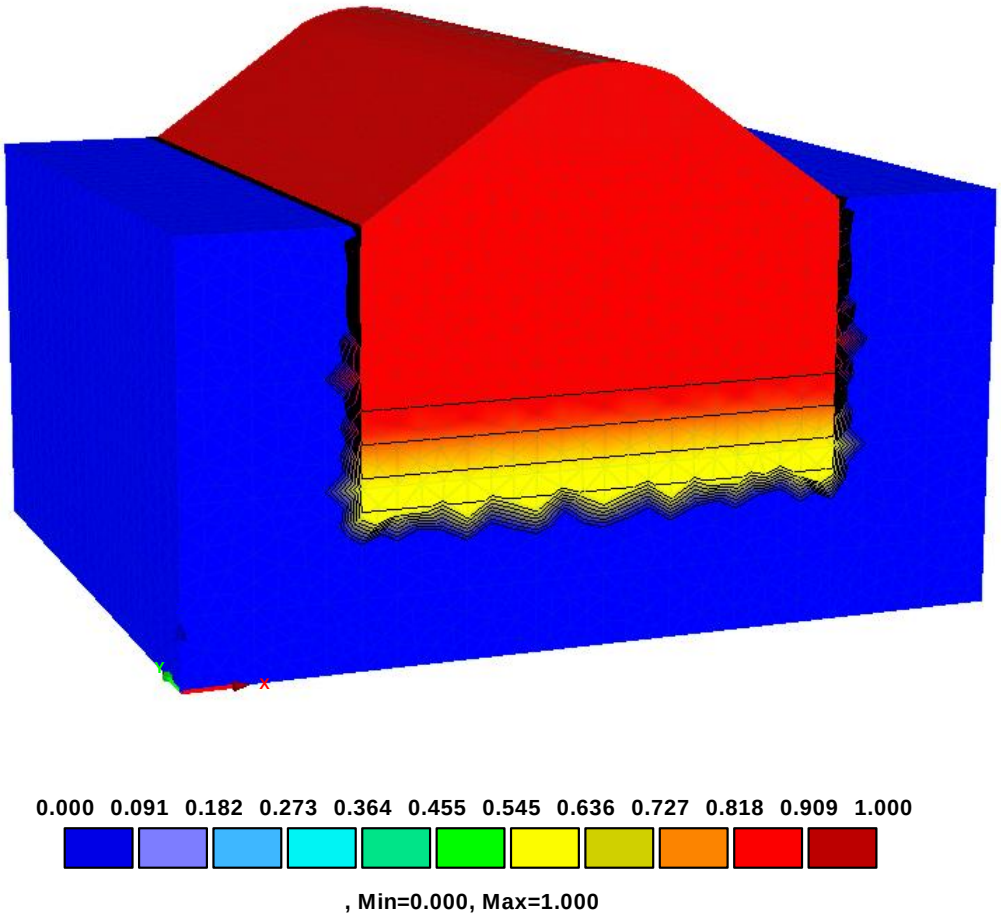

Figure 3.36: Root spatial distribution of the hop plants used in Hydrus-2D/3D simulations. The colour scale shows the root distribution range from dark blue (0) no roots to dark red (1) maximum roots
Slika 3.36: Prostorska distribucija korenin rastlin hmelja, uporabljena v Hydrus-2D/3D simulacijah. Barvna skala prikazuje razpon od temno modre barve (0), ki pomeni, da korenine niso prisotne, do temno rdeče barve (1), ki pomeni, da je korenin največ

The root system was, according to root survey data, located in and below the soil ridge. No roots were located in the compacted zone. It was assumed the maximum root concentration was in the ridge where adventitious roots develop after hop shedding process, and around the root stock which is located at the depth of around 0 and 20 cm, excluding the ridge. From the soil depth of 20 cm to 40 cm the root density linearly decreased to a value of 0.6. Simulation period corresponded to the mid to end growth period during which plants were fully developed and root system was constant. To reduce the potential root water uptake to actual one, the root water uptake stress response function, as suggested by Feddes et al. (1978) was used. Critical Stress Index was set at 1, meaning there was no root water uptake compensation. The Fedde's parameters are presented in Table 3.18.

Table 3.18: Fedde's parameters for root water uptake of hop plants used for Hydrus-2D/3D simulations
Preglednica 3.18: Feddesovi parametri za odvzem vode zkozi korenine hmelja, uporabljeni za Hydrus-2D/3D simulacije

Fedde's parameters	h_1 (cm)	h_2 (cm)	$h_{3\,high}$ (cm)	$h_{3\,low}$ (cm)	h_4 (cm)	*TH* (cm/h)	*TL* (cm/h)
	-10	-855	-3917	-3917	-15000	0.02083	0.00416

The Fedde's parameters above were set according to measured soil water retention data at the experimental location. Water retention data, according to VG function, for all soil layers (P, A_1, A_2 and AG_0), were plotted as a pairs of values for θ and pressure head (h). θ values for all soil layers were averaged for any given h. Parameter h_1 was selected at soil macroporosity at h of -10 cm, parameter h_2 was selected as average FC of all soil layers, according to Table 3.18. The parameters TH and TL were chosen as to represent the average of all soil layers at 50 % of soil water depletion (as suggested by Allen et al., 1998). Parameter h_4 was selected at WP and parameters TH and TL as independent of potential transpiration because TH = TL was set.

Hourly ETo (mm/h) values were calculated from daily ETo (mm/day) values. ETc (mm/h) values were calculated using the given Kc factors. For the purpose of simulations, ETc values in mm/h were transformed to ETc in cm/h. Evaporation from the soil surface was neglected because the experiment was covered with the plastic foil. Therefore entire ETc (cm/h) was attributed to transpiration process. Surface area associated with transpiration was selected as 8000 cm^2 (80 cm × 100 cm) and was calculated as follows. As shown on Figure 3.37, along the hop row two sprouts in V shaped form were growing from each plant. Each of them was 40 cm wide. It was assumed that if we eliminate V shape and put plants together (side to side), they are 80 cm wide. Along the hop row plants canopy was assumed to be continuous. This gives along the row continuous 80 cm wide strip of soil surface covered by plants from which transpiration process occurs. In Hydrus transpiration and surface area associated with transpiration (A) are multiplied to give the total transpiration flux from the transport domain. This total transpiration flux is, proportionally to values of root distribution, distributed over the entire root zone.

Figure 3.37: Hop plants canopy shape characteristics, at the experimental site, used for calculation of surface area associated with transpiration needed as input for Hydrus-2D/3D model
Slika 3.37: Značilnosti oblike krošnje hmeljne rastline na eksperimentalni lokaciji, uporabljenimi za izračun površine, povezane s transpiracijo, ki je bila uporabljena kot vhodni podatek za Hydrus-2D/3D model.

During simulations soil water content was observed at the same locations (using observation nodes) as in the field experiment TDR probes were located. Two TDR probes had to be removed because Hydrus-2D/3D can display only 20 observation nodes. We decided to remove TDR probes 1 and 18 from further comparison with simulations. The TDR probe 1 was the deepest probe in the soil profile (located 50 cm below the soil ridge) and TDR probe 18 was located in the soil compacted zone and were removed because TDR readings showed that water applied through irrigation events did not reach them in entire investigated period. Figure 3.38 is showing observation nodes as inserted in Hydrus model.

The observation nodes 9, 11, 12, 10, 1, 8, 3, 13, 16, 2, 7, 4, 14, 15, 5 and 6 were inserted 20 cm from the front vertical wall. This location corresponded to the TRD probes tips (location at the end of the probe). The same was true for nodes 17, 18, 19 and 20 which were placed at the depth of 10 cm (excluding the ridge) or 30 cm from the top of the ridge.

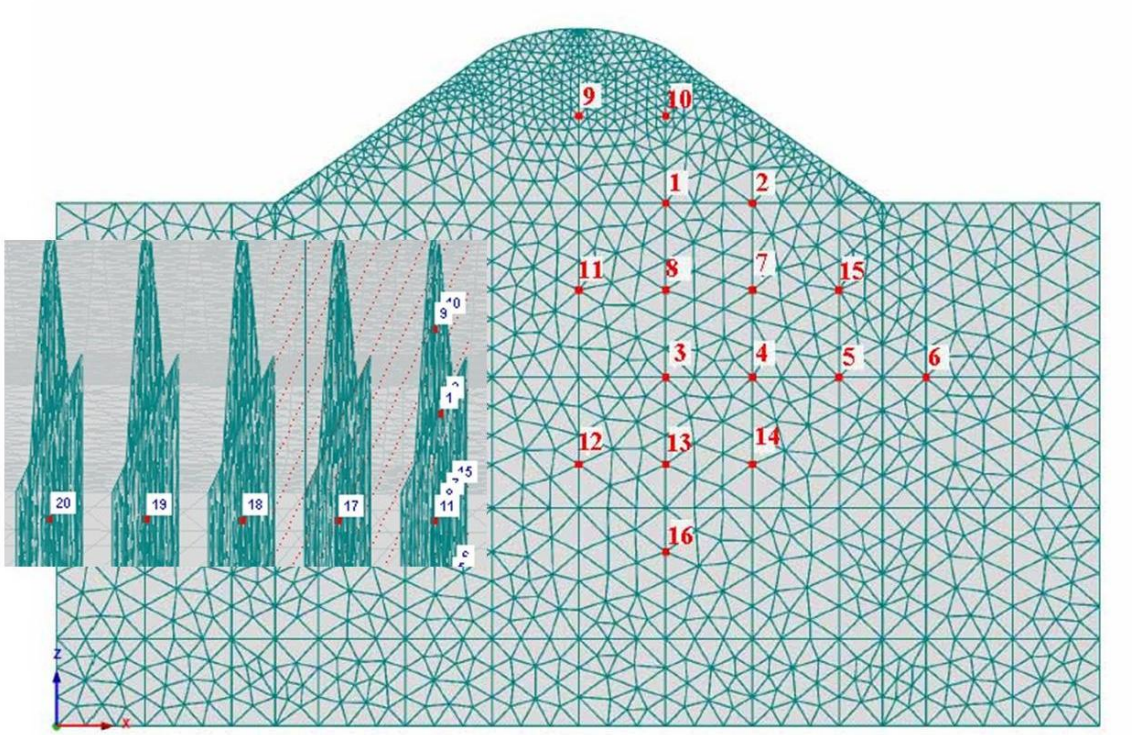

Figure 3.38: Placement of a) horizontal and b) vertical observation nodes used in Hydrus-2D/3D simulations of hop irrigation. Note that the TDR numbering and nodes numbering in Hydrus model are not the same (Hydrus does not allow manual nodes numbering and does this automatically)
Slika 3.38: Namestitev a) horizontalnih in b) vertikalnih opazovalnih točk, uporabljenih v Hydrus-2D/3D simulacijah namakanja hmelja. Upoštevati je potrebno, da se oštevilčevanje opazovalnih točk v Hydrus modelu ne ujema z oštevilčevanjem TDR sond v talnem profilu (Hydrus ne omogoča ročnega oštevilčevanja sond, ampak naredi to avtomatično).

3.8 APPLICATION OF NUMERICAL STUDY TO OTHER IRRIGATION DESIGN PARAMETERS

Influence of various surface drip irrigation design parameters on the water movement under hop plants was in this part investigated only numerically using Hydrus-2D/3D (v2.0). The purpose was to optimize emitter spacing, amount of applied water and initial soil water content at the start of irrigation, to optimize the wetting pattern and water movement extend and match wetting depth with roots main depth.

Hydrus-2D/3D simulations were run for a period of 5 days (120 h). Irrigation was carried out for all days of simulations, except for the first day. Irrigation started at 15:00 h for all simulations. Soil water distribution was simulated between two adjacent emitters for all simulations. The root distribution, root water uptake parameters, soil material distribution and finite element mesh used for those simulations, were the same as those used for comparison of field experiment with Hydrus-2D/3D simulations. There were 18

simulations conducted, testing different surface drip irrigation design parameters and their combinations, as presented in Tables 3.19 and 3.20.

Table 3.19: Different irrigation strategies used for simulations (a and b letters denote different soil water initial conditions presented in Table 3.20). Volume of applied water per irrigation is presented as % of plants potential evapotranspiration (ETc)
Preglednica 3.19: Različne strategije namakanja, uporabljene za simulacije (a in b črke označujejo različne začetne vsebnosti vode v tleh in so predstavljene v preglednici 3.20). Volumen dodane vode na cikel namakanja je predstavljen kot % potencialne evapotranspiracije (ETc) rastlin.

Strategy	Emitter distance (m) × Hop plants width (m)	Volume of water applied (% ETc)	Plants water demand (mm/day)	Irrigation requirement (L/day)	Irrigation cycle duration (min)
1 a, b	0.4 × 0.8	100	3.8	1.22	49.70
2 a, b	0.3 × 0.8	100	3.8	0.91	37.28
3 a, b	0.2 × 0.8	100	3.8	0.61	24.85
4 a,b	0.4 × 0.8	200	7.6	2.43	99.41
5 a, b	0.3 × 0.8	200	7.6	1.82	74.56
6 a, b	0.2 × 0.8	200	7.6	1.22	49.70
7 a, b	0.4 × 0.8	300	11.4	3.65	149.11
8 a, b	0.3 × 0.8	300	11.4	2.74	111.83
9 a, b	0.2 × 0.8	300	11.4	1.82	74.56

Table 3.20: Different initial soil water conditions (θ (cm^3/cm^3)) used for simulations. Letter a) denotes soil water initial conditions at field capacity (FC) – potential evapotranspiration (ETc), letter b) denotes initial conditions at soil critical point (CP) – ETc
Preglednica 3.20: Različne začetne vsebnosti vode v tleh (θ (cm^3/cm^3)), uporabljene za simulacije. Črka a označuje začetno vsebnost vode v tleh pri poljski kapaciteti tal za vodo (FC) – potencialna evapotranspiracija (ETc), črka b označuje začetno vsebnost vode v tleh pri kritični točki vode v tleh (CP) – ETc.

Strategy	a	b
	Initial conditions (FC-ETc)	Initial conditions (CP+ETc)
1 a, b	0.33	0.27
2 a, b	0.33	0.27
3 a, b	0.33	0.27
4 a,b	0.33	0.27
5 a, b	0.33	0.27
6 a, b	0.33	0.27
7 a, b	0.33	0.27
8 a, b	0.33	0.27
9 a, b	0.33	0.27

Emitter measured Q of 1.47 L/h was the same for all simulations. ETc of 3.8 mm (occurred on 4th of Sept. 2012) was selected as representative for all successive days of irrigation simulations. Three emitter distances (0.2, 0.3 and 0.4 m), three different volumes of water

applied (100 %, 200 % and 300 % of ETc) and two different soil water initial conditions (set at soil FC - ETc and Critical point (CP) + ETc). CP is the level below which the available water is not allowed to drop and it represents the lower limit of readily available water (RAW). According to Table 3.21 RAW is 26 mm (θ =0.27 cm^3/cm^3) and was calculated multiplying Total Available Water (TAW) by depletion fraction (taken at 0.5) (Allen et al., 1998). It has to be noted that the ridge (layer P) was excluded from the calculations in Table 3.21 because of irregular rounded shape which made calculations impossible.

Table 3.21: Soil field capacity (FC), wilting point (WP) and the total available water (TAW) in (θ (cm^3/cm^3)) and mm for the main root zone depth
Preglednica 3.21: Poljska kapaciteta tal za vodo (FC), točka venenja (WP) in celotna razpoložljiva voda v tleh (TAW) v (θ (cm^3/cm^3)) in mm za glavno globino korenin

Soil layer	Soil layer/root zone depth (m)	Soil FC (θ)	Amount of water retained at FC for given layer depth (mm)	Soil WP (θ)	Amount of water retained at WC for given layer depth (mm)	TAW (mm/m depth)
A_1 (0-20 cm)	0.2	0.34	68	0.21	42	26
A_2 (20 - 35 cm)	0.15	0.32	48	0.2	30	18
AG_o (35-50 cm)	0.05	0.36	18	0.2	10	8
Total	0.4		134		82	52

The irrigation requirement in (L/day) was computed from the hop ETc (cm/day) and the irrigated soil area. The irrigation cycle duration was determined from irrigation requirement and the emitter discharge rate.

Observation nodes were placed below the dripper (BD) and in the middle of two drippers zone (centre of the overlap zone (COZ)), in 10 cm increments. The domain dimensions, dripper and observation nodes placement are shown on Figure 3.39 (example for strategy 1a).

It has to be noted that domain length was different for strategies with different emitter distances. For instance, domain was 80 cm long for emitter distances of 40 cm (strategies 1, 4 and 7). In this case the first emitter was placed 20 from the front vertical wall of domain and the second dripper was placed at 40 cm from the first dripper, or 20 cm from the last vertical wall of domain (Figure 3.39). The same approach was followed for other strategies with different emitter spacings. For further analysis only 6 observation nodes were selected. Below the dripper nodes 6 (10 cm below the top of the ridge), 3 (20 cm below the soil surface) and 9 (40 cm below the soil surface or at the depth of main root zone considered for irrigation purposes) were selected and in the centre of overlap zone the

nodes 15 (10 cm below the top of the ridge), 12 (20 cm below the soil surface) and 18 (40 cm below the soil surface) were selected for further investigation.

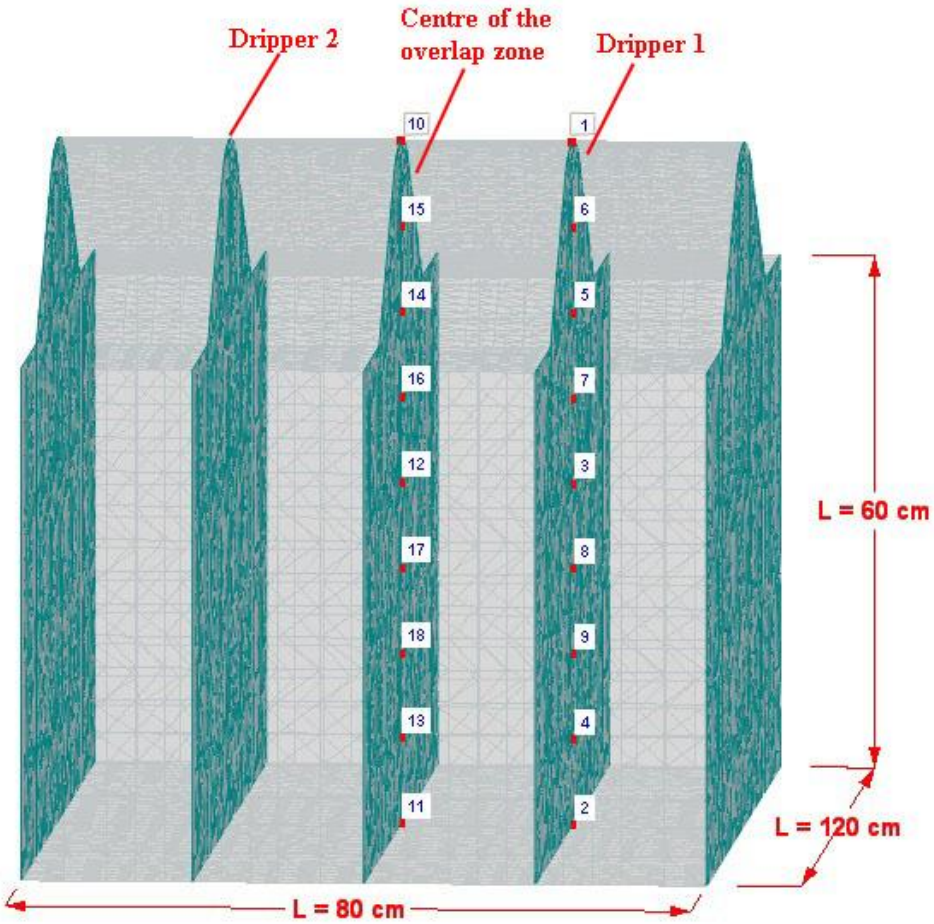

Figure 3.39: Layout of the vertical mesh layers of the soil domain (in 20 cm increments), dripper placement and observation points location used for simulations. Figure is showing example for strategy 1a
Slika 3.39: Načrt vertikalnih mesh slojev v pretočni domeni (v 20 cm razmakih), lokacija kapljača in lokacije opazovalnih točk, uporabljenih za simulacije. Slika prikazuje primer za strategijo 1a.

The irrigation amounts for simulations 1, 2 and 3 were 3.8 mm, for simulations 4, 5 and 6 7.6 mm and for simulations 7, 8 and 9 11.4 mm. Evaporation from soil surface was neglected in all strategies.

3.9 STATISTICAL ANALYSIS

For statistical analysis root-mean-square-error (RMSE) and modelling efficiency (EF) statistical parameters were used to test the performance of different empirical models and to test goodness of fit between simulated and observed values. RMSE calculation, as given by Wallach (2006) and used by Kandelous et al. (2011) and Phogat et al. (2011), for the

measured and simulated wetting pattern dimensions represents the mean distance between measured and simulated values. The EF as given by Smith et al. (1996) and Wallach (2006) has the maximum at 1, in which case the predicted values perfectly match with the observed ones. A model that gives *EF* = 0 has the same degree of agreement with the data as using the average value. A model with *EF* close to 0 would not normally be considered as a good model.

$$RMSE = \sqrt{\frac{1}{n}\sum_{i=1}^{n}(Mi - Si)^2} \quad \text{... (33)}$$

where *Mi* and *Si* are observed and simulated values and *n* is the number of observations. And

$$EF = \frac{(\sum_{i=1}^{n}(Mi - \bar{M})^2 - \sum_{i=1}^{n}(Si - Mi)^2)}{\sum_{i=1}^{n}(Mi - \bar{M})^2} \quad \text{... (34)}$$

where, *Mi* and *Si* are measured and observed values, $\bar{M}$ is the mean of the observed (measured) data and *n* is the number of observations.

4 RESULTS AND DISCUSSION

4.1 SOILS FROM SEISMIC DATABASE

In this section the surface wetted radius and wetted depth are presented as a function of volume of applied water (L). Volume of applied water is a product of the application rate (L/h) and water application time (h). Figures show the relation between wetting pattern radius (X) and depth (Y) with volume of applied water for all soil texture classes from SEISMIC database for different emitter *Q* and different soil water initial conditions (presented as % depletion from soil FC).

4.1.1 Influence of soil texture

The results from this section are the same to those from Naglič (2011). Because they are used for empirical model improvement in this work, only brief summary is given here. The wetting pattern sizes for four selected soil textural classes (out of 11 textural classes) are shown in Figure 4.1, which is a plot of the wetted soil dimension in X and Y directions as a function of volume of applied water.

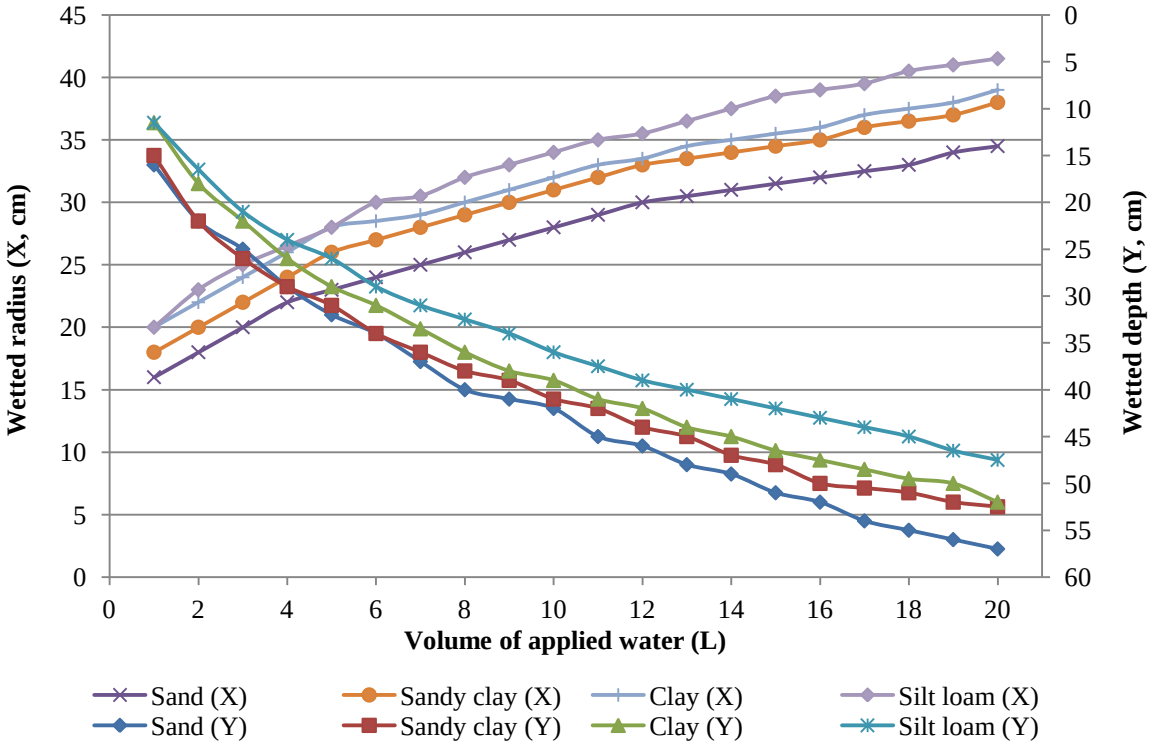

Figure 4.1: Dimensions of the simulated wetted soil radius (X) and depth (Y) as a function of volume of applied water for sand, sandy clay, clay and silt loam at emitter discharge rate of 2L/h and at 50 % depletion
Slika 4.1: Dimenzije simuliranega omočenega radija (X) in globine (Y) tal kot funkcije volumna dodane vode za peščena, glinasta in meljasto ilovnata tla pri pretoku kapljača 2 L/h in 50 % stanju razpoložljive vode v tleh

The size of the wetting pattern in both directions increased with the volume of applied water. The wetted X for a given volume of water applied was larger for fine-textured soils, such as silt loam, silty clay, clay loam, sandy silt loam and clay and smaller for course-textured ones, such as sand, loamy sand, sandy clay loam and sandy loam. In general Y tends to be larger for coarse-textured soils, as sand, loamy sand and sandy clay. The smallest wetted depth occurred in fine-textured soils, as silty clay loam, silty clay and silt loam.

The wetting front moved faster at the beginning of water application, in both directions. The wetted Y increased more than the wetted X for all soils from Figure 4.1.

The water content distribution results obtained with the numerical simulations show wetted X and wetted Y for the two most contrasting soil textures (sand and clay), at the end of the water application cycle, are compared in Figure 4.2. The wetting front Y in clay with low permeability is smaller than in the highly permeable sand. On the other hand, the wetted X in the clay is bigger than that of the sand.

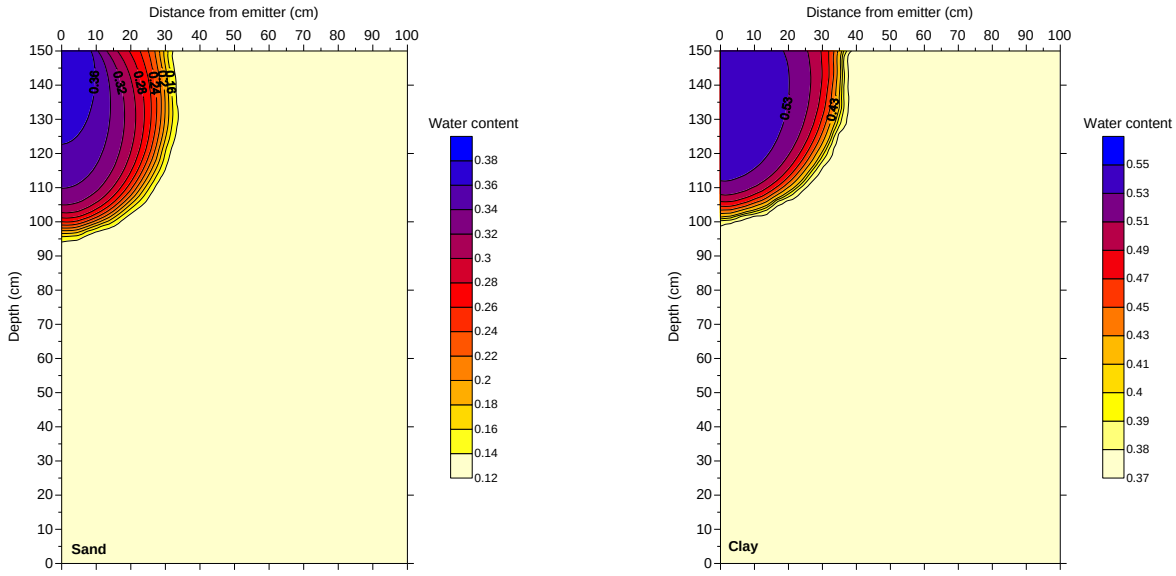

Figure 4.2: Soil water content (θ (cm^3/cm^3)) distribution for sand and clay soil as simulated with Hydrus-2D/3D, at the end of irrigation cycle at emitter discharge rate (Q) of 2 L/h and 50 % depletion
Slika 4.2: Distribucija vode v tleh (θ (cm^3/cm^3)) za peščena in glinasta tla kot rezultat simulacije z Hydrusom-2D/3D, na koncu namakalnega cikla pri pretoku kapljača (Q) 2 L/h in pri 50 % stanju razpoložljive vode v tleh

Maximum X and Y obtained at the end of the last irrigation cycle for each soil texture are further compared and discussed in more detail in Naglič (2011). In general, the wetting patterns for coarse-textured soils tend to extend in Y direction more than in X one.

4.1.2 Influence of emitter discharge rates

Measurements of wetting patterns dimensions for three contrasting soil texture classes (sand, silt loam and clay), as a function of volume of applied water (irrigation duration), for the four different surface drip emitter *Q*, are presented in Figures 4.3, 4.4 and 4.5.

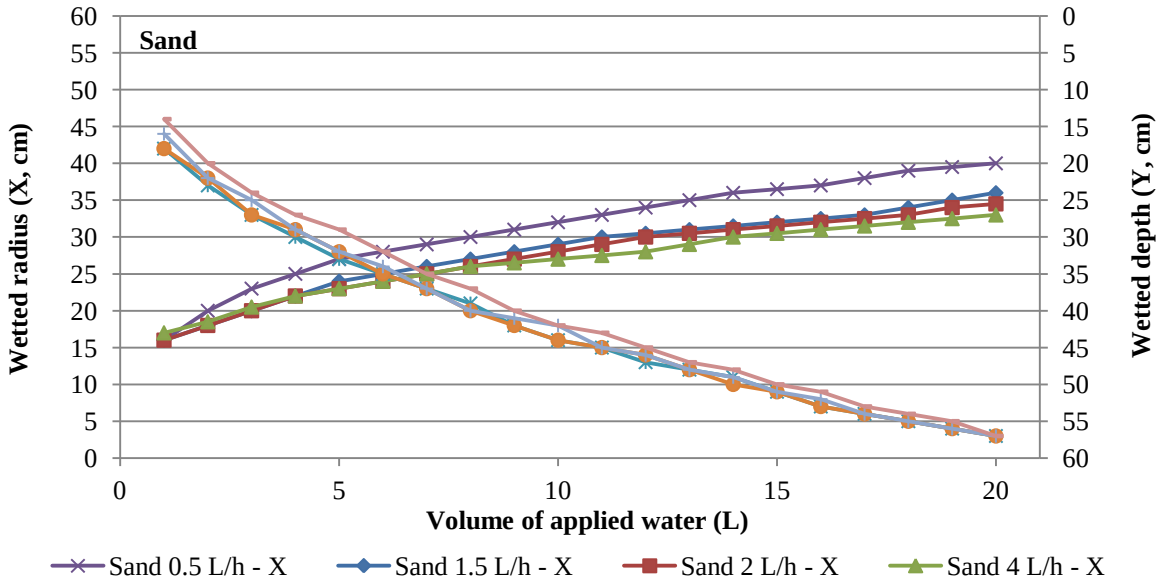

Figure 4.3: Measured simulated wetting pattern dimensions (in X and Y direction) in sand soil as a function of volume of applied water for emitter discharge rates (*Q*) of 0.5, 1.5, 2 and 4 L/h
Slika 4.3: Izmerjene simulirane dimenzije omočenih tal (v X in Y smer) v peščenih tleh, kot funkcija volumna dodane vode, za pretok kapljača (*Q*) 0,5; 1,5; 2 in 4 L/h

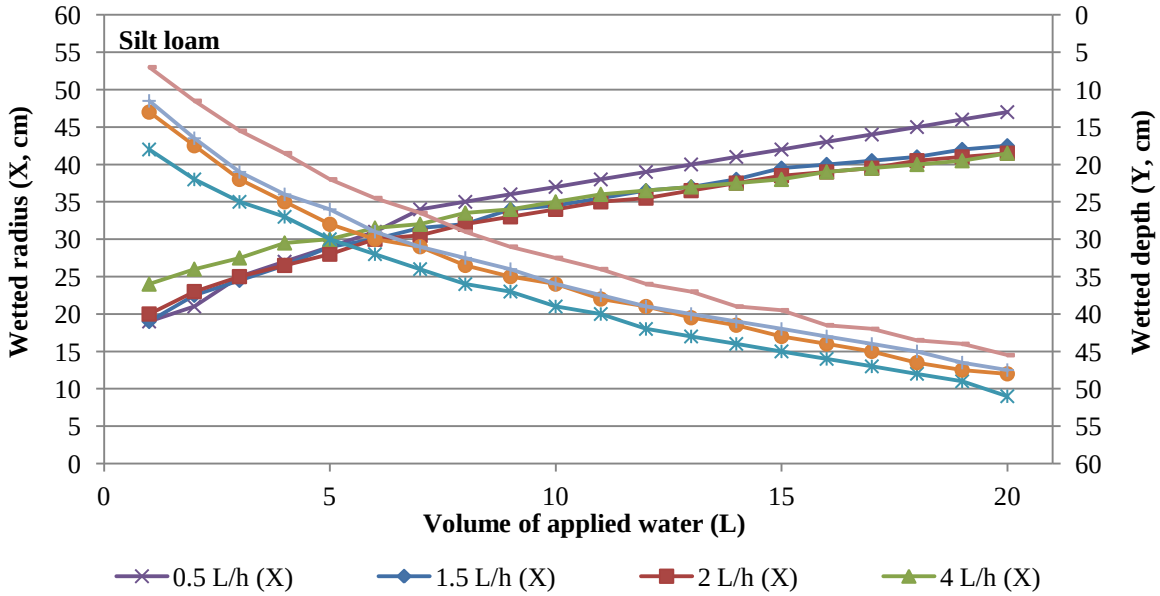

Figure 4.4: Measured simulated wetting pattern dimensions (in X and Y direction) in silt loam soil as a function of volume of applied water for emitter discharge rates (*Q*) of 0.5, 1.5, 2 and 4 L/h
Slika 4.4: Izmerjene simulirane dimenzije omočenih tal (v X in Y smer) v meljasto ilovnatih tleh, kot funkcija volumna dodane vode, za pretok kapljača (*Q*) 0,5; 1,5; 2 in 4 L/h

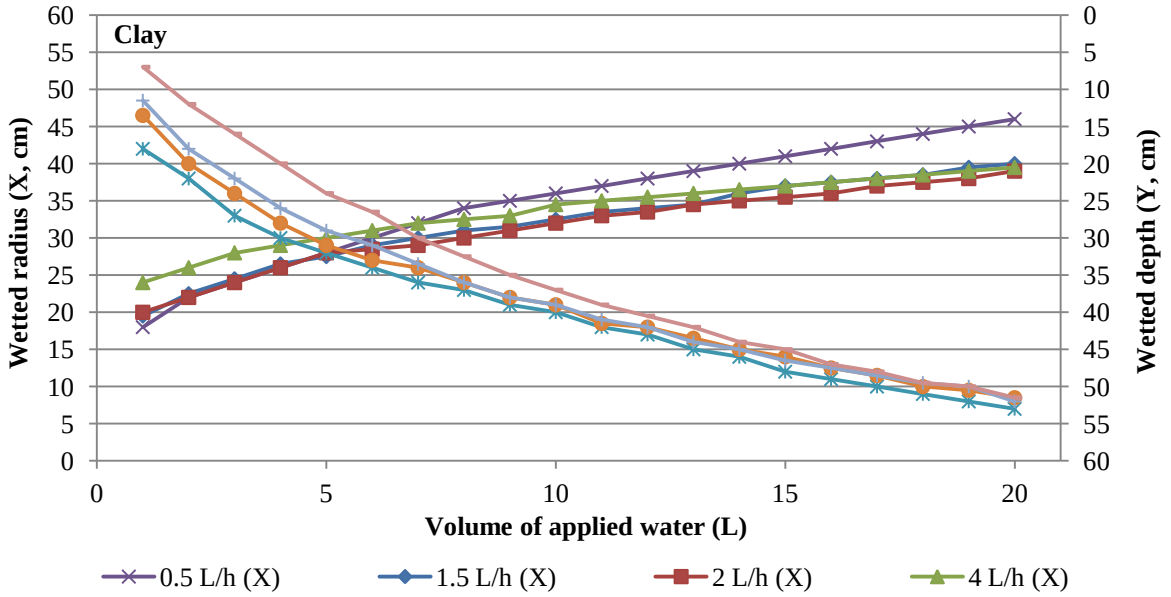

Figure 4.5: Measured simulated wetting pattern dimensions (in X and Y direction) in clay soil as a function of volume of applied water for emitter discharge rates (*Q*) of 0.5, 1.5, 2 and 4 L/h
Slika 4.5: Izmerjene simulirane dimenzije omočenih tal (v X in Y smer) v glinastih tleh, kot funkcija volumna dodane vode, za pretok kapljača (*Q*) 0,5; 1,5; 2 in 4 L/h

In the silt loam and clay soils (Figures 4.4 and 4.5), at the beginning of irrigation, the higher emitter *Q* (4 L/h) produced a bigger X in both directions. This was not true for the sand soil (Figure 4.3), where different emitter *Q* had minimal or almost no effect on the X at the beginning of irrigation. In the sand soil, differences in wetting pattern size in X direction occurred only at the end of irrigation, where the lower emitter *Q* (0.5 L/h) resulted in a larger X. Conversely, at the end of water application minimal differences in the size of the wetted X occurred in silt loam and clay soils for all emitter *Q*, excluding for 0.5 L/h treatment, where the largest X was produced almost at all volumes of applied water. The wetted Y increased with decrease of emitter *Q* in the clay and silt loam soils. In the clay soil this effect vanished after around 15 L of water applied. In the sand soil emitter discharge rate had almost no effect on the wetted Y from the beginning till the end of water application.

The sizes of the wetting patterns extend at the end of water application (20 L of water applied) (Figure 4.6 and 4.7) showed that the *Q* slightly affected radial water movement in all simulations. The *Q* of 1.5, 2, and 4 L/h had only small effect on the X in the sand soil and Y in the silt loam soil. On the other hand, the smallest *Q* of 0.5 L/h resulted in the largest X for all soils and the largest Y in silt loam and clay soil. In sand soil *Q* had no effect on the Y, which was probably due to the longer application time needed for the *Q* of 0.5 L/h to apply the same amount of water. Therefore more time was allowed for soil water to redistribute in a radial direction due to capillary forces. Higher emitter discharge rates

caused faster horizontal water spreading and shorter water application times, allowing less time for water to redistribute, through soil capillarity forces.

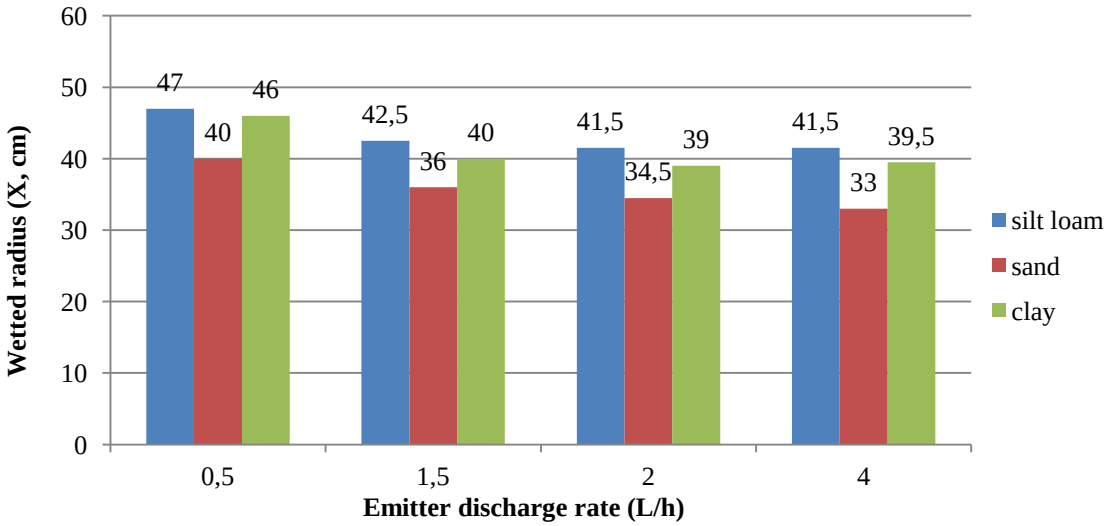

Figure 4.6: Simulated wetted radius X (cm) at the end of water application (20 L of water applied) for four different emitter discharge rates (*Q*) of 0.5, 1.5, 2 and 4 L/h and three different soil textures (silt loam, sand and clay)
Slika 4.6: Simuliran omočen radij X (cm) na koncu namakanja (20 L dodane vode) za štiri različne pretoke kapljačev (*Q*) (0,5; 1,5; 2 in 4 L/h) in za tri različne teksture tal (meljasta ilovica, pesek in glina)

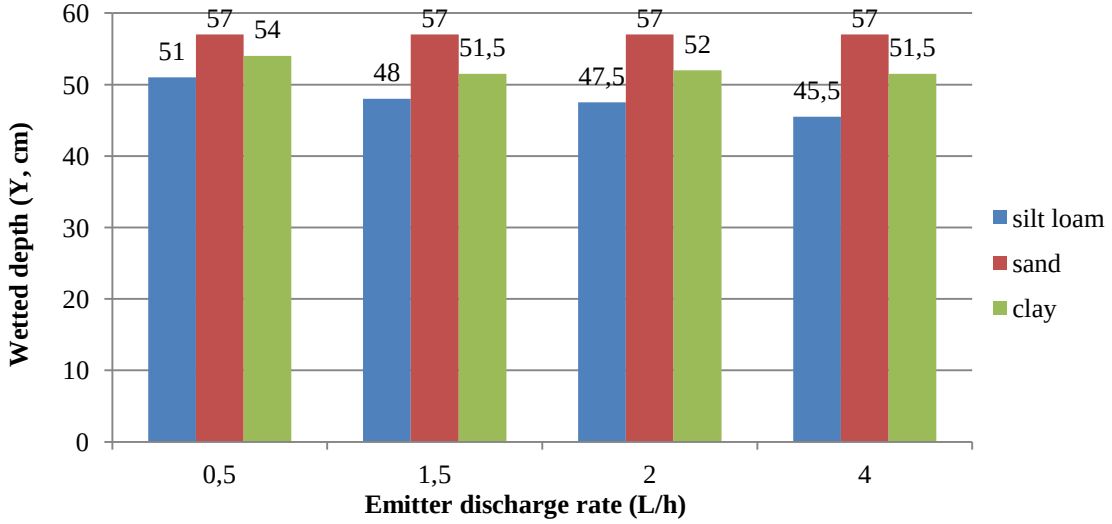

Figure 4.7: Simulated wetted depth Y (cm) at the end of water application (20 L of water applied) for four different emitter discharge rates of 0.5, 1.5, 2 and 4 L/h and three different soil textures (silt loam, sand and clay)
Slika 4.7: Simulirana omočena globina Y (cm) na koncu namakanja (20 L dodane vode) za štiri različne pretoke kapljačev (*Q*) (0,5; 1,5; 2 in 4 L/h) in za tri različne teksture tal (meljasta ilovica, pesek in glina)

Figures 4.6 and 4.7 show that the *Q* of 1.5, 2 and 4 L/h had a very small effect on the final size of the wetting pattern. The only major difference was observed for $Q = 0.5$ L/h where, in the comparison to highest *Q* of 4 L/h, the largest X was observed in all soils. The same

was true for wetted depth, with exception of sandy soil, where exactly the same wetting pattern size was observed for all *Q*. Just the opposite to above results, the large differences in the position of the wetted front close to saturation were observed (Figures 4.8 and 4.9).

The saturated wetted front was anticipated as the volumetric water content difference of 0.005 cm^3/cm^3 from the saturated water content. In this case *Q* had much larger effect on the position of the saturated wetted front compared with the position of the general wetting front (Figures 4.8 and 4.9). Higher emitter *Q* resulted in larger saturated wetting pattern in both directions. This was more pronounced for Y in the soils with coarser texture and can be clearly seen for sand soil. When only the wetting pattern with water content close to saturation is considered, the influence of *Q* had a bigger effect on radius and depth of wetting pattern in all soil textures.

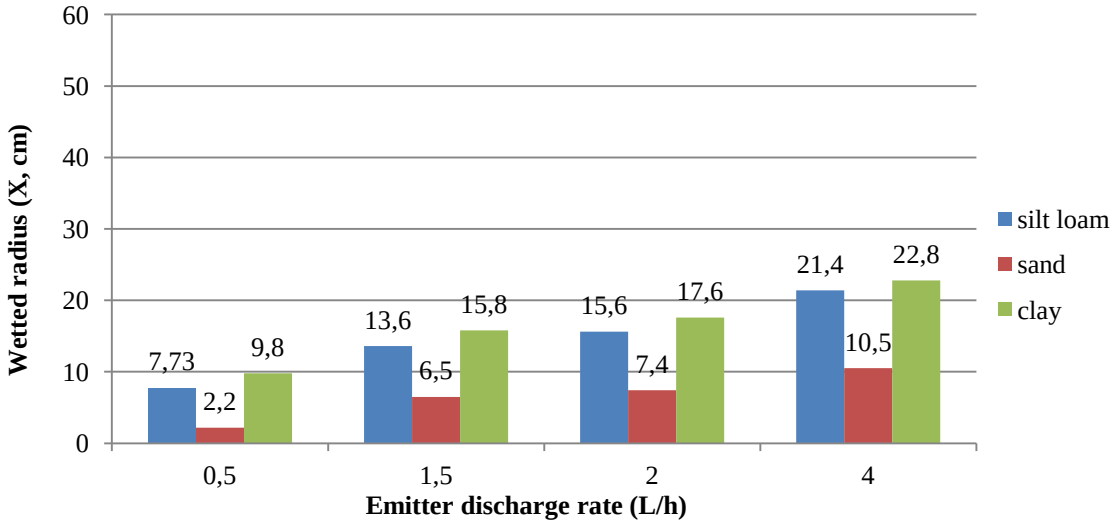

Figure 4.8: Simulated wetted radius (X) close to saturation at the end of water application (20 L of water applied) for four different emitter discharge rates of 0.5, 1.5, 2 and 4 L/h and three different soil textures (silt loam, sand and clay)
Slika 4.8: Simuliran omočen radij (X) blizu saturacije tal na koncu namakalnega cikla (20 L dodane vode) za štiri različne pretoke kapljačev (*Q*) (0,5; 1,5; 2 in 4 L/h) in za tri različne teksture tal (meljasta ilovica, pesek in glina)

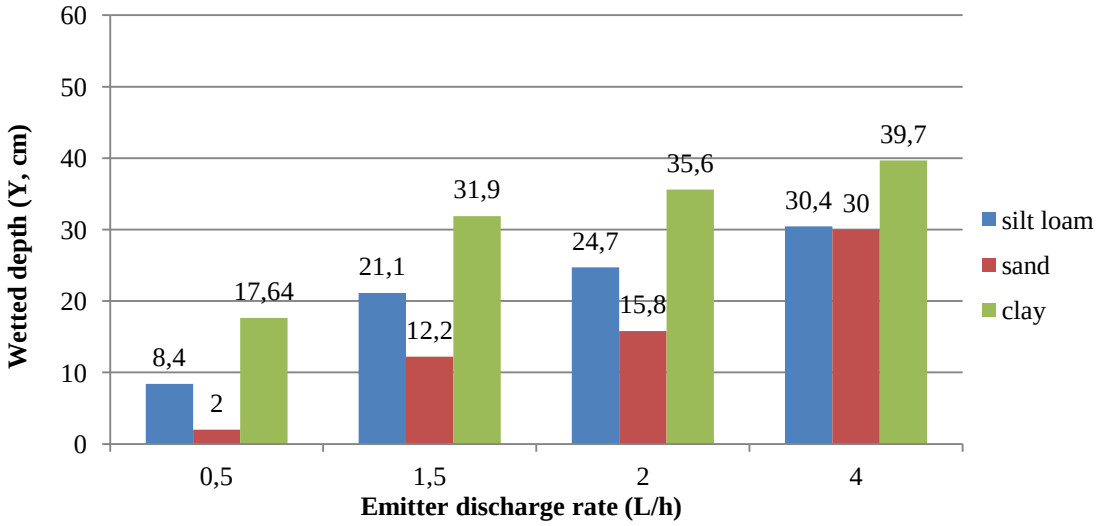

Figure 4.9: Simulated wetted depth (Y) close to saturation at the end of water application (20 L of water applied) for four different emitter discharge rates of 0.5, 1.5, 2 and 4 L/h and three different soil textures (silt loam, sand and clay)
Slika 4.9: Simulirana omočena globina (Y) blizu saturacije tal na koncu namakalnega cikla (20 L dodane vode) za štiri različne pretoke kapljačev (*Q*) (0,5; 1,5; 2 in 4 L/h) in za tri različne teksture tal (meljasta ilovica, pesek in glina)

The results of saturated wetted fronts are similar to the Levin et al. (1971) results, where for sand soil the highest *Q* resulted in the highest wetting pattern advance in both directions. However, their discharge rates used were higher (8 L/h) and initial water content of the soil was chosen close to field capacity. Above results also agree with Bresler et al. (1971), Levin et al. (1979), Khan et al., (1996) and Li et al. (2003, 2004) studies, but just for wetting patterns extend in horizontal direction. In their case the Y decreased with increase of emitter *Q*, which is opposite to this study.

It is important to note that wetting patterns in both directions were observed immediately after irrigation cut off, therefore allowing no time for soil water redistribution in the soil. According to Levin et al. (1977), the advantage gained by using *Q* to extend wetting pattern lateral movement in sand is valid only for a short time during the first irrigation cycle. After 24 h of water redistribution in the soil this difference is reduced to minimal amount. Skaggs et al. (2011) also concluded that none of the studies on sandy loam soil, testing different emitter *Q* and pulsed irrigation, produced a wetting pattern that was different from the others.

Finally, figures 4.3, 4.4 and 4.5 can help to establish the proper spacing between the emitters, to give complete lateral soil wetting for which the shape of the wetting pattern is of great importance. For example, to wet a root system to a depth of 40 cm in sand soil, the emitter spacing for emitter flow rate of 4 L/h should be about 53 cm (2×X) and about 9L of water should be applied with one surface drip emitter.

4.1.3 Influence of soil water initial conditions

Similarly to section 4.1.1, the results presented here are detailed in Naglič (2011) and only the most important findings are highlighted here. The size of the wetting pattern in X and Y direction was measured for three soils (sand, silt loam and clay). In this section three different initial soil water conditions are presented as % of depletion of the available water (AW) which corresponds to the amount of water between field capacity (FC) and permanent wilting point (PWP). % depletion represents the % of AW that is no longer available. A field capacity corresponding to a water content at 10 kPa (-100 cm) matric potential was chosen for all three soils. The size of the wetting pattern in a horizontal (X) and vertical (Y) direction was measured for three different initial soil water conditions corresponding to depletions of 30 %, 50 % and 70%. Emitter *Q* of 2 L/h was used in all cases.

The dimensions of the wetting patterns for the three soils as a function of the volume of applied water (irrigation duration) and for the three different soil water depletions are represented in Figures 4.10, 4.11 and 4.12.

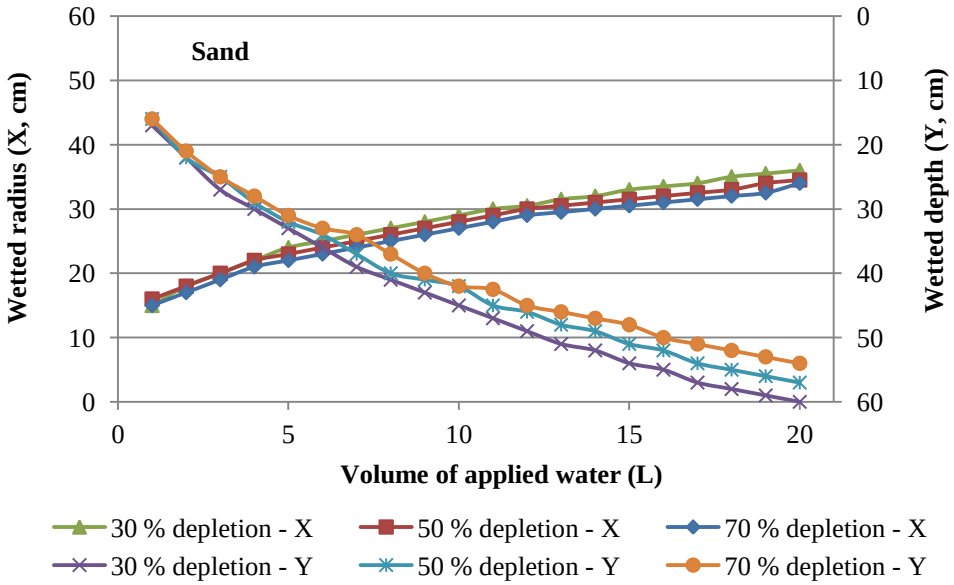

Figure 4.10: Measured simulated wetting pattern dimensions in X and Y direction for sand soil as a function of volume of applied water (L) for soil water initial conditions (represented as % depletion) of 30, 50 and 70 %

Slika 4.10: Izmerjene simulirane dimenzije omočenih tal v X in Y smer za peščena tla, kot funkcija volumna dodane vode (L), za začetna stanja razpoložljive vode v tleh pri 30, 50 in 70 %

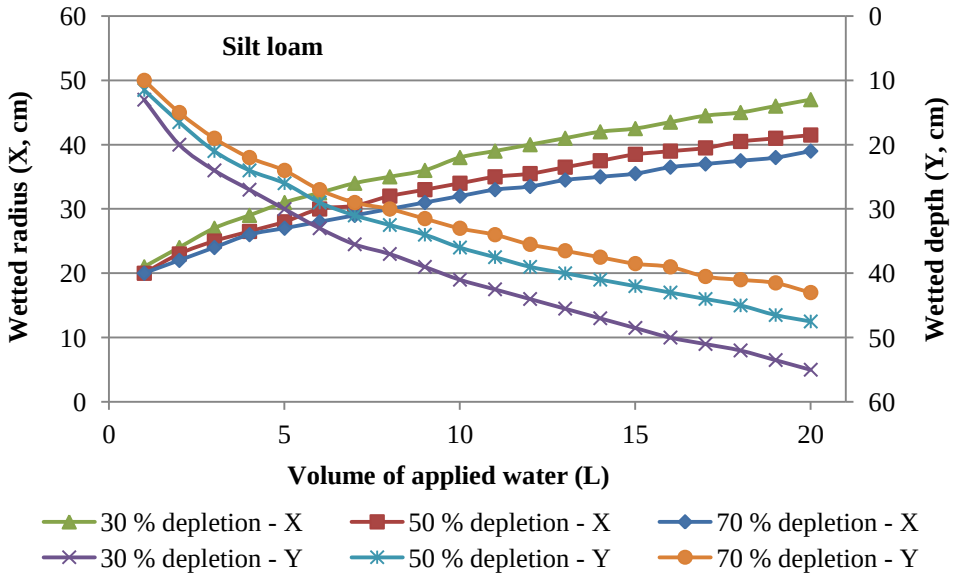

Figure 4.11: Measured simulated wetting pattern dimensions in X and Y direction for silt loam soil as a function of volume of applied water (L) for soil water initial conditions (represented as % depletion) of 30, 50 and 70 %
Slika 4.11: Izmerjene simulirane dimenzije omočenih tal v X in Y smer za meljasto ilovnata tla, kot funkcija volumna dodane vode (L), za začetna stanja razpoložljive vode v tleh pri 30, 50 in 70 %

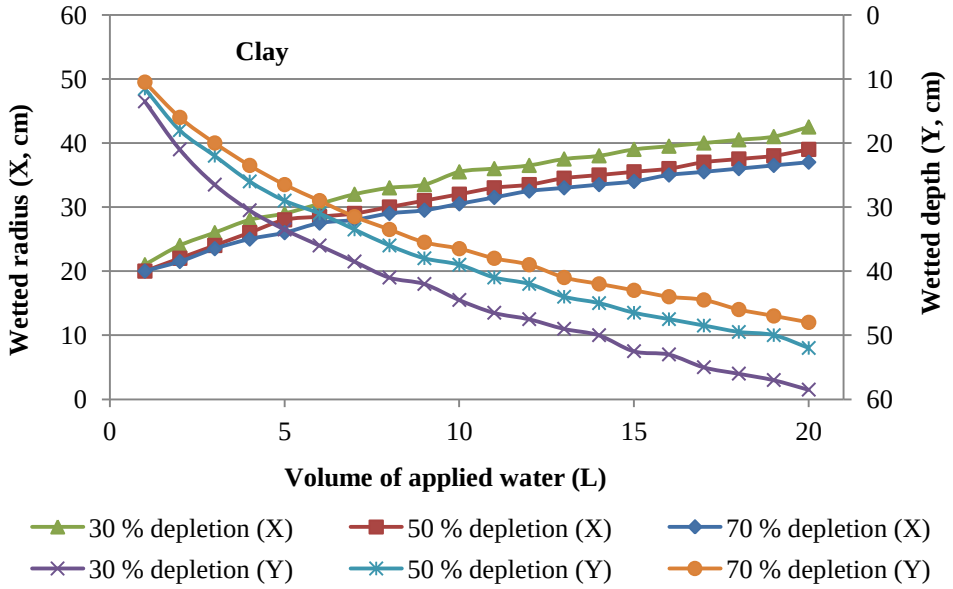

Figure 4.12: Measured simulated wetting pattern dimensions in X and Y direction for clay soil as a function of volume of applied water (L) for soil water initial conditions (represented as % depletion) of 30, 50 and 70 %
Slika 4.12: Izmerjene simulirane dimenzije omočenih tal v X in Y smer za glinasta tla, kot funkcija volumna dodane vode (L), za začetna stanja razpoložljive vode v tleh pri 30, 50 in 70 %

The largest X occurred in the silty loam soil for all depletion rates, followed by the clay and sand soils. The opposite occurred for Y, which was largest in the sand for all depletion rates, followed by the clay and silt loam soils. Higher initial soil water conditions (or lower

depletions) caused an increase in spreading in both X and Y directions for all soils. These results agree with previous studies on subsurface drip irrigation (Provenzano, 2007; Skaggs et al., 2010) and surface drip irrigation (Li et al., 2003, 2004).

It has to be noted soil depletion had a larger effect on fine-textured soils (clay and silt loam) in both directions. Because depletion (%) was calculated, based on the FC of each soil at -100 cm suction (matric potential), the sand soil had, at that suction, more air-filled pore space (or less available water) than other fine-textures soils. Therefore, applying different percentages of depletion to an already dry sand soil did not cause much difference in initial water content. The wetting pattern for all soils and in both directions increased with higher initial soil water (or lower depletion percentage). This was expected, because with higher soil water content less pore volume is available for water which has to infiltrate a larger soil volume.

Visual results of simulations with water distribution in the sand, silt loam and clay soil, using 2 L/h emitter discharge and the three different initial water contents, are presented on Figure 4.13.

Results confirm the conclusions of Skaggs et al. (2010) and Li et al. (2003, 2004), where higher initial soil water content resulted in increased water spreading from shallow subsurface drip irrigation system, with larger spreading in the Y than in the X direction. The larger overall spreading is due to a decrease in the available pore space at higher water content while the lower spreading in X direction can be explained by lower capillary forces at larger initial water content (smaller depletions). However, the rate of increase in the wetted Y and wetted X is not higher for dryer soils (70% depletion) as it would be expected because of higher capillary forces at the wetting front. This is because the rate of wetting pattern increase is governed by the infiltration rates at the soil surface, which is in this case constant at 2 L/h.

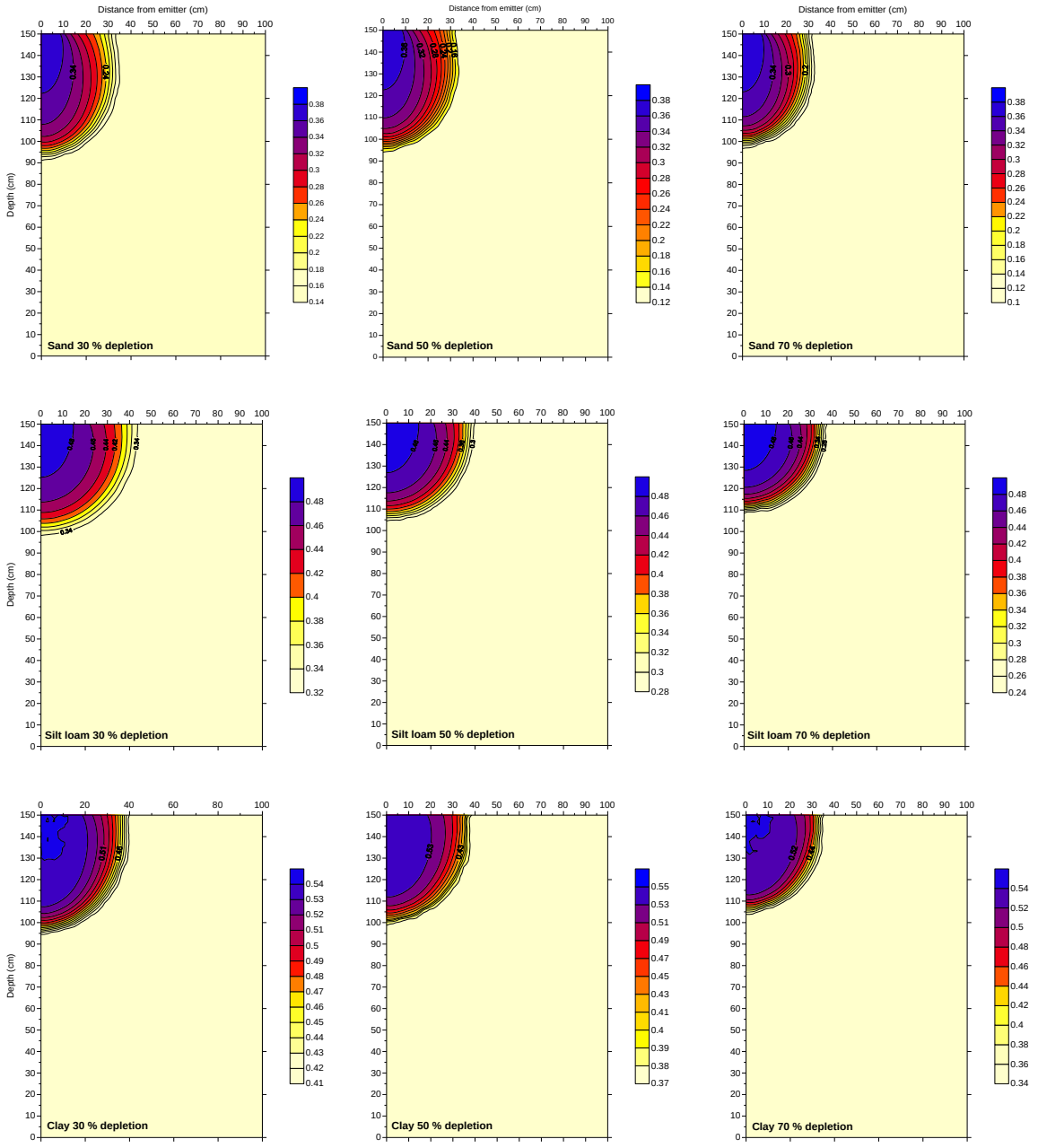

Figure 4.13: Hydrus-2D/3D simulations of water distribution in sand, silt loam and clay soils with 30 %, 50 % and 70 % depletions at the end of water application (20 L applied). Colour scale represents water content (θ (cm^3/cm^3))

Slika 4.13: Hydrus-2D/3D simulacije distribucije vode v peščenih, meljasto ilovnatih in glinastih tleh s 30, 50 % in 70 % stanjem razpoložljive vode v tleh, na koncu namakalnega cikla (20 L dodane vode). Barvna skala predstavlja vsebnost vode v tleh (θ (cm^3/cm^3)).

4.2 COMPARISON OF EXPERIMENTAL AND NUMERICAL SOIL TANK RESULTS

The comparison between the experimental and simulated wetting patterns for the sand and the silty clay loam for *Q* of 0.11, 0.49, 0.99, 1.51 and 2.05 L/h is shown on Figure 4.14. Note that for the silty clay loam soil *Q* higher than 0.11 L/h could not be used. This is because these higher rates resulted in water spreading across the entire soil surface area of the tank before any meaningful measurements could be achieved (Naglič, 2011).

The Y and D of the simulated and measured wetting patterns were in good agreement for all soils. As *Q* decreased, the wetted D increased. In general, as the *Q* decreased the wetted Y increased but the influence was smaller than in the horizontal direction (Naglič, 2011).

To see the results from another perspective Figure 4.15 shows the wetting pattern during soil tank experiment next to a 2D Hydrus water content picture for three examples of sandy soil at *Q* of 0.99 and 2.05 L/h and silty clay loam soil at *Q* of 0.11 L/h (Naglič, 2011).

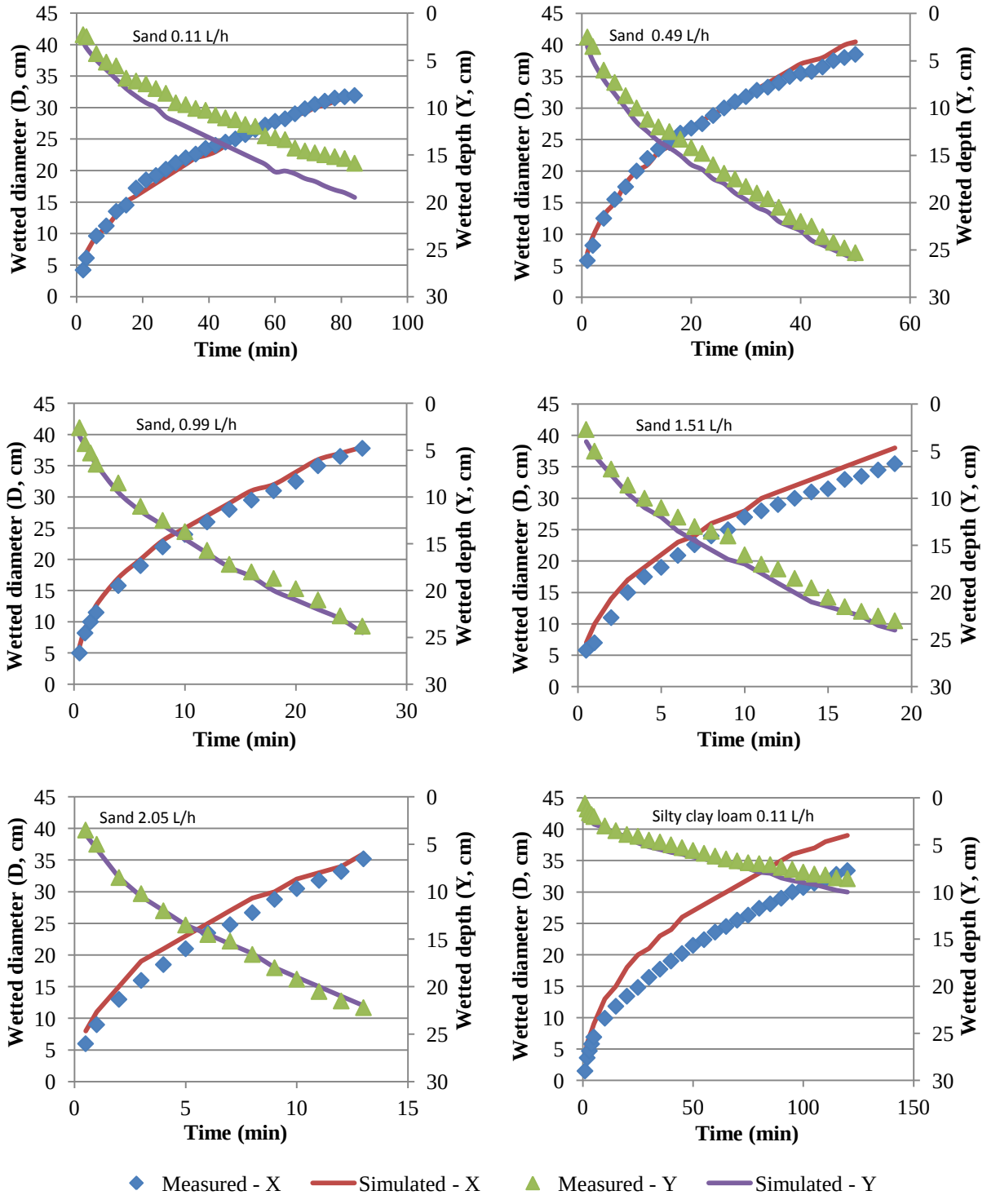

Figure 4.14: Measured and simulated wetting pattern diameters (D) and depths (Y) as a function of time (min) for sandy and silty clay loam soil at different emitter discharge rates (*Q* (L/h))
Slika 4.14: Izmerjena in simulirana diameter (D) in globina (Y) omočenih tal kot funkcija časa namakanja (min.) za peščena, meljasto ilovnata in glinasta tla pri različnih pretokih kapljačev (*Q* (L/h))

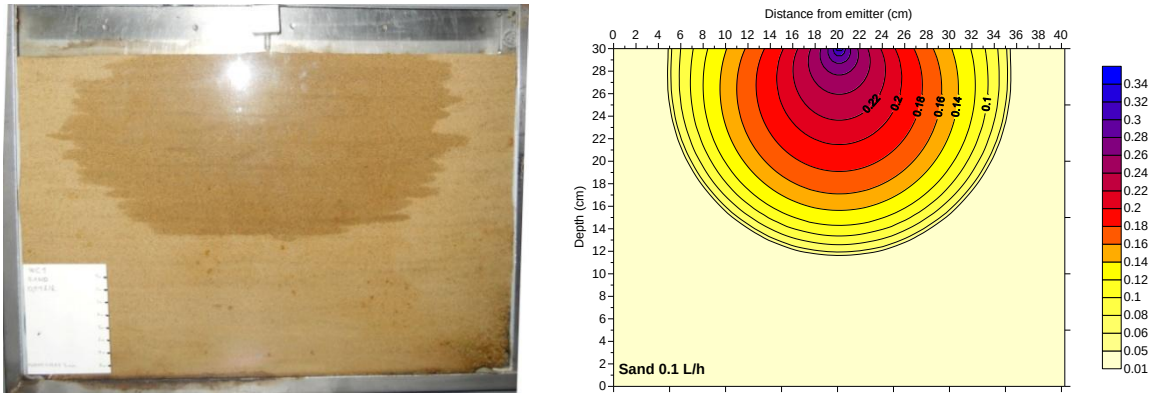

Sand 0.99 L/h at the end of irrigation cycle – 84 min (0,15 L of water applied)

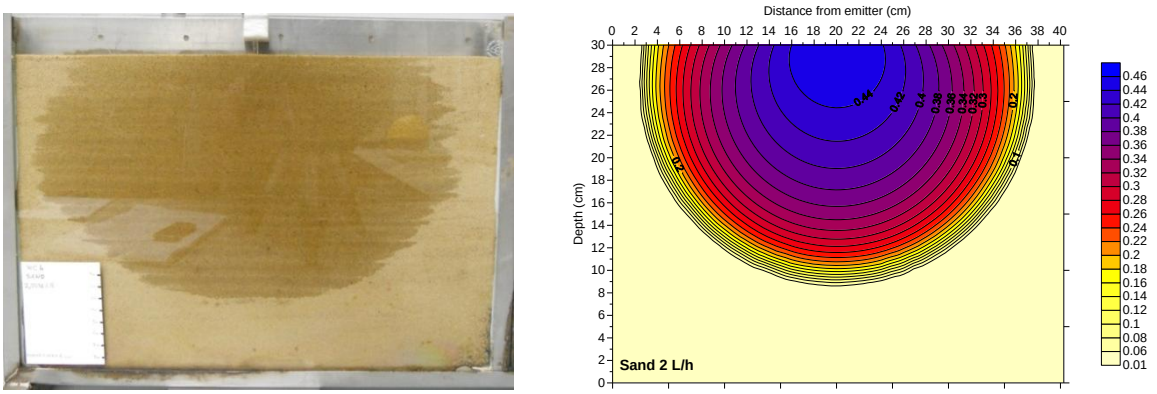

Sand 2.05 L/h at the end of irrigation cycle – 13 min (0,44 L of water applied)

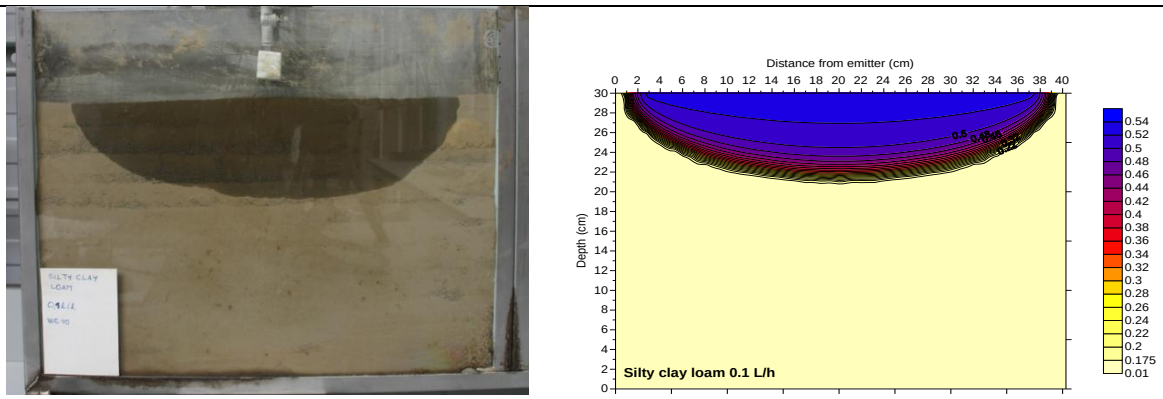

Silty clay loam 0.11 L/h at the end of irrigation cycle – 120 min (0,23 L of water applied

Figure 4.15: Measured (left side) and simulated (right side) wetting patterns for sand and silty clay loam soils at the end of the water application for emitter discharge rates (*Q*) of 0.99, 2.05 and 0.11 L/h (Naglič, 2011)
Slika 4.15: Izmerjeni (leva stran) in simulirani (desna stran) vzorci omočenosti za peščena, meljasto glinasto ilovnata tla na koncu namakanja za pretoke kapljačev (*Q*) 0,99; 2,0 5 in 0,11 L/h (Naglič, 2011)

The statistical comparison between observed and predicted data is presented in Table 4.1.

Table 4.1: Root mean square error (RMSE) between measured and simulated wetting pattern diameters (D) and depths (Y) for emitter discharge rates (*Q*) ranged from 0.1 to 2 L/h (Naglič, 2011)
Preglednica 4.1: Efektivna srednja kvadratna napaka (RMSE) med izmerjenimi in simuliranimi diametri (D) in globinami (Y) omočenih tal za pretoke kapljačev (*Q*) od 0,1 do 2 L/h (Naglič, 2011)

Soil texture	RMSE (cm)									
	Q									
	0.11 L/h		0.49 L/h		0.99 L/h		1.51 L/h		2.05 L/h	
	D	Y	D	Y	D	Y	D	Y	D	Y
Sand	0.8	2.6	1.0	1.3	1.0	0.7	2.2	1.3	1.9	0.4
Silty clay loam	5.0	0.8	-	-	-	-	-	-	-	-

The model predicted correctly the distribution of water in Y direction for both soils, with RMSE values < 2.6 cm. Good predictions of distribution in D direction were also obtained with RMSE values < 5.0 cm over the five flow rates (Naglič, 2011).

4.3 CORRELATIONS BETWEEN SOIL TEXTURE, HYDRAULIC PROPERTIES AND HORIZONTAL AND VERTICAL WETTING PATTERN DIMENSIONS

Soil parameters (soil texture, soil physical parameters and VG constants) as presented in section 3.4 were used in multiple linear regression analysis to examine their effects on wetting pattern radius (X) and depth (Y). Pareto chart of those effects was used to represent the influence of soil properties on wetting pattern X and Y dimensions (Figure 4.16 and 4.17). The Pareto chart's purpose is to highlight the most important parameters, among typically, a large set of parameters. The *p* value of 0.05 indicates which parameters are statistically significant; *t*-test checks the significance of individual regression coefficients.

It can be seen on Figure 4.16 that volume of applied water (L), θ_f (cm^3/cm^3), *Ks* (cm/day) and α (1/cm) have the highest significance in predicting the wetted radius (X) and are therefore used to build a model. All parameters, except % of sand and % of clay, are statistically significant. In figure 4.17 the volume of applied water, θ_f (cm^3/cm^3), *Q* (L/h) and *Ks* (cm/day) have the highest significance in predictions of wetted depth (Y) and, although all the other parameters are statistically significant, they add very little to wetted depth explanation.

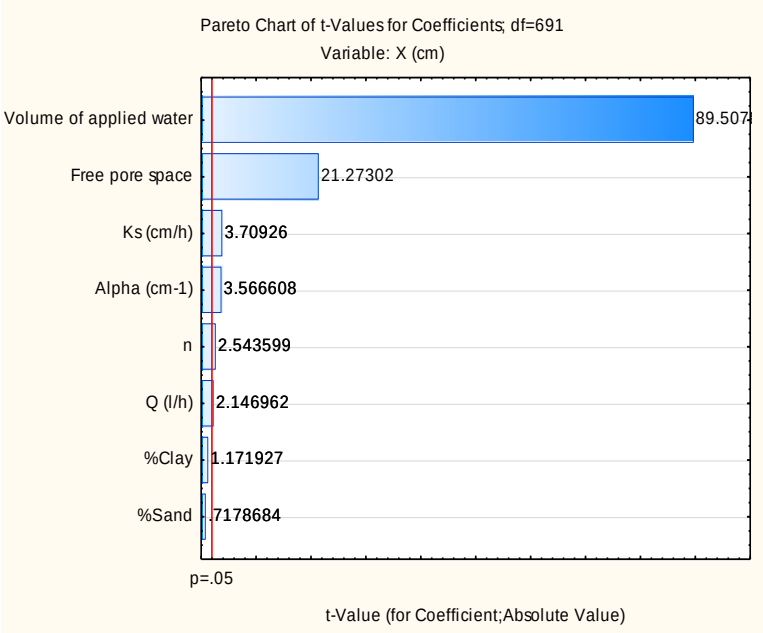

Figure 4.16: Pareto chart showing the relative frequency of soil parameters, affecting the soil wetting radius (X) (Naglič, 2011)
Slika 4.16: Pareto diagram, ki prikazuje relativno frekvenco parametrov tal, z vplivom na polmer (X) omočenih tal (Naglič, 2011).

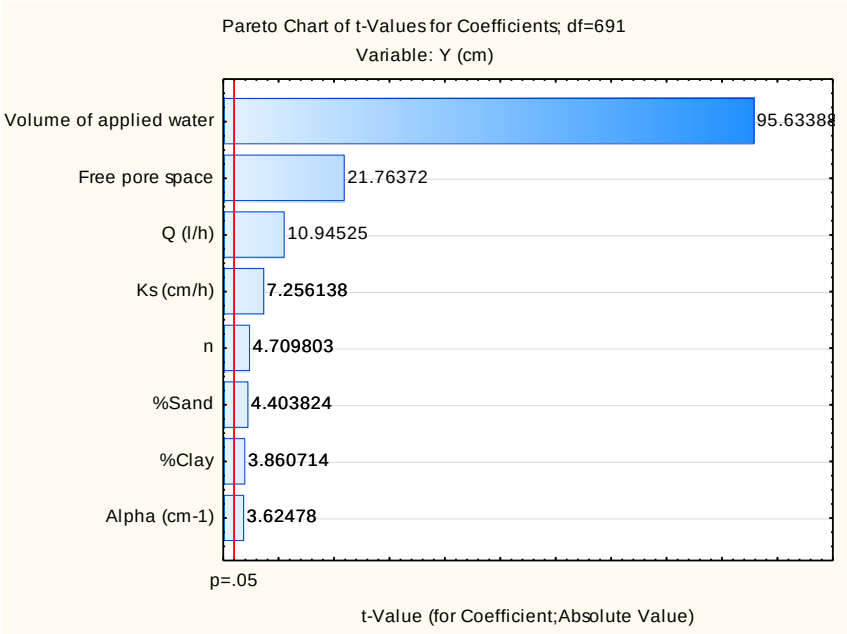

Figure 4.17: Pareto chart showing the relative frequency of soil parameters, affecting the depth (Y) of wetting pattern (Naglič, 2011)
Slika 4.16: Pareto diagram, ki prikazuje relativno frekvenco parametrov tal, z vplivom na globino (Y) omočenih tal (Naglič, 2011).

In both cases the parameters without or with lower statistical significance were removed from the model and new predictions, as presented in Table 4.2, were made (Naglič, 2011)

Table 4.2: Dependent and independent variables and multiple regression equations describing the relationship between soil parameters and soil wetted radius (X) and depth (Y) (Naglič, 2011)
Preglednica 4.2: Odvisne in neodvisne spremenljivke in enačbe multiple regresije, ki opisujejo zvezo med parametri tal in radiusom (X) ter globino (Y) omočenih tal (Naglič, 2011).

Dependent variable	Independent variable	Equation	Adj. R^2	p
X (cm)	Volume of water (V) (L), α (1/cm), θ_f (cm^3/cm^3), Ks (cm/h)	$x = -57.9*\alpha - 34.14*\theta_f + 0.94*V + 0.09*Ks + 31.52$	0.92	$p < 0.001$
Y (cm)	Volume of applied water (V) (L), Q (L/h), θ_f (cm^3/cm^3), Ks (cm/h)	$y = 1.22*Ks - 1.27*Q - 90.8*\theta_f + 1.87*V + 31.8$	0.92	$p < 0.001$

The volume of applied water (L), θ_f (cm^3/cm^3), Ks (cm/day) and α (1/cm) explained 92 % of variability of the wetted radius (X). Volume of applied water (L), θ_f (cm^3/cm^3), Q (L/h) and Ks (cm/h) explained 92 % of variability of wetted depth (Y). Analysis showed that independent variables, presented in Table 4.2, sufficiently explained the variability of X and Y. The full model, including all selected variables from Figures 4.16 and 4.17, explained 92 % of variability of X and 94 % of variability of Y (Naglič, 2011).

Figure 4.18 shows observed vs. predicted values for relationship X and volume of applied water (L), θ_f (cm^3/cm^3), Ks (cm/h) and α (1/cm).

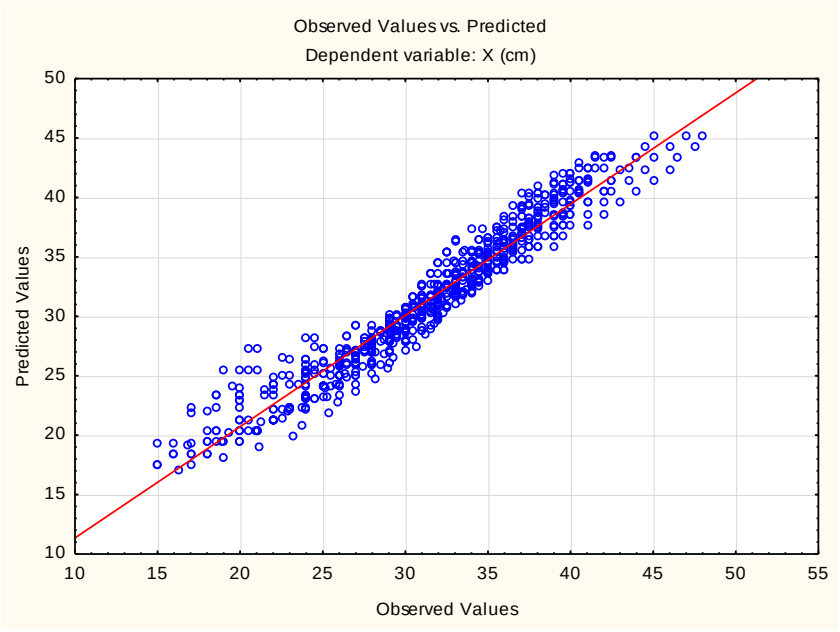

Figure 4.18: Observed values of X (cm) against those predicted from the relationship between X and volume of applied water (L), *θf, Ks* (cm/h) and α (1/cm) (Naglič, 2011)
Slika 4.18: Opažene vrednosti X (cm) proti tistim, ki so bile napovedane iz odnosa med X in volumnom dodane vode (L), *θf, Ks* (cm/h) in α (1/cm) (Naglič, 2011).

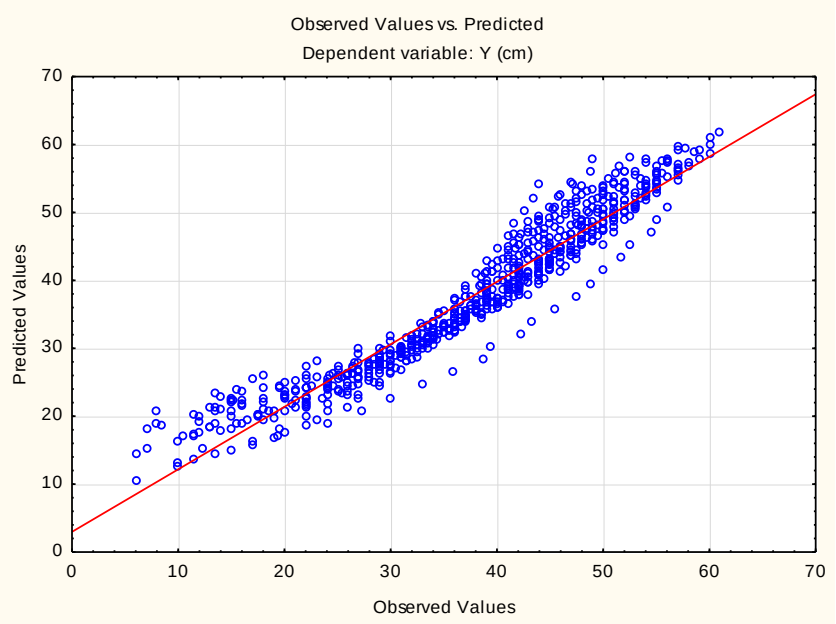

Figure 4.19: Observed values of Y (cm) against those predicted from the relationship between Y and volume of applied water (L), θ_f, Q (L/h) and Ks (cm/day) (Naglič, 2011)
Slika 4.19: Opažene vrednosti Y (cm) proti tistim, ki so bile napovedane iz odnosa med Y in volumnom dodane vode (L), θ_f, Q (L/h) in Ks (cm/dan) (Naglič, 2011).

Predicted values cluster closely and homogeneously around the 1:1 line, indicating a good fit of the linear model. On the basis of that it can be concluded that the volume of applied water (L), θ_f (cm^3/cm^3), Ks (cm/h) and α (1/cm) provide a good fit for the dependent variable of wetted pattern radius (X). Figure 4.19 shows observed vs. predicted values for relationship Y and Volume of applied water θf (cm^3/cm^3), Q (L/h) and Ks (cm/h). Predicted values cluster quite closely and homogenously around the 1:1 line. It can be concluded that volume of applied water, free pore space (θf), Q (L/h) and Ks (cm/h) provide a good fit for wetted depth (Y) (Naglič, 2011).

4.4 COMPARISON WITH EXISTING SIMPLE EMPIRICAL MODEL

The Schwartzman and Zur (1986) empirical model parameters were improved on the data obtained with the Hydrus-2D/3D simulations. 880 measurements were fitted to the model (Equations 28 and 29 in section 3.5.1), which included the measured wetting patterns from 11 soil textures at 50 % depletion and emitter Q (L/h) and all possible combinations of three contrasting soil textures, three emitter discharge rates and three different initial soil water conditions.

The dimensionless wetted radius (X*), wetted depth (Y*) and amount of water applied (V*) were calculated from the X and Y data obtained with the numerical simulations for each

volume of applied water, using the appropriate values of *Ks* for each soil texture and the known emitter *Q*.

The relationship between dimensionless *V** and *X** from Figure 4.20 resulted in following power equation with value coefficient of determination (R^2) of 0.94 (Equation 35).

$$X^* = 1.56V^{*0.29} \quad \text{... (35)}$$

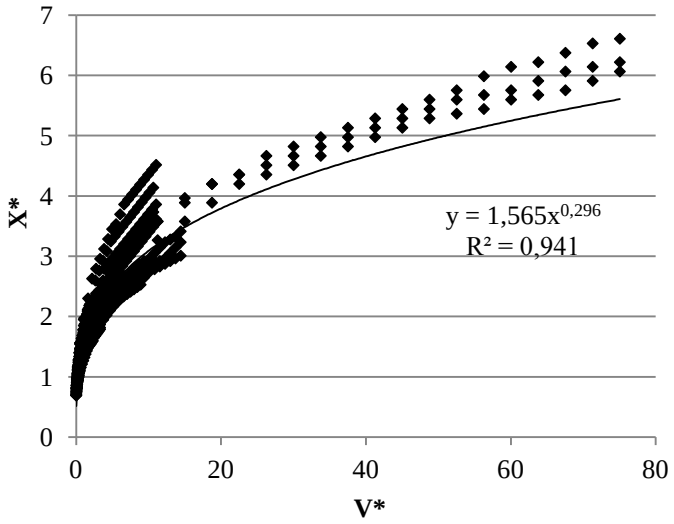

Figure 4.20: Relationship between *V** and *X** obtained from Hydrus-2D/3D simulated results for all treatments
Slika 4.20: Zveza med *V** in *X**, pridobljena iz rezultatov Hydrus-2D/3D simulacij za vsa obravnavanja.

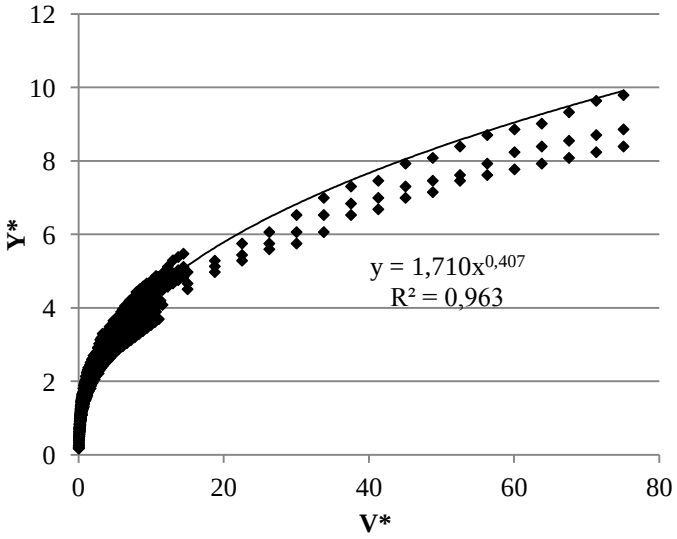

Figure 4.21: Relationship between *V** and *Y** obtained from Hydrus-2D/3D simulated results for all treatments
Slika 4.21: Zveza med *V** in *Y**, pridobljena iz rezultatov Hydrus-2D/3D simulacij za vsa obravnavanja.

Similarly, the relationship between dimensionless V^* and Y^* from Figure 4.21 resulted in following power equation (Equation 36) with value R^2 of 0.96.

$$X^* = 1.71V^{*0.41} \quad \text{... (36)}$$

Values of constants A1, A2 n1 and n2, regarding to equations 26 and 27 from the model, were 1.56, 1.71, 0.26 and 0.41, respectively. With converting dimensionless equations 35 and 36 to dimensional ones, using equations 28 and 29, resulted in the following relation (Equations 37 and 38).

$$X=1.56\ V^{0.29}\left(\frac{Ks}{Q}\right)^{-0.057} \quad \text{... (37)}$$

$$Y=1.71\ V^{0.41}\left(\frac{Ks}{Q}\right)^{0.11} \quad \text{... (38)}$$

The performance of improved parameters of Schwartzman and Zur (1986) model is illustrated on Figures 4.22 and 4.23. Observed and predicted values for wetted radius and depth were transformed, using logarithmic transformation. Linear regression analysis of the results was done and R^2 of 0.77 for wetted radius and of 0.89 for wetted depth, were observed.

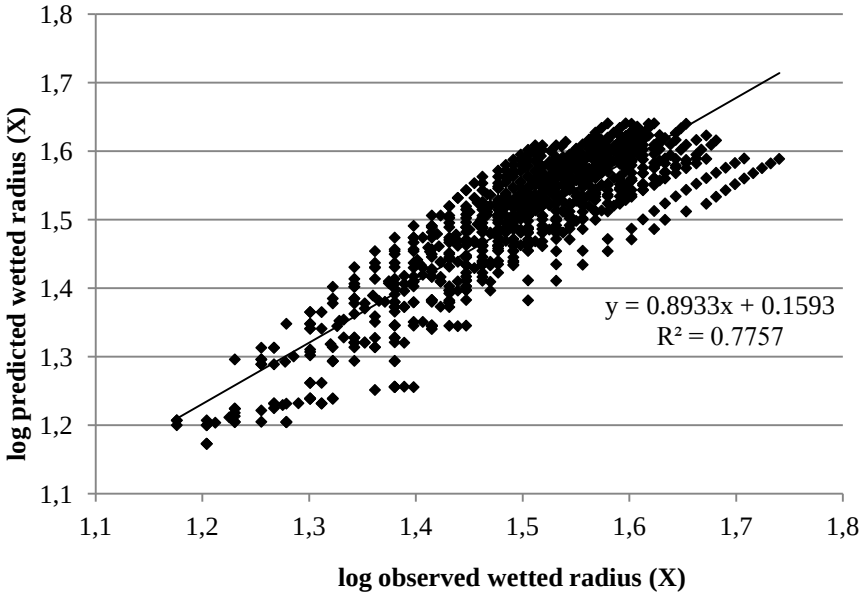

Figure 4.22: Logarithmic observed and predicted wetted radius (X) under surface drip emitter showing performance of Schwartzman and Zur model with improved parameters
Slika 4.22: Logaritem opaženega in napovedanega omočenega radija (X) pod nadzemnim kapljačem, ki prikazuje uspešnost Schwartzman and Zur modela z izboljšanimi parametri.

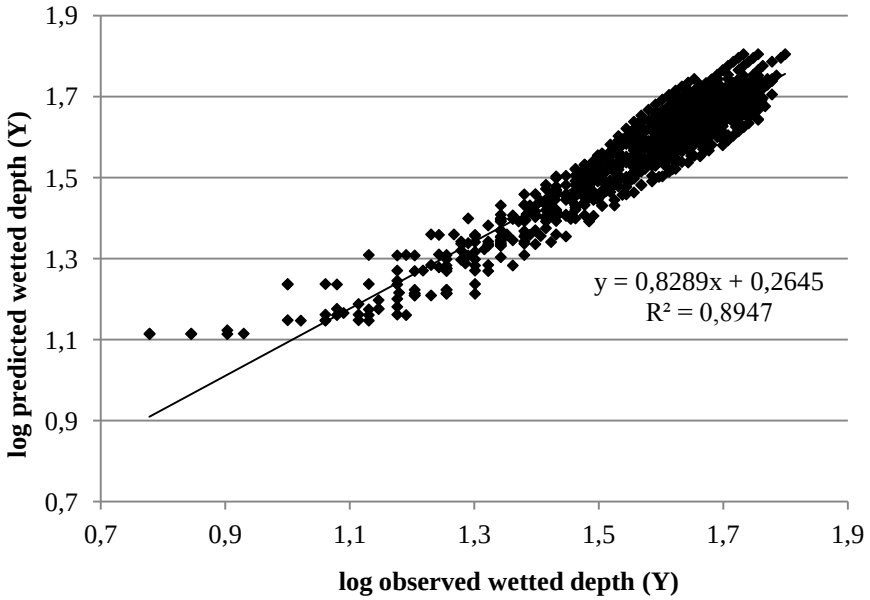

Figure 4.23: Logarithmic observed and predicted wetted depth (Y) under surface drip emitter ushowing performance of improved parameters of Schwartzman and Zur model
Slika 4.23: Logaritem opažene in napovedane omočene globine (Y) pod nadzemnim kapljačem, ki prikazuje uspešnost Schwartzman and Zur modela z izboljšanimi parametri.

Schwartzman and Zur (1986) model with original constants is based on two soils and two different emitter discharge rates of Bresler (1978) research and is as such unlikely to represent the best fit for most of soil textures. The new model constants result from the best fit for many more soil textural classes, different emitter discharge rates and different initial soil water initial conditions.

The Schwartzaman and Zur (1986) model using both our new (derived in this study) and the old (original) model constants, and Malek and Peters (2011) model, were compared to experimental results (real data about advance of wetting pattern dimensions with volume of applied water) published by Li et al. (2003, 2004) and Moncef et al. (2002). They provided the data of the wetted fronts for different soil types (sand, loam and silt) and different emitter Q. In research of Li et al. (2003) the soil was a loam with 54 % sand, 34 % silt and 12 % clay. The θ_s, Ks and ρ_b were 0.47 cm^3/cm^3, 1.85 cm/h and 1.32 g/cm^3, respectively. To test the models, the experiments with emitter Q of 0.6, 0.9 and 2 L/h were chosen. The soil from the Li et al. (2004) study was sand with θ_s, Ks and ρ_b of 0.42 cm^3/cm^3, 2.1 cm/h and 1.46 g/cm^3, respectively. The emitter Q of 0.5 and 1.0 L/h were used to compare the models. In the experiments done by Moncef et al. (2002) the silt soil was used. The θ_s, Ks and ρ_b were 0.58 cm^3/cm^3, 5.8 cm/h and 1.28 g/cm^3, respectively. Emitter discharge rates of 1, 2 and 4 L/h were used to compare the models. Figures 4.24 and 4.25 show two examples of comparison of the observed and predicted wetting pattern dimensions (using three investigated empirical models) for different emitter Q (L/h). Statistical evaluation of models performance is shown in Table 4.3.

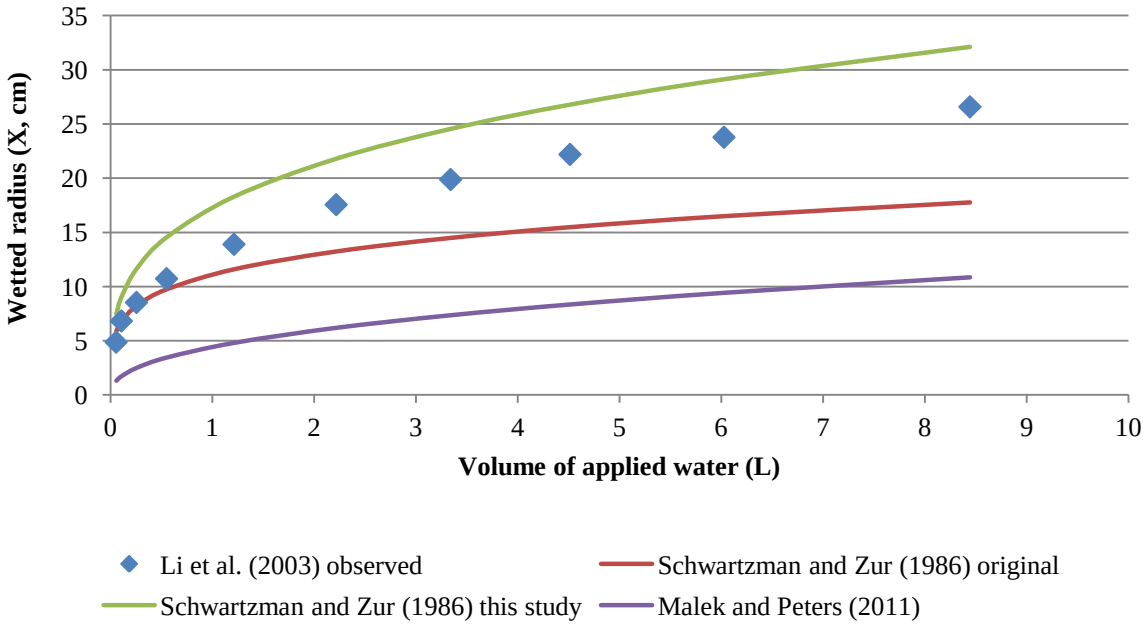

Figure 4.24: Real observed (Li et al., 2003) data compared to predicted wetted radius (X) with models of Schwartzman and Zur (1986) with constants improved in this study, Schwartzman and Zur (1986) model with original constants and Malek and Peters (2011) model, for emitter discharge rate (*Q*) of 0.6 L/h
Slika 4.24: Realni podatki (Li in sod., 2003) v primerjavi z napovedanimi omočenimi radiji (X) z modeli Schwartzman ain Zur (1986) s konstantami izboljšanimi v tej študiji, Schwartzman in Zur (1986) modelom z originalnimi konstantami in Malek in Peters (2011) modelom za pretok kapljača (*Q*) 0.6 L/h

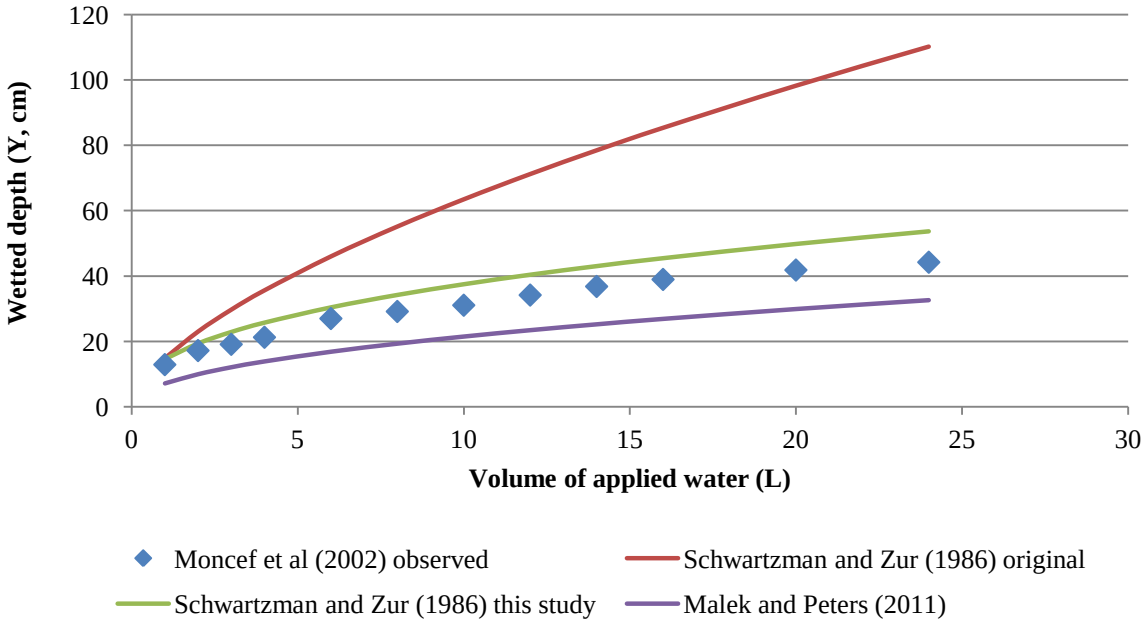

Figure 4.25: Real observed (Moncef et al., 2002) data compared to predicted wetted depth (Y) with models of Schwartzman and Zur (1986) with constants improved in this study, Schwartzman and Zur (1986) model with original constants and Malek and Peters (2011) model, for emitter discharge rate (*Q*) of 2 L/h
Slika 4.25: Realni podatki (Moncef in sod., 2003) v primerjavi z napovedanimi omočenimi globinami (Y) z modeli Schwartzman in Zur (1986) s konstantami izboljšanimi v tej študiji, Schwartzman in Zur (1986) modelom z originalnimi konstantami in Malek in Peters (2011) modelom za pretok kapljača (*Q*) 0.6 L/h

Table 4.3: Statistical analysis of the comparison between wetting pattern dimensions obtained experimentally by Li et al. (2003, 2004) and Moncef et al. (2002) for different soil textural classes and different emitter Q to those predicted with the empirical models of Schwartzman and Zur (1986) (with original parameters and those derived in this study) and Malek and Peters (2011); n is the number of measurements of each wetting pattern dimensions

Preglednica 4.3: Statistična analiza primerjave med dimenzijami omočenosti tal, pridobljenimi eksperimentalno od Li in sod. (2003, 2004) in Moncef in sod. (2002) za različne teksturne razrede in pretoke kapljačev (Q) ter tistimi, ki so bile predvidene z empiričnimi modeli Schwartzman in Zur (1986) (z originalnimi konstantami in v tej študiji izboljšanimi konstantami) in Malek in Peters (2011); n je število meritev vsakega vzorca omočenosti.

	Wetted radius X (cm)			Wetted depth Y (cm)		
	RMSE (cm)	EF	*n*	RMSE (cm)	EF	*n*
	Li et. al. (2003) for Q = 0.6 L/h; loam soil					
Schwartzman and Zur (original)	4.80	0.31	10	46.19	-4.54	8
Schwartzman and Zur (this study)	4.20	0.47	10	8.39	0.82	8
Malek and Peters	10.68	-2.42	10	4.61	0.94	8
	Li et. al. (2003) for Q = 0.9 L/h; loam soil					
Schwartzman and Zur (original)	5.53	0.41	8	36.95	-23.04	6
Schwartzman and Zur (this study)	4.36	0.63	8	8.77	-0.36	6
Malek and Peters	12.35	-1.95	8	3.49	0.79	6
	Li et. al. (2003) for Q = 2 L/h; loam soil					
Schwartzman and Zur (original)	2.78	0.70	7	16.23	-5.07	6
Schwartzman and Zur (this study)	4.85	0.10	7	5.75	0.24	6
Malek and Peters	11.33	-3.92	7	4.77	0.48	6
	Li et. al. (2004) for Q = 0.5 L/h; sandy soil					
Schwartzman and Zur (original)	4.52	0.37	9	13.55	-1.50	9
Schwartzman and Zur (this study)	4.30	0.43	9	2.21	0.93	9
Malek and Peters	8.90	-1.43	9	3.47	0.84	9
	Li et. al. (2004) for Q = 1 L/h; sandy soil					
Schwartzman and Zur (original)	2.98	0.68	7	6.26	0.32	7
Schwartzman and Zur (this study)	5.37	-0.04	7	2.41	0.90	7
Malek and Peters	8.08	-1.35	7	2.72	0.87	7
	Moncef et. al. (2002) for Q = 1 L/h; silty soil					
Schwartzman and Zur (original)	6.27	-0.22	12	37.31	-37.24	12
Schwartzman and Zur (this study)	6.06	-0.14	12	8.32	-0.90	12
Malek and Peters	1.45	0.93	12	5.69	0.11	12
	Moncef et. al. (2002) for Q = 2 L/h; silty soil					
Schwartzman and Zur (original)	6.88	-0.03	12	35.63	-12.31	12
Schwartzman and Zur (this study)	8.29	-0.50	12	5.71	0.66	12
Malek and Peters	3.71	0.70	12	9.79	0.00	12
	Moncef et. al. (2002) for Q = 4 L/h; silty soil					
Schwartzman and Zur (original)	4.61	0.61	12	39.27	-9.76	12
Schwartzman and Zur (this study)	13.92	-2.54	12	9.19	0.41	12
Malek and Peters	12.66	-1.93	12	8.05	0.55	12

The RMSE (cm) values varied in both directions from 2.87 to 46.19 cm for Schwartzman and Zur (1986) model with original constants, from 2.21 to 13.92 cm for Schwartzman and Zur (1986) model with improved parameters (in this study) and from 1.45 to 12.66 cm for model of Malek and Peters (2011) model. The EF values varied from -37.24 to 0.70 for Schwartzman and Zur (1986) model with original constants, from -2.54 to 0.93 for Schwartzman and Zur (1986) model with improved constants and from -3.92 to 0.94 for Malek and Peters (2011) model. The results show that the wetted radius and wetted depth predicted with Schwartzman and Zur (1986) model were in better agreement with observed data when using the new constants derived in this study. Figure 4.26 shows data of how many times RMSE (cm) of predicted wetting pattern dimensions of each model was the smallest (best), medium and worst (largest RMSE) when compared to observed data. Each models' performance was evaluated 16 times – 8 times in vertical and 8 times in horizontal direction.

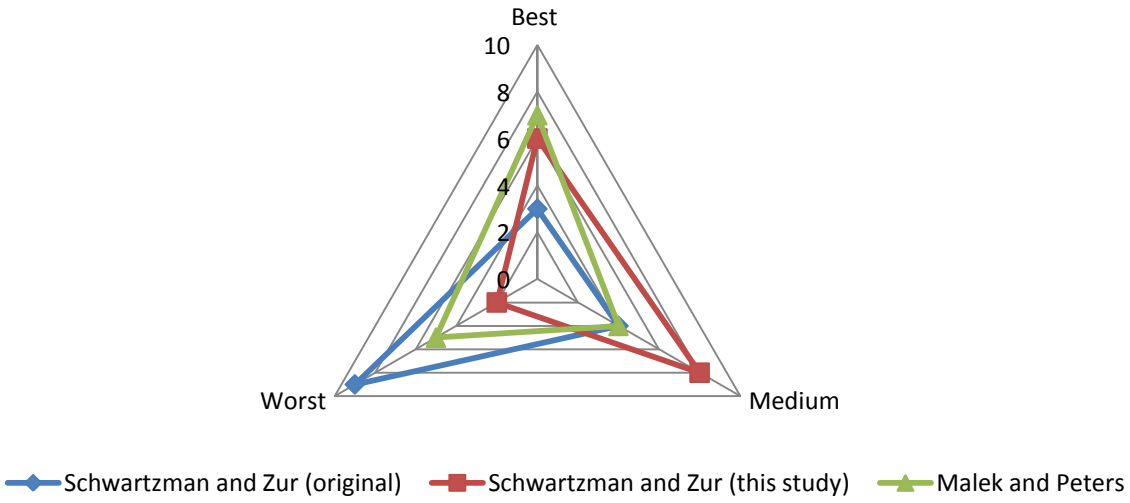

Figure 4.26: Prediction capabilities of selected empirical models (Schwartzman and Zur (1986) with constants improved in this study, Schwartzman and Zur (1986) model with original constants and Malek and Peters (2011) model)
Slika 4.26: Napovedne zmogljivosti izbranih empiričnih modelov (Schwartzman in Zur (1986) z originalnimi konstantami in v tej študiji izboljšanimi konstantami in Malek in Peters (2011) modelom)

Overall, analysis of RMSE (cm) values showed that the improved Schwartzman and Zur (1986) model provided the best estimations of the wetted fronts, followed by Malek and Peters (2011) and existing Schwartzman and Zur (1986) models. The difference between Schwartzman and Zur (1986) model with improved constants and Malek and Peters (2011) model was small and it can be concluded that both models performed well. But, on the other hand, when taking into account the simplicity of Schwartzman and Zur (1986) model, where the only soil parameter required is *Ks* (m/day), the model has a big advantage over other models.

4.5 APPLICATION TO SURFACE DRIP IRRIGATION OF SWEET CORN

4.5.1 Wetting pattern size influence

Figure 4.27 shows the water content distribution for all simulated strategies at the end of water application.

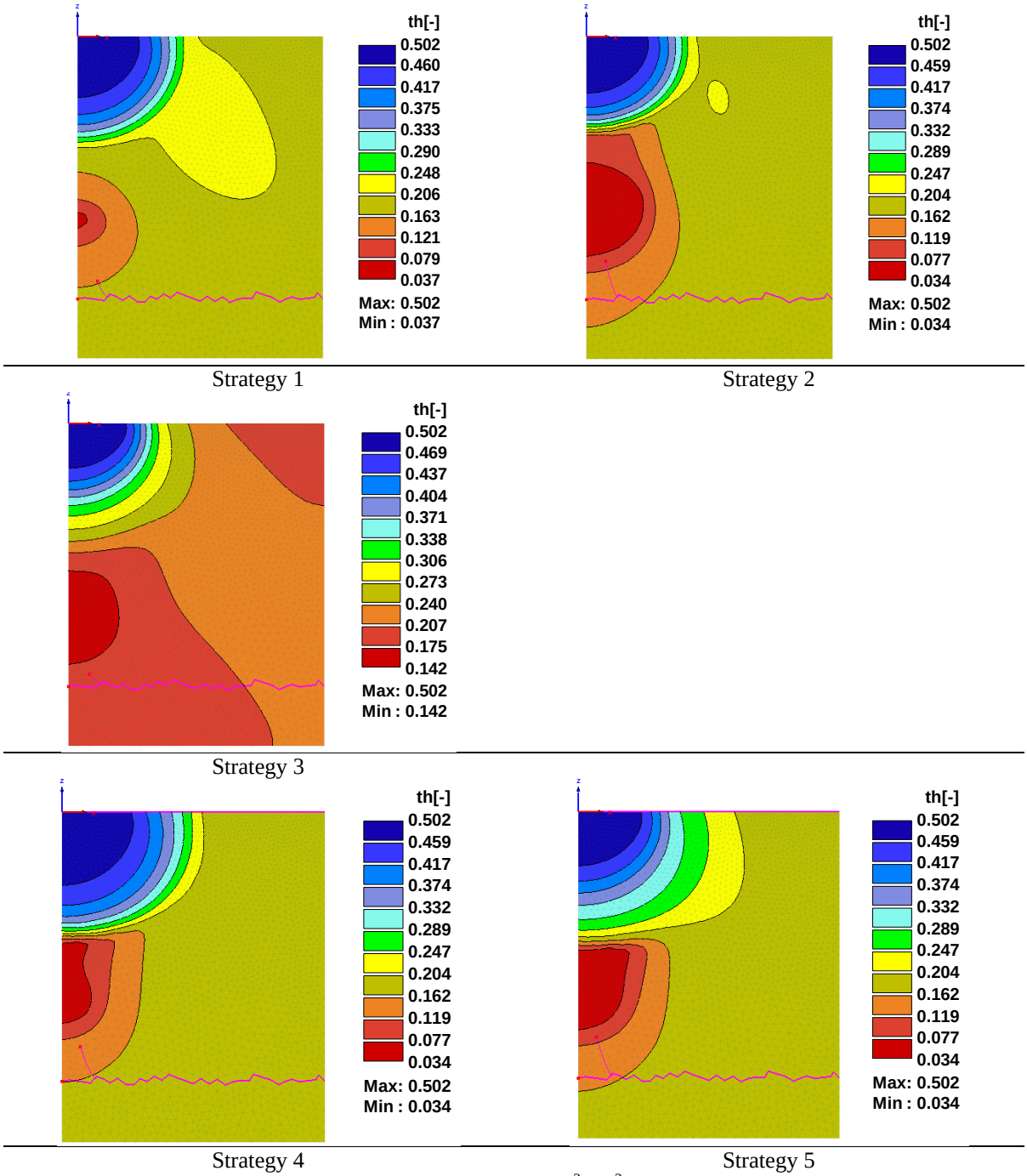

Figure 4.27: Simulated water content distribution (th = θ (cm^3/cm^3)) under sweet corn irrigation in sandy soil in Senegal at the end of last irrigation event for all 5 strategies

Slika 4.27: Simulirana distribucija vode (th = θ (cm^3/cm^3)) pod namakanim posevkom sladke koruze v peščenih tleh v Senegalu, na koncu namakalnega cikla, za vseh 5 strategij

In strategies 1, 2 and 3 the same amount of water (8.26 mm or 2.047 L per 1 emitter), equal to plant ETc, was applied on the daily basis (difference between strategies was in irrigation frequency (continous or pulsing) and time of the day when irrigation started). In strategies 4 and 5 the same amount of water (16.52 mm or 4.094 L per one emitter) was applied every second day to meet plant water needs (difference between strategies 4 and 5 was in irrigation frequency (continous or pulsing)).

Figure above clearly shows that beneath the wetting patterns dry zone occurred in all strategies, which was due to the root water uptake. Between irrigation events this dry zone spread to the top of the soil according to the plant root distribution. The wetting pattern extend in both directions, as shown on Figure 4.27, can serve as preliminary step to determine the emitter in line distances. In this case the wetting pattern horizontal (radial) extend is 18, 17, 24, 21 and 24 cm for irrigation strategies 1, 2, 3, 4 and 5. Because the emitter distances for sweet corn irrigation are 33 cm (radius of 16.5 cm) it can be concluded that the wetting patterns are overlapping in all cases and therefore producing continuous wetted strip in the soil. The wetted depths were 17, 15, 18, 20, and 21 cm for strategies 1, 2, 3, 4 and 5, respectively. The results show that irrigation is not wetting the entire root zone, which extends to the depth of 40 cm. On the other hand, wetting pattern reaches the zone of maximum root intensity at around 15 cm in all strategies. In practice the root system will always look for water and will in this case stay shallow with its main root mass close to the surface. On the other hand the results showed that the upper half of the plants root system was wetted, which is also a main purpose of irrigation.

As can be clearly seen at the Figures 4.28 and 4.29 the sizes of the wetting patterns (in vertical and horizontal direction) for strategies 1 and 2 are about the same. The wetting pattern size for pulsed irrigation (strategy 3) is slightly bigger because water is applied slowly and it has enough time to redistribute between irrigation events. This resulted in less sharp (smoother) water content gradient, especially in vertical direction and therefore small increase in extend of wetting pattern. For strategies 4 and 5 the bigger wetting pattern sizes are due to the higher amounts of water applied, either continuously or with pulsing. For pulsed irrigation (strategy 5) the smoother water content gradient occurred when compared to strategy 3.

The positions of saturated wetted fronts (Figures 4.28 and 4.29) were in radial direction about the same for all strategies. However, small differences occurred in vertical direction, where strategy 4 resulted in the biggest saturated zone and strategy 3 in the smallest one. This is due to the gravity and matric forces working in the soil. In strategy 4, the biggest amount of water was applied in one irrigation event and there were gravitational forces dominant. Just the opposite happened for strategy 3 where the smallest amount of water

was applied in short pulses over the day. In this case matric potential forces were dominant over gravity. This resulted in less sharp wetting pattern front.

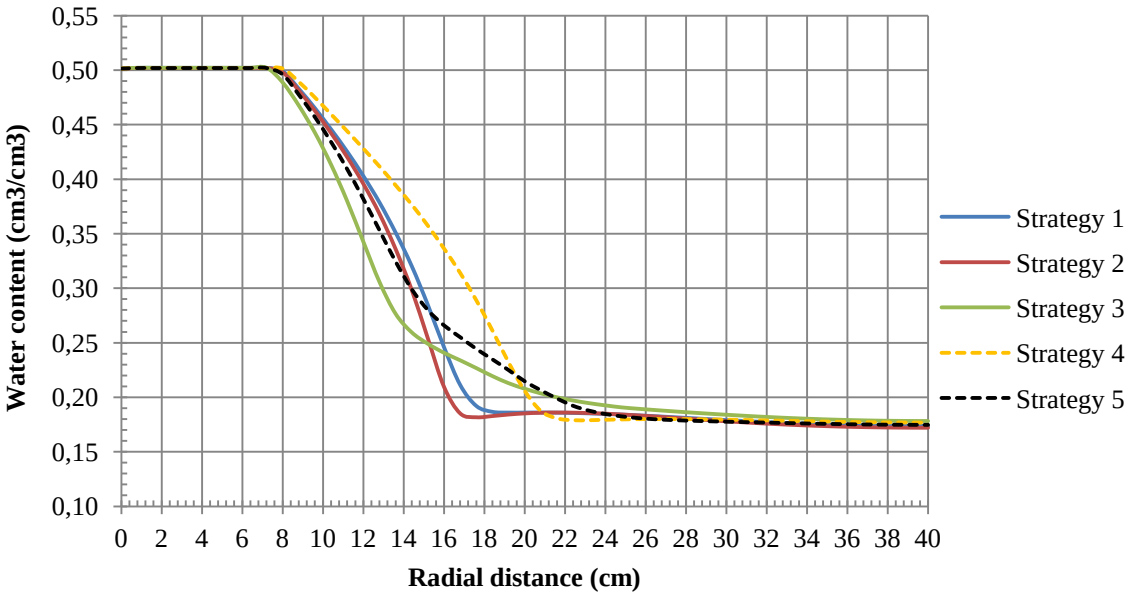

Figure 4.28: Simulated water content at sand soil surface in sweet corn crop as a function of radial distance at the end of last irrigation event
Slika 4.28: Simulirana vsebnost vode na površini peščenih tal v posevku sladke koruze, kot funkcija radialne razdalje, na koncu zadnjega cikla namakanja

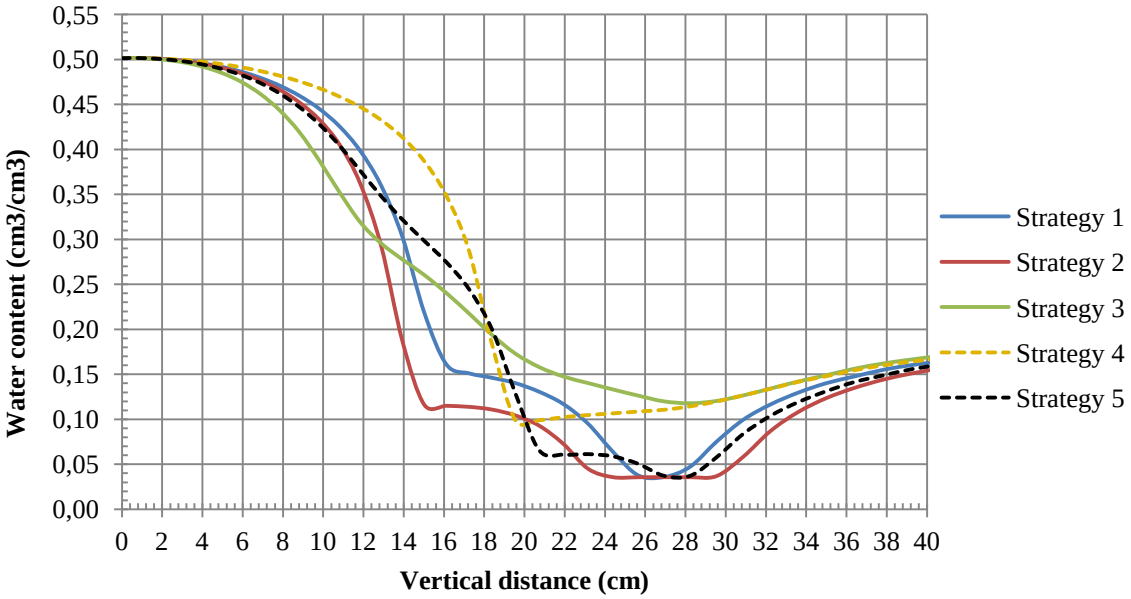

Figure 4.29: Simulated water content at sand soil surface in sweet corn crop as a function of vertical distance at the end of last irrigation event
Slika 4.29: Simulirana vsebnost vode na površini peščenih tal v posevku sladke koruze, kot funkcija vertikalne razdalje, na koncu zadnjega cikla namakanja

4.5.2 Soil water dynamics in different soil depths

With the purpose of water content monitoring during irrigation simulations three observation nodes were placed beneath the emitter in three different soil depths. Node 1 was placed at 10 cm, node 2 at 20 cm and node 3 at 40 cm depth.

Figures 4.30 and 4.31 show water content dynamics during 15 days (Strategies 1, 2 and 3) or 16 days (Strategies 4 and 5) of irrigation simulations at the soil depth of 10 cm. At the start of simulations water content was set just below soil FC of (0.21 cm^3/cm^3). During irrigation events the water content increased, but not to saturation (0.502 cm^3/cm^3) of the soil. The highest or peak water content at depth of 10 cm was observed for irrigation strategy 4 (0.47 cm^3/cm^3) and 1 (0.46 cm^3/cm^3), where water was applied continuously. The highest water content lasted only for a short time interval and afterwards dropped down to 0.20 for strategy 1 and 0.07 cm^3/cm^3 for strategy 4. For strategy 2, where crop was irrigated every day during the night, the water content was maintained between minimum of 0.12 and maximum of 0.44 cm^3/cm^3. Strategy 3, where crop was irrigated with pulsing, the water content was maintained between minimum of 0.24 and maximum of 0.43 cm^3/cm^3 and for strategy 5 between 0.12 and 0.44 cm^3/cm^3. The highest average water content was maintained with strategy 3. Water content minimum and maximum values at the depth of 10 cm approached to a steady state values for all strategies.

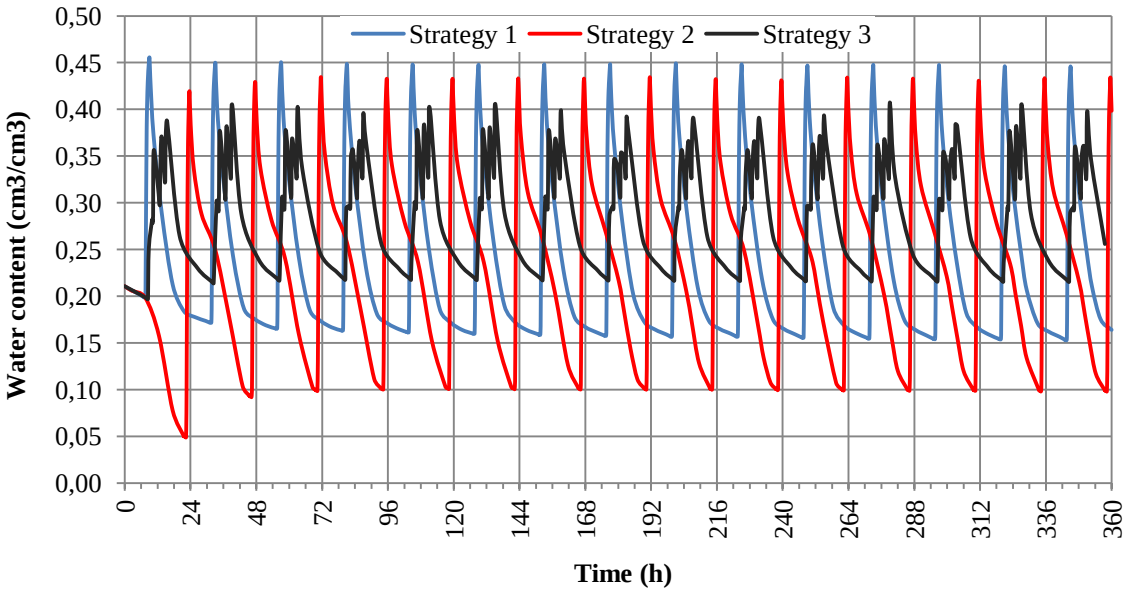

Figure 4.30: Simulated water content (cm^3/cm^3) dynamics under sweet corn surface drip irrigation at soil depth of 10 cm for strategies 1, 2 and 3
Slika 4.30: Simulirana dinamika vsebnosti vode (cm^3/cm^3) pod površinskim kapljičnim namakanjem sladke koruze, na globini tal 10 cm, za strategije 1, 2 in 3

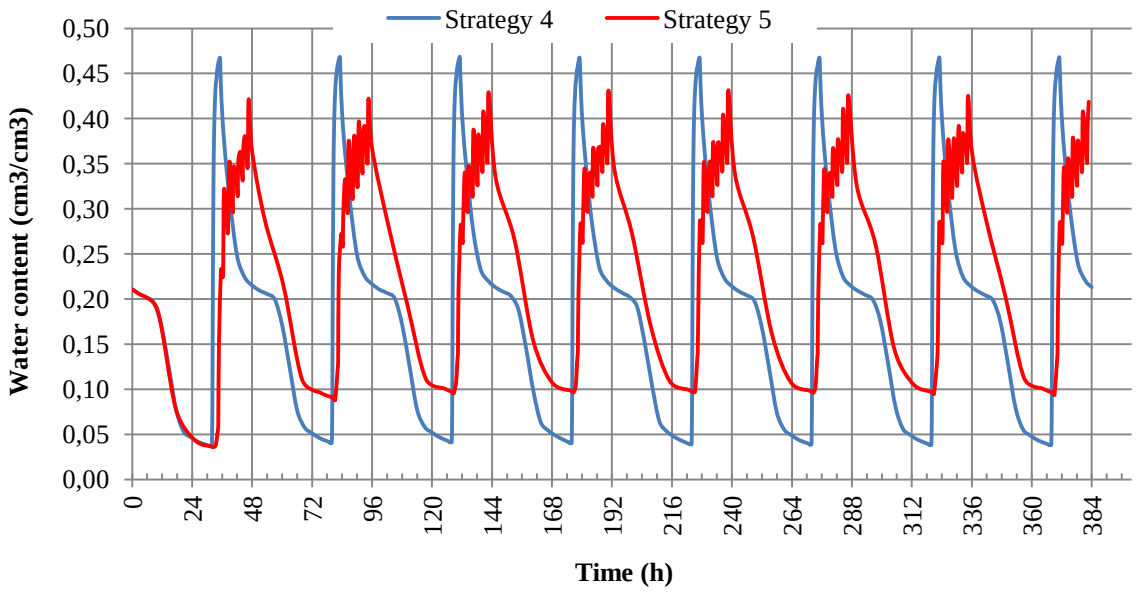

Figure 4.31: Simulated water content (cm^3/cm^3) dynamics under sweet corn surface drip irrigation at soil depth of 10 cm for strategies 4 and 5
Slika 4.31: Simulirana dinamika vsebnosti vode (cm^3/cm^3) pod površinskim kapljičnim namakanjem sladke koruze, na globini tal 10 cm, za strategiji 4 in 5

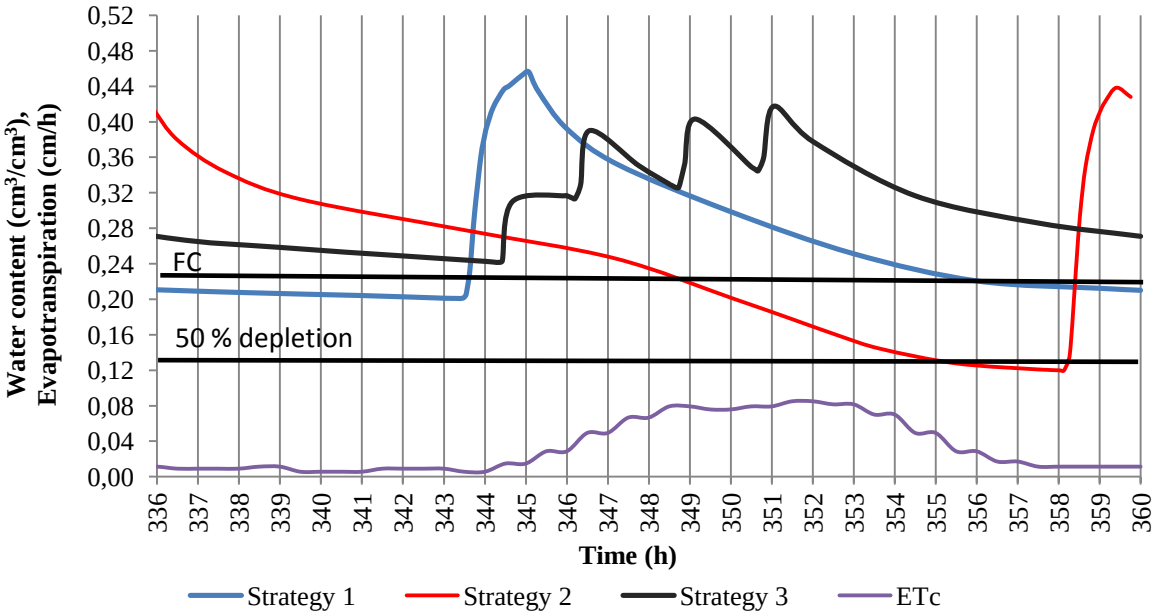

Figure 4.32: Simulated water content change at the soil depth of 10 cm for sweet corn surface drip irrigation strategies 1, 2 and 3 for the last (15^{th}) day or irrigation event. The root water uptake is highest between field capacity (FC) and 50 % depletion marks
Slika 4.32: Simulirana sprememba vsebnosti vode v tleh na globini 10 cm pod posevkom površinsko kapljično namakane sladke koruze, za strategije 1, 2 in 3, za zadnji (15.) dan namakanja. Odvzem vode skozi korenine je najvišji med poljsko kapaciteto tal za vodo (FC) in 50 % stanja razpoložljive vode v tleh.

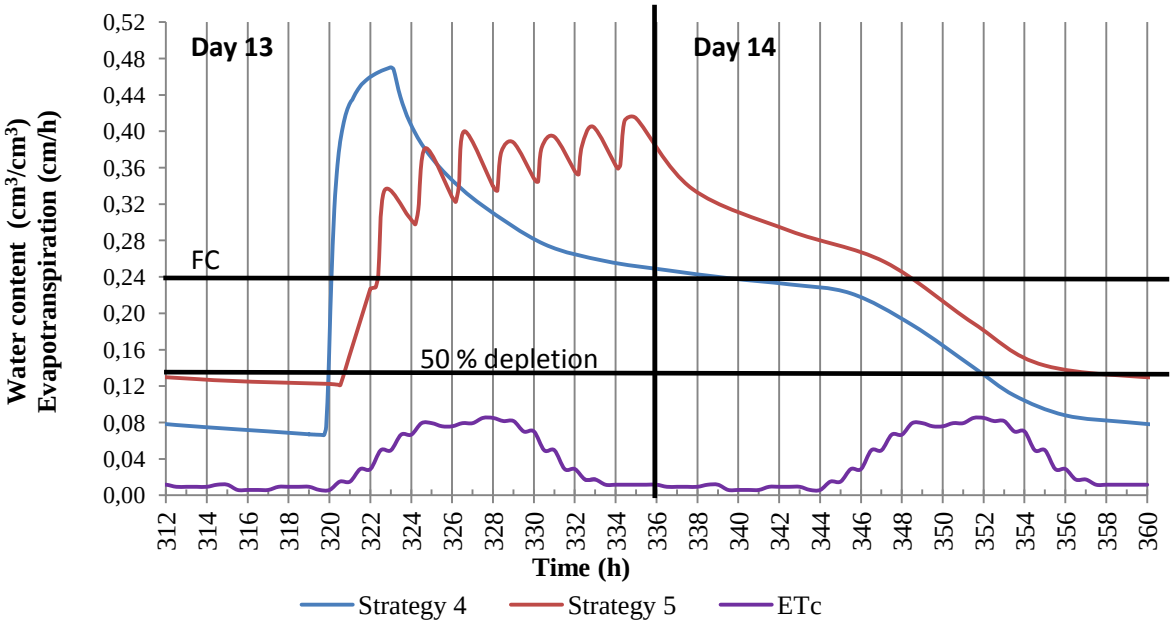

Figure 4.33: Simulated water content change at the soil depth of 10 cm for sweet corn surface drip irrigation strategies 4 and 5 the 7th irrigation event (on 13th and 14th day). The root water uptake is highest between FC and 50 % depletion marks
Slika 4.33: Simulirana sprememba vsebnosti vode v tleh na globini 10 cm pod posevkom površinsko kapljično namakane sladke koruze, za strategiji 4 in 5, za 7. cikel namakanja (13. in 14. dan). Odvzem vode skozi korenine je najvišji med poljsko kapaciteto tal za vodo (FC) in 50 % stanja razpoložljive vode v tleh.

Between soil FC and crop tolerated water depletion (for corn 50 % depletion is recommended by Allen et al. 1998) the plants experience no stress and water content is optimum for plants growth. Consequently root water uptake is highest in this water content range. The best irrigation strategy when considering above mentioned on Figures 4.32 and 4.33, was strategy 2, because water had enough time over the night to redistribute in the soil which resulted in optimum water content when the ETc of the plants was highest.

At the soil depth of 20 cm, the water content at the irrigation cut off was again highest for strategy 4 at 0.26 cm^3/cm^3 and strategy 1 at 0.25 cm^3/cm^3 (Figures 4.34 and 4.35) The lowest water content before the onset of new irrigation event was observed for strategies 5 at 0.03 cm^3/cm^3 and 2 at 0.08 cm^3/cm^3. The dynamics of water content change was again maintained at the highest average water content with irrigation strategy 3. In all strategies the average water content reached the steady state after 15 or 16 days (15 and 8 irrigation cycles) of irrigation. For additional insight into soil water content dynamics, Figures 4.36 and 4.37 show water content dynamics for all strategies during 24 h of last irrigation event.

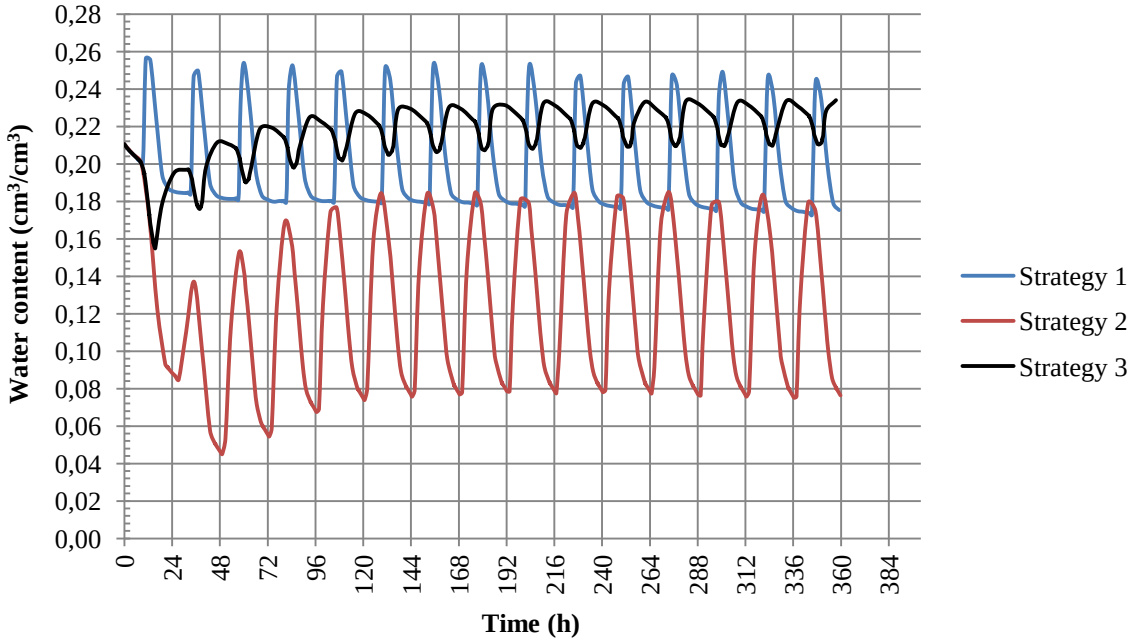

Figure 4.34: Simulated water content (cm^3/cm^3) dynamics under sweet corn surface drip irrigation at soil depth of 20 cm for strategies 1, 2 and 3
Slika 4.34: Simulirana dinamika vsebnosti vode (cm^3/cm^3) pod površinskim kapljičnim namakanjem sladke koruze, na globini tal 20 cm, za strategije 1, 2 in 3

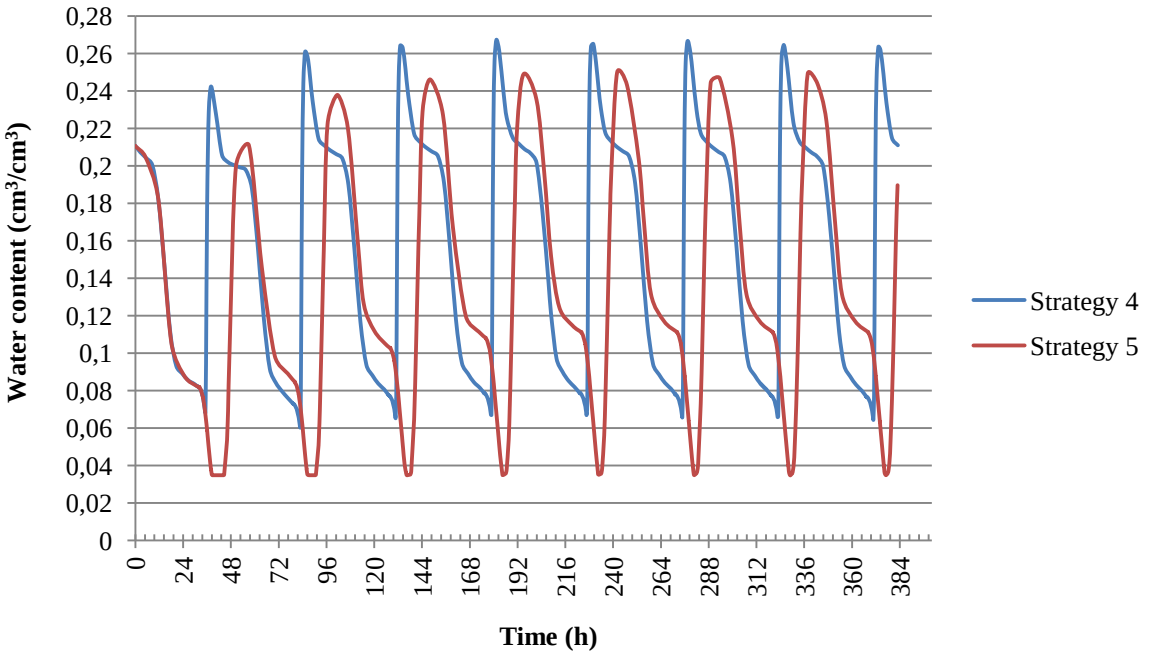

Figure 4.35: Simulated water content (cm^3/cm^3) dynamics under sweet corn surface drip irrigation at soil depth of 20 cm for strategies 4 and 5
Slika 4.35: Simulirana dinamika vsebnosti vode (cm^3/cm^3) pod površinskim kapljičnim namakanjem sladke koruze, na globini tal 20 cm, za strategiji 4 in 5

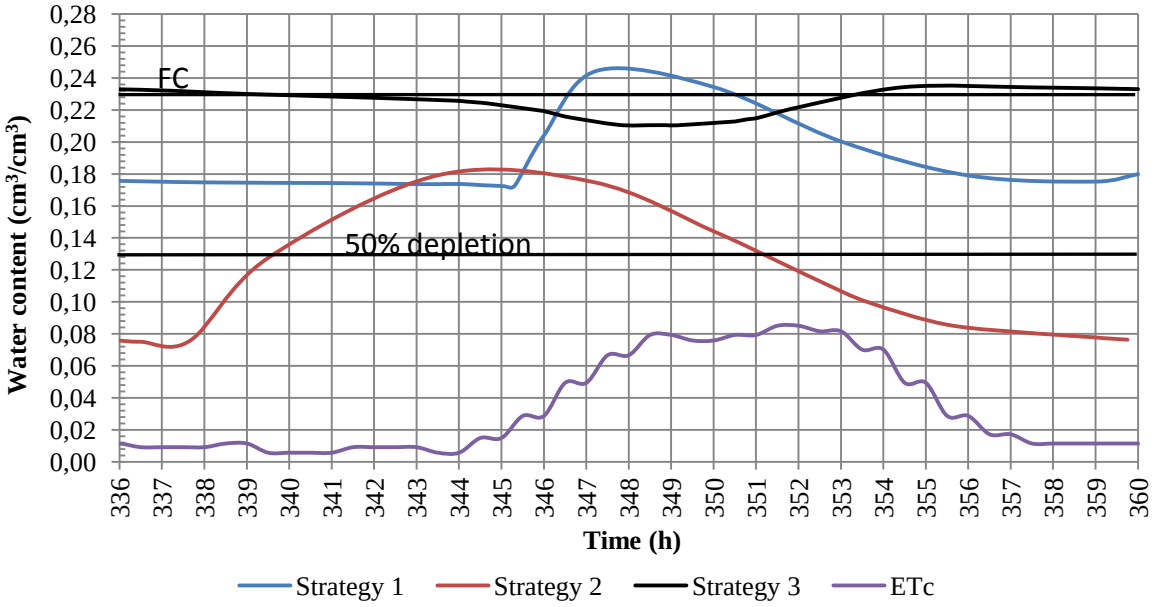

Figure 4.36: Simulated water content change at the soil depth of 20 cm for sweet corn surface drip irrigation strategies 1, 2 and 3 for the last (15th) day or irrigation event. The root water uptake is highest between FC and 50 % depletion marks

Slika 4.36: Simulirana sprememba vsebnosti vode v tleh na globini 20 cm pod posevkom površinsko kapljično namakane sladke koruze, za strategije 1, 2 in 3, za zadnji (15.) dan namakanja. Odvzem vode skozi korenine je najvišji med poljsko kappaciteto tal za vodo (FC) in 50 % stanja razpoložljive vode v tleh.

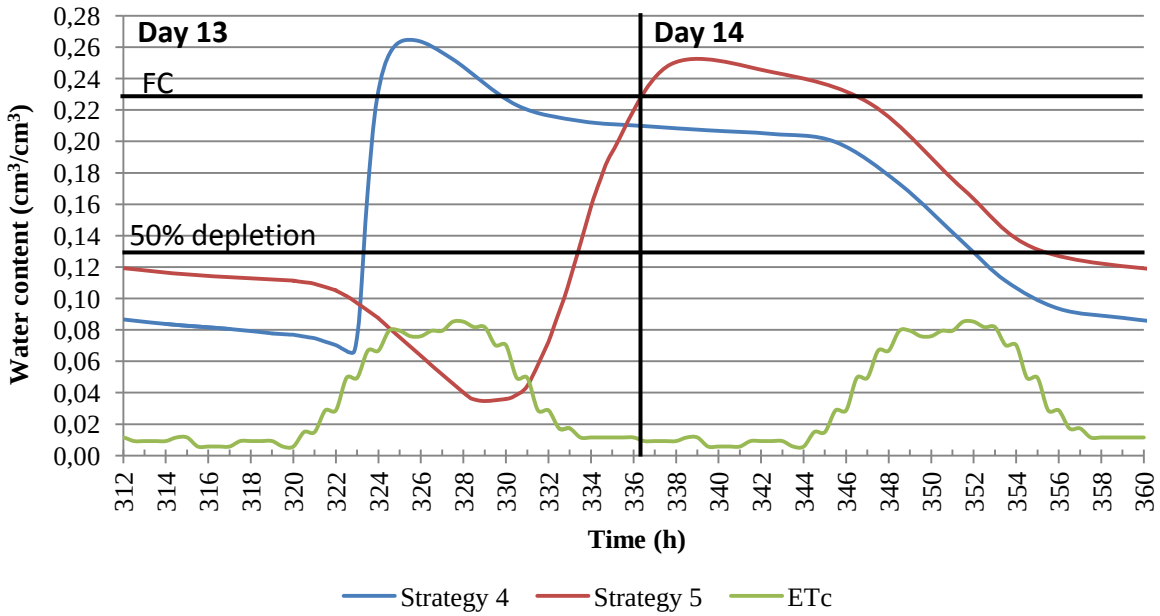

Figure 4.37: Simulated water content change at the soil depth of 20 cm for sweet corn surface drip irrigation strategies 4 and 5 for the 7th irrigation event (on 13th and 14th day). The root water uptake is highest between FC and 50 % depletion marks

Slika 4.37: Simulirana sprememba vsebnosti vode v tleh na globini 20 cm pod posevkom površinsko kapljično namakane sladke koruze za strategiji 4 in 5, za 7. cikel namakanja (13. in 14. dan). Odvzem vode skozi korenine je najvišji med poljsko kapaciteto tal za vodo (FC) in 50 % stanja razpoložljive vode v tleh.

As can be seen of Figures 4.36 and 4.37 the water content was for the longest time at the highest ETc maintained at the optimal θ for strategies 1 and 3 and on the second day for strategies 4 and 5.

Figures 4.38 and 4.39 show water content dynamics was monitored at the depth of 40 cm. Water content decrease during 15 or 16 days of simulation was observed for strategies 1, 2, 4 and 5. A slight water content increase was observed only for strategy 3, where water was applied in short pulses, but only after 7 days of irrigation. The highest water content at the end of simulations was observed at 0.183 cm^3/cm^3 for strategy 3 and the lowest at 0.149 cm^3/cm^3 for strategy 2. For strategy 5 the water content of 0.155 cm^3/cm^3 was observed at the end of irrigation simulations. For additional insight into soil water content dynamics, Figures 4.40 and 4.41 show water content oscillations for all strategies during 24 h of last irrigation event for the soil depth of 40 cm.

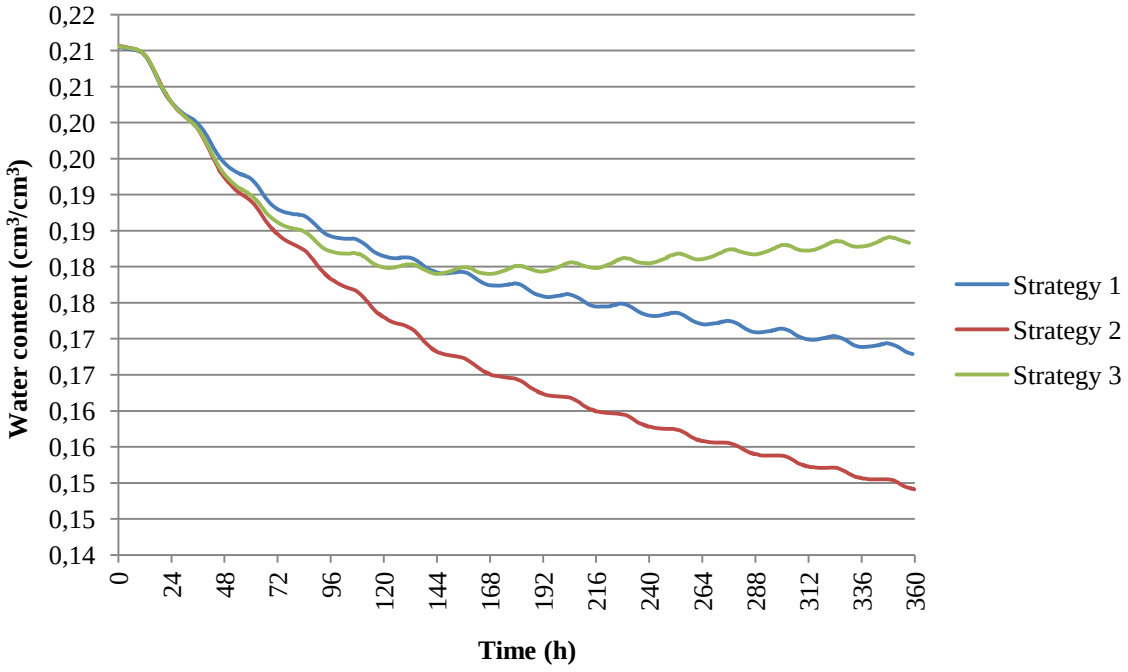

Figure 4.38: Simulated water content (cm^3/cm^3) dynamics under sweet corn surface drip irrigation at soil depth of 40 cm for strategies 1, 2 and 3
Slika 4.38: Simulirana dinamika vsebnosti vode (cm^3/cm^3) pod površinskim kapljičnim namakanjem sladke koruze, na globini tal 40 cm, za strategije 1, 2 in 3

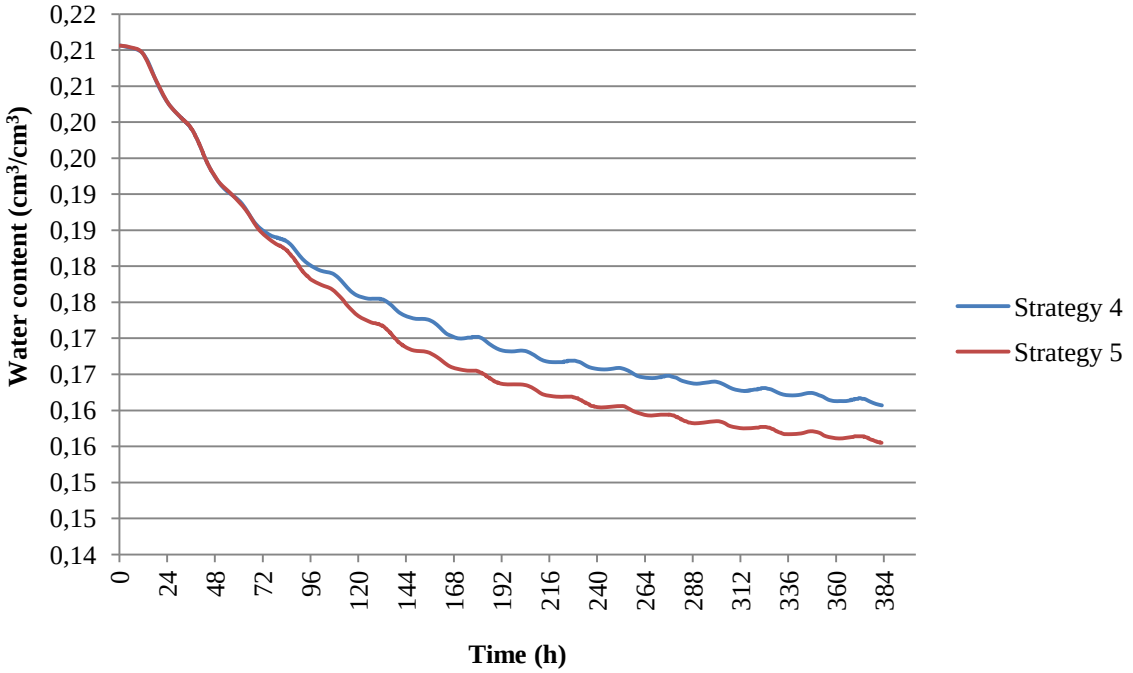

Figure 4.39: Simulated water content (cm^3/cm^3) dynamics under sweet corn surface drip irrigation at soil depth of 40 cm for strategies 4 and 5

Slika 4.39: Simulirana dinamika vsebnosti vode (cm^3/cm^3) pod površinskim kapljičnim namakanjem sladke koruze, na globini tal 40 cm, za strategiji 4 in 5

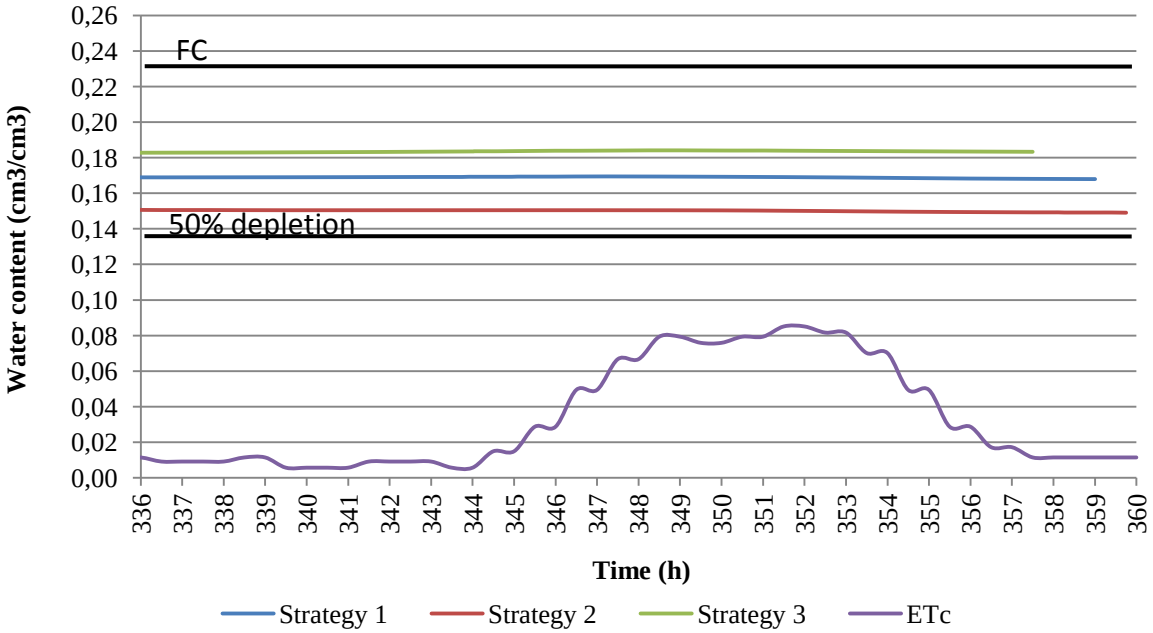

Figure 4.40: Simulated water content change at the soil depth of 40 cm for sweet corn surface drip irrigation strategies 1, 2 and 3 for the last (15^{th}) day or irrigation event. The root water uptake is highest between FC and 50 % depletion marks

Slika 4.40: Simulirana sprememba vsebnosti vode v tleh na globini 40 cm pod posevkom površinsko kapljično namakane sladke koruze za strategije 1, 2 in 3, za zadnji (15.) dan namakanja. Odvzem vode skozi korenine je najvišji med poljsko kapaciteto tal za vodo (FC) in 50 % stanja razpoložljive vode v tleh.

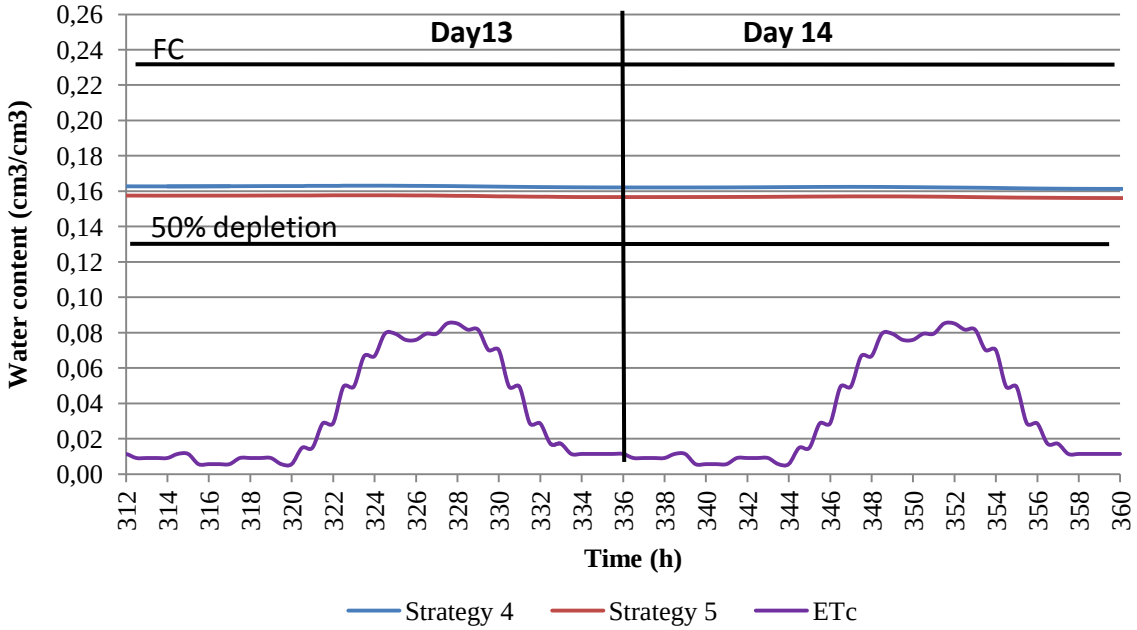

Figure 4.41: Simulated water content change at the soil depth of 40 cm for sweet corn surface drip irrigation strategies 4 and 5 for the 7th irrigation event (on 13th and 14th day). The root water uptake is highest between FC and 50 % depletion marks

Slika 4.41: Simulirana sprememba vsebnosti vode v tleh na globini 40 cm pod posevkom površinsko kapljično namakane sladke koruze za strategiji 4 in 5, za 7. cikel namakanja (13. in 14. dan). Odvzem vode skozi korenine je najvišji med poljsko kapaciteto tal za vodo (FC) in 50 % stanja razpoložljive vode v tleh.

As can be seen of Figures 4.40 and 4.41 the optimal water content was at the highest ETc maintained for all five irrigation strategies.

Overall results show that for all depths the highest water (on average) content was maintained with pulsed irrigation on the daily basis (strategy 3) at all soil depths. On the other hand strategy 3 resulted in the lowest peak water content after irrigation cut off at the soil depths of 10 and 20 cm. At 40 cm only strategy 3 resulted in slight water content increase after 7 days of irrigation. With strategy 2, when irrigation took place over the night, the lowest maintained water content was observed at all soil depths. The same was true for maximum water content, reached just after irrigation cut off for depths at 40 and 20 cm. Irrigation strategies 2, 4 and 5 resulted in the highest water content changes over the day for the depths of 10 and 20 cm. The highest water content just after irrigation cut off was observed for strategy 1 at the depths of 10 and 20 cm.

4.5.3 Root water uptake

Figure 4.42 shows potential and actual cumulative root water uptake for all irrigation at the end of 14th day of irrigation simulations. Actual and potential root water uptakes are compared to see how much root water uptake was reduced because of plants stress (non

optimal water content) for all irrigation strategies. The actual root water uptake was lowest for irrigation strategy 3 with which the water content level was highest, as can be seen from earlier results. The reason for this may be found in modelling of root water pressure head reduction. The parameter P0 (the value of the pressure head below which roots start to extract water from the soil) was in all cases set to -10 cm. When the pressure head was above -10 cm the root system was not active and did not extract water from the soil. Because in strategy 3 water was applied with short pulses 4 times a day, the water content in the wetting pattern increased (pressure head was less than -10 cm) after every pulse and roots did not extract water until pressure head was more than -10 cm (or the water redistributed). Also, optimum root water uptake was set to be at -50 cm or when water content was close to 0.228 cm^3/cm^3. Because the water content with strategy 3 was maintained above 0.228 cm^3/cm^3 at the depth of 10 and sometimes also at 20 cm the roots did not extract water at the maximum rate. With other words, soil was simply too wet and the plants were stressed due to the lack of oxygen in the soil.

The highest root water uptake was observed for strategy 2 where plants were irrigated continuously over the night. Because with this strategy water was applied when the Etc was low, more water was stored in the soil profile for the next day. Also, after water redistribution, the water content in the wetting pattern was not so high. When the ETc of the plants was highest the water content was close to 0.228 cm^3/cm^3 (at -116 cm) and roots extracted water at the maximum rate. With other words, at the soil depth of 10 and 20 cm, the water content in the soil profile was lowest, meaning the roots were not stressed and extracted water at the maximum rate.

The same as for strategy 3, soil water content with strategy 1 was above 0.228 cm^3/cm^3 when ETc was highest. This strategy was better than strategy 3 and worst than strategy 2.

Actual cumulative root water uptake for strategy 5 (continuous irrigation) was a bit higher than for strategy 4 (continuous irrigation). This happened because at the soil depth of 10 and 20 cm the water content in strategy 4 was longer closer to water content where the root water uptake is maximum. It has to be noted that the differences in root water uptake between strategies 4 and 5 were minimal.

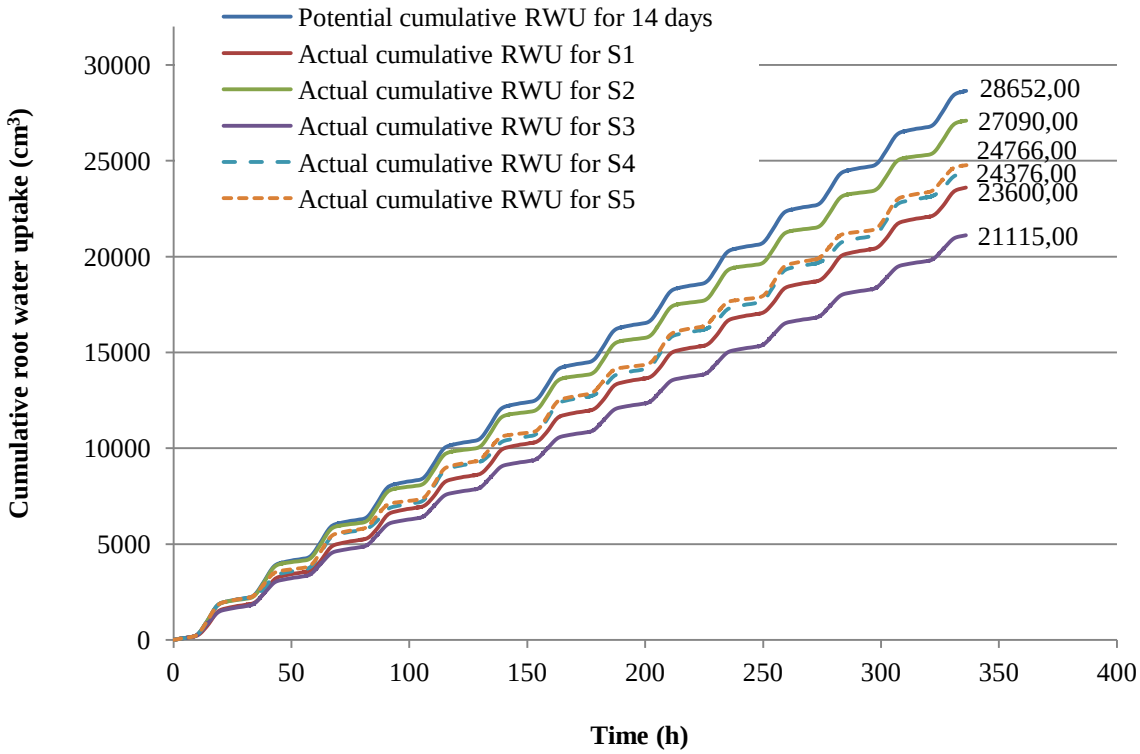

Figure 4.42: Potential and cumulative actual root (RWU) water uptake as a function of time for irrigation strategies 1, 2, 3, 4 and 5 (S1, S2, S3, S4 and S5)

Slika 4.42: Potencialen in kumulativen dejanski odvzem vode skozi korenine rastlin (RWU) kot funkcija časa za strategije namakanja 1, 2, 3, 4 in 5 (S1, S2, S3, S4 and S5)

Overall, the highest cumulative actual root water uptake was observed for strategy 2 (27090 cm^3), followed by strategies 5 (24766 cm^3), 4 (24376 cm^3), 1 (23600 cm^3) and 3 (21115 cm^3). The highest actual root water uptake was observed for strategies where the soil water content at the depth of maximum root intensity was maintained between 0.23 cm^3/cm^3 (FC) and 0.132 cm^3/cm^3 (50 % depletion) at the time when ETc of plants was highest. Because the root density was highest at soil depth of 15 cm (exactly between 9 and 16 cm), the root water uptake at the depth of 20 and 40 cm, when compared to the depth of 10 cm, did not have such a large influence on the cumulative actual root water uptake. However, at the soil depth of 20 and 40 cm the water content was lower and was, when compared to 10 cm depth, maintained at the level of maximum root water uptake throughout all simulation period.

4.6 APPLICATION TO SURFACE DRIP IRRIGATION OF HOP

4.6.1 Comparison of TDR field measurements with numerical study

The measured volumetric soil water content distribution was compared with the Hydrus-2D/3D simulated values at the same locations as the selected 20 TDR probes inserted in the soil profile (for help, Figure 4.43 is showing again TDR probes locations and their numbering). Figures 4.44, 4.45, 4.46 and 4.47 are showing measured (calibrated) and simulated volumetric water content, θ (cm^3/cm^3) dynamics as well as irrigation events (in volume of added water per 1 emitter) for all 20 TDR probes locations for the period from 28th of August 2012 until 5th of September 2012. Potential evapotranspiration rates (ETc) and irrigation amount and duration were set as presented in Figure 3.21 and Table 3.14 in sections 3.7.2 and 3.7.3.

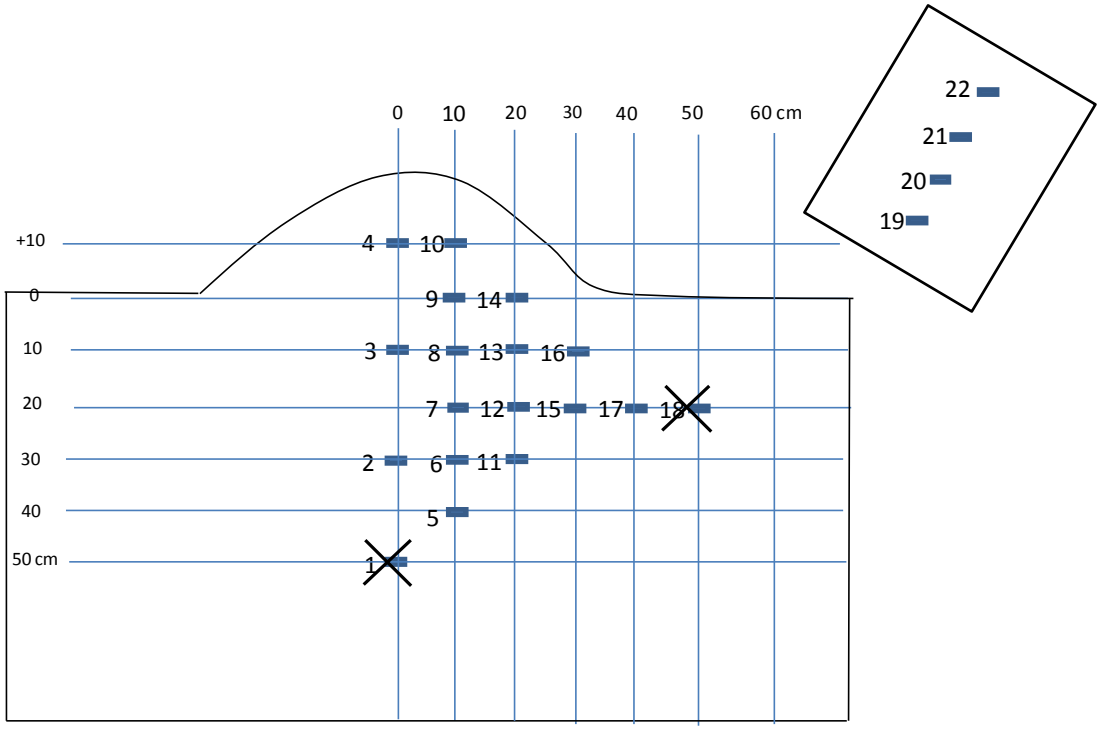

Figure 4.43: Schematic layout of the experimental location with 22 considered TDR probes. Probes from 19 to 22 were inserted vertically along the ridge. Probes 1 and 18 were not compared with the simulations
Slika 4.43: Shematski prikaz eksperimentalne lokacije z vstavljenini 22 TDR-sondami. Sonde od 19 do 20 so bile vstavljene vertikalno vzdolž grebena. TDR-sondi 1 in 18 nista bili primerjani s simulacijami.

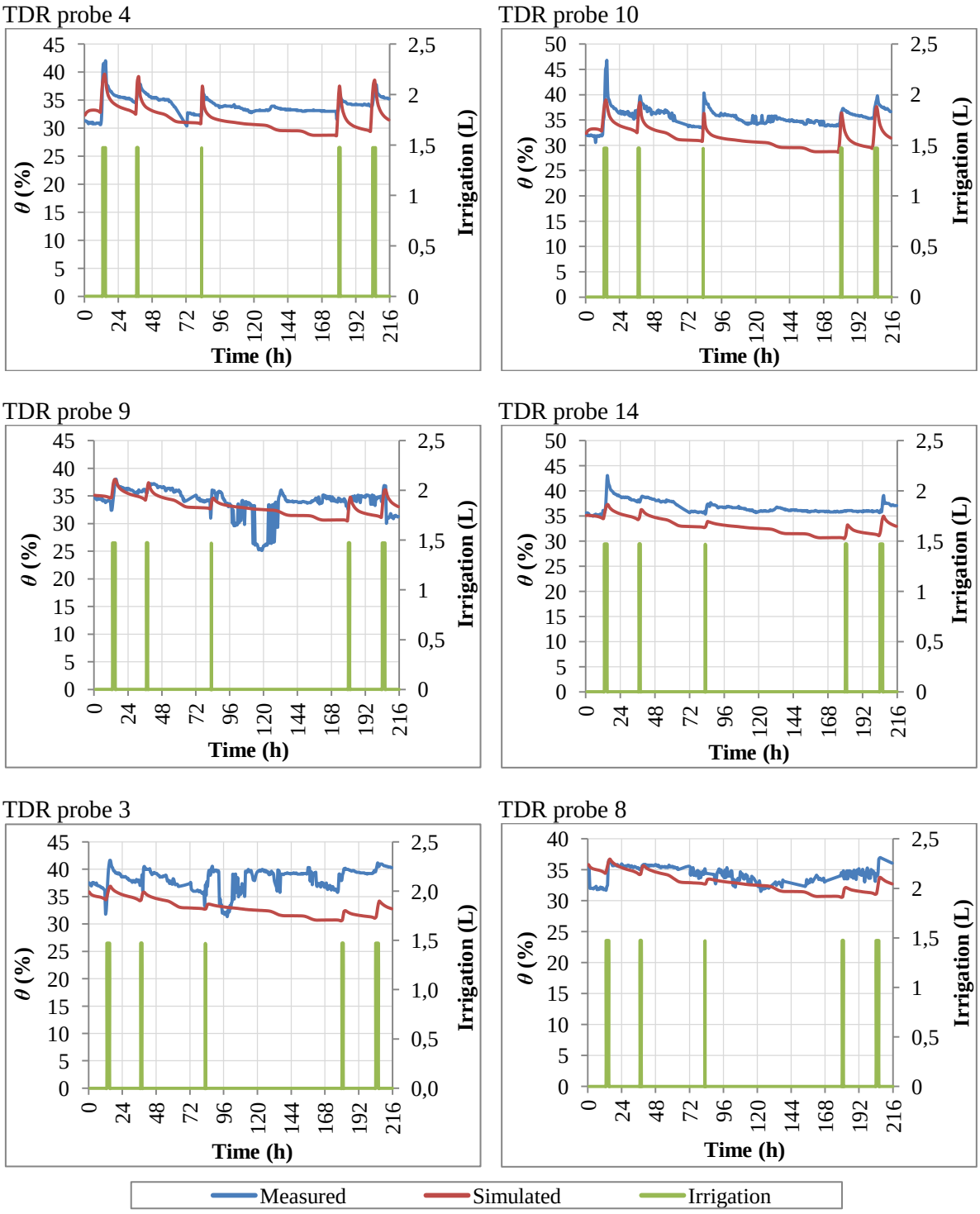

Figure 4.44: Measured and simulated volumetric water content (θ) and irrigation events (L) during 216 h (from 28th August to 5th September) of the experiment, for TDR probes 4, 10, 9, 14, 3 and 8
Slika 4.44: Izmerjeni in simulirani volumski deleži vode (θ) in dogodki namakanja (L) med 216 urami (od 28. avgusta do 5. septembra) izvajanja eksperimenta za TDR-sonde 4, 10, 9, 14, 3 in 8

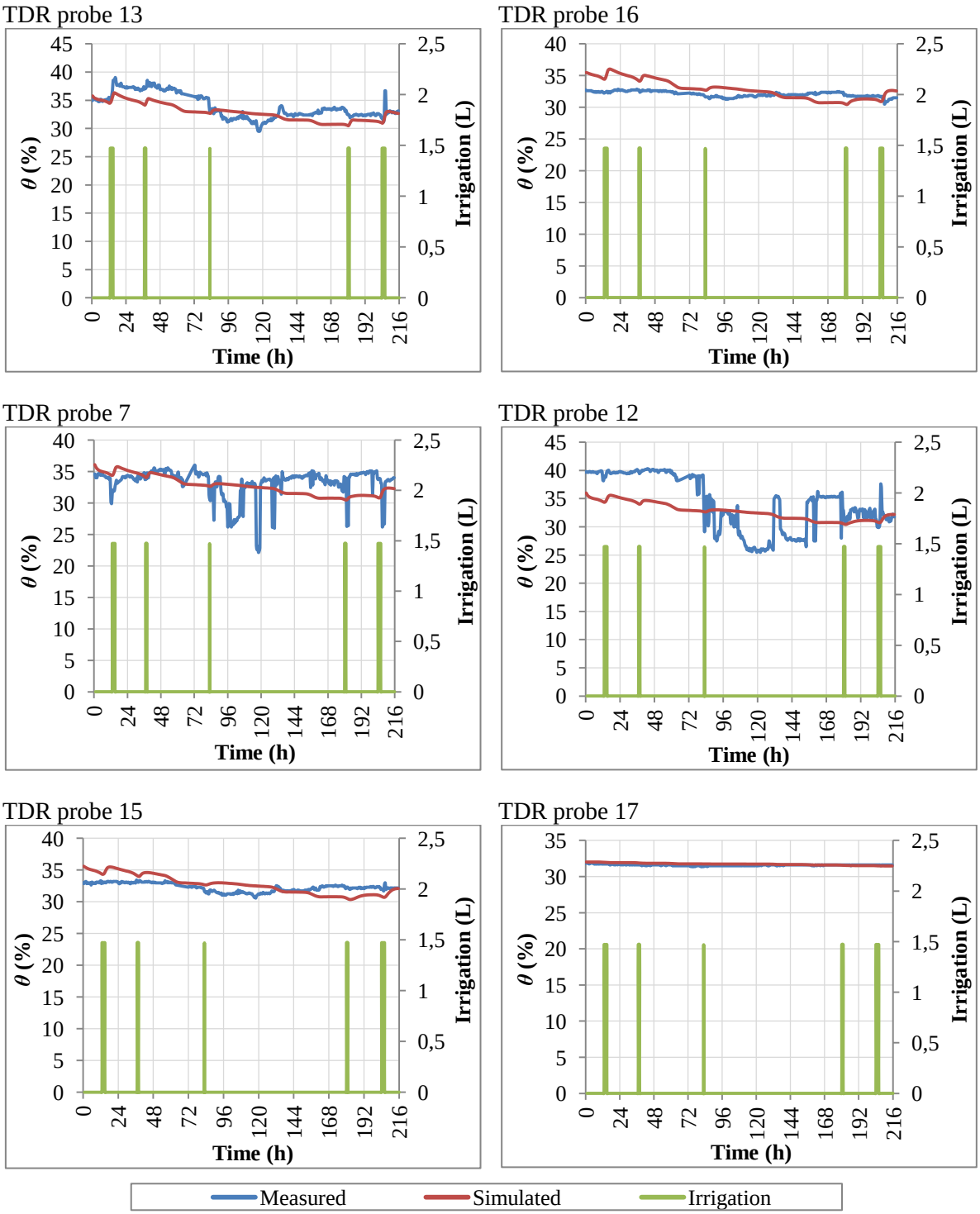

Figure 4.45: Measured and simulated volumetric water content (θ) and irrigation events (L) during 216 h (from 28th August to 5th September) of the experiment, for TDR probes 13, 16, 7, 12, 15 and 17
Slika 4.45: Izmerjeni in simulirani volumski deleži vode (θ) in dogodki namakanja (L) med 216 urami (od 28. avgusta do 5. septembra) izvajanja eksperimenta za TDR-sonde 13, 16, 7, 12, 15 in 17

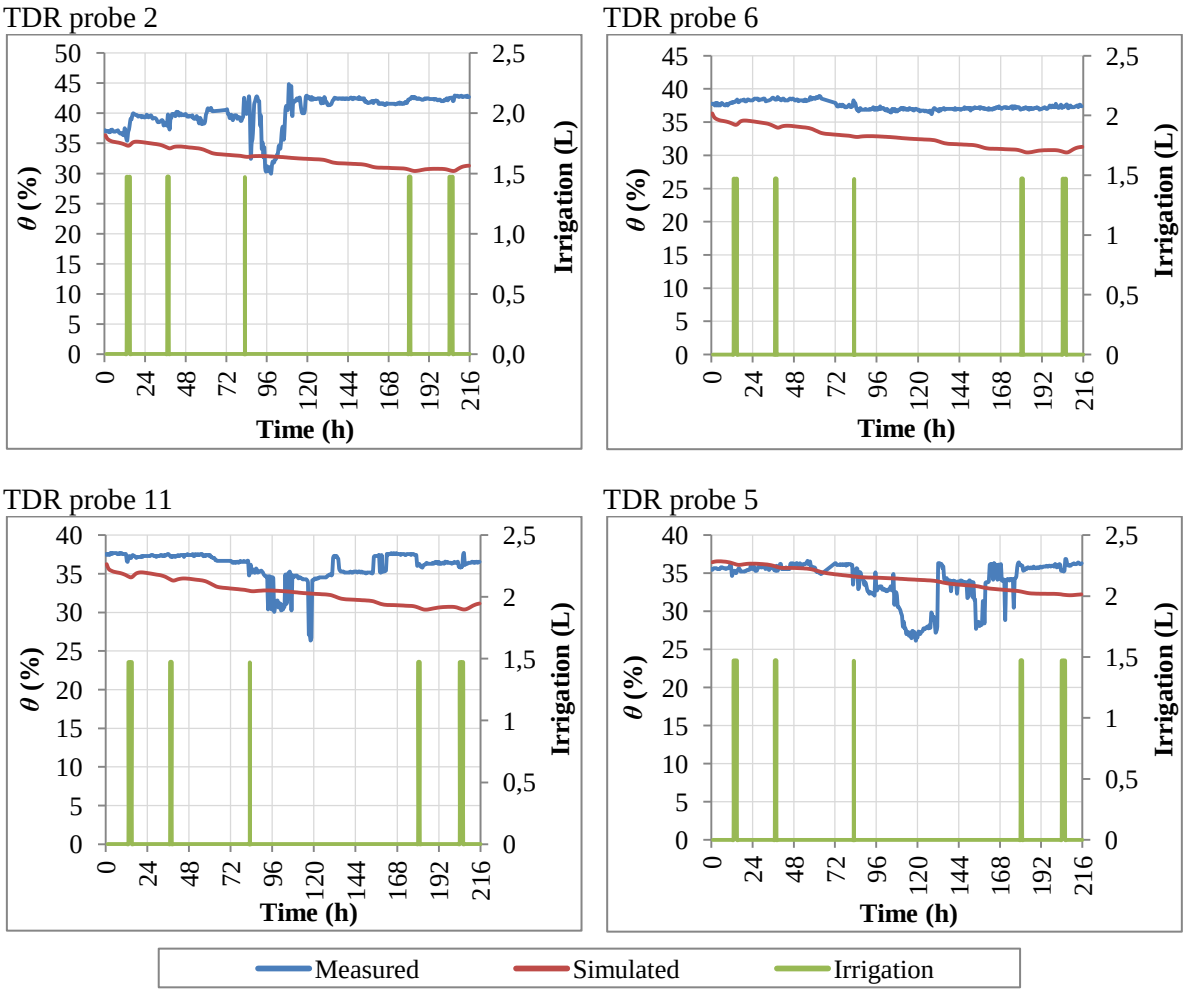

Figure 4.46: Measured and simulated volumetric water content (θ) and irrigation events (L) during 216 h (from 28th August to 5th September) of the experiment, for TDR probes 2, 6, 11 and 5
Slika 4.46: Izmerjeni in simulirani volumski deleži vode (θ) in dogodki namakanja (L) med 216 urami (od 28. avgusta do 5. septembra) izvajanja eksperimenta za TDR-sonde 2, 6, 11 in 5

It can be clearly seen from the figures that between long intervals between irrigation events some probes (like probes 2, 5, 7, 9, 11, 12 and 13) are drying and then they suddenly recover. The reason for this behaviour of TDR probes is unknown but it can be due to sudden loss of probes contact with soil (because of soil drying). It has to be noted that from the 1st of September till including the 2nd of September 2012 almost 80 mm of rain fell. Despite the experiment was covered with plastic sheet, that amount of rain could reach some probes or electronic equipment and disturb some TDR probes measurements by influencing trace (electrical waveform) noise.

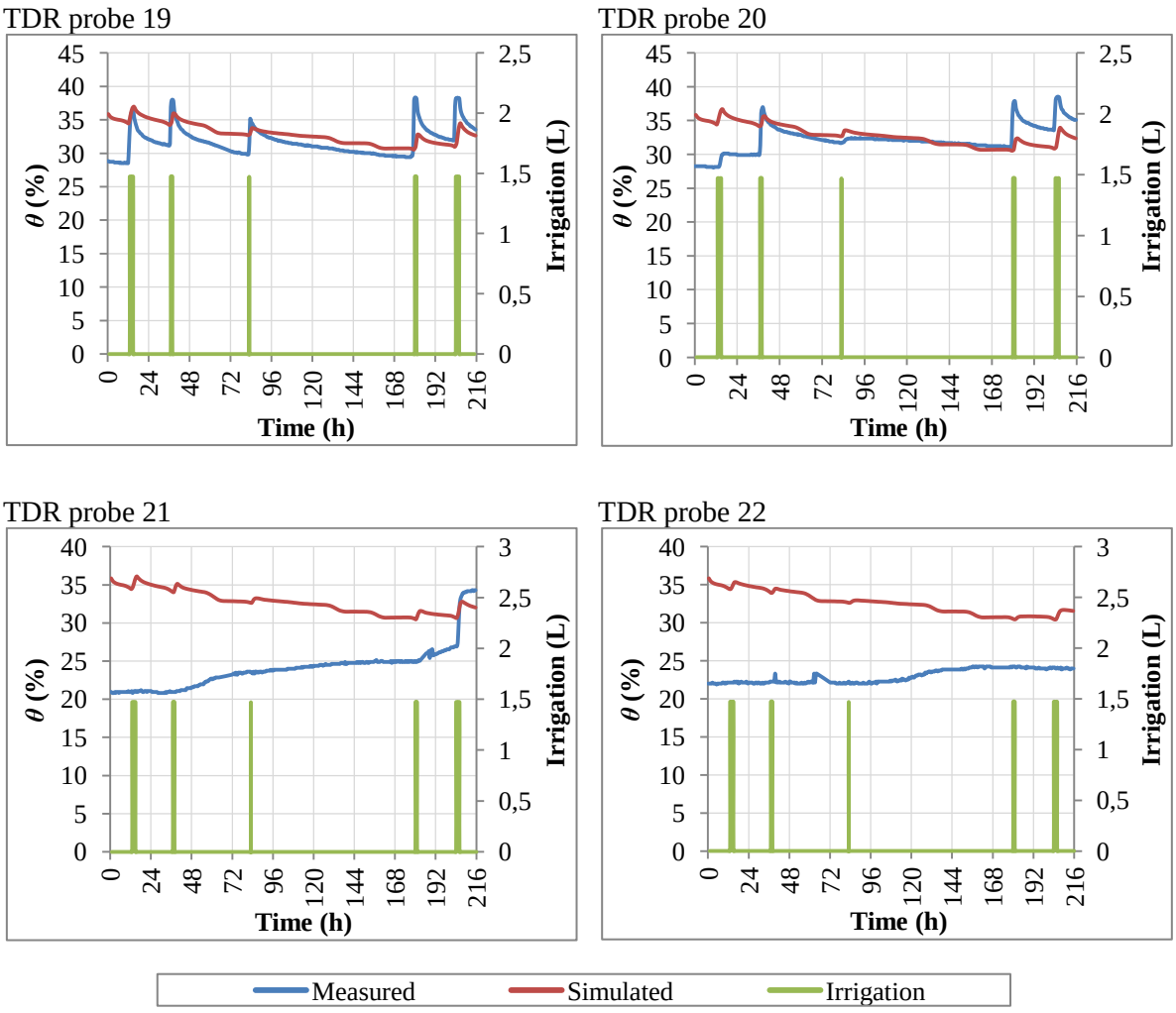

Figure 4.47: Measured and simulated volumetric water content (θ) and irrigation events (L) during 216 h (from 28th August to 5th September) of the experiment for TDR probes 19, 20, 21 and 22
Slika 4.47: Izmerjeni in simulirani volumski deleži vode (θ) in dogodki namakanja (L) med 216 urami (od 28. avgusta do 5. septembra) izvajanja eksperimenta za TDR-sonde 19, 20, 21 in 22

On the other hand, TDR probes 6 and 8 also did not work correctly during the experiment. Figure 4.48 is showing example of the malfunctioning of TDR probe 6. The reason for this error in TDR measurement, when soil water suddenly jumps to 90 % or more, is also unknown. However, to overcome this problem, the linear interpolation method was used to estimate the missing value between two known values. Interpolated values are on Figure 4.48 denoted with green colour (measured – interpolated).

According to Carlsson (1998) the TDR measurement errors can be consequence of two error groups. In first group are the errors that influence the determination of the *Ka* which includes noise caused by improper grounding (a trace affected by an improper grounding is characterised by a fluctuating trace which pattern reminds of sinus curves. Consequently

the software program which interprets the trace pattern fails to interpret the trace correctly), signal attenuations (this problem often occurs when long cables connecting TDR probes are used In those cables loss of energy makes noise more significant and the trace becomes difficult to interpret. This is even more significant when short probes are used since the shorter probe length gives a shorter trace which can, due to the relative long transmission zones, easily be interpreted incorrectly) and noise due to the use of long cables in combination with short unbalanced probes. The second group are errors which occur when *Ka* is converted to soil water content. Those errors concern the interpretation of the trace which is conducted with the software programmes which determine the beginning and the end of the trace. Under some circumstances (very wet sandy soil), the software is unable to recognise the end of the trace, which results in unreasonably high *Ka* and consequently soil water content values.

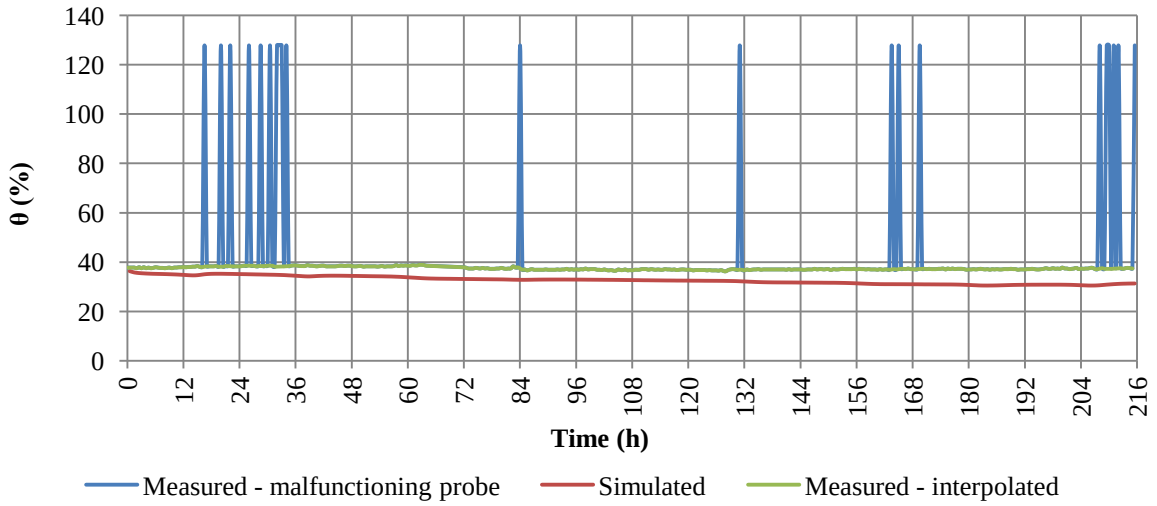

Figure 4.48: Measured, simulated and measured – interpolated volumetric water content (θ) during 216 h (from 28th August to 5th September) of the experiment for malfunctioning TDR probe 6
Slika 4.48: Izmerjene, simulirane in izmerjene-interpolirane vrednosti deleži vode (θ) med 216 urami (od 28. avgusta do 5. septembra) izvajanja eksperimenta za TDR-sondo 6 z montnjami v delovanju

From Figures 4.44, 4.45, 4.46 and 4.47 the goodness of comparison between simulated and measured values can be inspected only visually. It can be seen that the simulated values of θ were in general lower when compared to measured ones. Also, simulated and measured θ difference increased with increase with simulation time, but only for some probes (i.e. TDR probe 2, 3, 5, 6 and 11. According to Buffon et al. (2011) this happens because of error accumulation that comes from two sources. First source is increase in input data error (increase in measured and simulated ET_c or root distribution) and the second one is error accumulation through simulation time steps. As he described, the initial conditions from previous simulation time step is the basis for the next simulation time step, so a natural error accumulation over time steps occurs. The initial conditions assumptions accuracy therefore deteriorates as the simulation advances to further time steps. When looking at the

measured θ with TDR probes, some oscillations of unknown reason occurred during the measurements (TDR probes 2, 3, 5, 7, 9, 11 and 12). For instance, looking at the TDR probe 7, the water content was at 116 h 32.3 % then at 119 h decreased down to 22.8 % and at 121.5 h increased again to 32.4 %. It has to be noted, there was no irrigation during that period. In general, the numerical model performed well and managed to predict changes in soil θ comparable to the measured values at the field. However, some major discrepancies between simulated and measured θ values occurred for TDR probes 2 (Figure 4.46), 21 and 22 (Figure 4.47). There may be many reasons for deviation of TDR node 2, such as complex and heterogeneous soil profile, groundwater contribution, high evapotranspiration demands, and complexity of root water uptake at different depths. Different problem occurred for TDR 21 and 22. As can be seen from Figures 4.37, 4.38, 4.39 and 4.40 the initial soil water content at the beginning of TDR measurements and at the beginning of simulations is not the same for all nodes. This happened because the soil θ was averaged for specific TDR probes which were inserted in the middle of each soil layer, as mentioned in section 3.7.5 (Hydrus 2D/3D setup). If initial volumetric water content for simulation was determined for each specific TDR node, according to TDR measured values, the soil water content redistribution in simulation, because of soil matric forces, forced water to move from low matric forces to higher ones, or from wet to dry conditions. In simulations this eliminated the variability in selected soil water initial conditions within each soil layer. The same happened when along the soil ridge, for probes 21 and 22 (probes 30 and 40 cm from the dripper), drier initial soil water initial conditions were selected. In this case water moved from wet conditions, where probes 19 (beneath the emitter) and 20 (10 cm from the emitter) were located, to drier conditions (probes 21 and 22). Therefore the TDR measured initial θ for TDR probes 21 and 22 were just above 20 % and simulated ones around 30 %.

Statistical evaluation of the goodness of comparison between measured and simulated θ was not possible for all 9 days considered on Figures 4.44, 4.45, 4.46 and 4.47 because the TDR measurements were interrupted on 30th of August because of data downloading. In Hydrus-2D/3D the information concerning θ was selected to be printed (determined) at the same time intervals as for TDR probes measurements (every 0.5 hours). Because TDR measurements were interrupted the simulation and measured times did not coincide and statistical comparison was not possible. Therefore, statistical comparison for the goodness of comparison was made for period of three days (from 28th to 30th of August 2012). The TDR measurements were on the 30th of August stopped at 16 h because of data downloading. Figures 4.49, 4.50, 4.51 and 4.52 are showing measured and simulated θ dynamics for period of 64 h (2 days and 16 h) for which the statistical comparison (RMSE) was carried out. Figures also give more detailed insight into measured and simulated soil water content dynamics.

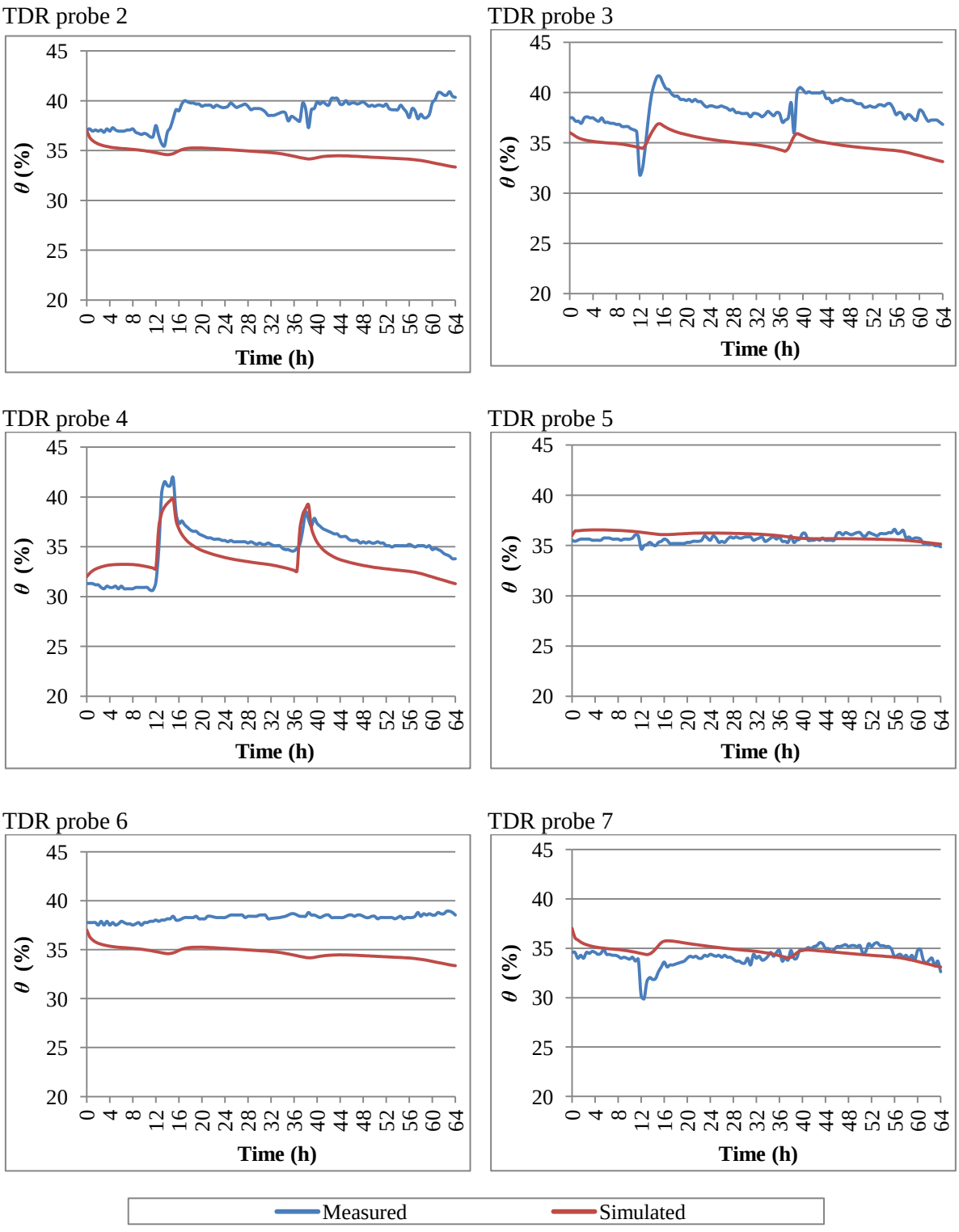

Figure 4.49: Measured and simulated volumetric water content (θ) during 64 h (from 28th to 30th August) of the experiment for TDR probes 2, 3, 4, 5, 6 and 7
Slika 4.49: Izmerjeni in simulirani volumski deleži vode (θ) med 64 urami (od 28. do 30. avgusta) izvajanja eksperimenta za TDR-sonde 2, 3, 4, 5, 6 in 7

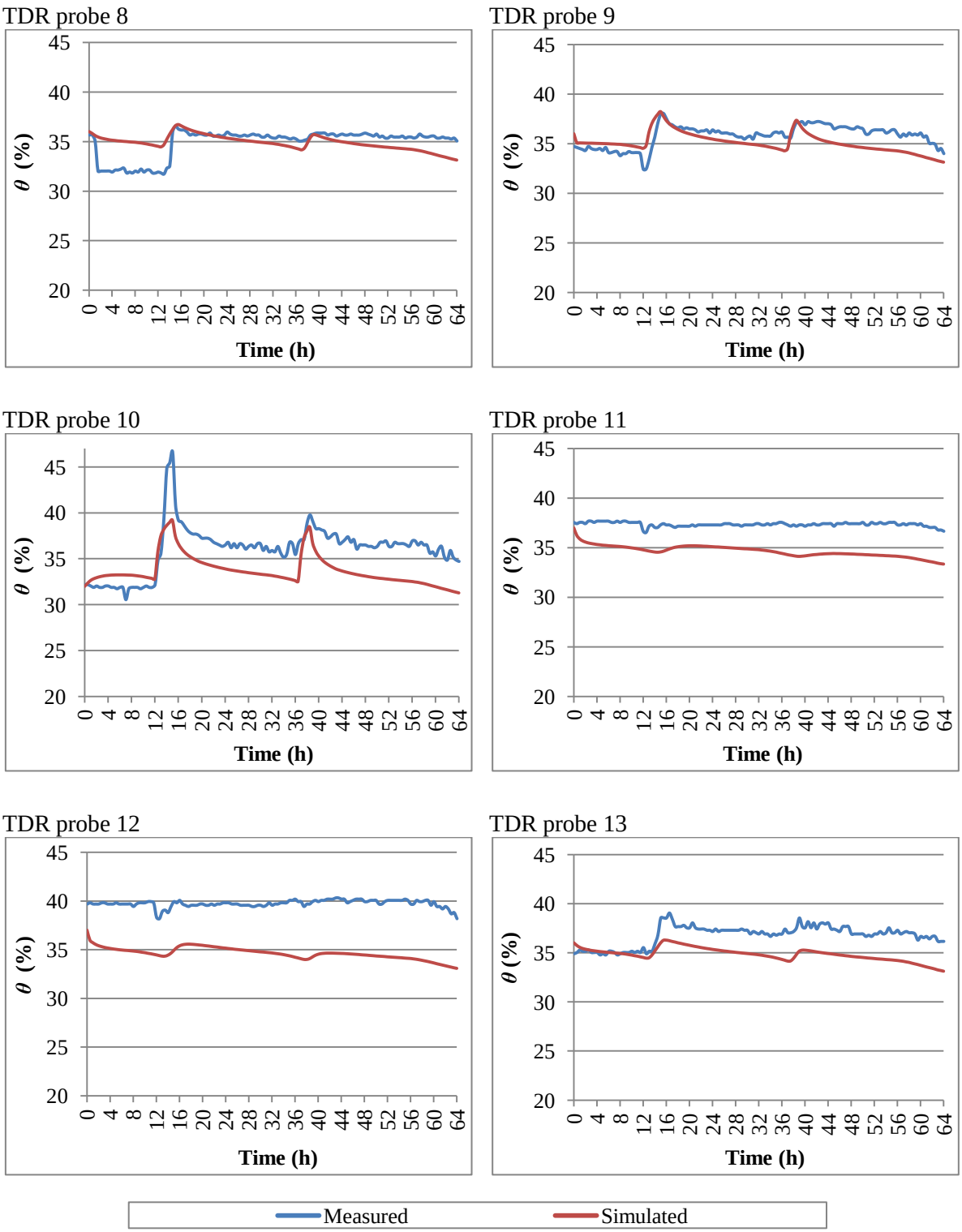

Figure 4.50: Measured and simulated volumetric water content (θ) during 64 h (from 28th to 30th August) of the experiment for TDR probes 8, 9, 10, 11, 12 and 13
Slika 4.50: Izmerjeni in simulirani volumski deleži vode (θ) med 64 urami (od 28. do 30. avgusta) izvajanja eksperimenta za TDR-sonde 8, 9, 10, 11, 12 in 13

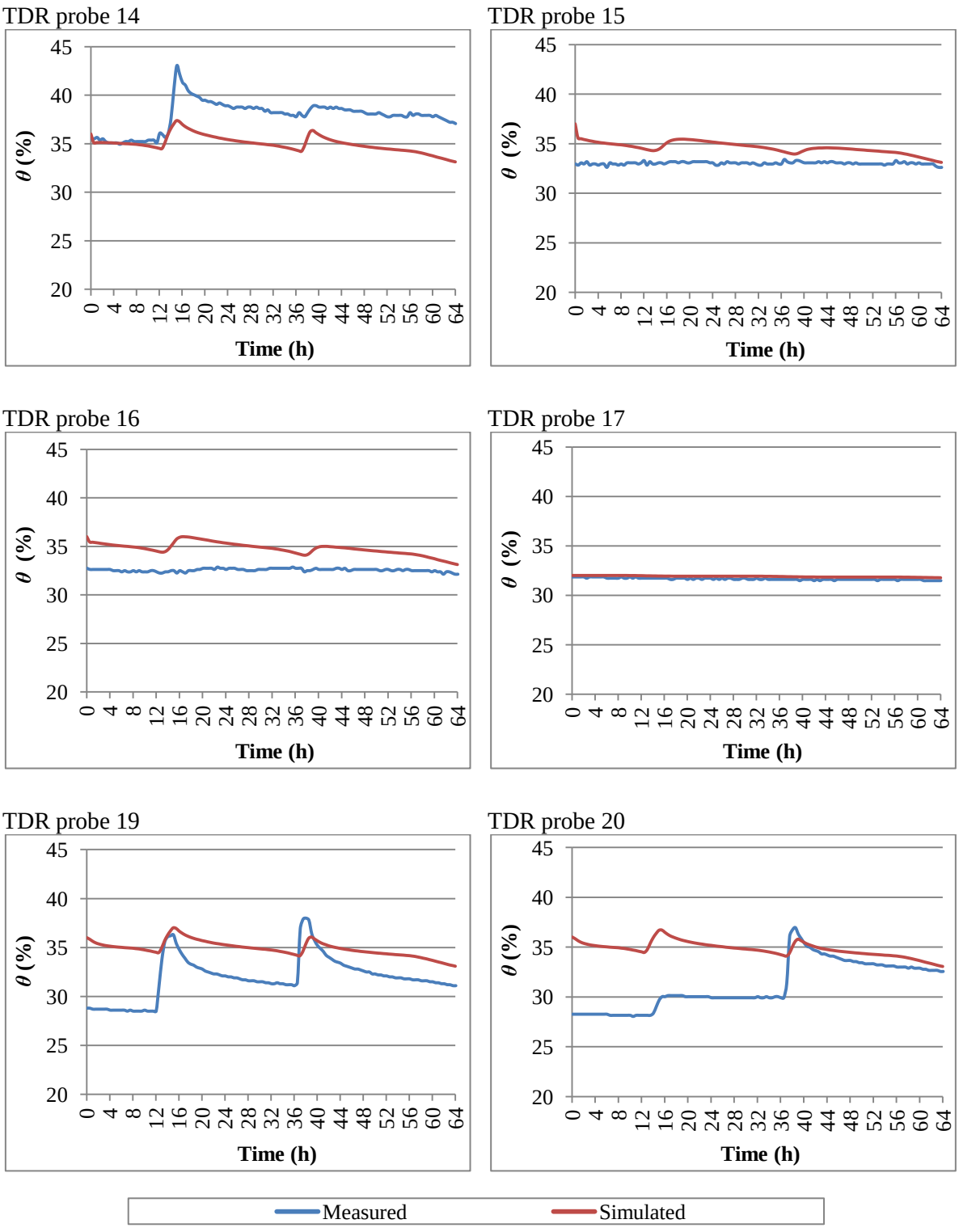

Figure 4.51: Measured and simulated volumetric water content (θ) during 64 h (from 28th to 30th August) of the experiment for TDR probes 14, 15, 16, 17, 19 and 20
Slika 4.51: Izmerjeni in simulirani volumski deleži vode (θ) med 64 urami (od 28. do 30. avgusta) izvajanja eksperimenta za TDR-sonde 14, 15, 16, 17, 19 in 20

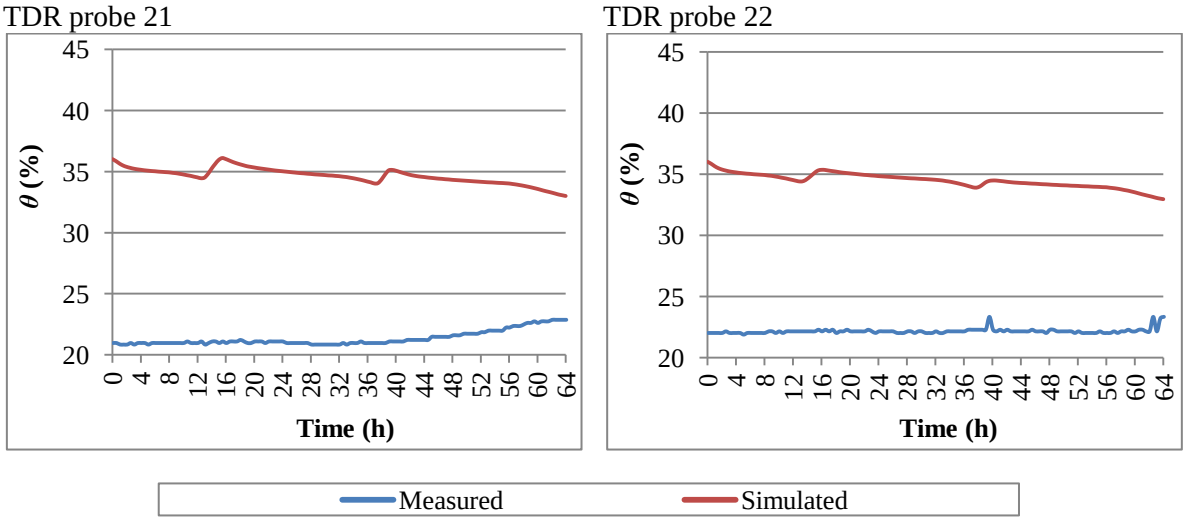

Figure 4.52: Measured and simulated volumetric water content (θ) during 64 h (from 28th to 30th August) of the experiment for TDR probes 21 and 22
Slika 4.52: Izmerjeni in simulirani volumski deleži vode (θ) med 64 urami (od 28. do 30. avgusta) izvajanja eksperimenta za TDR-sondi 21 in 22

The measured θ values, presented on Figures 4.49, 4.50, 4.51 and 4.52, were compared with the Hydrus-2D/3D simulated values at 20 different locations beneath the surface drip emitter for 129 time steps (64 h were divided in 0.5 h long time steps; including 0 h time step) (Table 4.4).

Two irrigation events (on 28th and 29th of August) happened during investigated time. The RMSE values between measured and simulated θ (%) ranged from 0.25 (0.0025 cm^3/cm^3) to 13.37 % (0.1337 cm^3/cm^3) for all locations. If the TDR probes 21 and 22, where comparison of measured and simulated values was the poorest because of the reasons mentioned earlier, are removed from the analysis, the RMSE values ranged from 0.25 % (0.0025 cm^3/cm^3) to 5.13 % (0.0513 cm^3/cm^3). The main advantage of using RMSE measure is that it uses the same units as measured and observed values and is thus easy to understand. Unfortunately, large differences are heavily weighted. It is suggested by Wallach et al. (2006) that those specific cases where large differences occur they have to be examined separately. Low RMSE values indicate that the predicted (simulated) values tend to be close to the measured ones. The lowest RMSE values for volumetric water content of 0.25 % and 0.65 % were obtained for probes 17 and 5, respectively. The highest RMSE was obtained for probes 21 and 22, resulting in 13.37 and 12.35 %, respectively.

Table 4.4: Root mean square error (RMSE) for measured and simulated soil volumetric water content (θ) for 64 hours of experiment for all TDR probes locations
Preglednica 4.4: Efektivna srednja kvadratna napaka (RMSE) za izmerjene in simulirane volumske deleže vode (θ) med 64 urami eksperimenta za vse TDR sonde

TDR probe	RMSE (%)
2	4.39
3	3.53
4	2.12
5	0.65
6	3.67
7	1.24
8	1.58
9	1.31
10	3.08
11	2.75
12	5.13
13	2.24
14	3.18
15	1.70
16	2.30
17	0.25
19	3.64
20	4.56
21	13.37
22	12.35

When looking at the RMSE values for probes representing the middle of the specific soil layer, the lowest RMSE for layer P (20 – 0 cm) was obtained for probe 4 (2.12 %). For soil layer A_1 (0 – 20 cm) the lowest RMSE was obtained for probe 8 (1.58 %), for soil layer A_2 (20 – 35 cm) for probe 11 (2.75 %) and for soil layer AG_o (35 – 50 cm) for probe 5 (0.65 %). Compacted zone was represented by probe 17, where the lowest RMSE among all probes was obtained, as mentioned earlier. Among four vertical probes, numbered 19, 20, 21 and 22, the lowest RMSE of 3.64 % was obtained for probe 19, which was located 10 cm beneath the surface drip emitter.

The potential sources of errors associated with TDR measurements were mentioned earlier in this chapter. However, when comparing measured and simulated results, many other factors also exist that can be source of potential errors in Hydrus-2D/3D simulations or field experiment (excluding TDR measurements). Potential sources of errors associated with Hydrus simulations can be mainly due to the empirical nature of the constitutive models incorporated into the programme itself (selected hydraulic model of van Genuchten–Mualem to describe soil hydraulic properties (assumed and true water retention

functions are especially critical near soil saturation and the dry end of the curve) and the selected root water uptake reduction model of Feddes). During the field experiment the possible sources of errors can be found in determination of water release curve with evaporation method (Hyprop), determination of soil bulk density or especially determination of soil saturated hydraulic conductivity, which, as mentioned in chapter 3.7.3, varied by orders of magnitude between soil layers. When uncertainty in determination (or the shortcuts used) of all those input parameters is considered, the model and the TDR probes results compare very well. Already good results change for the better, when the fact, that for the purpose of this research the Hydrus model was not calibrated using inverse modelling option incorporated into the model, is considered.

If only one TDR probe with best RMSE comparison between measured and observed θ (%) values is chosen as representative for each soil layer, the RMSE varied from 0.25 % (0.0025 cm^3/cm^3) to 3.64 % (0.0364 cm^3/cm^3). Overall, numerical model Hydrus-2D/3D successfully simulated changes in soil water content when considering the complexity of root water uptake process beneath the surface drip emitter. The accuracy of the model simulations, when compared to measured values, was shown to be good with RMSE values smaller than 5.13 % (0.0513 cm^3/cm^3) excluding the TDR probes 21 and 22, where Hydrus failed to simulate the soil θ dynamics. Some possible explanations, from numerical point of view, for discrepancies between simulation and measurement results for probes 21 and 22 are given earlier in this chapter. However, many other possible explanations exist for this discrepancy. First of all, vertical TDR probes (19, 20, 21 and 22) were in experiment inserted only with a reason to determine how far from the surface dripper will water move along the soil ridge. It is unrealistic to expect that simulation and experiment results will compare well, if the vertical probe is inserted through 2 soil layers with different soil physical parameters, especially when taking into account the fact that the TDR probes give results in linear weighted average water contents irrespective of the water distribution along the probe (in Hydrus water content was determined for a single point at 10 cm below the soil ridge which represented entire 20 cm long TDR probe). Vertically inserted TDR probes can be therefore used only for water balance measurements where a single measurement gives the total quantity over depth spanned and is not dependent on the depth water distribution. It has to be noted here that horizontally embedded TDR probes are much more appropriate for precise water content movement measurements. Also, a possibility exists that the soil hydraulic properties for those two layers were not well characterised, that the boundary between those two soil layers did not represent the reality very well. The reason for this discrepancy can be found in soil water preferential flow which according to Radcliffe and Šimůnek (2010) occurs because of the presence of macropores, fractures, biological channels (dead rotten roots) through which water is moving preferentially. Preferential flow often occurs in field soils.

Other studies, as that of Phogat et al. (2011) and Buffon et al. (2011) who considered root water uptake in layered soil profile acquired similar results, with RMSE values of soil θ (%) smaller than 5 %. Similar results were reported by Skaggs et al. (2004, 2010) where RMSE values of soil θ (%) varied from 1 – 4 %, but no root water uptake and homogeneous soil profile were considered.

However, the simulation in this study was more complex because of simulated soil domain characteristics (which included soil ridge) and surface point source water redistribution process, which made given problem impossible to be simulated in any other than in 3D environment. 3D simulations as shown in Hydrus-2D/3D are presented in Figure 4.53 which is showing the simulated soil water distribution pattern in the soil profile at three different times.

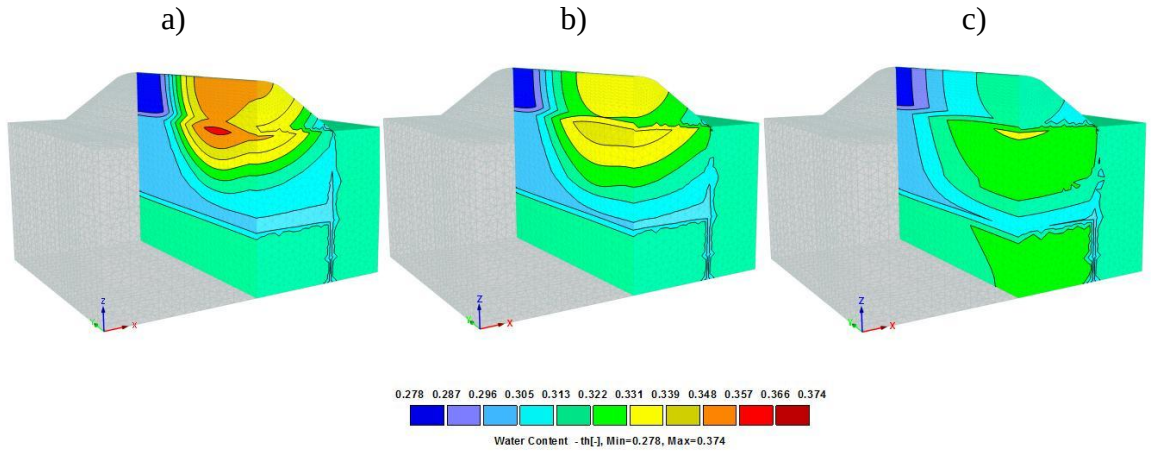

Figure 4.53: The figures show Hydrus-2D/3D simulation results. The water content conditions at 207 (a), 209 (b) and 216 h (c) are illustrated. Figure a) shows soil water distribution just after last irrigation event (lasted from 204 to 206 h). The transport domain is cut on the half in the middle of the soil ridge
Slika 4.53: Slike prikazujejo rezultate Hydrus-2D/3D simulacij. Prikazana je distribucija vsebnosti vode TH = θ (cm^3/cm^3) pri 207 (a), 209 (b) in 216 (c) urah. Slika a) prikazuje distribucijo vode takoj za zadnjim namakalnim dogodkom (zadnje namakanje je trajalo od 204 do 206 ur). Transportna domena je prerezana na polovico po sredini grebena.

4.7 NUMERICAL STUDY OF INFLUENCE OF HOP IRRIGATION DESIGN AND MANAGEMENT PARAMETERS ON SOIL WATER DYNAMICS

This section offers a detailed insight into the effects of different emitter spacing, volumes of applied water and soil water initial conditions on the soil water content distribution between two adjacent surface drip emitters in hop plantation. The flow geometry and soil properties were kept the same as in previous section, where the comparison of measured and simulated water content dynamics below one dripper in the hop plantation was investigated. All simulations were done considering root water uptake. All together 18

simulations (18 strategies) using Hydrus-2D/3D were done, as presented in Tables 3.19 and 3.20. The water content distribution was monitored in six locations in the soil profile using observation nodes. Three node locations were considered directly below the dripper (BD), at the soil depth of 10 cm (middle of the 20 cm high soil ridge), at 40 cm (20 cm below the soil surface without considering soil ridge) and at 60 cm (40 cm below the soil surface without considering the soil ridge). The other three locations were considered at the centre of the dripper overlap zone (COZ) at the same locations as the nodes below the dripper (Figure 3.39). When the water dynamics for all observation nodes was investigated this resulted in 36 graphs. Each strategy was divided in two parts, regarding soil water content initial conditions (for instance, strategy 1 was divided into strategy 1a and 1b).

4.7.1 Influence of dripper distance and initial water content

In this section Strategies 1a, b, 2a, b and 3a, b with dripper spacing 40, 30 and 20 cm were compared. In all strategies the volume of applied water per irrigation cycle was covering 100 % of the plants ETc. According to Table 3.20, both initial conditions were tested for this purpose.

Figures 4.54 and 4.55 are a plot of soil water dynamics in time for different dripper spacings and at different soil depths. Soil water initial conditions were set at FC-ETc (0.33 cm^3/cm^3).

Strategy 1a (40 cm dripper spacing)

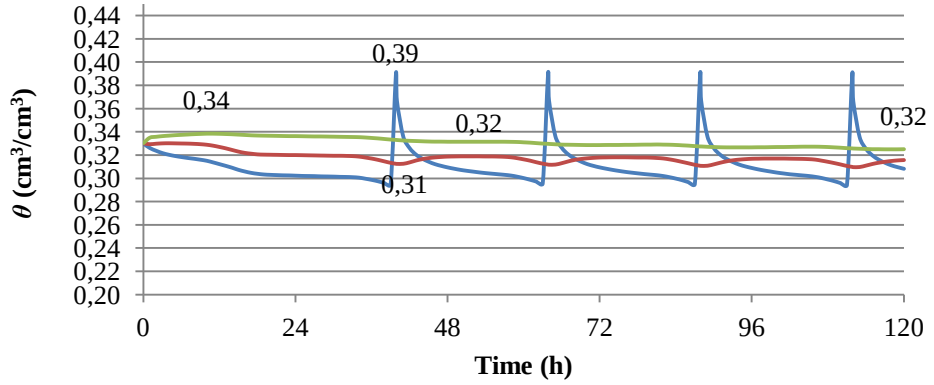

Strategy 2a (30 cm dripper spacing)

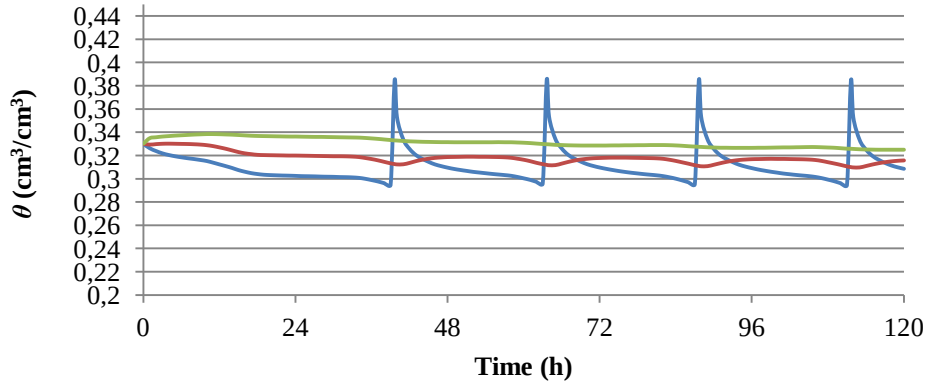

Strategy 3a (20 cm dripper spacing)

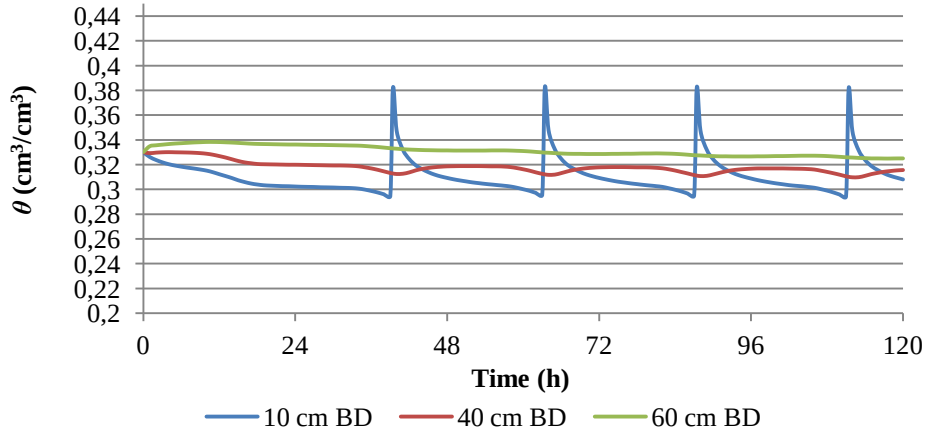

Figure 4.54: Soil water content dynamics at three different soil depths at location below the dripper (BD) for three different dripper distances with soil water initial conditions set to field capacity (FC) – potential evapotranspiration (ETc)
Slika 4.54: Dinamika stanja vode v tleh na treh različnih globinah, na lokacijah pod kapljačem (BD) za tri različne razdalje med kapljači, z začetno vsebnostjo vode v tleh pri poljski kapiceti (FC) – potencialni evapotranspiraciji (ETc)

Strategy 1a (40 cm dripper spacing)

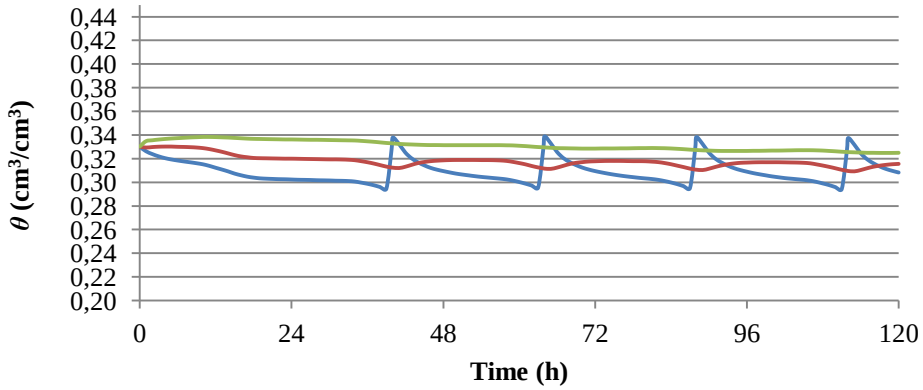

Strategy 2a (30 cm dripper spacing)

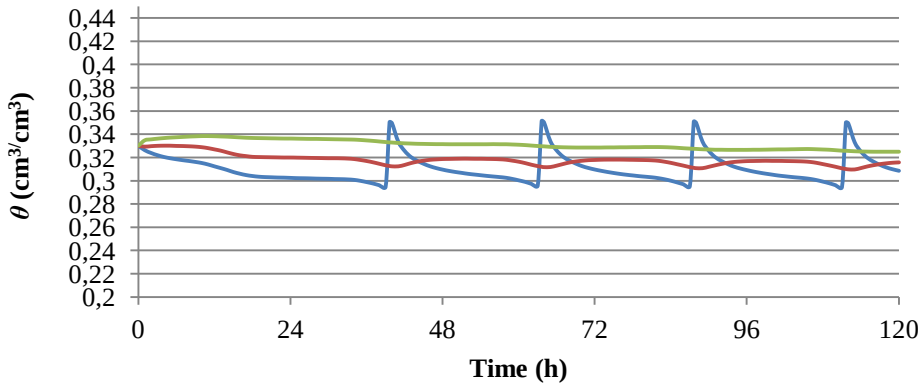

Strategy 3a (20 cm dripper spacing)

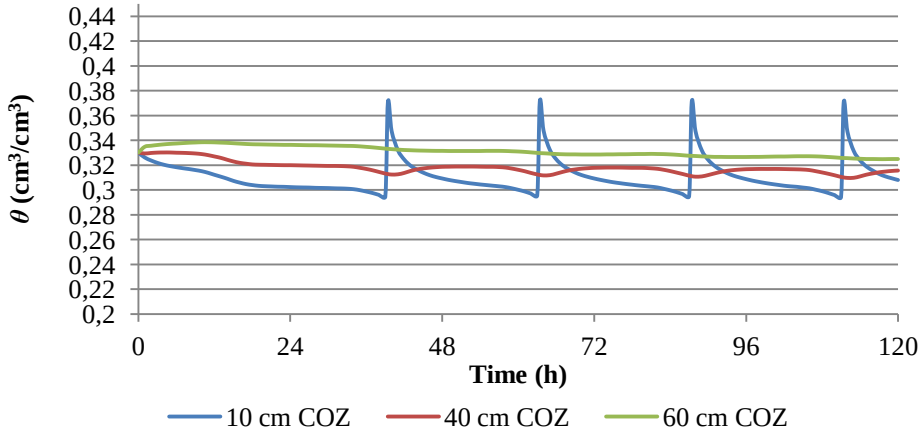

Figure 4.55: Soil water content dynamics at three different soil depths located at the centre of the overlap zone (COZ) for three different dripper distances with soil water initial conditions set to field capacity (FC) – potential evapotranspiration (ETc)

Slika 4.55: Dinamika stanja vode v tleh na treh različnih globinah, na lokaciji na sredini med kapljačema(COZ) za tri različne razdalje med kapljači, z začetno vsebnostjo vode v tleh pri poljski kapiceti (FC) – potencialni evapotranspiraciji (ETc)

It can be seen that the soil water content observed at locations BD and at the COZ just before another irrigation event (at 39, 63, 87 and 111h) are identical at all soil depths and all strategies. It can be seen that wetting patterns overlapped in all considered strategies and forming a continuous wetted strip of soil. To provide greater insight into the effect of soil water dynamics under different dripper spacings, Tables 4.5 and 4.6 show water content at 111 h observed at different soil depth at locations BD and COZ.

The water redistribution process and root water uptake (which was the same as volume of added water) in 24 h after irrigation completely eliminated the influence of surface dripper spacing on soil water distribution in the soil profile.

Table 4.5: Soil water content for irrigation strategies 1a, 2a and 3a, observed at different soil depths at 111 h (just before last irrigation event) at location below dripper (BD)
Preglednica 4.5: Vsebnost vode v tleh za strategije namakanja 1a, 2a in 3a, opažena na različnih globinah pri 111. uri (takoj pred zadnjim ciklom namakanja) na lokaciji pod kapljačem (BD)

Spacing (cm)	Soil depth BD		
	10 cm	40 cm	60 cm
40 cm (1a)	0.29	0.31	0.33
30 cm (2a)	0.29	0.31	0.33
20 cm (3a)	0.29	0.31	0.33

Table 4.6: Soil water content for irrigation strategies 1a, 2a and 3a, observed at different soil depths at 111 h (just before last irrigation event) at the centre of the overlap zone (COZ)
Preglednica 4.6: Vsebnost vode v tleh za strategije namakanja 1a, 2a in 3a, opažena na različnih globinah pri 111. uri (takoj pred zadnjim ciklom namakanja) na lokaciji na sredini med kapljačema (COZ)

Spacing (cm)	Depth COZ		
	10 cm	40 cm	60 cm
40 cm (1a)	0.29	0.31	0.33
30 cm (2a)	0.29	0.31	0.33
20 cm (3a)	0.29	0.31	0.33

On the other hand, minor soil water content differences at the soil depth of 10 cm were observed on Figures 4.54 and 4.55, immediately after irrigation cut off. The highest peak water content at the location BD was observed for Strategy 1a (40 cm dripper spacing) at 0.39 cm^3/cm^3, followed by Strategy 2a (30 cm dripper spacing) at 0.3841 cm^3/cm^3 and Strategy 3a (20 cm dripper spacing) at 0.3815. When considering location at the COZ the highest peak water content at the irrigation was observed for Strategy 3a at 0.3706 cm^3/cm^3, followed by Strategy 2a at 0.3502 cm^3/cm^3 and Strategy 1a at 0.34 cm^3/cm^3. The highest peak soil water content observed 10 cm below the dripper caused the lowest peak soil water content in the centre of the drippers overlap zone. This can be explained with the water application time needed to satisfy 100 % of plant water needs (determined by ETc) when different dripper distances are used. The irrigation cycle

duration for Strategy 1 was 49.7 min, for Strategy 2 37.28 min and for Strategy 3 24.85 min. Because of longest irrigation cycle duration for Strategy 1, the biggest amount of water per one emitter was applied, which resulted in highest water content directly below the dripper. Still, the water content did not reach the soil water saturation point at 0.437 cm^3/cm^3. Because of dripper distance of 40 cm, wetting patterns formed below the drippers at that time did not overlap at the COZ causing slightly lower soil water content. After around 3 h of soil water redistribution this effect vanished, as can be seen on Figures 4.54 and 4.55. These minor peak soil water content differences occurred only at the soil depth of 10 cm. Figures 4.54 and 4.55 show that water content at observation nodes, placed at 10 and 40 cm BD and at the COZ, remained constant, which means that the amount of water applied with irrigation was sufficient to maintain constant water content level (between 0.31 and 0.32 cm^3/cm^3) for Simulations 1a, 2a and 3a. When considering water content at the soil depth of 60 cm, a slight water content decrease from 0.34 to 0.32 cm^3/cm^3 in 5 days was observed at locations BD and at the COZ, for all simulations.

Figures 4.56 and 4.57 show soil water content dynamics for soil water initial conditions set at CP+ETc (0.27 cm^3/cm^3) for Strategies 1b, 2b and 3b. To see soil water dynamics from different perspective as for Strategies 1a, 2a and 3a the different dripper spacings are here plotted for each investigated soil depth. Where only one line presenting data is visible, three lines, which present soil water dynamics for different strategies, are perfectly matching.

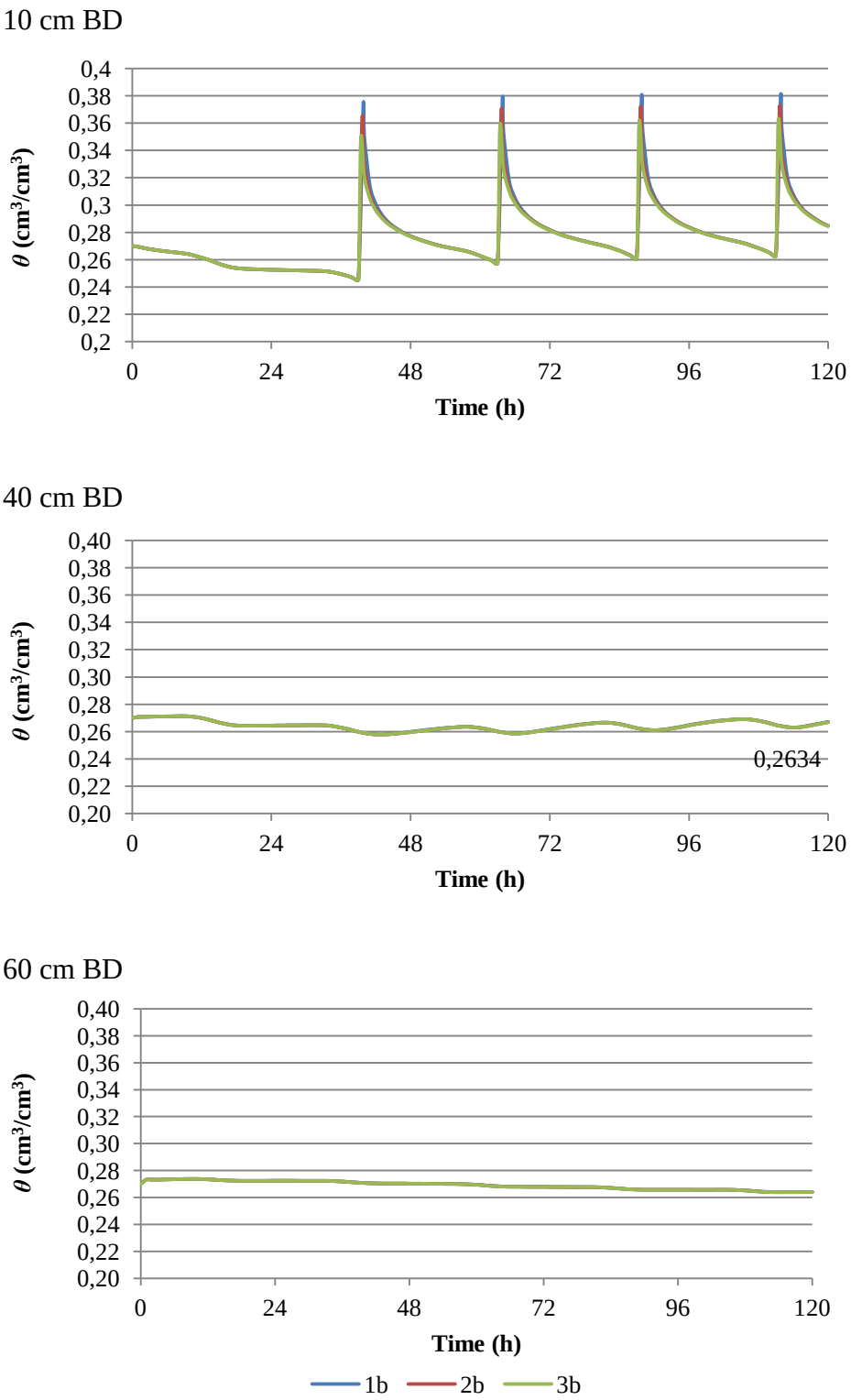

Figure 4.56: Soil water content dynamics for three different dripper distances (40 cm (1b), 30 cm (2b) and 20 cm (3b)) for three different soil depths at location below the dripper (BD) and soil water initial conditions at critical point (CP) + potential evapotranspiration (ETc)
Slika 4.56: Dinamika stanja vode v tleh za tri različne razdalje med kapljači (40 cm (1b), 30 cm (2b) in 20 cm (3b)) na treh različnih globinah tal, na lokaciji pod kapljačem (BD) in ob začetni vsebnosti vode v tleh pri kritični točki (CP) + potencialni evapotranspiraciji (ETc)

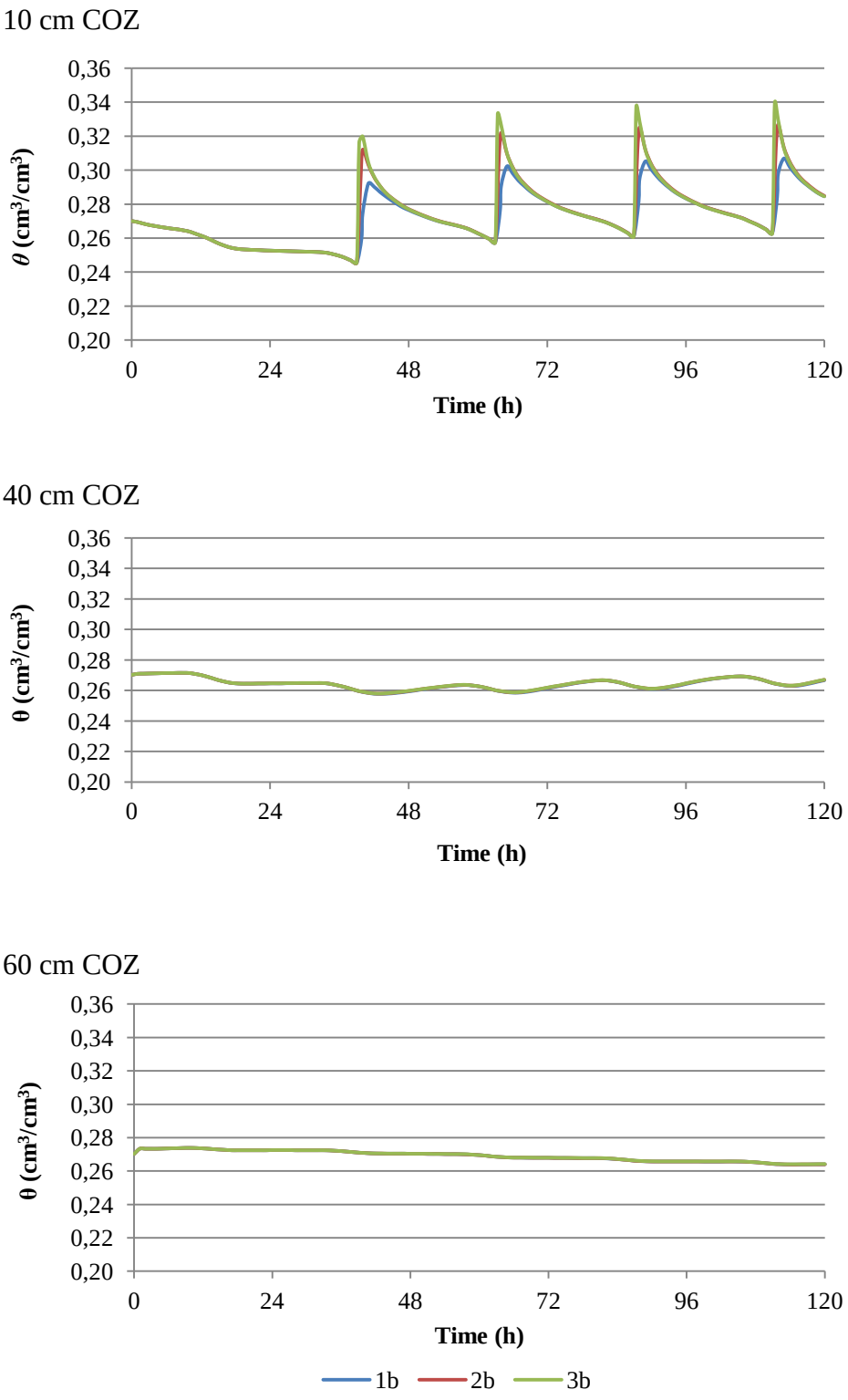

Figure 4.57: Soil water content dynamics for three different dripper distances (40 cm (1b), 30 cm (2b) and 20 cm (3b)) for three different soil depths located at the centre of the overlap zone (COZ) and soil water initial conditions at critical point (CP) + potential evapotranspiration (ETc)
Slika 4.57: Dinamika stanja vode v tleh za tri različne razdalje med kapljači (40 cm (1b), 30 cm (2b) in 20 cm (3b)) na treh različnih globinah tal, na lokaciji na sredini med kapljačema (COZ) in ob začetni vsebnosti vode v tleh pri kritični točki (CP) + potencialni evapotranspiraciji (ETc)

The soil water content observed BD and in the COZ was in all soil depths and for all dripper distances almost identical. The only difference was observed at the soil depth of 10 cm where immediately after irrigation cut off the highest water content was observed below the dripper for Strategy 1b, as already seen in the previous simulations with initial conditions at FC-ETc. When looking at the water content just before the next irrigation event, there was no difference observed between locations BD and at COZ.

At 10 cm of soil depth a slight increase of soil water content was observed for all Strategies. The water content observed before the last irrigation event at that depth was for strategies 1b and 2b and 3b almost identical, resulting in 0.26 cm^3/cm^3. At the soil depth of 40 cm (20 cm excluding the ridge), the soil water content for all Strategies was slightly rising (from 0.258 cm^3/cm^3 to 0.263 cm^3/cm^3 on the last day) throughout all days of simulations. At the soil depth of 60 cm (40 cm excluding the ridge) the soil water content was slightly decreasing (from 0.27 to 0.265 cm^3/cm^3) for all the Strategies.

Overall, when dripper distances and initial soil water effects were investigated the results showed that the initial soil water content affects the soil water distribution in all soil depths, which was expected. When soil water initial conditions were set to FC – ETc the water content was throughout 5 days of simulations kept constant at the soil depths of 10 and 40 cm, but was slightly decreasing at the depth of 60 cm (40 cm excluding the ridge). On the other hand, when soil water initial conditions were set to CP+ETc the soil water content at the soil depth of 10 and 40 cm slightly increased, but identically to simulations with initial conditions set to FC-ETc, decreased at the soil depth of 60 cm. Thus, all strategies studied above failed to maintain constant soil water content at 60 cm (40 cm without soil ridge). Simulations also showed that the soil water content, observed just before the next irrigation event and when the amount of applied water was equal to plants ETc, was for the given soil depth the same below the dripper and at the centre of overlap zone. This suggests that wetting patterns overlapped for all simulated Strategies.

When comparing the results of different dripper distances at different soil water initial conditions for other strategies with volume of applied water equal to 200 and 300 % of ETc (i.e. Strategies 7 a, b; 8 a, b; 9 a, b), the similar results as presented above, were observed.

To provide additional insight into the strategies presented in this section, Table 4.7 presets cumulative free drainage from the soil profile and cumulative root water uptake against cumulative potential RWU for Strategies 1a, b, 2 a, b and 3 a, b.

Table 4.7: Cumulative free water drainage (cm^3), actual and potential root water uptake (RWU) (cm^3) for different emitter distances (strategies) and different soil water initial conditions
Preglednica 4.7: Kumulativna drenaža vode (cm^3), dejanski in potencialni odvzem vode skozi korenine (RWU) (cm^3) za različne razdalje med kapljači (strategije) in različne začetne vsebnosti vode v tleh

Strategy	Free drainage (cm^3)	Cumulative actual root water uptake (RWU) (cm^3)	Cumulative potential RWU (cm^3)
1a	3850	12100	12200
2a	2890	9030	9080
3a	1930	5990	6030
1b	277	11300	12200
2b	208	8450	9080
3b	139	5610	6030

Higher free water drainage was observed for strategies where soil water initial conditions were set to FC-ETc (strategies denoted with letter b). The highest water drainage of 3.85 L (in 5 days of simulations) was observed for Strategy 1a. For Strategy 1b the water drainage was remarkably smaller, resulting in 0.208 L for 5 simulation days. This was due to higher soil water conditions maintained with Strategies 1a, 2a and 3a which at the soil depth of 60 cm resulted in water content around soil FC which increased the possibility of water drainage below the main root zone. The same trend was observed for other strategies (2a, 2b; 3a, 3b), as seen in Table 4.7. On the other hand, the smallest amount of drained water was observed for Strategy 3b, at 0.139 L. However, it has to be pointed out that smallest amount of water drained from the soil profile for Strategies 3a and 3b were due to the smaller dripper distances and therefore smaller simulations flow domain with consequently smallest volumes of water applied per irrigation event. Comparing the results of actual cumulative RWU of Simulations 1a, 2a and 3a and Simulations 1b, 2b and 3b, lower RWU was observed for the latter. This happened because the RWU was below 50 % of AWC (below 0.27 cm^3/cm^3) already reduced. Strategies with lower soil water initial conditions (set at CP+ETc) maintained soil water content at all soil depths close to CP. However, if the simulations with initial soil water conditions set to CP+ETc would maintain soil water content just above CP at 0.27 cm^3/cm^3 the results may have been different.

4.7.2 Influence of volume of applied water

The model was run for different amounts of applied water represented as 100, 200 and 300 % of plants ETc (mm) with the purpose to investigate which strategy sufficiently wets the entire 40 cm (60 cm including the soil ridge) of the hop root zone. Therefore amount of water applied each day exceeded the plants daily water needs (ETc) for 100 % with strategies 4 a, b, 5 a, b and 6 a, b, and for 200 % with Strategies 7 a, b, 8 a, b and 9 a, b. Initial soil water conditions were kept the same as presented in Tables 3.20. Irrigation was carried out each day, except on the first day. Two additional simulations are also presented

showing how soil water content behaves if 200 % of plants ETc is applied every second day and 300 % ETc is applied every third day, making water applied with irrigation equal to plants ETc. Because the results in previous section showed that soil water content below the dripper (BD) and at the centre of the drippers overlap zone (COZ), observed just before next irrigation event, are identical, only the water distribution observations at the COZ were selected as representative throughout this results section.

To investigate soil water distribution at different soil depths, when different amounts of water are applied, Figure 4.58 shows soil water content dynamics for Strategies 1a (100 % ETc), 4a (200 % ETc) and 7a (300 % ETc) at soil water initial conditions set to FC-ETc.

Comparing the results of different numerical experiments denoted as Strategies 1a, 4a and 7a showed that the highest soil water content at all soil depths developed under 300 % ETc (7a) irrigation, followed by 200 % ETc (4a) and 100 % ETc (1a). At the soil depth of 10 cm soil water content, observed just before the next irrigation event was maintained at the constant level of 0.30 cm^3/cm^3 only with Strategy 1a. With Strategy 4a a slight water content increase from 0.29 to 0.31 cm^3/cm^3 was observed. Strategy 7a resulted in water content increase from 0.29 to 0.326 cm^3/cm^3 over five simulation days. At soil depth of 40 cm soil water content was maintained at constant level of 0.31 cm^3/cm^3 only with Strategy 1a. Water content increase from 0.31 cm^3/cm^3 to 0.326 for Strategy 4a and from 0.31 to 0.34 cm^3/cm^3 for Strategies 7a, were observed. At soil depth of 60 cm soil water increased from 0.332 cm^3/cm^3 to 0.34 and 0.36 cm^3/cm^3 for Strategies 4a and 7a, respectively. However, a slight water content decrease from 0.332 to 0.326 cm^3/cm^3 was observed for Strategy 1 over 5 simulated days.

Figure 4.59 shows soil water content dynamics for Strategies 1a (100 % ETc), 4a (200 % ETc) and 7a (300 % ETc) but this time for soil water initial conditions set to CP+ETc.

10 cm COZ

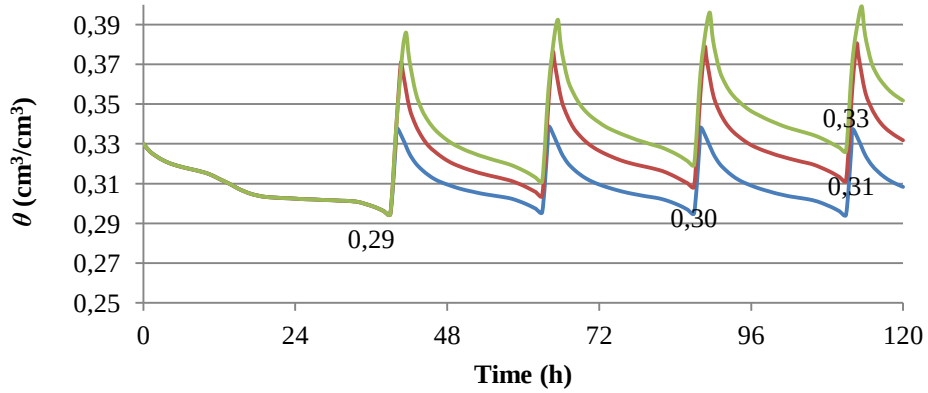

40 cm COZ

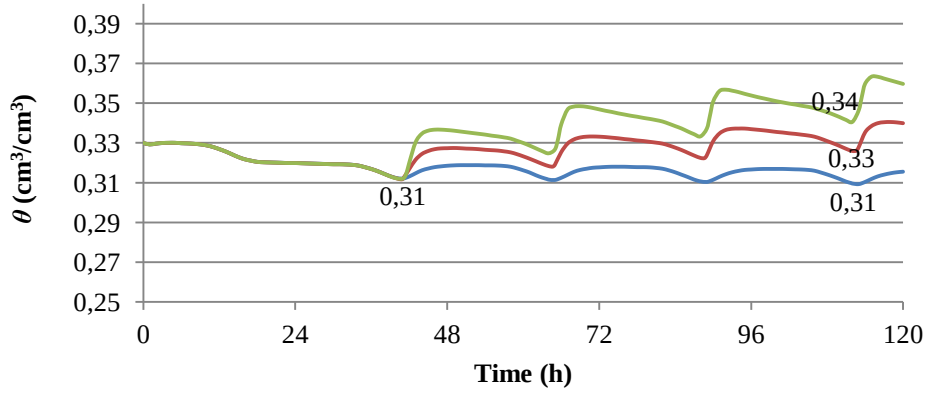

60 cm COZ

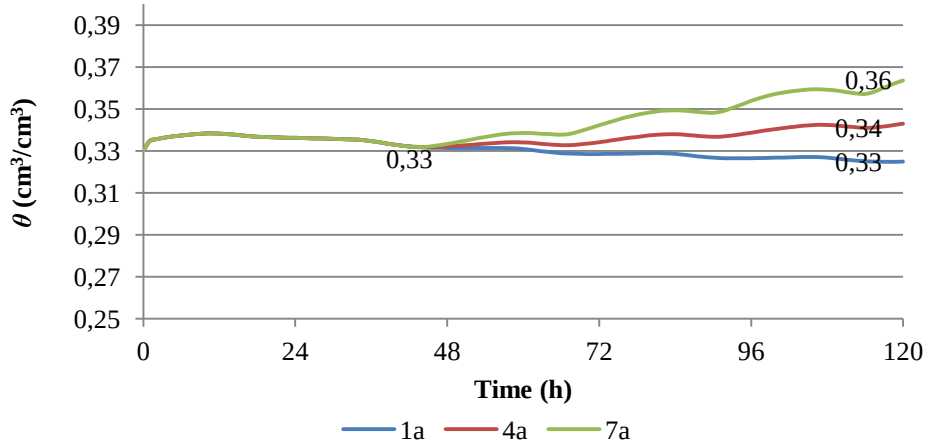

Figure 4.58: Soil water content dynamics for three different volumes of water applied presented as 100 % ETc (Strategy 1a), 200 % ETc (Strategy 4a) and 300 % ETc (Strategy 7a) for three different soil depths at initial conditions set to field capacity (FC) – potential evapotranspiration (ETc)
Slika 4.58: Dinamika stanja vode v tleh za tri različne volumne dodane vode, prikazane kot 100 % ETc (strategija 1a), 200 % ETc (strategija 4a) in 300 % ETc (strategija 7a), za tri različne globine tal in začetno vsebnostjo vode v tleh pri kritični točki (FC) – potencialni evapotranspiraciji (ETc)

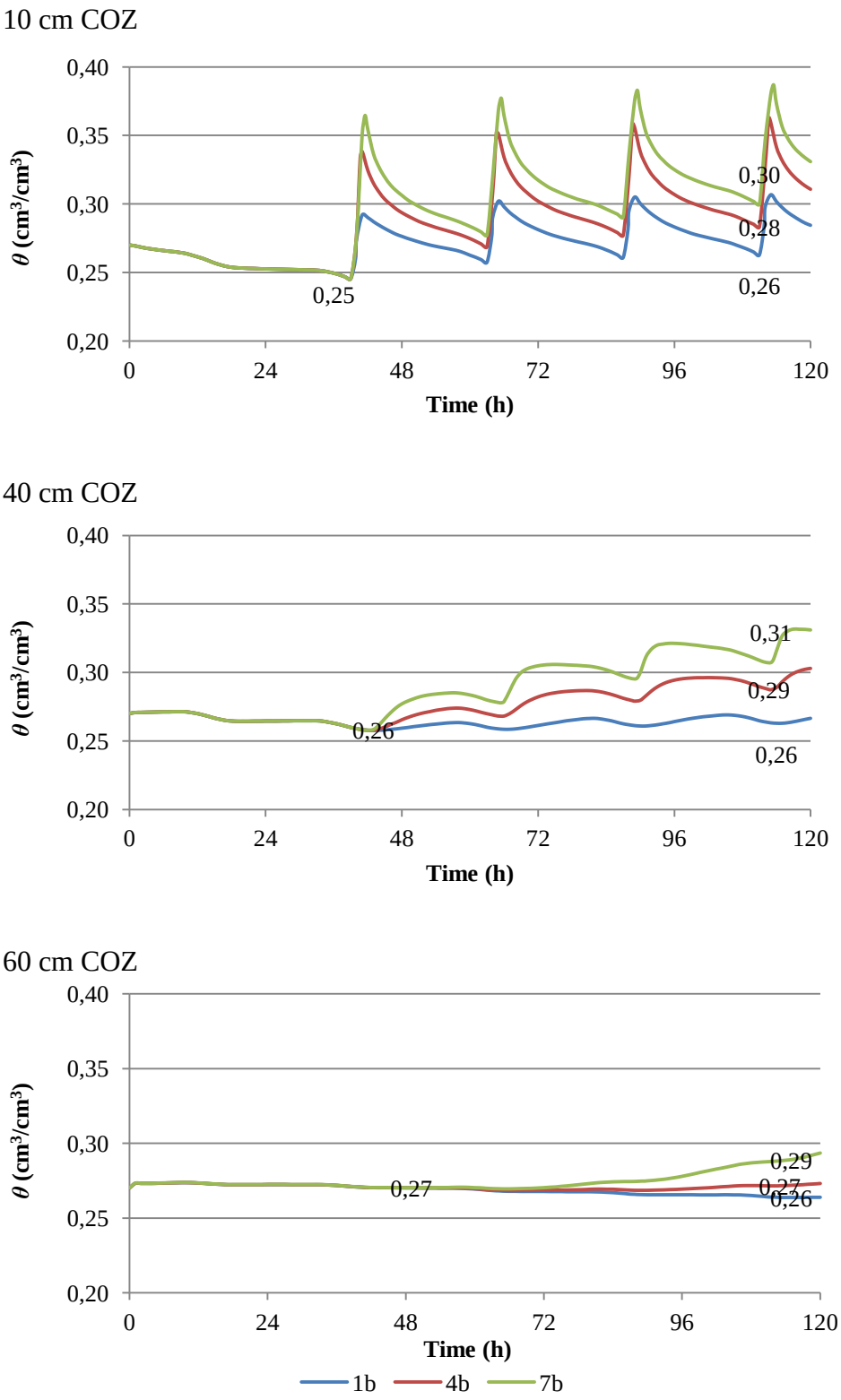

Figure 4.59: Soil water content dynamics for three different volumes of water applied presented as 100 % ETc (Strategy 1b), 200 % ETc (Strategy 4b) and 300 % ETc (Strategy 7b) for three different soil depths at initial conditions set to critical point (CP) + potential evapotranspiration (ETc)
Slika 4.59: Dinamika stanja vode v tleh za tri različne volumne dodane vode, prikazane kot 100 % ETc (strategija 1b), 200 % ETc (strategija 4b) in 300 % ETc (strategija 7b) za tri različne globine tal in začetno vsebnostjo vode v tleh pri kritični točki (CP) + potencialni evapotranspiraciji (ETc)

The results on Figure 4.59 are similar to those from Figure 4.58. The highest soil water content just before the next irrigation event was observed for Strategy 7b and followed by Strategies 4b and 1b. At the soil depth of 10 cm the soil water content increase with time was observed for all Strategies. At the soil depth of 10 cm soil water content increase from 0.246 cm^3/cm^3 to 0.26 cm^3/cm^3 was observed for Strategy 1b, from 0.264 cm^3/cm^3 to 0.283 cm^3/cm^3 for Strategy 4b and from 0.264 cm^3/cm^3 to 0.30 cm^3/cm^3 for Strategy 7b. At soil depth of 40 cm soil water increased from 0.258 cm^3/cm^3 to 0.24, 0.29 and 0.31 cm^3/cm^3 for Strategies 1b, 4b and 7b, respectively. At soil depth of 60 cm soil water in five simulation days increased from 0.27 cm^3/cm^3 to 0.272 and 0.29 cm^3/cm^3 for Strategies 4b and 7b, respectively. Results showed that at the soil depth of 10 and 40 cm soil water content was kept constant only with Strategy 1b. However, Strategy 1b resulted in soil water content decrease of 0.02 cm^3/cm^3 (2 %) at the soil depth of 60 cm.

The increase of soil water content, observed before the first irrigation event compared to soil water content before the last (4^{th}) irrigation event, was for all Strategies with water initial conditions at CP+ETc greater when compared to Strategies with soil water initial conditions set to FC-ETc. When soil water dynamics for different volumes of water applied were tested with other dripper (emitter) spacings (i.e. 30 and 20 cm) the similar results as shown on Figures 4.58 and 4.59 were obtained.

Figure 4.60 shows the soil water dynamics for strategies 1a, 4a and 7a when water applied with irrigation is equal to plants ETc. In this case irrigation is carried out every day for strategy 1a, every second day for strategy 4a (modified) and every third day for strategy 7a (modified). All strategies were simulated for 5 days. As for all strategies simulated in this work, there was no irrigation on the first day, which allowed water to redistribute in the soil profile. This resulted in 4 irrigation cycles for strategy 1a and two irrigation cycles for strategies 4a (on second and fourth day) and strategy 7a (on second and fifth day).

Strategy 1a

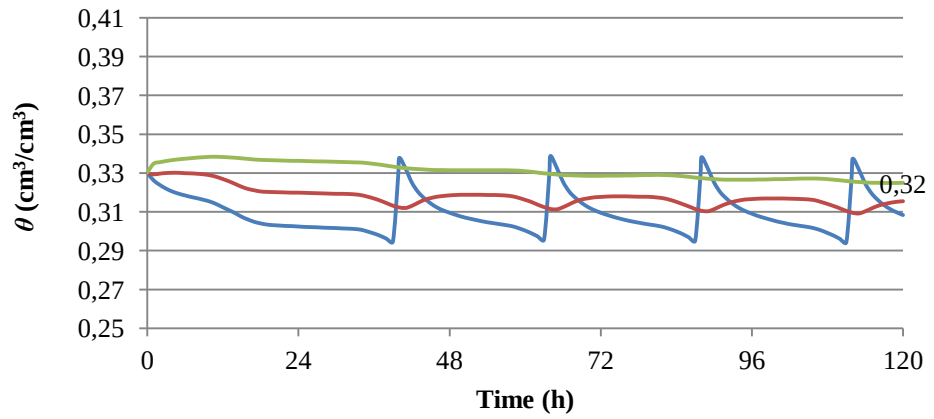

Strategy 4a (modified)

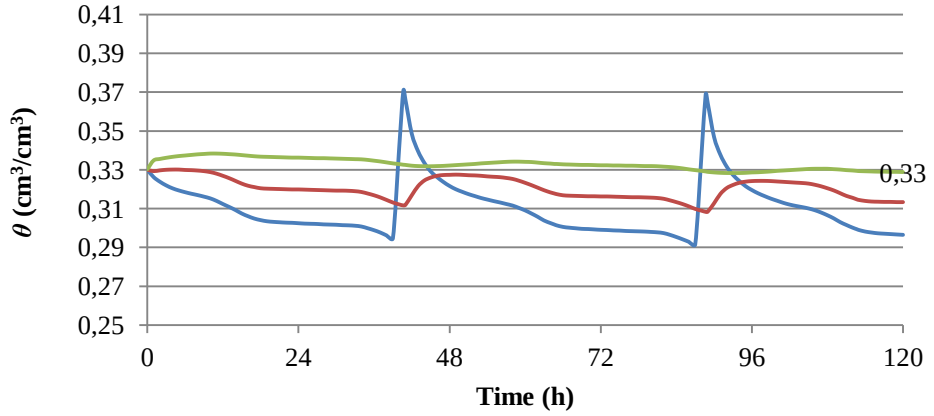

Strategy 7a (modified)

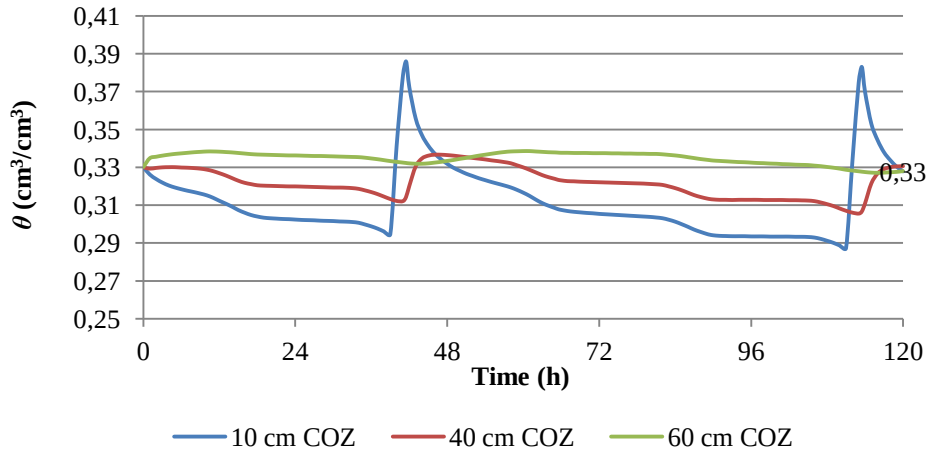

Figure 4.60: Soil water content dynamics at three different soil depths, with dripper spacing of 40 cm and soil water initial conditions at field capacity (FC) – potential evapotranspiration (ETc)for strategies 1a, 4a (modified) and 7a (modified) when the applied water is equal to 100 % of plants ETc

Slika 4.60: Dinamika stanja vode v tleh na treh različnih globinah tal z razdaljo med kapljači pri 40 cm in začetno vsebnostjo vode v tleh pri polski kapaciteti (FC) – potencialni evapotranspiraciji (ETc), za strategije 1a, 4a (prilagojena) in 7a (prilagojena), ko je volumen dodane vode z namakanjem enak 100 % ETc

If changing the amounts of added water per irrigation cycle and at the same time applying 100 % of plants ETc, as shown on Figure 4.60, this changes the irrigation frequency (every day, every second day and every third day). The differences between soil water contents observed before the last irrigation event for strategies presented on Figures 4.60 are very small. This is partly because of the short duration (5 days) of simulations. If simulations would be extended to 14 or 21 days, the differences would probably be bigger. Observed soil water content just before the last irrigation event at soil depth of 10 and 40 cm was maintained at the constant level only with Strategy 1a. At the same soil depths a very small soil water content decrease was observed for modified Strategies 4a and 7a. At soil depth of 60 cm (40 cm excluding soil ridge) a slight water content decrease was observed for all Strategies. This suggests that the volume of applied water, for all Strategies tested on Figure 4.60, which is equal to 100 % of plants ETc, does not wet the entire plants root zone (40 cm excluding soil ridge). At the same time the highest soil water content is observed at that depth because water from the upper soil profiles is, because of gravity forces, moving downwards. Unfortunately the amount of this water is not big enough to maintain constant water level at that depth also because of the process of plant root water uptake in the above soil layers and possibly water drainage below the root zone depth. On the other hand, as already mentioned, soil water content at that depth is maintained just around the limit of soil FC. This means that if more water is added with irrigation, this would increase soil water content above soil FC which would result in water drainage below effective root zone depth, representing water losses. Therefore, as the simulated strategies on Figure 4.60 suggest, volume of applied water should just exceed the plants water needs so that the water content at the soil depth of 60 cm (40 cm without soil ridge) would be maintained at constant level. However, as proposed previously, water content at this depth is already maintained close to the soil FC and because the soil water decrease over period of 5 days is very small, there is no concern that water content will at this depth reach soil CP in short time (at the given water content decrease from Figure 4.60 a soil CP would be reached after around 24 days for Strategy 1a and after 73 days for modified Strategies 4a and 7a).

Additional insight into water content distribution below two surface drippers at the time just before (111 h for strategy1a and 7a, 87 h for strategy 4a) and just at the irrigation cut-off (88.66 h for strategy 4a, 113.49 h for strategy 7a, 111.82 h for strategy 1a) for the last irrigation event is shown on Figure 4.61 which is Hydrus-2D/3D graphical output for the same strategies as presented on Figure 4.60. The soil domain is cut off at the middle of the soil ridge and aligned in X direction.

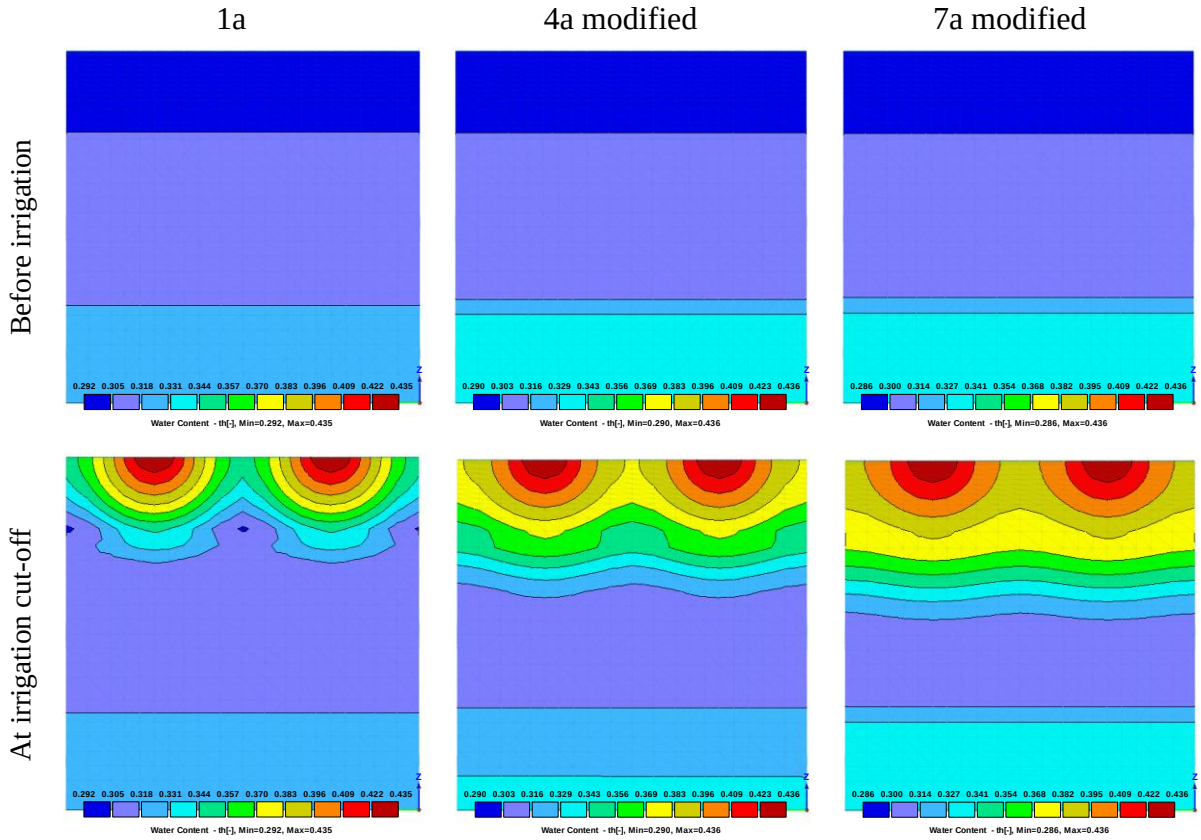

Figure 4.61: Hydrus-2D/3D graphical output of simulated soil water distribution with dripper spacing of 40 cm and soil water initial conditions at field capacity (FC) – potential evapotranspiration (ETc) for strategies 1a, 4a (modified) and 7a (modified) before and after irrigation when the applied water is equal to 100 % of plants ETc. The soil domain depth and length are 80 cm

Slika 4.61: Hydrus-2D/3D grafični prikaz simulirane distribucije vode v tleh, pri 40 cm razdalje med kapljači in začetno vsebnostjo vode v tleh pri poljsko kapaciteto (FC) – potencialno evapotranspiracijo (ETc), za strategije 1a, 4a (prilagojena) in 7a (prilagojena), pred in po namakanju, ko je količina z namakanjem dodane vode enaka 100 % ETc. Globina in širina domene je 80 cm.

The same as on Figure 4.60, no differences in soil water content distribution, before next irrigation event, were observed on Figure 4.61. However, just after irrigation cut-off important differences occurred between different irrigation strategies. Because of the biggest amount of water applied per irrigation cycle, the wetting pattern sizes in all directions was the biggest for strategy 7a modified, where water was applied every third day and was followed by strategy 4a modified and strategy 1a, where the smallest wetting pattern dimensions just after irrigation cut-off were observed. These results were expected, since it is well known that the biggest amount of water produces the biggest wetting pattern sizes in all directions. This can be clearly seen also on Figure 4.60, where the biggest amount of water applied per irrigation event (strategy 7a modified) resulted in the highest peak θ (cm^3/cm^3) just after the end of irrigation event at all soil depths at the centre of the overlap zone. But, on the other hand, when the soil water θ (cm^3/cm^3) was analyzed just before the next irrigation event, the differences between considered irrigation strategies were very small.

5 CONCLUSIONS AND RECOMMENDATIONS

5.1 CONCLUSIONS

The literature is generally suggesting that higher emitter (dripper) discharge rates extend the wetting pattern in horizontal direction, especially in fine textured soils. This can be true for higher discharge rates, causing water to pond on the soil surface and then infiltrate into soil. This was not the case in first part of this research, most probably because emitter discharge rates used were small in comparison to discharge rates used in other research. The sizes of wetting patterns in first part of this work were measured immediately after irrigation cut off. The influence of 1.5, 2 and 4 L/h emitter discharges on the final size of wetting pattern was very small and almost negligible. The only difference was observed for 0.5 L/h treatment, where the biggest wetting patterns in all directions were observed. However, the literature is suggesting that differences caused by the different emitter discharge rates, become even less pronounced, after allowing the water to redistribute after irrigation cut off. All irrigation simulations done with different antecedent soil water contents or depletions showed that higher initial water content conditions at the beginning of irrigation caused larger wetting pattern sizes in all directions

The number of emitters on laterals, allowable length and diameter of the pipes and laterals, sizes of the pumps and all necessary supporting equipment largely determine the price of drip irrigation system. Therefore the goal is to maximize the horizontal water spreading from the emitters and to use the smallest emitter discharge rate possible which will, at the same time, maintain desired soil water content at the depth of the main root zone. According to this study the smallest emitter discharge rate of 0.5 L/h and highest soil water content initial conditions, produced the biggest wetting pattern in both directions and can be therefore suggested as optimal for crops irrigation. In addition, because of small discharge rates the lateral pipes can be longer, the number or power of pumps with supporting equipment smaller and the distance between emitters (drippers) bigger. However, lower emitter discharge rates and bigger emitter distance will increase the duration of irrigation which will affect the irrigation management and scheduling considerably.

Hydrus-2D/3D simulations results with different soil texture classes from SEISMIC database, different emitter (dripper) discharge rates and different antecedent soil water contents were used for the second part of the research and allowed deriving new parameter constants for the Schwartzman and Zur (1986) model. The improved model parameters, tested on data from three independent studies, showed a good performance of the Schwartzman and Zur (1986) model resulting in root mean square values varying from 2.21 to 13.92 cm and modelling efficiency values varying from -2.54 to 0.93. A good comparison of the model is suggesting that the model can be used by irrigation systems

designers with the simple and sole knowledge of the soil's saturated hydraulic conductivity. However, it has to be noted that further research on how such empirical models perform under in situ conditions, when other factors affecting soil water movement, such as soil structure and layering, are considered.

In the third part of research numerical study under sweet corn field was carried out to investigate the influence of five different irrigation management strategies on the spreading of water from the surface drip emitters when at the same time considering root water uptake. The difference in wetting patterns sizes in uniform soil between five irrigation strategies (continuous or pulsing), when applying the same amount of water, was up to 28.6 % in the vertical and up to 29.2 % in the radial direction. Water content in the soil profile was on average higher for irrigation strategies where water was applied in daily pulses and lowest when irrigation was carried out over the night. Plants root water uptake was significantly affected by irrigation strategy and was lowest for irrigation strategy 3, where soil water content was maintained at the highest average level. This was due to the parameters of root water uptake which entirely depend on selected physical properties of the soil. This means that root water uptake was highest between soil FC and crop tolerated water depletion (for corn 50 % depletion is recommended by Allen et al. 1998). For irrigation strategies where soil water content was maintained above soil FC or below 50 % depletion, at the stage of highest ETc and at the depth of maximum root intensity, resulted in more stress for plants and lower water uptake. Strategy where continuous irrigation started every day at 21.30 h and lasted until 23.33 h (strategy 2) performed best, because soil water redistributed over the night which resulted in optimum water content during the next day at the time when ETc was highest. Overall, the results are shoving that with the present surface drip system design for highly permeable sandy soils the best option for sweet corn irrigation is continuous daily irrigation at night (strategy 2) and that with the emitter spacing of 33 cm, a continuous wetted strip of soil was maintained with all strategies to the maximum soil depth of 21 cm where highest root density occurs for the strategy where water was applied in eight pulses every second day. However, further simulations with different drip system design parameters should be carried out to determine the optimal emitter discharge rates, timing and spacings and therefore provide better irrigation efficiency. This part of research was a case study and it did not relate to previous parts of research, but presented introduction to more complex numerical modelling approaches with realistic input parameters which are presented in the following parts of research.

In the fourth part the accuracy of Hydrus-2D/3D simulations of water infiltration and redistribution from a surface point source for a layered silty clay loam soil when considering root water uptake, was evaluated in a hop field. Simulated soil volumetric water contents were found to be in good agreement with TDR measured experimental data

at 20 locations considered. The root mean square values for three studied days and for all TDR probes varied between 0.0025 and 0.1337 cm^3/cm^3. If only one representative location for each soil layer was selected, root mean square values varied from 0.0025 to 0.0364 cm^3/cm^3. Hydrus-2D/3D failed to correctly simulate initial soil water values for two vertically inserted probes resulting in root mean square values of 0.13337 and 0.1235 cm^3/cm^3. Because measured and simulated results were in good agreement, this set up a good basis for the last part of the research.

In the fifth part the evaluated model allowed evaluation of the effects of various surface drip irrigation design and management parameters for surface drip hop irrigation, such as different soil water initial conditions at the onset of irrigation, different emitter (dripper) spacings and volumes of water applied presented as 100, 200 and 300 % of plants ETc. For this purpose all together 18 different irrigation strategies were investigated. The graphical comparisons of simulated soil water contents at different depths and different vertical plane locations (below the dripper and in the centre of the drippers overlap zone) considering two surface drip emitters have been carried out. Results showed that, when water contents at different soil depths are compared just before the next irrigation event (after 24 h of water redistribution), the influence of dripper spacing (20, 30 and 40 cm apart), when applying the same volumes of water, was completely eliminated. Also, after soil water redistribution, no difference in soil water content at various soil depths was observed for locations below the dripper and in the centre of the drippers overlap zone. This suggests that neighbouring wetting patterns formed below surface drippers overlapped at all dripper spacings (20, 30 and 40 cm). The results of simulations with different soil water initial conditions (FC-ETc, CP+ETc) showed that antecedent soil water content affects the soil water distribution in all soil depths. At soil water initial conditions set close to soil FC, when applied water was equal to 100 % of plants ETc, the water content at soil depths of 10 and 40 cm was constant, but with the soil water initial conditions set close to critical point, the water contents at the same depths were slightly increasing with time. For both initial conditions investigated the soil water content was decreasing at the soil depth of 60 cm (40 cm below soil surface if the soil ridge is excluded), when amount of water applied with irrigation was equal to 100 % of plants ETc. Results also showed that water drainage below the root zone, when daily applying 100 % of plants ETc was higher for strategies with higher initial soil water conditions. resulting in 16.8 m^3/ha of lost water for strategies with higher soil water initial conditions (strategies 1a, 2a and 3a) compared to 1.2 m^3/ha of lost water for strategies with lower soil water initial conditions (strategies 1b, 2b and 3b).

In general, for hop irrigation, the emitter spacing had very little effect on the soil water distribution below the surface drippers for given soil and root water uptake conditions. But, when at the same time, soil water initial conditions and volume of applied water per irrigation cycle are considered, it is suggested that the irrigation water applied should just

exceed plant water needs so that the soil water content level at the soil depth of 60 cm is maintained at constant level. Results also suggest that dripper spacing of 40 cm is appropriate for hop irrigation in silty clay loam soil. However, more simulations with different dripper spacings and volumes of water applied per irrigation cycle should be carried out to determine even more optimal irrigation system design and management parameters.

5.2 KEY CONCLUSIONS

The first hypothesis (Wetting volumes will strongly correlate with soil texture (% sand, % silt, % clay) and they will be wider and shallower for finer textured soils) is proved true the Hydrus-2D/3D modelling and soil tank experiments with three different soil textures, which have been conducted in Naglič (2011). The wetting patterns for coarse-textured soils tend to extend in Y direction more than in X one. This is due to high infiltration capacity of coarse-textured soils, where water infiltrates easily through the soil profile and the domination of gravity forces. On the other hand, in fine-textured soils, the wetting patterns tends to move more in X than in Y direction because of high capillarity forces, especially at the beginning of water application process. However, as results in Naglič (2011) (which in some aspects supplements this thesis) showed, the percentages of sand silt and clay fractions do not correlate with the sizes of the wetting patterns.

Hypothesis two (Higher flow rate for equal irrigated volumes will create wider shallower wetting patters for all drip systems) was not proven to be correct. It was shown with simulations that emitter (dripper) discharge (flow) rates of 1.5, 2 and 4 L/h had a very small effect on the final size of the wetting patterns observed just after irrigation cut off. Just the opposite was observed for the smallest discharge rate of 0.5 L/h which produced the largest wetting patterns in all directions. The only exception occurred in sandy soil, where exactly the same wetting pattern depth was observed for all emitter discharge rates. On the other hand, larger differences were observed when the wetted fronts close to soil saturation point were observed, where higher emitter discharge rates resulted in larger wetting pattern dimensions in all directions.

Hypothesis three (Different initial soil water conditions at given evapotranspiration will affect the size of the wetting pattern) was proven to be correct. Higher initial soil water content caused larger wetting pattern sizes in all directions. For a given volume of water applied the wetted radius tended to be larger and wetted depth smaller for fine textured soils. For coarse textured soils the wetted radius was smaller and wetted depth larger. The effect of evapotranspiration or plants root water uptake influence on the wetting pattern size was studied throughout different irrigation strategies of sweet corn irrigation. Results

showed that drip irrigation strategy strongly affected plants root water uptake. The root water uptake was largest for irrigation strategies where high water content was maintained in the zone of maximum root intensity at the time when plants evapotranspiration was highest which directly affects the wetting pattern shape and soil water distribution in the soil profile.

6 SUMMARY (POVZETEK)

6.1 SUMMARY

Future improvements in irrigation, as modified irrigation technology or techniques, will play a very important role. These improvements can in the future increase the productivity of water used by irrigation and may provide significant adaptation potential under a changing climate.

The great potential of drip irrigation lies in improving water management by improving crop yield and quality using less water, and by localising chemical and fertiliser applications to enhance their efficient use and to reduce the risk of pollution. But, to design drip irrigation systems effectively, the soil water dynamics needs to be predicted using all necessary soil, plant and atmosphere variables. Information about temporal evolution of the wetted soil volume can be helpful in establishing the optimal emitters spacing and the duration of irrigation for the volume of soil where the main crop roots are located.

There are some guidelines published to help end users operate surface drip irrigation systems. Unfortunately, there are few, if any, clear guidelines on how to design surface drip irrigation systems by taking into account differences in soil hydraulic properties. In engineering terms, systems are often designed to an economic optimum, which may result in insufficient or excessive irrigation. On the other hand, models that simulate the dynamics of water in the soil beneath surface drip irrigation can help in predicting soil water content distribution. One such model is the numerical model Hydrus. The use of such models can, in comparison to field experiments, save financial resources and time-demanding laborious work, which would have to be undertaken to examine the dimensions of wetting patterns under different drip irrigation strategies and field/soil conditions.

The main purpose of this project is to investigate numerically and experimentally the influence of soil texture, relevant hydraulic properties, evapotranspiration, vegetation root distribution and rate of water applied on the size of the wetted area and therefore emitter spacing under surface drip irrigation systems that are appropriate for Slovenian climate conditions.

The hypotheses examined in the dissertation are: wetting volumes will strongly correlate with soil texture (% sand, % silt, % clay), they will be wider and shallower for finer textured soils, higher flow rate for equal irrigated volumes will create wider shallower wetting patters for all drip systems and different initial soil water conditions and evapotranspiration will affect size of the wetting pattern.

Work in this thesis was divided into five main parts. For the first part of this work, numerical simulations were done for soils, from arable land use, covering all texture classes according to the UK soil textural triangle which were selected from the Spatial Environmental Information System for Modelling the Impact of Chemicals (SEISMIC) database. In the second part selected empirical model parameters were improved based on simulations data from the first part. In the third part numerical model was used to investigate surface drip irrigation management of sweet corn when considering root water uptake. In the fourth part, numerical model results were compared with experimental data from hop surface drip irrigation. Finally, in the fifth part, numerical simulations were carried out to investigate the influence of different hop surface drip irrigation design parameters on soil water dynamics between two adjacent emitters.

The simulation results testing influence of different emitter discharge rates showed a small influence of 1.5, 2 and 4 L h^{-1} emitter discharge rates on the final size of the wetting pattern. The only major difference was observed for the discharge rate of 0.5 L/h, where the largest wetting pattern in all directions was observed. Higher initial soil water content at the beginning of irrigation caused larger wetting pattern sizes in all directions in all contrasting soil textures. However, for a given volume of water applied the wetted radius tended to be larger and wetted depth smaller for fine textured soils. For coarse textured soils the wetted radius of wetting pattern was smaller and wetted depth larger.

The numerical data obtained for a wide range of soil textures provided the opportunity to refine the parameters of the Schwartzman and Zur model. The improved model parameters, tested on data from three independent studies, showed a good performance of the Schwartzman and Zur (1986) model resulting in root mean square values varying from 2.21 to 13.92 cm and modelling efficiency values varying from -2.54 to 0.93. A good comparison of the model is suggesting that the model can be used by irrigation systems designers with the simple and sole knowledge of the soil's saturated hydraulic conductivity.

Simulation results with sweet corn drip irrigation showed that irrigation strategy strongly affected plants root water uptake. The root water uptake was largest for strategies where high water content was maintained in the zone of maximum root intensity at the time when ETc was highest. The results are shoving that with the present surface drip system design for highly permeable sandy soils the best option for sweet corn irrigation is continuous daily irrigation at night and that with the emitter spacing of 33 cm, a continuous wetted strip of soil was maintained with all strategies to the maximum soil depth of 21 cm where highest root density occurs for the strategy where water was applied in eight pulses every second day.

The accuracy of Hydrus-2D/3D simulations of water infiltration and redistribution from a surface point source for a layered silty clay loam soil when considering root water uptake, was evaluated in a hop field in Žalec. Simulated soil volumetric water contents were found to be in good agreement with TDR measured experimental data at 20 locations considered. The root mean square values for three studied days and for all TDR probes varied between 0.0025 and 0.1337 cm^3/cm^3. If only one representative location for each soil layer was selected, root mean square values varied from 0.0025 to 0.0364 cm^3/cm^3. However, Hydrus-2D/3D failed to correctly simulate initial soil water values for two vertically inserted probes resulting in root mean square values of 0.13337 and 0.1235 cm^3/cm^3.

The evaluated model allowed evaluation of the effects of various surface drip irrigation design and management parameters for surface drip hop irrigation, such as different soil water initial conditions at the onset of irrigation, different emitter (dripper) spacings and volumes of water applied presented as 100, 200 and 300 % of plants ETc. In general, for hop irrigation, the emitter spacing had very little effect on the soil water distribution below the surface drippers for given soil and root water uptake conditions. But, when at the same time, soil water initial conditions and volume of applied water per irrigation cycle are considered, it is suggested that the irrigation water applied should just exceed plant water needs so that the soil water content level at the soil depth of 60 cm is maintained at constant level. Results also suggest that dripper spacing of 40 cm is appropriate for hop irrigation in silty clay loam soil.

The research done proposes that the Hydrus-2D/3D can be successfully used for optimizing different irrigation design and management strategies to increase the surface drip irrigation systems efficiency. However, it has to be noted that further research on how such empirical models perform under in situ conditions, when other factors affecting soil water movement, such as soil structure and layering, are considered. Also, further simulations with different drip system design parameters should be carried out to determine the optimal emitter discharge rates, timing and spacings and therefore provide even more optimal irrigation system design and management parameters.

6.2 POVZETEK

Z večanjem števila prebivalstva in večanjem porabe vode v urbanih regijah mora kmetijska proizvodnja, ki temelji na namakanju, pridelati več hrane s porabo manj vode in hkrati preprečiti degradiranje tal in vodnih virov. Fischer in sod. (2007) je analiziral, da prilagajanje lahko in tudi mora igrati pomembno vlogo pri zmanjševanju vpliva podnebnih sprememb na vodne vire, namenjene za kmetijstvo, tako regionalno kot globalno. Za vzdrževanje ali povečanje kmetijske proizvodnje bodo morali novi namakalni sistemi, kot

so nadzemno ali podzemno kapljično namakanje, zagotoviti še večjo učinkovitost rabe vode kot sistemi, ki se tradicionalno uporabljajo danes. Kapljično namakanje ponuja velik potencial za izboljšanje upravljanja z vodo in tako prispeva k z izboljšanjeu kakovosti in donosu posevkov, s porabo manj vode in z možnostjo lokalnega gnojenja ter kemičnega apliciranja, ki povečuje učinkovito rabo in zmanjšuje tveganje za onesnaženje. Glavna prednost tega načina namakanja je potencial, da se zmanjša porabo vode in doseže zelo veliko učinkovitost namakanja, medtem ko se hkrati povečujeta kvaliteta in pridelek posevkov.

Kapljični namakalni sistemi običajno delujejo v presledkih in so sestavljeni iz točkovnih ali linijsko razporejenih kapljačev, ki so včasih razvrščeni tako, da med njimi prihaja do interakcije. Med procesom infiltracije se vsebnost vode v tleh spreminja tako prostorsko kot časovno in je močno odvisna od oblikovnih parametrov kapljičnega namakalnega sistema (razdalja med kapljači in lateralami, tlak v sistemu, pretok posameznega kapljača, vrst kapljača), podnebnih razmer, tipa tal, rastlinskega koreninskega sistema in upravljanja namakanja (obroka dodane vode). Za učinkovit načrt in uporabo kapljičnih namakalnih sistemov je potrebno predvideti dinamiko vode v tleh ob upoštevanju vseh zgoraj naštetih dejavnikov. Upravljanje, spremljanje in modeliranje distribucije vode v tleh zahteva tudi informacije o odvzemu vode skozi koreninski sistem rastlin. Ta odvzem vode vpliva na distribucijo vode v tleh in tako predstavlja osnovo za zagotovitev zanesljivih napovedi distribucije vode in matričnega potenciala v coni omočenih tal. Informacije o odvzemu vode skozi korenine so pomembne za planiranje kapljičnih namakalnih sistemov, da se prilagodi uniformnost aplikacije, razmik med kapljači in pretok kapljačev obsegu rastlinskega koreninskega sistema in da se zagotovi enotna dostopnost korenin do omočenega volumna tal. Poznavanje dinamike vode v tleh pri namakanju predstavlja predpogoj za načrtovanje namakalnih sistemov kakor tudi upravljanje (gospodarjenje) z vodo. Poznavanje časovnega razvoja omočene cone okoli kapljača v danem tipu tal lahko prispeva k vzpostavitvi ustreznih razdalj med kapljači in trajanje namakanja kot funkcije volumna tal, kjer so locirane korenine.

Za izpolnitev potrebe rastlin po vodi so lahko dnevne količine vode za namakanje dostavljene na več načinov. Voda je lahko dodana dnevno v enem samem obroku skozi celotno rastno sezono. Dodana je lahko dnevno, vendar v visokih ali nizkih frekvencah, ali pa je dodana izmenoma: vsa naenkrat v nekaterih dnevih in v pulzih v drugih dneh. Vsaka namakalna strategija bo imela za posledico drugačen vzorec vlaženja tal in drugačno obliko omočene cone tal, kar bo posledično vplivalo na drugačno distribucijo rastlinskega koreninskega sistema in odvzem vode preko korenin. Kot sta zapisala Vermairen in Jobling (1984), oblika omočenega vzorca tal ni odvisna samo od kapilarnih in gravitacijskih sil, teksture tal in hidravličnih lastnosti tal, ampak tudi od horizontalne in

vertikalne prepustnosti tal za vodo, neprepustnih slojev v tleh, volumna dodane vode, stopnje aplikacije vode ter začetne vsebnosti vode v tleh. Gradient vodnega potenciala je dodatno potreben za pomikanje vode v tleh. Simulacije za peščeno ilovnata tla, ki jih je opravil Skaggs in sod. (2010), so pokazale, da višja začetna vsebnost vode v tleh poveča volumen omočenih tal, a so povečanja večja v vertikalno kot v horizontalno smer. V raziskavi je bilo na splošno ugotovljeno, da tekstura tal, hidravlične lastnosti tal in začetna vsebnost vode v tleh v veliki meri določajo distribucijo vode v tleh, medtem ko imajo dodajanje vode v pulzih in sprememba pretoka kapljačev minimalen učinek.

Za izračun pomikanja vode v tleh obstaja veliko število empiričnih, analitičnih in numeričnih modelov. Analitični in numerični uporabljajo glavne enačbe za pretok za specifične začetne in robne (mejne) pogoje. To vključuje modele, ki temeljijo na reševanju Richardsove enačbe, in tudi bolj enostavne modele, ki izračunajo distribucijo vode v tleh na osnovi karakteristik tal. Čeprav so analitični modeli enostavni za uporabo, je njihova aplikacija za namene kapljičnih namakalnih sistemov omejena, ker so rešitve osnovane na omejujočih predpostavkah, ki se nanašajo na konfiguracijo vira vode, linearizacijo enačb tokov in homogene hidravlične lastnosti tal. Na osnovi poljskih opazovanj, regresijske analize, dimenzijske analize ali Artificial Neural Networks analize, so Schwartzman in Zur (1986), Amin in Ekhmaj (2006) in Malek in Peters (2011) razvili empirične enačbe za določanje širine in globine omočenega volumna tal pod nadzemnim točkovnim virom. Šimünek in sod. (1999) je razvil numerični programski paket Hydrus-2D, ki je bil posodobljen, da omogoča tudi tretjo dimenzijo, in se sedaj imenuje Hydrus-2D/3D (Šimünek in sod, 2006). Program omogoča implementacijo 3D, axialno-simetričnega pretoka vode, transporta raztopin, odvzema vode in hranil preko korenin na osnovi končnih elementov (finite element) numeričnih rešitev enačb toka. Programski paket Hydrus-2D/3D se lahko uporablja za reševanje dvo- ali tridimenzionalnega toka vode ali kontaminantov. Modeliranje toka vode ali transporta raztopin v tleh je uporabno za modeliranje vodnih virov ali ekološka upravljanja. Zaradi večjih računalniških hitrosti in razpoložljivosti učinkovitejših računalniških numeričnih modelov se numerični pristopi, kot je Hydrus-2D/3D, zdaj vse bolj uporabljajo tudi za ocenjevanje vodnega toka pri kapljičnih namakalnih sistemih.

Zgoraj omenjeni pristopi modeliranja so bili večinoma narejeni in testirani le za omejeno število talnih tipov in se nanašajo na predpostavke, kot so homogene hidravlične lastnosti tal. Večina od njih ne upošteva odvzema vode preko korenin, ET in slojevitosti tal. Prav tako ni generične in vzpostavljene relacije med geometrijo omočenih tal in splošnimi lastnostmi tal, kot so tekstura in njihove hidravlične lastnosti.

Pomanjkanje časa in potrebnih finančnih sredstev za testiranje vseh možnih namakalnih strategij pod različnimi pogoji je običajno preveliko, da bi bilo eksperimentalno določeno. Praktičen pristop za modeliranje vodnih tokov v tleh, rast korenin in odvzem vode iz tal je uporaba modelov, ki simulirajo različne strategije kapljičnega namakanja in ocenijo možne strategije za načrtovanje sistemov. Potem so lahko najbolj obetavne strategije izbrane in testirane pod poljskimi pogoji. V tem kontekstu je sprejetje tehnologije kapljičnega namakanja v kombinaciji s simulacijskim modelom, kot je Hydrus, dober primer te aplikacije.

Glavni namen tega projekta je numerično in eksperimentalno raziskati vpliv teksture tal, ustreznih hidravličnih lastnosti tal, metode namakanja, evapotranspiracije rastlin, rastlinskega koreninskega sistema (globina) in obroka dodane vode, na velikost vzorca omočenih tal in s tem povezanih razdalj med kapljači, za nadzemne kapljične namakalne sisteme, ki so veljavni za slovenske podnebne razmere. Raziskava se bo usmerila na medsebojne odnose med zgoraj naštetimi parametri, ki so pomembni za učinkovito kapljično namakanje. Cilj je vzdrževati oziroma ustvariti čim bolj uniformno distribucijo vode med kapljači, da se bo še ustvarjala homogena vlažna cona v tleh, ki je pomembna za pridelovanje vrstnih posevkov, brez izgub vode v podtalnico.

Ta premišljevanja vodijo do naslednjih specifičnih ciljev:

- Simulirati infiltracijo vode in izračunati širine in globine vlažnih con pod posameznimi kapljači z numeričnim modelom Hydrus-2D/3D za različne vrste tal z različnimi teksturami.
- Preučiti odnose širine in globine vlažne cone v tleh s teksturo in hidravličnimi parametri tal z namenom razvoja enačbe, ki bi napovedala dimenzije omočenih tal.
- Preučiti vpliv pretoka kapljačev in začetne vsebnosti vode v tleh na površino omočenih tal.
- Preučiti vpliv interakcije dveh sosednjih vzorcev omočenosti tal na geometrijo in distribucijo vlage vzorcev omočenosti z uporabo numeričnih simulacij v 3D okolju.
- Numerično preučiti vpliv evapotranspiracije z uporabo dejanskih meteoroloških podatkov in podatkov o rastlini (posevku) kot mejnih pogojev za model.
- Preveriti rezultate numeričnega modela v dejanskih razmerah s serijami poljskih poskusov pri kulturah, namakanih s sistemi kapljičnega namakanja.

Disertacija proučuje numeričen in eksperimentalen vpliv različnih dejavnikov načrtovanja in upravljanja nadzemnih kapljičnih namakalnih sistemov na geometrije omočenosti tal. Hipoteze so tako naslednje:

- Volumni omočenih tal bodo v močni korelaciji s teksturo tal (% peska, % melja, % gline), širši in plitvejši bodo za tla s težjo teksturo.

- Večji pretoki kapljačev bodo ob enaki količini dodane vode ustvarili širše in plitvejše vzorce omočenosti za vse kapljične namakalne sisteme.
- Različne začetne vsebnosti vode v tleh in evapotranspiracija bosta vplivala na velikost omočenih tal.

V prvem delu te raziskave so bile narejene numerične simulacije za enajst teksturnih razredov tal, ki ustrezajo teksturnemu trikotniku Združenega kraljestva (UK), pridobljenih iz baze podatkov Spatial Environmental Information System for Modelling the Impact of Chemicals database (SEISMIC). Iz baze podatkov so bila izbrana tla obdelovalnih zemljišč. Izbrana tla so tako pokrivala vse teksturne razrede glede na UK teksturni trikotnik. Baza podatkov je vsebovala vse potrebne van Genuchtnove parametre in nasičeno hidravlično prevodnost tal, ki so potrebni za delovanje Hydrus-2D/3D modela. Simulacije so bila narejene v treh različnih sklopih. V vsakem sklopu je bilo z namakanjem dodanih 20 L vode. Prvi sklop simulacij je bil namenjen proučevanju vpliva teksture tal, kjer smo simulacije izvedli za tla iz vseh 11 teksturnih razredov, pri pretoku kapljača 2 L/h in začetni vsebnosti vode v tleh pri 50 % razpoložljive vode. Pri drugem sklopu simulacij je bil proučen vpliv začetne vsebnosti vode v tleh na velikost omočene cone. Simulacije so bile izvedene za tri kontrastne teksturne razrede (pesek, meljasta ilovica in glina) pri pretoku kapljača 2 L/h ter za tri začetne vsebnosti vode v tleh, ki so ustrezale 30, 50 in 70 % razpoložljive vode v tleh. Končno, za iste tri kontrastne teksturne razrede je bil opravljen tretji niz simulacij, ki je bil izveden z namenom proučiti vpliv štirih različnih pretokov kapljačev (0,5; 1,5; 2 in 4 L/h) pri začetni vsebnosti vode v tleh pri 50 % razpoložljive vode. V vseh sklopih simulacij je bila velikost omočenih tal v obe smeri (horizontalno – polmer (X) in vertikalno – globina (Y)) izmerjena po vsakem litru dodane vode. Skupaj je bilo opravljenih 44 simulacij, od katerih je bilo le 32 uporabljenih v prvem delu te raziskave. Rezultati vseh 44 simulacij so bili uporabljeni za izboljšanje parametrov modela Schwartzman in Zur (1986).

V drugem delu so se izboljšali parametri izbranega Schwartzman in Zur (1986) empiričnega modela. Za ta namen so bili uporabljeni podatki vseh simulacij iz prvega dela raziskave. Nabor podatkov je tako vseboval rezultate dimenzij omočenih tal pod kapljačem v X in Y smer, za vsak liter od skupno 20 L dodane vode. Nabor podatkov je vključeval tla iz 11 teksturnih razredov pri pretoku kapljača 2 L/h in začetno vsebnostjo vode pri 50 % razpoložljive vode in tri kontrastne teksturne razrede tal, namakane pri treh različnih začetnih vsebnostih vode v tleh in štirih različnih pretokih kapljačev. Skupaj je bilo za izboljšanje parametrov modela uporabljenih 880 meritev v vsako smer cone omočenosti (X in Y).

V tretjem delu raziskave je bil model Hydrus-2D/3D uporabljen za preučitev upravljanja površinskega kapljičnega namakanja sladke koruze v homogenih peščenih tleh ob hkratnem upoštevanju realnih podatkov potencialne evapotranspiracije (ETc). Preučili smo vpliv petih različnih strategij kapljičnega namakanja, kjer je bila razdalja med kapljači 33 cm, pretok kapljačev 1 L/h in količina z namakanjem dodane vode enaka ETc. Pri prvi in drugi strategiji je bilo namakanje neprekinjeno zjutraj ali ponoči, pri tretji strategiji pa je se je namakanje izvedlo v štirih krajših pulzih čez dan. Pri četrti in peti strategiji je bilo namakanje izvedeno vsak drug dan in sicer neprekinjeno ali v kratkih pulzih.

V četrtem delu so bili numerični rezultati modela Hydrus-2D/3D primerjani z eksperimentalnimi podatki TDR meritev vsebnosti vode na 20 lokacijah v talnem profilu v meljasto-glinasto-ilovnatih tleh, pridobljenimi iz poljskega poskusa površinskega kapljičnega namakanja hmelja v Žalcu.

Nazadnje, v petem delu, so bile za raziskovanje vpliva različnih oblikovnih parametrov in strategij upravljanja nadzemnega kapljičnega namakanja hmelja, na dinamiko vode v tleh med dvema sosednjima kapljačema, uporabljene samo Hydrus-2D/3D numerične simulacije. Numerično smo preučili vpliv 9 različnih strategij namakanja pri dveh različnih začetnih vsebnostih vode v tleh (skupaj 18 strategij). Namen je bil optimizirati razmak med kapljači, količino z obrokom namakanja dodane vode in začetno vsebnost vode v tleh, da bomo na globini tal, kjer je največja masa korenin hmelja, še vzdrževali homogeno vlažno cono v tleh. Strategije so bile tako razdeljene na dva dela, glede na začetno vsebnost vode v tleh. In sicer, pri strategijah od 1 do 9, ki so bile označene s črko a, je bila začetna vsebnost vode v tleh določena pri poljski kapaciteti tal za vodo (FC) – dnevna ETc. Pri strategijah, označenih s črko b, je bila začetna vsebnost vode enaka kritični točki vode v tleh (CP) + dnevni ETc. Pri strategijah 1 a, b; 4 a, b in 7 a, b je bila razdalja med kapljači 40 cm, pri strategijah 2 a, b; 5 a, b in 8 a, b 30 cm in pri strategijah 3 a, b; 6 a, b in 9 a, b 20 cm. Pri strategijah 1 a, b; 2 a, b in 3 a, b je bila količina z namaknjem dodane vode enaka 100 % ETc, pri strategijah 4 a, b; 5 a, b in 6 a, b je bila količina dodane vode enaka 200 % ETc in pri strategijah 7 a, b; 8 a, b in 9 a, b enaka 300 % ETc. Dodatno sta bili uvedeni dve strategiji, in sicer 4 a (modificirana) in 7 a (modoficirana), kjer je bila količina z namakanjem dodane vode enaka ETc. Z drugimi besedami, namakanje pri strategiji 4 a (modificirana), se je izvedlo vsak drugi dan, saj je bil obrok dodane vode enak 200 % ETc, pri strategiji 7 a (modificirana) pa vsak tretji dan, saj je bil obrok dodane vode enak 300 % ETc. Hydrus-2D/3D simulacije smo za vse strategije zagnali za obdobje petih dni. Namakanje je bilo izvedeno v vseh dneh simulacij, razen za prvi dan in se je v vseh primerih pričelo ob 15. uri. Distribucija vode v tleh je bila spremljana na različnih globinah (10, 40 in 60 cm) na lokacijah pod kapljačem (BD) in na sredini med dvema sosednjima kapljačema (COZ) za vse strategije namakanja.

Rezultati simulacij v prvem delu raziskave so pokazali, da je vpliv pretoka kapljačev 1,5 in 2 in 4 L/h na končno velikost omočenih tal zelo majhen ali skoraj zanemarljiv. Edina razlika je bila opažena pri pretoku kapljača pri 0,5 L/h, kjer je bila opažena največja velikost omočenih tal v vse smeri (X in Y). Velikosti omočenih tal pod kapljačem so bile v tej raziskavi izmerjene takoj po prenehanju namakanja. Kakorkoli, literatura omenja, da postanejo razlike v velikosti omočenih tal ob uporabi različnih pretokov kapljačev še manj izrazite, če pustimo, da se voda v tleh prerazporedi po koncu namakanja. Rezultati simulacij namakanja z različnimi začetnimi vsebnostmi vode v tleh so pokazali, da povzroči višja vsebnost vode v tleh ob začetku namakanja večje velikosti omočenih tal v vse smeri.

Rezultati Hydrus-2D/3D simulacij z različnimi teksturnimi razredi tal iz baze podatkov SEISMIC, različnimi pretoki kapljačev in različnimi začetnimi vsebnostmi vode v tleh so omogočili določitev novih konstant za Schwartzman in Zur (1986) model. Izboljšani parametri modela, testirani na podatkih iz treh neodvisnih študij, so pokazali dobre rezultate modela Schwartzman in Zur (1986) z oceno efektivne srednje kvadratne napake (RMSE) od 2,21 do 13,92 cm in učinkovitostjo modeliranja (ME) od -2,54 do 0,93. Dobri doseženi rezultati modela kažejo na to, da se model lahko uporablja za planiranje (določanje oblikovnih lastnosti) površinskih kapljičnih namakalnih sistemov, za kar se potrebuje preprosto in edino znanje o nasičeni hidravlični prevodnosti tal. Vendar pa je potrebno opozoriti, da so potrebne nadaljnje raziskave o tem, kako se takšni empirični modeli izkažejo v *'in situ'* pogojih, ko so prisotni še drugi dejavniki, kot sta struktura in slojevitost tal, ki lahko v veliki meri vplivata na gibanje vode v tleh.

Numerična študija kapljičnega namakanja sladke koruze je bila izvedena z namenom, da se razišče vpliv petih različnih strategij upravljanja namakanje na distribucijo vode iz nadzemnega kapljača ob hkratnem upoštevanju odvzema vode preko koreninskega sistema. Razlika v velikosti vzorcev omočenosti v homogenih tleh je bila med petimi strategijami namakanja (neprekinjeno ali v pulzih) ob uporabi enake količine vode od 28,6 % v vertikalni (Y) in do 29,2 % v radialni (X) smeri. Vsebnost vode v talnem profilu je bila v povprečju višja za strategije, kjer je namakanje potekalo v pulzih, in nižja za strategijo, kjer se je namakanje izvajalo ponoči. Strategija namakanja je pomembno vplivala na odvzem vode skozi korenine koruze, ki je bila najnižja pri strategiji 3, kjer se je namakanje izvajalo v 4 kratkih pulzih čez dan in kjer se je vsebnost vode v tleh ohranjala na najvišji povprečni ravni. To je bila posledica izbranih parametrov odvzema vode preko korenin, ki je bila v celoti odvisna od izbranih fizikalnih parametrov tal. To je pomenilo, da je bil odvzem vode skozi korenine najvišji med FC tal in stopnjo za koruzo tolerirane najnižje vsebnosti vode v tleh, ki je bila določena pri 50 % (Določeno po Allen in sod. 1998) razpoložljive vode v tleh. Torej, pri strategijah namakanja, kjer je bila vsebnost vode v tleh

vzdrževana nad FC tal ali pod 50 % razpoložljive vode v tleh, ob stanju najvišje ETc in na globini maksimalne gostote korenin, so bile rastline pod stresom, kar je vplivalo na manjši odvzem vode. Strategija, pri kateri se je neprekinjeno namakanje pričelo vsak dan ob 21.30 h in končalo ob 23.33 h (strategija 2) je bila najboljša, ker se je voda v tleh po namakanju prerazporedila čez noč, posledica česar je bila optimalna vsebnost vode v tleh naslednji dan, ko je bila ETc najvišja. Če povzamemo, so rezultati pokazali, da je bila, za dane oblikovne parametre površinskega kapljičnega namakanja sladke koruze v peščenih tleh, najboljša strategija 2 (neprekinjeno namakanje ponoči). Prav tako se je pokazalo, da je 33 cm razdalje med kapljači dovolj, da se v danih tleh ustvari enotna vlažna cona na globini največje gostote korenin (21 cm). Za dani primer namakanja so potrebne dodatne simulacije z različnimi oblikovnimi parametri kapljičnega namakalnega sistema, da bi določili optimalne pretoke kapljačev in razdalje med njimi, kar bi pripomoglo k boljši učinkovitosti namakanja sladke koruze v peščenih tleh.

Natančnost Hydrus-2D/3D simulacij infiltracije vode v tla in njene redistribucije v slojevitih meljasto-glinasto-ilovnatih tleh pod nadzemnim točkovnim virom vode (kapljačem) in ob hkratnem upoštevanju odvzema vode skozi korenine rastlin je bila ocenjena na praktičnem primeru namakanja hmelja. Pokazalo se je, da se simulirani volumski deleži vode v tleh dobro ujemajo z dejanskimi TDR izmerjenimi podatki na 20 preučenih lokacijah. Vrednosti RMSE stanja vode v tleh za obdobje treh dni, za vse preučene TDR sonde, so variirale od 0.0025 do 0.1337 cm^3/cm^3. V primeru, da je bila za vsak sloj tal izbrana le ena reprezentativna TDR sonda, so vrednosti RMSE variirale od 0.0025 do 0.0364 cm^3/cm^3. Hydrus-2D/3D ni uspel pravilno simulirati začetnih vsebnosti vode v tleh za dve, vzdolž talnega grebena vertikalno vstavljenih TDR sond, kjer sta vrednosti RMSE znašali 0.13337 in 0.1235 cm^3/cm^3.

Ovrednoten Hydrus-2D/3D model je omogočil oceno vpliva različnih oblikovnih parametrov in načinov upravljanja nadzemnega kapljičnega namakanja hmelja. To je vključevalo različne začetne vsebnosti vode v tleh, različne razdalje med kapljači in različno količino v enem namakalnem obroku dodane vode. Za ta namen je bilo numerično preučenih 18 različnih strategij namakanja. Grafično so bile preučene primerjave simuliranih vrednosti stanja vode na različnih globinah v tleh in dveh različnih lokacijah (pod kapljačem in na sredini med dvema kapljačema). Rezultati so pokazali, da je ob primerjavi vrednosti vsebnosti vode v tleh, na različnih globinah, opaženih tik pred naslednjim namakanjem, vpliv razdalje med kapljači (20, 30 in 40 cm), ko se je z namakanjem dodajala enaka količina vode, v celoti izničen. Prav tako ni bilo opažene nobene razlike v stanju vode v tleh (po 24 urni redistribuciji) na različnih globinah, lociranih pod kapljačem, ali na sredini med dvema kapljačema. Ti rezultati kažejo na to, da

so se vzorci omočenosti pod sosednjima nadzemnima kapljačema v celoti prekrivali pri vseh preučenih razdaljah med kapljačema (20, 30 in 40 cm).

Rezultati simulacij z različnimi začetnimi vsebnostmi vode v tleh (FC-ETc in CP+ETc) so pokazali, da je začetna vsebnost vode v tleh imela vpliv na distribucijo vode pod kapljačema na vseh preučenih globinah tal. Pri začetni vsebnosti vode v tleh pri FC-ETc, ko je bila količina z namakanjem dodane vode enaka 100 % ETc, je bila vsebnost vode na 10 in 40 cm globine konstantna. Nasprotno je pri začetni vsebnosti vode v tleh, nastavljeni pri CP+ETc, vsebnost vode na enakih globinah rahlo povečevala s časom. Na 60 cm globine tal (oz. 40 cm pod grebenom) je pri obeh preučenih začetnih vsebnostih vode v tleh vsebnost vode s časom padala. Rezultati so tudi pokazali, da je bila drenaža (izguba) vode pod globino glavne mase korenin, ko je bila dnevna količina dodane vode enaka 100 % ETc, večja pri strategijah (1 a, 2 a in 3 a), kjer je bila začetna vsebnost vode v tleh višja (izgubilo se je 16,8 m^3/ha vode), v primerjavi z 1,2 m^3/ha izgubljene vode pri strategijah (1 b, 2 b in 3 b) z nižjo začetno vsebnostjo vode v tleh.

Če povzamemo, je bil pri simulacijah namakanja hmelja pod nadzemnim kapljačem za dana tla in pri danih pogojih evapotranspiracije zaznan minimalen vpliv preučenih razdalj med kapljači na distribucijo vode v tleh. Če hkrati upoštevamo še vpliv začetne vsebnosti vode v tleh ob namakanju in količino dnevno dodane vode z namakanjem, lahko predlagamo, da mora biti količina dnevno dodane vode na cikel kapljičnega namakanja malo večja od potreb rastlin po vodi (oziroma ETc), kar bi povzročilo, da bi se količina vode v tleh na globini glavne mase korenin (40 cm brez upoštevanja grebena tal) vzdrževala na konstantnem nivoju. Rezultati tudi kažejo, da je 40 cm razdalje med kapljači primerno za namakanje hmelja v meljasto-glinasto-ilovnatih tleh. Gotovo pa bo potrebno je preučiti več simulacij z različnimi oziroma večjimi razdaljami med kapljači in različnimi količinami dodane vode ciklu namakanja, da bi lahko določili še bolj optimalne oblikovne parametre površinskega kapljičnega sistema in parametre upravljanja s temi sistemi pod danimi realnimi pogoji.

7 REFERENCES

Acar B., Topak R., Mikailsoy F. 2009. Effect of applied water and discharge rate on wetted soil volume in loam or clay - loam soil from an irrigated trickle source. African Journal of Agricultural Research, 4, 1: 49-54

Ah Koon P. D., Gregory P. J., Bell J. P. 1990. Influence of drip irrigation emission rate on distribution and drainage of water beneath a sugarcane and a fallow plot. Agricultural Water Management, 17: 267-282

Ainechee G, Boroomand-Nasab S, Behzad M. 2009. Simulation of soil wetting pattern under point source trickle irrigation. Journal of Applied Sciences, 9: 1170-1174

Allen R., Pereira L. S., Raes D., Smith M. 1998. Crop evapotranspiration. Irrigation and drainage paper No. 56. Rome, FAO: 300 p.

Amin M. S. M., Ekhmaj, A. I. M. 2006. DIPAC-drip irrigation water distribution pattern calculator. In: 7th International micro irrigation congress, 10–16 Sept, PWTC, Kuala Lumpur, Malaysia.
http://irrigationtoolbox.com/ReferenceDocuments/TechnicalPapers (July 2013)

Angelakis A. N., Rolston D. E., Kadir T. N., Scott V. N. 1993. Soil-water distribution under trickle source. Journal of Irrigation and Drainage Engineering, 119: 484-500

ARSO (Agencija Republike Slovenije za Okolje). 2013
http://meteo.arso.gov.si/met/sl/agromet/ (30.8.2013)

ASAE standard ASAE S526.3 September. 2007. Soil and water terminology. American Society of Agricultural and Biological Engineers (ASABE), St. Joseph, Michigan: 22 p.

ASCE-EWRI. 2005. The ASCE standardized reference evapotranspiration equation. In: Allen, R.G., Walter, I.A., Elliot, R.L., et al. (eds.) Environmental and Water Resources Institute (EWRI) of the American Society of Civil. Engineers, ASCE, Standardization of Reference Evapotranspiration Task Committee Final Report, Reston, VA: American Society of Civil Engineers (ASCE): 213
http://www.kimberly.uidaho.edu/water/asceewri/ascestzdetmain2005.pdf (December, 2012)

Assouline S. 2002. The effects of microdrip and conventional drip irrigation on water distribution and uptake. Soil Science Society of America Journal, 66: 1630-1636

Badr M. A., Taalab A. S. 2007. Effect of drip irrigation and discharge rate on water and solute dynamics in sandy soil and tomato yield. Australian Journal of Basic and Applied Sciences, 1, 4: 545-552

Bar-Yosef B; Sheikholslami M. R. 1976. Distribution of water and ions in soils irrigated and fertilized from a trickle source. Soil Science Society of America Journal, 40: 575-582

Bates B. C., Kundzewicz Z. W., Wu S., Palutikof J. P. 2008. Climate change and water. Technical Paper of the Intergovernmental Panel on Climate Change, IPCC Secretariat, Geneva: 210 p.

Benami A, Ofen A. 1995. Irrigation engineering, Haifa, Agripro-Agricultural Projects: 257 p.

Ben-Gal A., Lazarovitch N., Shani U. 2004. Subsurface drip irrigation in gravel-filled cavities. Vadose Zone Journal, 3: 1407–1413

Brandt A., Bresler E., Diner N., Ben-Asher I. K., Heller J., Goldberg D. 1971. Infiltration from a trickle source: I. Mathematical models. Soil Science Society of America Journal, 35: 683-689

Bresler E., Heller J., Diner N., Ben-Asher J., Brandt A., Goldberg D. 1971. Infiltration from a trickle source. II: Experimental data and theoretical predictions. Soil Science Society of America Proceedings, 35: 683–689

Bresler E. 1975. Two-dimensional transport of solutes during non-steady infiltration from a trickle source. Soil Science Society of America Proceedings, 39: 604-613

Brooks R. H., Corey A. T. 1964. Hydraulic properties of porous media, Hydrol. Paper No. 3, Colorado State Univ., Fort Collins, CO: 27 p.

Bruinsma J. 2003. World Agriculture: Towards 2015/2030. An FAO Perspective. London, Earthscan: 444 p.

Bucks D. A. 1995. Historical development in microirrigation. Proc. Fifth Int Microirrig Congr Orlando, Florida, ASAE Publ 4: 1-6. In: Drip irrigation. 1999. Dasberg, S. and Or, D. (eds). Berlin, Springer Verlag: 3-4

Bufon V. B., Lascano R. J., Bednarz C., Booker J. D., Gitz D. C. 2011. Soil water content on drip irrigated cotton: comparison of measured and simulated values obtained with the Hydrus 2-D model. Irrigation Science, 30, 4: 259-273

Burdine N. T. 1953. Relative permeability calculate on from pore size distribution data. Transactions of the American Institute of Mining Engineers, 198: 71-78

Camp C. R. 1998. Subsurface drip irrigation: a review. Transactions of the American Society of Agricultural Engineers, 41: 1353-1367

Cassel D. K., Nielsen D. R. 1986. Field capacity and available water capacity. In: Methods of soil analysis. Part 1, Physical and mineralogical methods. Klute A. (eds). American Society of Agronomy and Soil Science Society of America: Madison, WI: 901-926

Carlsson M. 1998. Sources of errors in time domain refloctometry measurements of soil moisture. MSc Thesis. Uppsala: 50 p. http://pub.epsilon.slu.se/4888/ (August, 2013)

Chesworth W. 2008. Encyclopedia of Soil Science. Springer, Dorderecht: 902 p.

Clark G. A. 1992. Drip irrigation management and scheduling for vegetable row crop production. Hort Technology, 2,1: 32-37

Coelho E. F., Or D. 1996. A parametric model for two-dimensional water uptake by corn roots under drip irrigation. Soil Science Society of America Journal, 60: 1039-1049

Coelho E. F., Or D. 1999. Root distribution and water uptake patterns of corn under surface and subsurface drip irrigation. Plant and Soil, 206: 123-136

Cook F. J., Thorburn P. J., Fitch P., Bristow K. L. 2003. Wet up: A Software Tool to Display Approximate Wetting Patterns from Drippers. Irrigation Science, 22: 129-134

Cote C. M., Bristow K. L., Charlesworth P. B., Cook F. J., Thorburn P. J. 2003. Analysis of soil wetting and solute transport in subsurface trickle irrigation. Irrigation Science, 22: 143-156

Couvreur V., Vanderborght J., Javaux M. 2012. A simple three-dimensional macroscopic root water uptake model based on the hydraulic architecture approach. Hydrology and Earth System Sciences, 16: 2957-2971

Dabach S., Lazarovitch N., Šimůnek J., Shani U. 2011. Numerical investigation of irrigation scheduling based on soil water status. Irrigation Science, 31, 1: 27-36

Dahiya R., Jhorar J. B. S., Malik R. S., Ingwersen J., Streck T. 2007. Simulation of water and heat transport in drip-irrigated sandy soil under mulched conditions. Journal of the Indian Society of Soil Science, 55, 3: 233-240

Dasberg S., Or D. 1999. Drip irrigation. Berlin, Springer Verlag: 162 p.

De Fraiture C., Wichelns D. 2010. Scenarios for meeting future water challenges in food production. Agricultural Water Management, 97, 4: 502-511

Deb S., Shukla M. K. 2012. Variability of hydraulic conductivity due to multiple factors. American Journal of Environmental Science, 8, 5: 489-502

Dirksen C., Matula S. 1994. Automated atomized water spray system for soil hydraulic conductivity measurements. Soil Science Society of America Journal, 58: 319-325

Dorenbos J., Pruitt W. O. 1977. Crop Water Requirements - guidelines for predicting crop water requirements. FAO Irrigation and Drainage Paper 24. Rome, FAO: 144 p.

DripTips. Toro's drip irrigation blog and educational website. 2013. http://driptips.toro.com/?p=40 (July, 2013)

Durner W. 1994. Hydraulic conductivity estimation for soils with heterogeneous pore structure. Water Resources Research, 32, 9: 211-223

Elmaloglou S., Malamos N. 2007. Estimation of width and depth of the wetted soil volume under a surface emitter, considering root water-uptake and evaporation. Water Resources Management, 21: 1325-1340

Elmaloglou S., Diamantopoulos E. 2009. Simulation of soil water dynamics under subsurface drip irrigation from line sources. Agricultural Water Management, 96, 1587–1595

Elmaloglou S., Diamantopoulos E. 2010. Soil water dynamics under surface trickle irrigation as affected by soil hydraulic properties, discharge rate, dripper spacing and irrigation duration, Irrigation and Drainage, 59, 3: 254-263

Evans R. G., Wu I. P., Smystrala A. G. 2007. Design of microirrigation systems. Chapter 17. In: Design and operation of farm irrigation systems. 2nd edition. Glenn J. Hoffman, Robert G. Evans, Marvin E. Jensen, Derrel L. Martin, Ronald L. Elliott (eds). ASABE Special Monograph: 633-683

FAO. 2001. Irrigation manual. Planning, development monitoring and evaluation of irrigated agriculture with farmer participation, Module 8: Sprinkler irrigation systems planning, design, operation and maintenance. Harare, FAO, Subregional Office for Southern and East Africa: 80 p.

FAO. 2002a. Irrigation manual. Planning, development monitoring and evaluation of irrigated agriculture with farmer participation, Module 9: Localized irrigation systems planning, design, operation and maintenance. Harare, FAO, Subregional Office for Southern and East Africa: 82 p.

FAO. 2002b. Irrigation manual. Planning, development monitoring and evaluation of irrigated agriculture with farmer participation, Module 4: Crop water requirements and irrigation scheduling. Harare, FAO, Subregional Office for Southern and East Africa: 138 p.

Feddes R. A., Kowalik P. J., Zaradny H. 1978. Simulation of field water use and crop yield. New York, NY, John Wiley & Sons: 188 p.

Feddes R. A., Raats P. A. C. 2004. Parameterizing the soil–water–plant root system. In: Proceedings of the unsaturated zone modelling: progress, challenges and applications. Feddes R. A., de Rooij G. H., van Dam J.mC. (eds). Wageningen UR Frontis Series, vol. 6., Dordrecht, The Netherlands, Kluwer Academic Publishers: 95-141

Fernandez-Galvez J., Simmonds L. P. 2006. Monitoring and modelling the three-dimensional flow of water under drip irrigation. Agricultural Water Management, 83, 3: 197-208

Ferre P. A., Topp G. C. 2002. Time domain reflectometry. In: Methods of soil analysis, Part 4 - Physical methods. Dane J. H., and Topp G. C. (eds). Soil Science Society of America Book Series No. 5. Madison, Wisconsin, Soil Science Society of America: 434-446

Fischer G., Tubiello F. N., van Velthuizen H., Wiberg, D. 2007. Climate change impacts on irrigation water requirements: Effects of mitigation, 1990–2080. Technological Forecasting and Social Change, 74: 1083-1107

Friškovec I. 2002. Obdelava tal v rastnem obdobju. In: Priročnik za hmeljarje. Majer, D. (eds). Žalec, Inštitut za hmeljarstvo in pivovarstvo Žalec: 165-167

Gao Y., Duan A., Qiu X., Liu Z., Sun J. 2010. Distribution of roots and root length density in a maize/soybean strip intercropping system. Agricultural Water Management, 98: 199-212

Gardenas A, Hopmans J. W., Hanson B. R., Šimůnek J. 2005. Two dimensional modeling of nitrate leaching for various fertigation scenarios under micro-irrigation. Agricultural Water Management, 74: 219-242

Gardner W. R. 1960. Dynamic aspects of water availability to plants. Soil Science, 89: 63-73

Gardner W. R. 1964. Relation of root distribution to water uptake and availability. Agronomy Journal, 56: 41-45

Gardner W. R. 1965. Dynamic aspects of soil-water availability to plants. Annual Review of Plant Physiology, 16: 323-342

Grossman R. B., Reinsch T. G. 2002. Bulk density and linear extensibility. In: Methods of soil analysis. Part 4. Physical methods. Dane J. H. and Topp G. C. (eds). SSSA Book Ser. 5. SSSA, Madison WI: 201-228

Hammami M., Daghari H., Balti J., Maalej M. 2002. Approach for predicting the wetting front depth beneath a surface point source: Theory and numerical aspect. Irrigation and Drainage, 51, 4: 347-360

Hanson B. R., Šimůnek J., Hopmans J. W. 2008. Leaching with subsurface drip irrigation under saline, shallow groundwater conditions. Vadose Zone Journal 7, 2: 810-818

Healy R. W., Warrick A. W. 1988. A generalized solution to infiltration from a surface point source. Soil Science Society of America Journal, 52: 1245-1251

Hess T. 2011. Sweetcorn irrigation at Société de Culture Legumièré (SCL), Cranfield, UK: 7 p.

Hillel D. 2004. Introduction to environmental soil physics. San Diego, CA, Elsevier/Academic Press: 494 p.

Hopmans J. W., Bristow K. L. 2002. Current capabilities and future needs of root water and nutrient uptake modelling. Advances in Agronomy, 77: 104-183

James I. 2010. Introduction to Soils. Cranfield University. (internal material, handouts).

Jarvis N. J. 1989. A simple empirical model of root water uptake. Journal of Hydrology, 107: 57-72

Kaiser Lopez P. 2012. Sustainable water management for sweetcorn in Senegal. Cranfield University, School of Applied Sciences, MSc Thesis: 91 p.

Kandelous M. M., Liaghat A., Abbasi F. 2008. Estimation of soil moisture pattern in subsurface drip irrigation using dimensional analysis method. Journal of Agricultural Sciences, 39, 2: 371-378 (in Persian), In: Numerical simulations of water movement in a subsurface drip irrigation system under field and laboratory conditions using HYDRUS-2D. Kandelous M. M., Šimůnek J. 2010b., Agricultural Water Management, 97: 1070-1076

Kandelous M. M., Šimůnek J. 2010a. Comparison of numerical, analytical and empirical models to estimate wetting pattern for surface and subsurface drip irrigation. Irrigation Science, 28: 435-444

Kandelous M. M., Šimůnek J. 2010b. Numerical simulations of water movement in a subsurface drip irrigation system under field and laboratory conditions using HYDRUS-2D. Agricultural Water Management, 97: 1070-1076

Kandelous M. M., Šimůnek J., van Genuchten M. Th., Malek K. 2011. Soil water content distributions between two emitters of a subsurface drip irrigation system. Soil Science Society of America Journal, 75, 2: 488-497

Kanzari S., Ba I., Hachicha M., Bouhlila R. 2013. Characterization and modelling of water and salt dynamics in a sandy soil under the effects of surface drip irrigation. In: HYDRUS Software Applications to Subsurface Flow and Contaminant Transport Problems. Šimůnek J., van Genuchten M. Th., Kodešová R. (eds). Proceedings of the 4th International Conference, March 21-22, 2013, Department of Soil Science and Geology, Czech University of Life Sciences, Prague, Czech Republic:175-181

Keller J., Karmeli D. 1974. Trickle irrigation design parameters. Transaction of the ASAE, 7: 678-684

Keller J., Bliesner R. 1990. Sprinkle and trickle irrigation. Chapman and Hall, New York: 739 p.

Khan A. A., Yitayew M., Warrick A. W. 1996. Field evaluation of water and solute distribution from a point source. Journal of Irrigation and Drainage Engineering, 22, 4: 221–227

Knapič M., Pintar M. 1998. Implementation of subsurface drip irrigation in hop growing as contribution to an environmentally acceptable production. Fresenius Environmental Bulletin, 7: 867-872

Knapič M. 2002. Namakanje hmeljskih nasadov. In: Priročnik za hmeljarje. Majer D. (eds). Žalec, Inštitut za hmeljarstvo in pivovarstvo Žalec: 169-179

Kosugi K. 1996. Lognormal distribution model for unsaturated soil hydraulic properties. Water Resources Research, 32, 9: 2697-2703

Lafolie F., Guennelon R., Van Genuchten M. 1989. Analysis of water flow under trickle-irrigation, I: theory and numerical solution. Soil Science Society of America Journal, 53: 1310-1318

Lamm F. R., Ayars J. E., Nakayama F. S. 2007. Microirrigation for Crop Production - Design, Operation and Management. Elsevier Publications: 608 p.

Laboski C. A. M., Dowdy R. H., Allmaras R. R., Lamb J. A. 1998. Soil strength and water content influences on corn root distribution in a sandy soil. Plant and Soil, 203: 239-247

Lazarovitch N., Šimůnek J., Shani U. 2005. System dependent boundary condition for water flow from subsurface source. Soil Science Society of America Journal, 69, 1: 46-50

Lazarovitch N, Warrick A. W., Furman A., Šimůnek J. 2007. Subsurface water distribution from drip irrigation described by moment analyses. Vadose Zone Journal, 6: 116-123

Levin I., Van Rooyen P. C., Van Rooyen F. C. 1979. The effect of discharge rate and intermittent water application by point source irrigation on soil moisture distribution pattern. Soil Science Society of America Journal, 43, 1: 8-16

Li J., Zhang J., Ren L. 2003. Water and nitrogen distribution as affected by fertigation of ammonium nitrate from a point source. Irrigation Science, 22,1: 12-30

Li J., Zhang J., Rao M. 2004. Wetting patterns and nitrogen distributions as affected by fertigation strategies from a surface point source. Agricultural Water Management, 67: 89–104

Lubana P. P. S., Narda, N. K. 2001. Modelling soil water dynamics under trickle emitters - a review. Journal Of Agricultural Engineering Research, 78, 3: 217-232

Malek K., Peters R. 2011. Wetting Pattern Models for Drip Irrigation: New Empirical Model. Journal of Irrigation and Drainage Engineering, 137, 8: 530-536

MKO (Ministrstvo za kmetijstvo in okolje). Javni pregledovalnik grafičnih podatkov MKO. 2013 http://rkg.gov.si/GERK/WebViewer/#map_x=500000&map_y=100000&map_sc=1828571 (30.8.2013)

Mmolawa K., Or D. 2000. Water and Solute Dynamics under a Drip-Irrigated Crop: Experiments and Analytical Model. Transactions of ASAE, 43: 1597-1608

Mmolawa K., Or D. 2003. Experimental and numerical evaluation of analytical volume balance model for soil water dynamics under drip irrigation. Soil Science Society of America Journal, 67, 6:1657-1671

Mostaghimi S., Mitchel J. K., Lembke W. D. 1981. Effect of discharge rate on distribution of moisture in heavy soils irrigated from a trickle source. American Society of Agricultural Engineers, 81: 975-980

Molz F.J. 1981. Models of water transport in the soil–plant system: a review. Water Resources Research, 17: 1245-1260

Moncef H., Hedi D., Jelloul B., Mohamed M. 2002. Approach for predicting the wetting front depth beneath a surface point source: Theory and numerical aspect. Irrigation and Drainage, 51, 4:347-360

Mualem Y. 1976. A new model for predicting the hydraulic conductivity of unsaturated porous media. Water Resources Research, 12: 513–522

Naglič B. 2011. Modelling and analysis of soil wetting patterns under surface drip irrigation. MSc Thesis. Cranfield, Cranfield University, School of Applied Sciences: 122 p.

Neve R. 1991. Hops. London, Chapman and Hall: 272 p.

Oosterbaan R. J, Nijland H. J. 1994. Determining the saturated hydraulic conductivity. In: Drainage principles and applications. Ritzema H. P. (eds). International Institute for Land Reclamation and Improvement (ILRI), Publication 16, second revised edition, Wageningen, The Netherlands: 435-475

Patel N., Rajput, T. B. S. 2008. Dynamics and modeling of soil water under subsurface drip irrigated onion. Agricultural Water Management, 95, 12: 1335-1349

Pavlovic M. 2012. Production character of the EU hop industry. Bulgarian Journal of Agricultural Sciences, 18, 2: 233-239

Peters A., Durner, W. 2008. Simplified evaporation method for determining soil hydraulic properties. Journal of Hydrology, 356: 147-162

Philip J. R. 1968. Steady infiltration from buried point sources and spherical cavities. Water Resources Research, 4: 1039-1047

Philip J. R. 1984. Travel-times from buried and surface infiltration point sources. Water Resources Research, 20: 990-994

Phogat V., Mahadevan M., Skewes M., Cox J. W. 2011. Modelling soil water and salt dynamics under pulsed and continuous surface drip irrigation of almond and implications of system design. Irrigation Science, 30, 4: 315-333

Phogat V., Skewes M. A., Mahadevan M., Cox, J. W. 2013. Evaluation of soil plant system response to pulsed drip irrigation of an almond tree under sustained stress conditions. Agricultural Water Management, 118: 1-11

Pintar M. 2006. Osnove namakanja s poudarkom na vrtninah in sadnih vrstah v zahodni, osrednji in južni Sloveniji. Ljubljana. Ministrstvo za kmetijstvo, gozdarstvo in prehrano: 54 p.

Provenzano G. 2007. Using HYDRUS-2D Simulation model to evaluate wetted soil volume in subsurface drip irrigation systems. Journal of Irrigation and Drainage Engineering, 133, 4: 342-349

Radcliffe D. E., Šimůnek J. 2010. Soil physics with HYDRUS modeling and applications. Boca Raton, CRC Press, Taylor & Francis Group: 373 p.

Ravi V., Williams J. R. 1998. Estimation of infiltration rate in the vadose zone: compilation of simple mathematical models. Report EPA/600/R-97/128a, vol 1. Washington, DC, Environmental Protection Agency: 26 p.

Reinders F. B. 2007. Micro-irrigation: world overview on technology and utilization. In: 7th International Micro-Irrigation Congress in Kuala Lumpur, Malaysia. http://www.icid.org/nletter/micro_nl2006_4.pdf (August 2012)

Richards L. A. 1931. Capillary conduction of liquids in porous mediums. Physics, 1: 318–333

Richards L. A. 1942. A pressure-membrane extraction apparatus for soil solutions. Soil Science, 53: 241-248

Rode J., Zmrzlak M., Kovačevič M. 2002. Hmeljna rastlina. In: Priročnik za hmeljarje. Majer, D. (eds). Žalec, Inštitut za hmeljarstvo in pivovarstvo Žalec: 21-30

Rodríguez-Sinobas L., Gil-Rodríguez M., Sánchez R., Losada A., Castañón G., Juana L., Laguna F. V., Benítez J. 2010. Simulation of soil wetting patterns in drip and subsurface irrigation. Effects in design and irrigation management variables. Geophysical Research Abstracts: 12 http://meetingorganizer.copernicus.org/EGU2010/EGU2010-15064.pdf (July, 2013)

Sansoulet J., Cabidoche Y. M., Cattan P., Ruy S., Šimůnek J. 2008. Spatially distributed water fluxes in an Andisol under banana plants: experiments and 3D modelling. Vadose Zone Journal: 7, 2: 819-829

Schindler U., Durner W., Von Unold G., Mueller L., Wieland R. 2010. The evaporation method – Extending the measurement range of soil hydraulic properties using the air-entry pressure of the ceramic cup. Journal of Plant Nutrition and Soil Science, 173: 563-572

Schindler U. 1980. Ein Schnellverfahren zur Messung der Wasserleitfa ¨higkeit im teilgesa¨ttigten Boden an Stechzylinderproben. Arch. Acker-u. Pflanzenbau u. Bodenkd. Berlin 24, 1–7. In: Simplified Evaporation Method for Determining Soil Hydraulic Properties. Peters, A., Durner, W. (2008). Journal of Hydrology, 356: 147-162

SEISMIC (Spatial Environmental Information System for Modelling the Impact of Chemicals). Cranfield, National Soil Resources Institute (NSRI) in Cranfield University, in collaboration with the British Agrochemicals Association (BAA) and the Pesticides Safety Directorate of Defra (internal material, April, 2011)

Shan Y. Y., Wang Q. J. 2012. Simulation of salinity distribution in the overlap zone with double-point-source drip irrigation using HYDRUS-3D. Australian Journal of Crop Science, 6, 2: 238-247

Schmitz G. H., Schutze N., Petersohn U. 2002. New strategy for optimizing water application under trickle irrigation. Journal of Irrigation and Drainage Engineering ASCE, 128, 5: 287–297

Schwartzman M., Zur B. 1986. Emitter spacing and geometry of wetted soil volume. Journal of Irrigation and Drainage Engineering, 112: 242-253

Smith J. U., Smith P. Addiscott T. M. 1996. Quantitative methods to evaluate and compare soil organice matter (SOM) models. In: Evaluation of soil organic matter models using existing long-term datasets. Powlson D. S., Smith P., Smith J. U. (eds). NATO Advanced Research Workshop Papers, NATO ASI Series 38. Heidelberg, Springer-Verlag: 181-199

Snyder R. L., Eching S. 2006. PMhr Penman-Monteith Hourly ETref for short and tall canopies. University of California, Davis.
http://biomet.ucdavis.edu (January, 2013)

Skaggs T. H., Trout T. J., Šimůnek J., Shouse P. J. 2004. Comparison of Hydrus-2D simulations of drip irrigation with experimental observations. Journal of Irrigation and Drainage Engineering, 130, 4: 304-310

Skaggs T. H., Van Genuchten M. Th., Shouse P. J., Poss J. A. 2006. Macroscopic approaches to root water uptake as a function of water and salinity stress. Agricultural Water Management, 86, 1-2: 140-149

Skaggs T. H., Trout T. J., Rothfuss Y. 2010. Drip Irrigation Water Distribution Patterns: Effects of emitter rate, pulsing, and antecedent water. Soil Science Society of America Journal, 74: 1886-1896

Subbaiah R. 2013. A review of models for predicting soil water dynamics during trickle irrigation. Irrigation Science, 31, 3:225-258

Šejna M., Šimůnek J., van Genuchten M. Th. 2011. The HYDRUS software package for simulating two- and three-dimensional movement of water, heat, and multiple solutes in variably- saturated media, User Manual, Version 2.0, PC Progress, Prague, Czech Republic: 284 p.

Šimůnek J., van Genucten M. Th. 1994. The chain_2d code for simulating two-dimensional movement of water, heat and multiple solutes in variably-saturated porous media, Version 1.1. Research Report No. 136, U.S. Salinity Laboratory, USDA, ARS, Riverside, California: 194 p.

Šimůnek J., Vogel T., van Genuchten M. Th. 1994. The SWMS_2D code for simulating water flow and solute transport in two-dimensional variably saturated media, Version 1.21. Research Report No. 132, U.S. Salinity Laboratory, USDA, ARS, Riverside, California: 197 p.

Šimůnek J., Šejna M., van Genuchten M. Th. 1996. The HYDRUS-2D software package for simulating water flow and solute transport in two dimensional variably saturated media. Version 1.0. IGWMC-TPS-53. Int. Ground Water Modeling Ctr., Colorado School of Mines, Golden: 167 p.

Šimůnek J. 2005. Models of water flow and solute transport in the unsaturated zone. In: Encyclopedia of hydrological sciences. Anderson M. G. (eds). Chichester, England, The John Wiley & Sons, Ltd: 25 p.

Šimůnek J., van Genuchten M. Th. 2006. Contaminant transport in the unsaturated zone: theory and modeling, Chapter 22. In: The handbook of groundwater engineering. Delleur J. (eds). Second Edition, CRC Press: 22.1-22.46

Šimůnek J., van Genuchten M. Th, Šejna M. 2006. The HYDRUS software package for simulating two- and three-dimensional movement of water, heat, and multiple solutes in variably-saturated media: Technical manual. Version 1.0. PC-Progress, Prague, Czech Republic: 161 p.

Šimůnek J., Hopmans J. W. 2008. Modeling compensated root water and nutrient uptake. Ecological Modeling, 220, 4: 505-521

Šimůnek J., van Genuchten M. Th., Šejna M. 2011. The HYDRUS software package for simulating two- and three-dimensional movement of water, heat, and multiple solutes in variably-saturated media: Technical manual. Version 2.0. PC-Progress, Prague, Czech Republic: 258 p.

Šimůnek J., van Genuchten M. Th., Šejna M. 2012. The HYDRUS Software Package for Simulating Two- and Three Dimensional Movement of Water, Heat, and Multiple Solutes in Variably-Saturated Media, Technical Manual, Version 2.0, PC Progress, Prague, Czech Republic: 258 p.

Šimůnek J., Šejna M., Jacques D., Langergraber G., Bradford A. S., van Genuchten M. Th. 2013. New Features of the HYDRUS Computer Software Packages. In: HYDRUS Software Applications to Subsurface Flow and Contaminant Transport Problems. Proceedings of the 4th International Conference. Šimůnek J., van Genuchten M. Th., Kodešová R. (eds). March 21-22, 2013, Department of Soil Science and Geology, Czech University of Life Sciences, Prague, Czech Republic:17-26

Taghavi S. A., Miguel M. A., Rolston D. E. 1984. Infiltration from trickle-irrigation source. Journal of Irrigation and Drainage Engineering. American Society of Civil Engineering, 10: 331-341

Thabet M, Zayani K. 2008. Wetting patterns under trickle source in a loamy sand soil of South Tunisia. American-Eurasian Journal of Agricultural and Environment Science, 3: 38-42

Twarakavi N. K. C., Sakai M., Šimůnek J. 2009. An objective analysis of the dynamic nature of field capacity. Water Resources Research, 45, 10: 4-10

van Genuchten M. Th. 1980. A closed-form equation for predicting hydraulic conductivity of unsaturated soils. Soil Science Society of America Journal, 44: 892-898

van Genuchten M. Th. 1987. A numerical model for water and solute movement in and below the root zone. Research Report No 121, U.S. Salinity Laboratory, USDA, ARS, Riverside, CA. In: The HYDRUS software package for simulating two- and three-dimensional movement of water, heat, and multiple solutes in variably-saturated media. 2006. Šimůnek J., van Genuchten, M. Th, Šejna M. (eds). Technical manual. Version 1.0. PC-Progress, Prague, Czech Republic: 7-13

van Genuchten M. Th., Leij F. J., Yates S. R. 1991. The RETC code for quantifying the hydraulic functions of unsaturated soils. Report No. EPA/600/2-91/065. R. S. Kerr Environmental Research Laboratory, U. S. Environmental Protection Agency, Ada, OK: 85 p.

Vermeiren L., Jobling, G. A. 1984. Localized irrigation. FAO Irrigation and Drainage Paper 36. Rome, Italy, FAO-UN: 203 p.

Vogel T., Císlerová M. 1988. On the reliability of unsaturated hydraulic conductivity calculated from the moisture retention curve. Transport in Porous Media. 3: 1-15

Vrugt J. A., Hopmans J. W., Šimůnek J. 2001a. Calibration of a two-dimensional root water uptake model. Soil Science Society of America Journal, 65, 4: 1027-1037

Vrugt J. A., van Wijk M. T., Hopmans J. W., Šimůnek J. 2001b. One-, two-, and three-dimensional root water uptake functions for transient modelling. Water Resources Research, 37, 10: 2457-2470

Wang F., Kang Y., Liu S. 2006. Effects of drip irrigation frequency on soil wetting pattern and potato growth in North China Plain. Agricultural Water Management, 79, 3: 248-264

Wang J., Shihong G., Di X., Sui J., Jianxin M. 2013. Numerical simulations and validation of water flow and heat transport in a subsurface drip irrigation system using HYDRUS-2D. Irrigation and Drainage, 62, 1: 97-106

Wallach D. 2006. Working with dynamic crop models - evaluation, analysis, parameterization and applications. Elsevier B.V: 462 p.

Warrick A. W. 1974. Time-dependent linearized infiltration: I. Point sources. Soil Science Society of America Journal, 38: 383-386

Weaver J. E. 1926. Root development of field crops. Chapter XVII, Methods of studying root development. New York, Mcgraw-Hill
http://www.soilandhealth.org/01aglibrary/010139fieldcroproots/010139ch17.html (August, 2013)

Wind G. P. 1968. Capillary conductivity data estimated by a simple method. In: Water in the unsaturated zone, vol. 1. Rijtema P. E., Wassink H. (eds). Proceedings of the Wageningen Symposium, 19–23 June 1966. Int. Assoc. Sci. Hydrol. Publ. (IASH), Gentbrugge, Paris, The Netherlands and UNESCO: 181-190

Wooding R. A. 1968. Steady infiltration from a shallow circular pond. Water Resources Research, 4: 1259-1273

ACKNOWLEDGEMENTS

Many thanks to my supervisor Dr. Marina Pintar, from the University of Ljubljana, for offering me support during the formation of this work and for offering me opportunity to study abroad.

I would like to express my gratitude to my co-supervisor Dr. Cédric Kéchavarzi for all the help, support and encouragement during the duration of this project.

Special thanks to Nataša Hrastnik and Boris Sirše from Plima d.o.o. for encouragement and financial support.

I would like to thank to Martina Zupančič from the Slovenian Institute of Hop Research and Brewing for enabling me to carry out an experimental part of this project and to Dr. Barbara Čeh for all support and help during duration of this project.

Many thanks to Peter Korpar for help with field and laboratory work and to Dr. Andreja Sušnik and Dr. Gregor Gregorič from the Slovenian Environmental Agency for help with providing and analysing meteorological data.

The project was partly founded by the European Union (European Social Found).